UNIVERSITE CATHOLIQUE DE LOUVAIN

INSTITUTE OF EXPERIMENTAL AND CLINICAL RESEARCH

POLE OF PHARMACOLOGY AND THERAPEUTICS

Influence of the tumor microenvironment on the humoral and cellular immune responses: insights for new specific cancer biomarkers and therapeutic targets.

Florence Defresne

Promoteur : Professeur Olivier Feron

Thèse présentée en vue de l'obtention du grade
de Docteur en Sciences Biomédicales et Pharmaceutiques
Orientations : Cancérologie, Protéomique

2011

A travers ces quelques mots, je tiens à remercier toutes les personnes ayant contribué de près ou de loin à l'aboutissement de ce travail.

Mes premiers remerciements sont adressés à mon promoteur, le Professeur Olivier Feron, pour m'avoir accueillie au sein de son laboratoire et pour m'avoir fait confiance en me laissant démarrer la protéomique au labo. Merci pour votre présence et vos conseils au cours de ces années et merci pour votre compréhension et la flexibilité que vous m'avez accordée face à l'arrivée d'Emilie.

Je remercie les membres du jury, le Docteur Jérôme Solassol et le Professeur Agnès Noël, qui ont accepté de lire et critiquer mon travail.

Je tiens également à remercier les membres de mon comité d'encadrement, les Professeurs Carine Michiels, Emmanuel Hermans, Bernard Gallez et Luc Bertrand, pour m'avoir suivie et conseillée durant ces quatre années. Je tiens à remercier plus particulièrement le Professeur Michiels pour m'avoir permis de m'initier à la protéomique au sein de son laboratoire.

Sans une équipe, un labo ne peut pas fonctionner. Je tiens donc à remercier toutes les personnes du labo FATH (passées ou présentes) qui contribuent chaque jour au bon fonctionnement du labo et à la bonne humeur qu'il y règne ! Merci aux Professeurs Jean-Luc Balligand, Chantal Dessy et Pierre Sonveaux ; merci aux techniciens pour leur aide précieuse Antoine, Audrey, Céline, Delphine, Elise, Hrag et Laurenne; merci aux doctorants Ann, Aude, Christophe, Gaëtane, Joanna, Manu, Marie, Nihed, Pierre et Virginie; merci aux post-docs Aline, Aurélia, Boris, Caroline, Elvira, Géraldine, Irina, Laila, Miguel, Nerea, Paolo, Suveera et Tamara et merci aux secrétaires Anne et Leila.

Je souhaite plus particulièrement remercier le Docteur Caroline Bouzin. Merci Caro pour toutes nos discussions et brainstormings, scientifiques ou non ! Merci d'avoir toujours été là pour moi durant toutes ces années et de m'avoir conseillée dans mes choix. Et n'oublie pas que quand tu as besoin d'aide pour écrire un mail… tu demandes ! ;)

Je remercie également Céline sans qui tout ce travail n'aurait pas pu se faire ! Merci Cé pour tous ces moments de délires en chanson (awimbowé !) et pour tout le reste ! Sans toi, ce boulot n'aurait pas abouti aussi rapidement et il aurait été beaucoup moins agréable au quotidien !

Je remercie ensuite le Docteur Aline Meulle (Madame Adipocyte!). Merci pour toutes nos discussions (scientifiques ou non), fou-rires et merci pour ta présence et tous tes précieux conseils et encouragements en cette fin de thèse. N'oublie pas de rester en phase avec tes adipocytes et de ne pas manger trop sucré!

Je remercie enfin Marie, qui me supporte au quotidien dans le bureau ! Je ne te remercie pas pour ton aide avec Acrobat Professional ;)

mais merci d'avoir agrandi l'équipe des 2D-girls avec autant de bonne humeur !

Une thèse est également l'occasion de faire des rencontres précieuses… je souhaite donc remercier Flo pour toutes les manips que nous avons partagées et plus particulièrement pour son amitié au quotidien. Merci choupinette !

Mes remerciements vont bien sûr à ma famille qui m'a encouragée à faire cette thèse. Je tiens également à remercier Julie Stockis, avec qui j'ai pu partager mes galères de labo pendant ces quelques années. On y est enfin arrivé !!!

Last but not least, je remercie Pascal qui m'a toujours soutenue au quotidien, qui a toujours été là pour moi et qui m'a permis de connaitre le bonheur d'être maman de notre petite canaille Emilie. Merci de m'avoir écoutée raconter mes joies et galères scientifiques… même si tu n'y comprenais pas toujours grand-chose ! ;) Merci pour tout !

Table of Contents

ABBREVIATIONS

2-DE	2 dimension-electrophoresis
Act4	Actin-related protein 4
ACY1	Aminoacylase 1
AFP	Alpha foetoprotein
Akt	Protein kinase B (PKB)
AldA	Putative aldehyde dehydrogenase A
ANXA	Annexin A
APC	Antigen presenting cell
ARNT	Aryl hydrocarbon receptor nuclear translocator
αSMA	α-smooth muscle actin
ATP	Adenosine triphosphate
Bcl-2	B-cell lymphoma 2
BCR	B-cell receptor
BiP	Immunoglobulin heavy-chain binding protein
BM	Bone marrow
BMDC	Bone marrow-derived cells
BTA	Bladder tumor antigen
BV	Bronchiole vein
BV8	Bombina Variegata 8
BVA	Biological variation analysis
CA-125	Carbohydrate antigen-125
CAF	Cancer-associated fibroblasts
CAI	Carbonic-anhydrase I
CapG	Capping-protein gelsolin-like
CCD	Charge-coupled device
CCR2	Chemokine (C-C motif) receptor 2
cDNA	Complementary DNA
CD4 Th	CD4 T helper lymphocyte
CEA	Carcinoembryonic antigen
CEC	Circulating endothelial cells
CNN2	Calponin 2
CSF1R	Colony stimulating factor 1 receptor
CTL	Cytotoxic T lymphocytes
CXCR4	C-X-C chemokine receptor type 4
Cy	Cyanine
DIA	Differential in-gel analysis
DIGE	Difference in gel electrophoresis
DNA	Deoxyribonucleic acid
EC	Endothelial cell
ECL	Enhanced chemiluminescence
ECM	Extra-cellular matrix
E.Coli	Escherichia Coli
EGF	Epidermal growth factor
EIF3G	Eukaryotic translation initiation initiation factor 3G

ELISA	Enzyme-linked immunosorbent assay
EMT	Epithelial to mesenchymal transition
EPC	Endothelial progenitor cell
EPO	Erythropoietin
ER	Endoplasmic reticulum
ESI	Electrospray ionization
FAK	Focal adhesion kinase
FAP	Fibroblast activating protein
FB	Fibroblast
FGF	Fibroblast growth factor
FIH	Factor inhibiting HIF-1α
FKBP52	Peptidyl-prolyl cis-trans isomerase FKBP4
FN	Fibronectin
FSP-1	Fibroblast specific protein-1
G-CSF	Granulocyte colony-stimulating factor
GLUT-1	Glucose transporter 1
GM-CSF	Granulocyte macrophage colony-stimulating factor
GRP	Glucose-regulated protein
HAP	Haptglobin
HBV	Hepatitis B virus
HCC	Hepatocellular carcinoma
HCV	Hepatitis C virus
HER2	Human epidermal growth factor receptor 2
HGF	Hepatocyte growth factor
HIF-1	Hypoxia Inducible Factor 1
HMGB1	High-mobility group protein B1
HnRNP	Heterogeneous ribonucleoprotein
HPC	Hematopoietic progenitor cells
HPLC	High performance liquid chromatography
HRE	Hypoxia responsive element
HSC	Hematopoietic stem cell
HSP	Heat-shock protein
ICTP	C-telopeptide pyridinoline cross-links of type I collagen
IFN	Interferon
Ig	Immunoglobulin
IGF-2	Insulin-like growth factor-2
IL	Interleukin
iNOS	Inducible NO synthase
IPG	Immobiline pH gradient
kDa	Kilo Dalton
LamC	Laminin C
LCM	Laser-capture microdissection
LOX	Lysyl oxidase

LRG1	Leucine-rich alpha-2-glycoprotein 1
LY6C	Lymphocyte antigen 6C
MAGE	Melanoma antigen
MALDI TOF	Matrix-assisted laser desorption ionization – Time of flight
MDSC	Myeloid-derived suppressor cell
MET	Mesenchymal to epithelial transition
MHC	Major histocompatibility complex
MICA/B	Major histocompatibility antigen related chain A and B
MMP	Matrix metalloproteinase
MMTV-PyMT	Mouse mammary tumor virus-Polyoma Middle T protein
MOMC	Monocyte-derived multipotential progenitor cells
MS	Mass spectrometry
MSC	Mesenchymal stem cell
mTOR	Mammalian target of rapamycin
MUC1	Mucin 1
MVP	Major Vault protein
Ng	Nanograms
NG2	Nerve/Glial antigen 2
NK cell	Natural killer cell
NKp46	Natural killer cell p46-related protein
NMP22	Nuclear matrix protein 22
NSE	Neuron-specific enolase
ODD	Oxygen-dependent degradation
OLA1	Obg-like ATPase 1
ORF	Open reading frame
p300	E1A binding protein p300
p53	Tumor protein 53
PDIA3	Protein-disulfide isomerase A3
PDGFR	Platelet-derived growth factor receptor
PHD	Prolyl-hydroxylase domain
pI	Isoelectric point
PI3K	Phospho inositol 3 kinase
PPAR	Peroxisome proliferator-activated receptors
PPIA	Peptidyl-prolyl cis-trans isomerase A
PRDX6	Peroxiredoxin 6
PROTEOMEX	combination of PROTEOMics and serEX
PSA	Prostate-specific antigen
PTEN	Phosphate and tensin homolog
Q-TOF	Quadrupole - Time of flight
Rae-1	Retinoic acid early inducible gene-1
Ras	RAt Sarcoma virus
RCC	Renal cell carcinoma

RNA	Ribonucleic acid
S100A8	S100 calcium binding protein A8
s.c.	Sub-cutaneous
Sca-1	Stem cell antigen-1
SCC	Squamous cell carcinoma antigen
SDF-1	Stromal cell-derived factor 1
SDS-PAGE	Sodium dodecyl sulfate – polyacrylamide gel electrophoresis
SEREX	Serological analysis of tumor antigens by recombinant cDNA expression cloning
SERPA	Serological proteome analysis
SM22α	Smooth muscle protein 22α
SOD	Superoxide dismutase
SPARC	Secreted Protein, acidic and rich in cysteine
STMN1	Stathmin 1
STR	Serotransferrin
TAA	Tumor-associated antigen
TAM	Tumor-associated macrophage
TB	Terminal bronchiole
TEM	Tie-2 expressing monocyte
TCR	T lymphocyte receptor
TGF-β	Transforming growth factorβ
Tie-2	Tyrosine kinase with immunoglobulin and EGF homology domain-2
TLR4	Toll-like receptor 4
TMB	Tetra methylbenzidine
TNFα	Tumor necrosis factor α
TP	Thymidine phosphorylase
TRAIL	TNF-related apoptosis-inducing ligand
Treg	T regulatory lymphocyte
TSC	Tumor suppressor complex
ULBP	UL16-binding protein
UPR	Unfolded protein response
VCP	Valosin containing protein
VEGF	Vascular endothelial growth factor
VEGFR	Vascular endothelial growth factor receptor
VHL	Von Hippel Lindau
VLA-4	Very late antigen 4

FOREWORD

Cancer is a complex network of tumor cells and host cells. Tumor cells by producing various proteins and recruiting cells, constantly communicate with “the extra-tumor” world. The tumor secretome and tumor-associated antigens both participate in this dialog by promoting the mobilization of endothelial progenitor cells from the bone marrow and the production of autoantibodies by B lymphocytes, respectively. Proteomics can now provide the tools to analyze the serological response to changes in the tumor biology, and to identify key players in the variety of proteins secreted by tumor cells and influencing tumor progression, including metastases formation. In this work, we used 2D-DIGE and SERPA technologies to address these issues in different mouse tumor models. In the introduction of this thesis, we will thus summarize key aspects of the tumor microenvironment and of the immune response to tumor development but also provide information on technologies related to cancer proteomics and detection of cancer biomarkers.

INTRODUCTION

1. The tumor microenvironment

1.1 Definition – Hallmarks of cancer revisited

The tumor microenvironment could be defined negatively as everything which is not "a cancer cell" in tumors (Figure1). This includes the extracellular matrix (ECM) and a large variety of different cell types, including endothelial cells, fibroblasts or CAF (cancer-associated fibroblasts) (Wels et al., 2008), bone marrow-derived cells (BMDC), macrophages or TAM (tumor-associated macrophages) (Wels et al., 2008), neutrophils, lymphocytes and natural killer cells (NK cells) (Table 1).

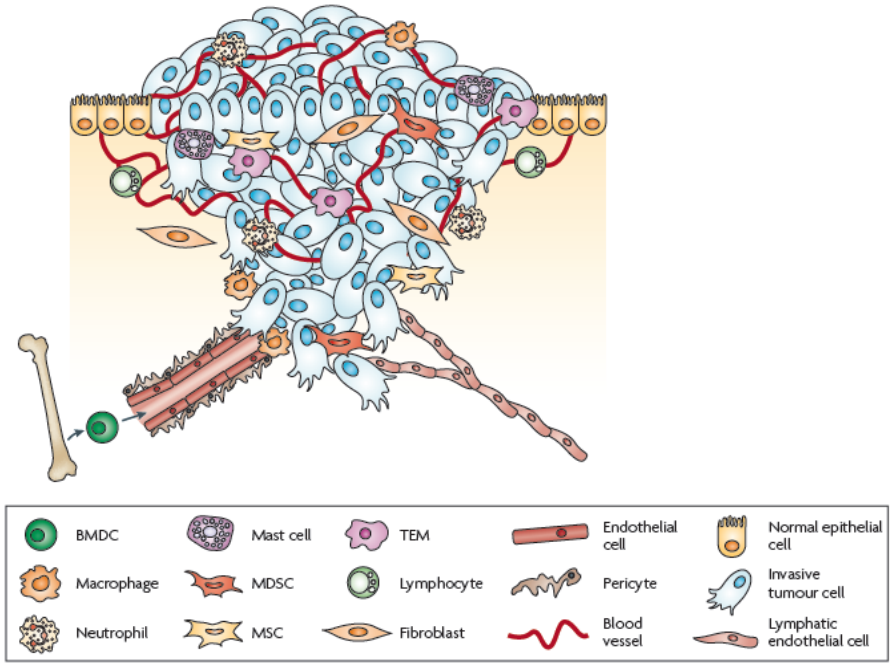

Figure 1: General representation of the tumor microenvironment. The tumor is a complex mass composed of different cell types including the bone marrow-derived cells (BMDC), mast cells, Tie-2 expressing monocytes (TEM), endothelial cells, macrophages, myeloid-derived suppressor cells (MDSC), lymphocytes, pericytes, neutrophils, mesenchymal tem cells (MSC) and fibroblasts. All these cell types participate to the tumor microenvironment and the remodelling of the ECM (Joyce and Pollard, 2009).

Table 1: Description of the different cell types present in the tumor microenvironment, their cell surface markers and their function in the tumor microenvironment (Joyce and Pollard, 2009).

Cell type	Cell surface markers*	Functions in the tumor microenvironment
TAM	$CD11b^+CD14^+CD31^-CD34^-$ $CD45^+CD68^+CD117^-CD133^-CD146^-$ $CD204^+CD206^+CCR2^+CSF1R^+MHC\ II^+$ $VEGFR1^+VEGFR2^-$ (m/h) $F4/80^+$ (m) $CD23^+CD163^+CXCR4^+$ (h)	'Classically activated' M1 macrophages contribute to tumour rejection through type 1 cytokine production and antigen presentation, whereas 'alternatively activated' M2 macrophages enhance angiogenesis and remodelling through type 2 cytokine production TAMs are proposed to share M2 characteristics; their presence in tumours is thought to be tumour promoting, and is associated with poor prognosis
MDSC	$CD11b^+CD14^{+/-}$ $MHC\ I^+MHC\ II^{low}$ (m/h) $GR1^+CD11b^+$ (m): can be further subdivided into $LY6G^+LY6C^{low}$ $CD11b^+$ $CD11c^{+/-}CD33^+CD34^+CD86^-$ (h)	MDSCs are increased in almost all patients and animal models with cancer. Because of the variation in MDSC gene expression between different tumour microenvironments, it has been challenging to identify a unique set of markers. This has emphasized the importance of showing their ability to suppress T cells as a defining trait
MSC	$CD14^-CD29^+CD31^-CD34^-CD44^+CD45^-$ $CD51^+CD71^+CD73^+CD90^+CD105^+CD133^-$ $CD166^+CD271^+$ (m/h)	MSCs infiltrate various human cancers and have been shown to increase cancer cell dissemination in animal models. MSCs are also immunosuppressive, in part through inhibition of T-cell proliferation
TEM	$CD11b^+CD14^+CD31^{low}CD34^-CD45^+$ $CD117^-CD133^-TIE2^+VEGFR2^-$ (m/h) $F4/80^+GR1^{low}SCA1^-$ (m) $CD11c^+CD13^+CD16^+CD33^+CD62L^-CD146^-$ $CCR2^-CCR5^+CSF1R^+$ (h)	Monocytes that express the angiopoietin receptor TIE2. TEMs have been implicated in angiogenesis from studies in animal models and have been detected in human tumours and at low frequency in the peripheral blood of cancer patients
Neutrophil	$CD11b^+CD14^{low}CD31^+CD66B^+CXCR2^+$ (m/h) $GR1^+VEGFR1^+CXCR1^-$ (m) $CD15^+CXCR1^+$ (h)	Levels of neutrophils are increased in patients with colon, gastric and lung cancer. Neutrophil infiltration is further enhanced in the invasive areas of CRCs, and increased numbers are associated with poor prognosis in bronchioalveolar carcinoma. Neutrophils have been implicated in enhancing angiogenesis and metastasis in animal models
Mast cell	$CD43^+CD117^+CD123^+CD153^+$(m/h) $CD11b^+CD16^+CD34^+SCA1^+$ (m) $CCR1^+CCR3^+CCR4^+CCR5^+CXCR1^+CXCR2^+$ $CXCR4^+$ (h)	Mast cells are important in generating and maintaining innate and adaptive immune responses. Increased mast cell numbers have been reported in a wide range of tumours and, in some cases, this correlates with poor prognosis. Mast cells have been implicated in angiogenic switching in several animal models
Endothelial cell	$CD31^+CD34^+CD105^+CD106^+CD144^+$ (m/h)	Endothelial cells comprise the blood vasculature of the tumour, and increased microvessel density is frequently associated with poor prognosis in a wide range of human cancers
EPC	$CD13^+CD31^{low}CD45^-CD105^+$ $CD133^+CD117^+CD146^+CD144^+$ (VE-cadherin: E4G10+ Ab)$VEGFR2^+$ (m/h)	EPCs contribute to blood vessel formation in various animal models and some patient studies, although the functional importance of EPCs in tumour angiogenesis remains controversial
Pericyte	$Desmin^{+/-}NG2^{+/-}\alpha SMA^{+/-}PDGFR\beta^{+/-}$	Pericytes are mural cells that provide physical support and stabilization, as well as pro-survival factors, to blood vessels. Pericytes may also be crucial in limiting metastasis by maintaining vessel integrity
Fibroblast	$Vimentin^+desmin^+\alpha SMA^{+/-}FSP1^+FAP^+$ (m/h)	CAFs are a large component of the stroma, and at later stages of tumour progression are generally tumour promoting, as shown in animal models and studies using patient samples
Platelet	$CD41^+CD42a$-$dCD51^+CD110^+$ (m/h)	Platelets are activated and circulate at higher levels in cancer patients, particularly those with advanced malignancy.
$CD4^+$ T cell	$CD3^+CD4^+CD45^+$ (m/h)	T helper type 1 cells aid $CD8^+$ T cells in tumour rejection, whereas T helper type 2 cells polarize immunity away from an anti-tumour response, and regulatory T cells block $CD8^+$ cell activation and NK cell killing
$CD8^+$ T cells	$CD3^+CD8^+CD45^+$ (m/h)	Also known as CTLs, these are the effector cells of the adaptive immune system and specifically recognize and destroy cancer cells through perforin- and granzyme-mediated apoptosis
B cell	$CD3^-CD19^+CD20^+CD45^+$ (m/h) $CD45RA^+B220^+$ (m)	B lymphocytes are important mediators of humoral immunity, but have been shown to promote malignancy in an animal model of squamous cell carcinogenesis
NK cell	$CD11b^+CD27^{+/-}$ $CD3^-CD16^{+/-}CD56^+$ $CD3^-CD335^+NKp46^+$ (m/h)	NK cells are effector lymphocytes of the innate immune system that are cytotoxic to cancer cells through the perforin– granzyme pathway NK cells contribute to immunosurveillance of cancer, and low NK-like cytotoxicity in the peripheral blood is associated with increased risk of cancer

One may also consider tumor cell-derived proteins such as chemokines, cytokines, growth factors and proteases as well as the numerous end-products of the tumor metabolism as part of the tumor microenvironment (Witz and Levy-Nissenbaum, 2006; Hynes, 2009; Joyce and Pollard, 2009; Lorusso and Ruegg, 2008; Hanna et al., 2009). Furthermore, some typical features of cancer have to be integrated in the notion of microenvironment, namely hypoxia and low extracellular pH (Witz and Levy-Nissenbaum, 2006; Ge et al., 2010). Also, necrotic cells and release of cell content due to tumor cell death bring their contribution to the stroma in which tumor cells live (Witz and Levy-Nissenbaum, 2006).

In the six major hallmarks of cancers described by Hanahan and Weinberg, two are more directly related to the tumor microenvironment, namely angiogenesis and invasiveness (Hanahan and Weinberg, 2000; Trosko et al., 2004). Futhermore, Gillies and Gatenby recently reviewed the original list of cancer hallmarks and proposed to now include physico-chemical peculiarities of tumors, such as hypoxia, acidosis and extrinsic interactions (positive and negative growth signals exchanged by normal cells with each other and the ECM) (Figure 2) (Gillies and Gatenby, 2007).

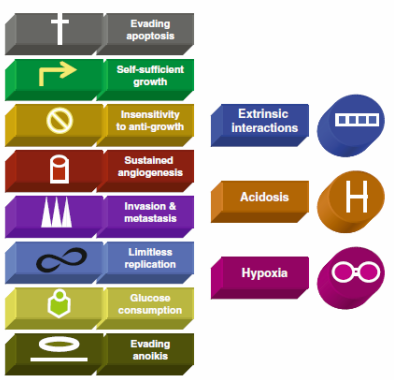

Figure 2: The eight hallmarks of cancer (adapted from Hanahan and Weinberg) (left icons) and three major components of the physiological microenvironment (right icons). Tumors present different features that allow them to grow and to escape to immune responses and regulating processes. They are able to evade apoptosis and anoïkis, to invade and metastasize at distant sites, to adapt the glucose metabolism and to induce angiogenesis. The tumor microenvironment presents different major characteristics such as acidosis and hypoxia. Tumor cells also modulate cell growth, favoring self-sufficient growth and being insensitive to anti-growth factors (Gillies and Gatenby, 2007).

Tumors exploit their particular microenvironment to progress into invasive disease (Joyce and Pollard, 2009). Indeed, the tumor microenvironment is directly linked to the alterations in tumor cell biology that will lead *in fine* to metastasis spreading (Liotta and Kohn, 2001). Tumor cells secrete for instance a lot of different proteases that can degrade the ECM, like the matrix metalloproteinases (MMP) (McCawley and Matrisian, 2001; Liotta and Kohn, 2001). These proteases are involved in tumor cell adhesion and motility, both processes regulating invasiveness (Mbeunkui and Johann, Jr., 2009; Bhowmick and Moses, 2005). It is also the balance between proteases and protease inhibitors that determine the extent of angiogenesis. Angiogenesis *per se* favors the immaturity of the tumor vasculature and thereby increases the chances of invasive tumor cells to reach the circulation (Sivridis et al., 2004). Cytokines, chemokines and growth factors mediate these interactions leading to tumor progression (Seruga et al., 2008; Dittmar et al., 2008).

Moreover, the primary tumor secretome also influences distant anatomic sites, like bone marrow, spleen or lungs (McAllister and Weinberg, 2010). Tumors can indeed mobilize BMDC into the tumor site wherein these inflammatory/immune cells favor tumor progression. BMDC may also contribute to the so-called premetastatic niches in the lungs (Kaplan et al., 2005; Hiratsuka et al., 2006). It is however still not clear whether premetastatic niches can be identified in other metastatic sites or arise from some peculiarities of the lung microenvironment (McAllister and Weinberg, 2010). Tumor cells also communicate with spleen which contains numerous cells from the myeloid lineage, in particular the myeloid-derived suppressor cells $CD11b^{+}$-$GR1^{+}$ (MDSC). These cells are thought to decrease the host immune reactivity to tumors in different experimental models (Ostrand-Rosenberg, 2010; Peranzoni et al., 2010), thereby favoring tumor development.

In the next paragraphs, we will focus on some of these hallmarks and factors directly or indirectly related to the tumor microenvironment: (i) hypoxia, (ii) angiogenesis, (iii) vasculogenesis, and (iv) invasiveness.

1.2 Tumor hypoxia

1.2.1. Hypoxia types

Tumor hypoxia is a common feature of solid tumors (Figure 3). A highly proliferative mass of tumor cells indeed always develop faster than the vasculature. Thus, growing tumor cells recurrently face avascular environment deprived of oxygen (Brahimi-Horn et al., 2007). There are actually three major types of hypoxia: diffusion-limited hypoxia (often called chronic hypoxia), perfusion-limited or cyclic hypoxia (often called acute hypoxia) and longitudinal hypoxia.

With tumor growth, intervessel distances increase, leading to an insufficient number of arterioles supplying oxygen and nutrients. The limit of diffusion of oxygen is usually proposed to be around 150 µm. Beyond this distance, tumor cells are considered to be hypoxic (Rofstad et al., 2010; Vaupel and Harrison, 2004; Brahimi-Horn et al., 2007).

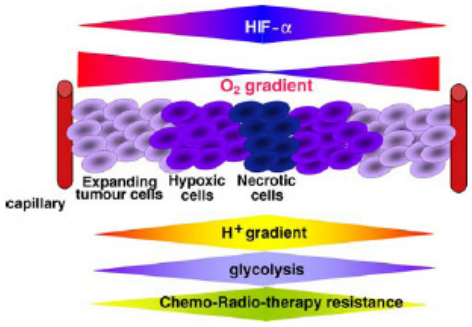

Figure 3: Characteristics of a hypoxic tumor. In tumors, there are expanding tumor cells in proximity to capillaries and a central region of necrotic cells. This gradient of cell viability parallels that of a decreasing gradient of oxygen. This is accompanied by an increase of HIF-1α, a decrease of the extracellular pH and an increase in the resistance of radio and chemotherapies (Brahimi-Horn et al., 2007).

On the contrary, acute hypoxia is a consequence of transient limitations in blood perfusion caused by vasomotor activity of feeding tumor arterioles, mechanical compression of tumor microvessels by proliferating cells, intravessel stasis or vessel obstruction. Tumor blood vessels present structural and functional abnormalities

(Rofstad et al., 2010; Dewhirst, 2009; Vaupel and Harrison, 2004). These vessels can present elongated or tortuous shape and even an incomplete endothelial lining (Vaupel and Harrison, 2004). In other words, blood vessels do exist in tumors but can be either structurally or functionally abnormal (Semenza, 2008).

Finally, a third form of hypoxia named longitudinal hypoxia can be described: it corresponds to the progressive decrease in oxygen availability from red blood cells along with the perfusing vascular tree inside the tumor.

Hypoxia induces changes in gene expression and promotes genomic instability and thereby may favor survival or anti-apoptotic pathways (Barnhart and Simon, 2007). It can for instance promote tumor progression by enabling cells to adapt to nutritive deprivation (Vaupel and Harrison, 2004). Moreover, hypoxia *per se* can lead to cell-cycle arrest, differentiation or cell death (Figure 4).

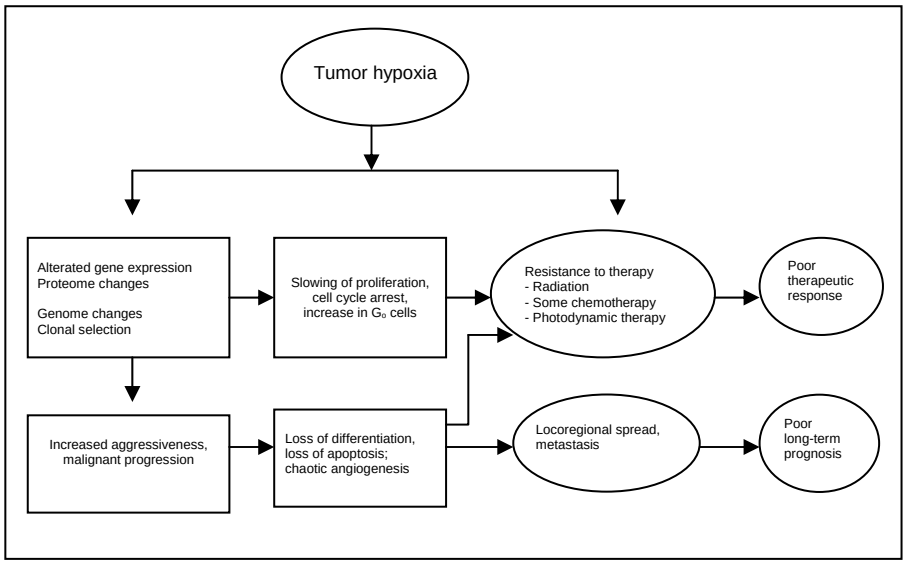

Figure 4: Schematic representation of the consequences of tumor hypoxia. Hypoxia accounts for genomic, transcriptomic and proteomic alterations, associated with limited tumor response and poor long-term prognosis. In particular, hypoxia drives malignant progression through loss of differentiation and apoptosis but also resistance to anticancer therapies (Vaupel and Harrison, 2004).

1.2.2. HIF-1

Hypoxia Inducible Factor-1 (HIF-1) is a transcription factor comprising two subunits: HIF-1α and HIF-1β. These two proteins are able to heterodimerize in the nucleus and bind to promoter regions of numerous genes involved in angiogenesis, metabolic adaptation, resistance to oxidative stress and invasiveness (Dewhirst, 2009). HIF-1β is constitutively expressed whereas HIF-1α is regulated by the oxygen concentration. Indeed, HIF-1α can be hydroxylated on two proline residues. This hydroxylation is required for the binding of the von Hippel-Lindau (VHL) tumor suppressor protein. This will lead to ubiquitination and final proteasome degradation (Semenza, 2008; Semenza, 2002). Under hypoxic conditions, hydroxylation is reduced and HIF-1α can accumulate and will thus dimerize with HIF-1β (Figure 5).

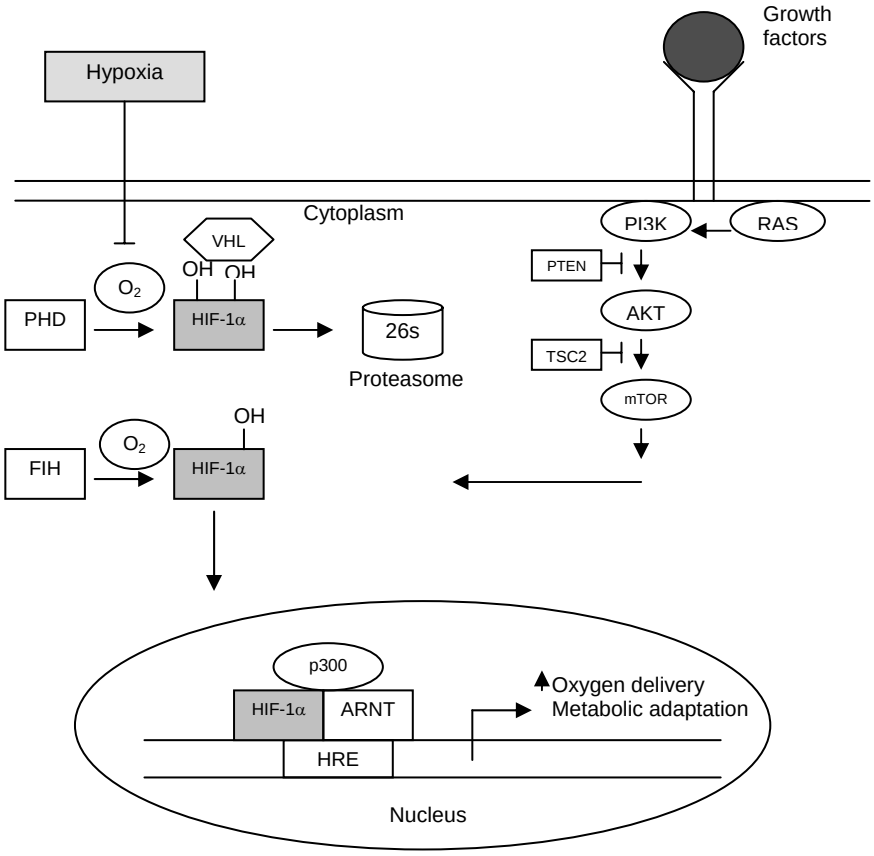

Figure 5: Mechanisms of HIF activation in cancer. Low oxygen tension inhibits the activity of prolyl-4-hydroxylase domain (PHD) and factor inhibiting HIF-1 (FIH-1). Under normoxic conditions, PHD enzymes utilize oxygen as a substrate to hydroxylate key proline residues located within the HIF-*α*- ODD domain. This hydroxylation event mediates Von Hippel Lindau (pVHL) binding and subsequent ubiquitination and degradation by the 26S proteasome. Under hypoxia or loss of pVHL, HIF-*α* is stabilized and translocates to the nucleus where it heterodimerizes with aryl hydrocarbon receptor nuclear translocator (ARNT) and binds to hypoxia responsive elements (HREs). The HIF heterodimer further activates gene expression at these sites upon cofactor (p300) recruitment. The interaction between HIF and p300 is regulated in an oxygen-dependent manner by FIH. HIF activity can also be induced in tumor cells through activation of the phospho-inositol-3 kinase (PI3K)/Akt-signaling pathway. PTEN: phosphatase and tensin homolog, mTOR: mammalian target of rapamycin, TSC2: tumor suppressor complex 2, RAS: Rat Sarcoma virus (Rankin and Giaccia, 2008).

Hypoxia, via HIF-1, induces transcriptional modifications of numerous genes involved in different events in tumor biology (Figure 6):

- Angiogenesis: HIF-1 induces the expression of VEGF-A, VEGF receptors 1 et 2, plasminogen activator inhibitor, angiopoietin 2 (Brahimi-Horn et al., 2007; Rankin and Giaccia, 2008).
- Cell survival or cell death: hypoxia can induce an adaptive response in tumor cells and favors the survival and the proliferation of these cells. Under severe conditions of hypoxia however, HIF-1 can also lead to cell death. The typical necrotic region observed in many solid tumors illustrates the hypoxia-induced cell death (Brahimi-Horn et al., 2007).
- Metabolism: cancer cells shift glucose metabolism from oxidative to glycolytic pathways (Brahimi-Horn et al., 2007; Rankin and Giaccia, 2008). This is known as the Warburg effect that involves an increased lactate production, even in the presence of oxygen. HIF-1 regulates genes implicated in glucose-to-lactate metabolism (glucose transporters, glycolytic enzymes, lactate dehydrogenase).
- Metastasis: HIF-1 activation is associated with metastasis development. It influences some crucial factors in the metastasis take, including E-cadherin, lysyl oxidase, CXCR4 and stromal cell-derived factor (SDF-1) (Rankin and Giaccia, 2008). Hypoxia is also known to favor metastatic spread (Barnhart and Simon, 2007; Christofori, 2006) by exerting a selection pressure on the tumor cell population (Erler and Weaver, 2009). Hypoxia can promote a decrease in E-Cadherin, known to be involved in the epithelial-to-mesenchymal transition, that further increases tumor cell motility (Barnhart and Simon, 2007).
- Finally, hypoxia has been associated to chemoresistance and radioresistance in different studies (Rankin and Giaccia, 2008; Semenza, 2002; Vaupel and Harrison, 2004; Brahimi-Horn et al., 2007).

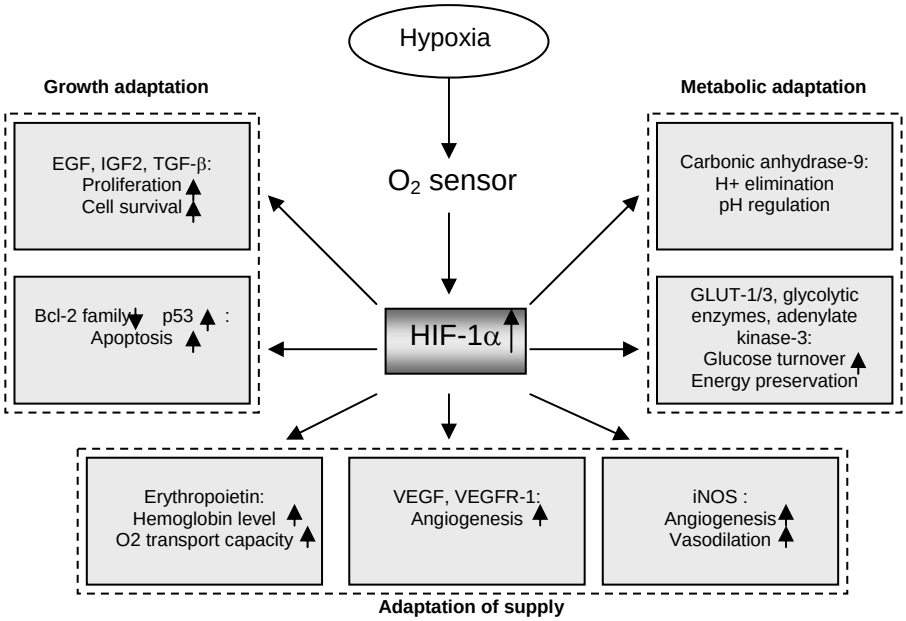

Figure 6: Schematic representation of the role of HIF-1α in human cancers. HIF-1-regulated gene products may play major roles in tumor progression, aggressiveness and metabolic adaptation. It may contribute to increased resistance of hypoxic tumors to radiotherapy and chemotherapy. EGF: Epidermal growth factor, IGF2: Insulin-like growth factor-2, Bcl-2: B-cell lymphoma 2, iNOS: inducible NO synthase (Vaupel and Harrison, 2004).

It has been shown that tumor cells but also endothelial cells subjected to cyclic hypoxia accumulate HIF-1α to a larger extent than the level reached during prolonged hypoxia. We have documented that endothelial cells exposed to cyclic hypoxia were more prone to migrate and form tubes *in vitro* and more radioresistant compared with normally oxygenated or chronically hypoxic cells (Martinive et al., 2006; Martinive et al., 2009).

1.3 Angiogenesis

Once a tumor mass reaches a critical size, tumor cells located too far from blood vessels lack an appropriate supply in oxygen and nutrients. Tumor cells are able to overcome this privation by inducing the formation of new blood vessels by angiogenesis and vasculogenesis (Dome et al., 2009) (Figure 7). Judah Folkman hypothesized more than 30 years ago that the neovasculature plays an important role in tumor progression (Folkman, 1971; Dome et al., 2009).

Tumor angiogenesis can be defined as the sprouting of new blood vessels from pre-existing vessels (Patenaude et al., 2010). This is different from vasculogenesis which can be defined as the *de novo* formation of blood vessels from endothelial progenitors (Patenaude et al., 2010; Eguchi et al., 2007).

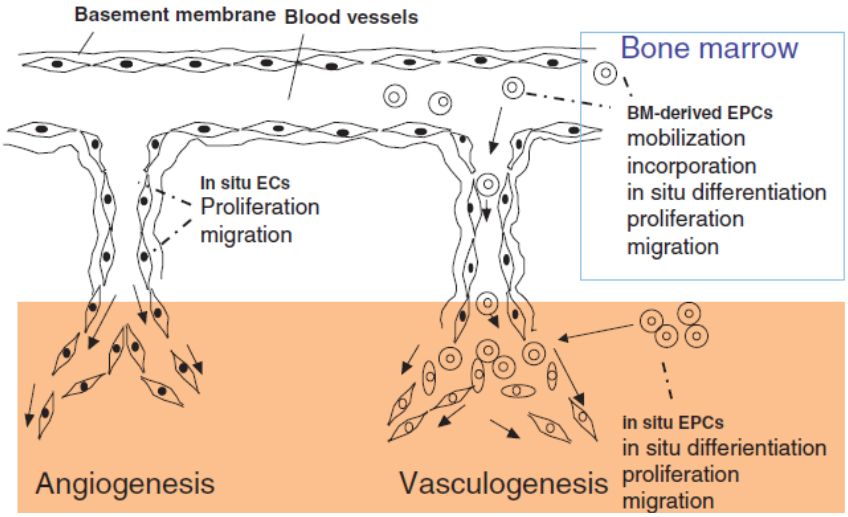

Figure 7: The two ways of tumor neovascularization : angiogenesis and vasculogenesis. Angiogenesis and vasculogenesis are driven by endothelial cells and endothelial progenitor cells, respectively. Angiogenesis consists in the formation of new blood vessels from pre-existing vessels whereas vasculogenesis implies the formation of new blood vessels from bone marrow-derived progenitor cells. EC: endothelial cells, EPC: endothelial progenitor cells (Eguchi et al., 2007).

While a tumor is progressing, the stroma reacts through the formation of a tumor-associated vasculature. The angiogenic process begins with the production of pro-angiogenic factors, such as VEGF, FGF, TNFα and interleukins, by both cancer

cells and stromal cells (Francavilla et al., 2009). The new forming vessels promote tumor growth because it allows an access to nutrients and oxygen. It also facilitates tumor cell entry into the circulation (Lorusso and Ruegg, 2008). Angiogenesis is initiated in a process called 'the angiogenic switch' (Baeriswyl and Christofori, 2009), which occurs when the balance between activators and inhibitors of angiogenesis is in favor of the formation of new blood vessels (De and Naldini, 2006).

To form new vessels, different events have to happen successively (Figure 8). Endothelial cells have first to exit dormancy. Then, they need to proliferate, migrate, differentiate, polarize and finally organize themselves into new vessels (Lorusso and Ruegg, 2008; Francavilla et al., 2009).

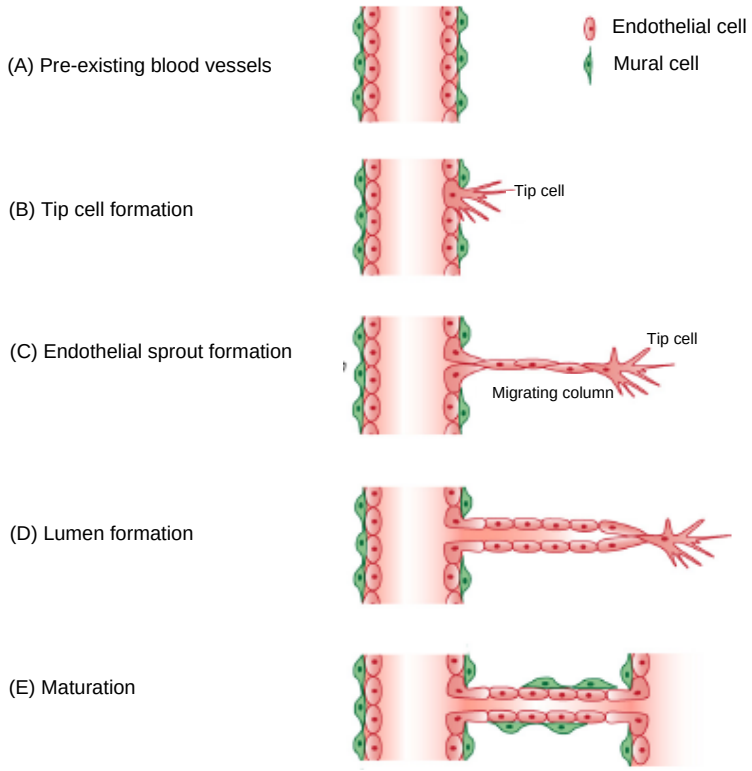

Figure 8: Schematic representation of angiogenesis. It starts from a pre-existing vessel (A), with the conversion of a previously quiescent endothelial cell into a tip cell (B). This induces a migrating column, formed by proliferating endothelial cells (C). During endothelial sprouting, the vascular lumen is formed (D). Finally, upon formation of the new vessel, it undergoes stabilization and maturation, a process mainly mediated by intercellular adhesion and mural cell coverage (E) (Francavilla et al., 2009)**.**

1.4 Vasculogenesis

1.4.1 Endothelial progenitor cells

Vasculogenesis is the second mechanism by which a tumor may develop its vasculature in order to get sufficient supply in oxygen and nutrients. It was first thought to only occur in the embryo (Larrivee and Karsan, 2007; Luttun et al., 2002). Different studies however showed that this phenomenon could happen in adults. The first study suggesting the existence of adult endothelial progenitor cells (EPC) was published in 1997 (Asahara et al., 1997). The EPC are commonly defined as the precursor cells that are recruited from the bone marrow to be integrated into nascent vessels at tumor sites and to differentiate into mature endothelial cells (Kassmeyer et al., 2009; Seandel et al., 2008; De and Naldini, 2006; Nolan et al., 2007). Under steady-state conditions, EPC contribute to a reservoir which can be mobilized in response to a vascular trauma (Larrivee and Karsan, 2007). These cells contribute to vasculogenesis during wound healing, ischemia, postmyocardial infarction, endothelialization of vascular grafts and development of tumor vasculature (Eguchi et al., 2007).

Besides acting as direct precursors of endothelial cells, progenitor cells also induced the secretion of pro-angiogenic cytokines that can improve neovascularization (Patenaude et al., 2010; Gao et al., 2009; Ahn and Brown, 2009; Gao et al., 2009; Dome et al., 2009). EPC may thus have both structural and paracrine roles in the formation of new blood vessels.

The EPC can originate from at least three potential cell types: hemangioblasts, myeloid cells and bone marrow-derived mesenchymal stem cells (Miller-Kasprzak and Jagodzinski, 2007; Asahara and Kawamoto, 2004) (Figure 9).

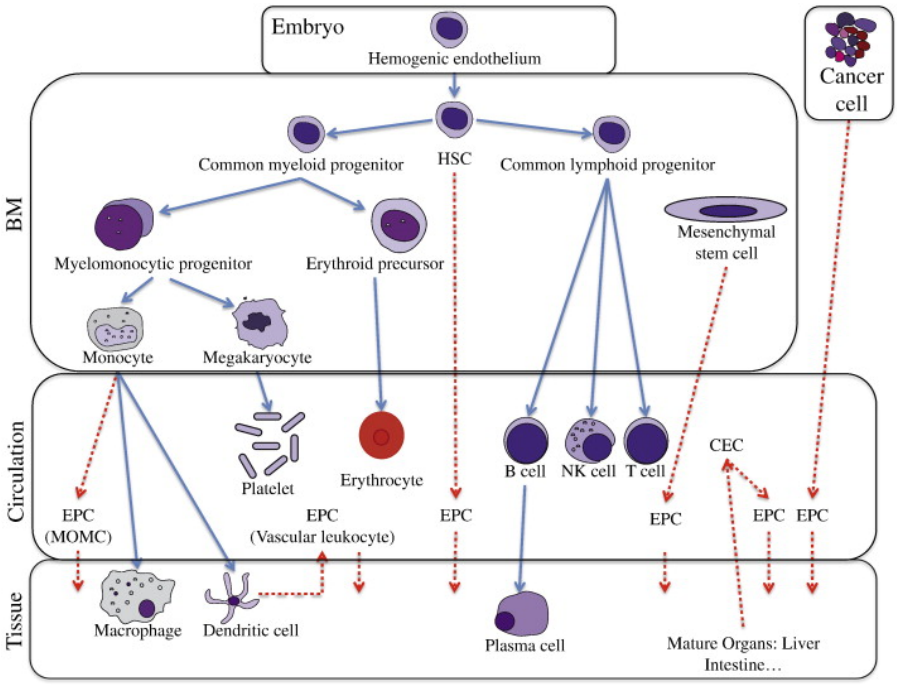

Figure 9: Different origins of the endothelial progenitor cells (EPC). Hemogenic endothelium gives rise to hematopoietic stem cells (HSC) during embryonic development. At the adult stage, bone marrow is responsible for the maintenance of the HSC pool, and gives rise to cells which undergo differentiation into myeloid and lymphoid cell lineages. EPC have been suggested to arise from HSC or progeny cells such as monocytes and dendritic cells referred to as monocyte-derived multipotential progenitor cells (MOMCs) and vascular leukocytes, respectively. Mesenchymal stem cells are recruited to the tumors and can differentiate into endothelial cells. Circulating endothelial cells (CEC) from organs such as liver and intestine are also suggested to be a potential source of EPC. Cancer stem cells have been suggested to differentiate into blood vessel structures that express endothelial cell molecular characteristics in tumors (Patenaude et al., 2010).

1.4.2 Contribution of EPC to vasculogenesis

The first step in the incorporation of EPC into nascent vessels is the mobilization from the bone marrow, depending of the local microenvironment (Figure 10). The release of EPC from the bone marrow is determined by various growth factors, enzymes, ligands and surface receptors (Hristov et al., 2003; Kaplan et al., 2006a). The activation of proteases such as MMP and more especially MMP-9, leads to the cleavage of EPC from stromal cells (Urbich and Dimmeler, 2004; Miller-Kasprzak and Jagodzinski, 2007; Hristov et al., 2003). MMP-9 releases soluble kit-ligand, which induces the mobility of progenitor cells and their mobilization into the

circulation (Chavakis et al., 2008; Miller-Kasprzak and Jagodzinski, 2007; Jodele et al., 2005; Gao and Mittal, 2009).

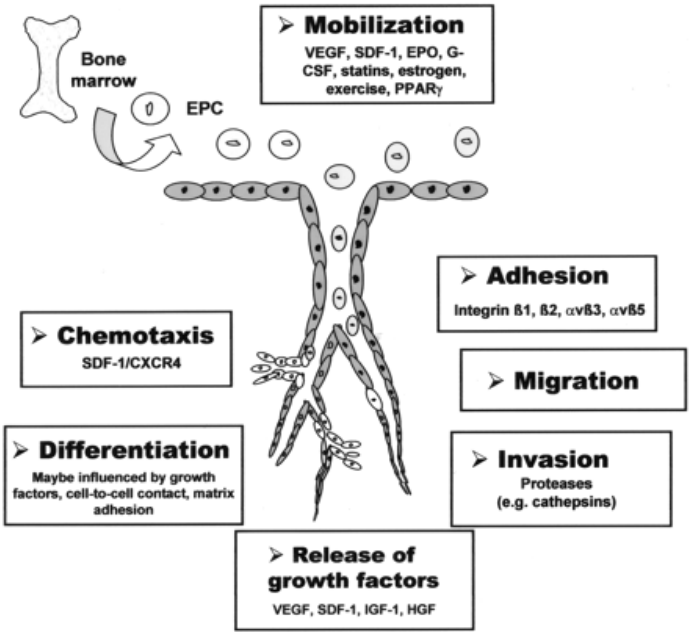

Figure 10: Different components of the vasculogenic process. Recruitment and incorporation of EPC into ischemic tissue require a coordinated multistep process including mobilization, chemoattraction, adhesion, transmigration, migration, tissue invasion, and in situ differentiation. Factors that are proposed to regulate the distinct steps are indicated. SDF-1: Stromal cell-derived factor 1, EPO: erythropoietin, G-CSF: Granulocyte colony-stimulating factor, PPAR: Peroxisome proliferator-activated receptors, CXCR4: C-X-C chemokine receptor type 4, IGF-1: Insulin-like growth factor, HGF: Hepatocyte growth factor (Urbich and Dimmeler, 2004).

The recruitment of circulating EPC to sites of neoangiogenesis is triggered by angiogenic growth factors or chemokines, such as VEGF, erythropoietin, granulocyte-macrophage colony-stimulating factor (GM-CSF) and SDF-1 (Ribatti, 2007; Dome et al., 2009; Eguchi et al., 2007; Asahara and Kawamoto, 2004; Sbaa et al., 2006).

EPC need then to arrest within tumor microvessels, extravasate into the interstitium and finally incorporate into the new forming vessels (Urbich and Dimmeler, 2004; Chavakis et al., 2008). The adhesion of EPC to endothelial cells is mediated by proteins involved in adhesion, namely the integrins. These proteins are glycosylated

heterodimeric proteins expressed on cell surface, mediating the adhesion of cells to ECM and to other cells. Integrins mediate cell-cell interactions mostly via the β-integrins and in particular the α4β1 integrin (Urbich and Dimmeler, 2004; Chavakis et al., 2008). The final step is the maturation and differentiation of the progenitor cells into mature endothelial cells.

1.4.3 Controversy about EPC contribution to vasculogenesis

In the recent years, the great enthusiasm in studying the role of progenitor cells in the cancer field has given place to controversy (Gao et al., 2009; De and Naldini, 2006; Shaked and Voest, 2009). Indeed, there is a lack of specific markers to identify very precisely the EPC (Dome et al., 2009; Timmermans et al., 2009). In fact, there is no clear phenotype of EPC and some common markers of these cells are also shared by hematopoietic or mature endothelial cells (Patenaude et al., 2010). The classical phenotype based on membrane markers for EPC are in mouse Sca^{+} - c-kit^{+} - Lin^{-} - $VEGFR1^{+}$ and in human $CD34^{+}$ - c-kit^{low} - $CD133^{+}$ - $VEGFR1^{+}$ - $VEGFR2^{+}$ (Patenaude et al., 2010; Ribatti, 2007).

Another subject of controversy is the contribution of EPC to the tumor vasculature (Shaked and Voest, 2009) (Table 2). Initial studies documented an integration of these cells up to 50% in the tumor endothelium (Garcia-Barros et al., 2003; Patenaude et al., 2010; Hilbe et al., 2004; Shaked et al., 2006; Kerbel et al., 2008). However, more recent studies suggested a reduced or inexistent integration of EPC in the nascent vessels (Larrivee et al., 2005; Rajantie et al., 2004; Wickersheim et al., 2009; Ahn and Brown, 2009; Purhonen et al., 2008). Potential explanation to these discrepancies could be the tumor type, the tumor size at time of analysis, the site of implantation or the mouse genetic background (De and Naldini, 2006; Gao and Mittal, 2009).

Table 2: Summary of studies showing the extent of EPC incorporation to the tumor vasculature (Ahn and Brown, 2009).

EPC incorporation (%)	Type of tumor	Refs
<0,01	B16 melanoma	(Purhonen et al., 2008)
<0,01	B16 melanoma	(Ahn and Brown, 2009)
80-100	lymphoma	(Lyden et al., 2001)
<0,01	lymphoma	(Gothert et al., 2004)
<0,01	Lewis Lung carcinoma	(Gothert et al., 2004)
<0,01	Lewis Lung carcinoma	(Ahn and Brown, 2009)
0,01-0,15	Lewis Lung carcinoma	(Shaked et al., 2008)
1-2	Lewis Lung carcinoma	(Shinde Patil et al., 2005)
50-100	Lewis Lung carcinoma	(Lyden et al., 2001)
50	MCA/129 fibrosarcoma	(Garcia-Barros et al., 2003)
7-10	MMTV-PyMT spontaneous mammary carcinoma	(Nolan et al., 2007)
2,5-3,5	MT1A2 mouse mammary carcinoma	(Ahn and Brown, 2009)
7-10	Namalwa lymphoma	(Capillo et al., 2003)
10-25	Spontaneous tumor (NOD/SCID/b-glucuronidase -/-)	(Li et al., 2006a)
0,5	TG1-1 mouse mammary carcinoma	(Suriano et al., 2008)
<0,01	TG1-1 mouse mammary carcinoma	(Ahn and Brown, 2009)

1.5 Invasiveness

The development of metastases accounts for 90% of deaths related to cancer (Yilmaz et al., 2007; Woodhouse et al., 1997; Gupta and Massague, 2006; Kopfstein and Christofori, 2006; Fokas et al., 2007). Strikingly, the metastasis process is very inefficient, with less than 0,1% of circulating tumor cells able to generate metastases (Bidard et al., 2008; Kaplan et al., 2006a). Millions cells are however thought to be released by a tumor into the circulation every day (Gupta and Massague, 2006).

Metastasis can be defined as the spread of tumor cells to areas not directly adjacent to the primary tumor. Such spread can occur by invasion of blood or lymph vessels, or by penetration of cancer cells into cavities surrounding organs (Oppenheimer, 2006).

The tumor cells are able to invade the surrounding tissues because they influence their environment and secrete various factors that allow them to disseminate. Tumor cells have actually to go through different steps to form metastases (Figure 11): (i) they have to be released from the tumor mass and to migrate through the ECM, (ii) they next enter the blood flow (“intravasation”) where they have to survive to mechanic stress, (iii) then they arrest, adhere and extravasate and (iv) finally, they have to migrate through their new environment and to develop into growing metastases via activation of angiogenesis and recruitment of different cell types.

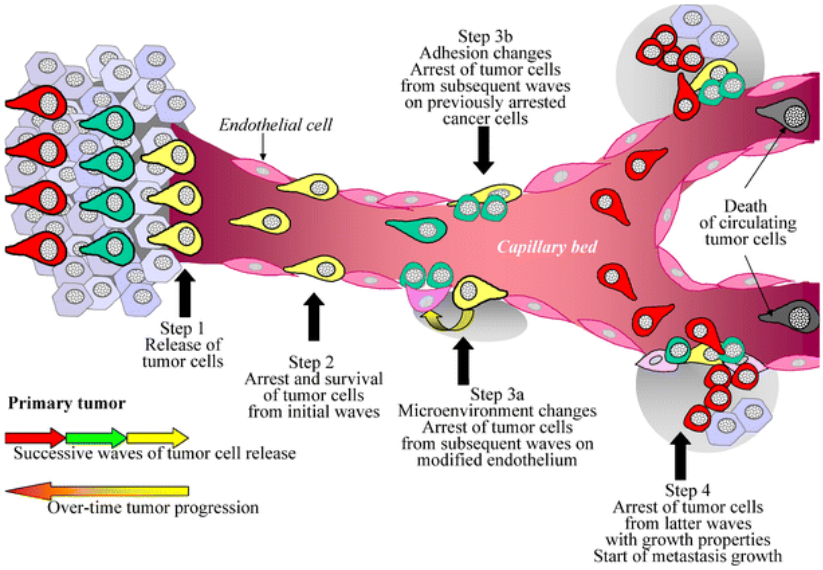

Figure 11: Schematic view of metastasis development. Possible cooperation between successive waves of circulating cancer cells. Tumors are known to release many tumor cells in the circulation each day. The first released malignant cells are able to arrest and survive. They induce changes in the microenvironment where they stopped. Subsequent waves of tumor cells can therefore arrest on this modified endothelium or on other cancer cells. When latter waves of tumor cells, presenting growth properties, finally arrest, they are able to induce the start of the metastasis growth (Bidard et al., 2008).

1.5.1 Invasion and migration of tumor cells: contribution of the EMT

The first event at the beginning of the metastasis process is the invasion of the surrounding tissues and the migration through the ECM. These two processes are coordinated and require morphologic modifications of the cancer cells. Pseudopodia are formed at the leading edge, and ECM proteases are released at the invasive front, thereby influencing cell adhesion and cellular movement (Bidard et al., 2008; Oppenheimer, 2006; Kumar and Weaver, 2009). The typical features required for these steps are obtained thanks to the epithelial-to-mesenchymal transition (EMT) (Scheel et al., 2007; Christofori, 2006). EMT can be induced by oncogenic events in tumor cells and secreted growth factors like TGF-β and FGF-2 (Kopfstein and Christofori, 2006). The EMT is characterized by loss of cell polarity and downregulation of epithelial proteins, like E-cadherin (Geiger and Peeper, 2009; Prindull, 2005; Kopfstein and Christofori, 2006) (Figure 12). The loss of E-cadherin disrupts adhesion junctions between neighboring cells, leading to detachment of

tumor cells from epithelial cell layer (Kopfstein and Christofori, 2006). The cells acquire a spindle-shaped morphology. The EMT enhances cell migration and induces mesenchymal proteins like N-cadherin or vimentin (Geiger and Peeper, 2009; Kalluri and Weinberg, 2009). Thus, the EMT favors (i) tumor cell invasion via the loss of E-cadherin, (ii) the expression of MMP to remodel the ECM, (iii) the overexpression of proteins promoting invasive and metastatic processes such as N-cadherin. Some of the EMT mediators also inhibit apoptosis of tumor cells (Geiger and Peeper, 2009).

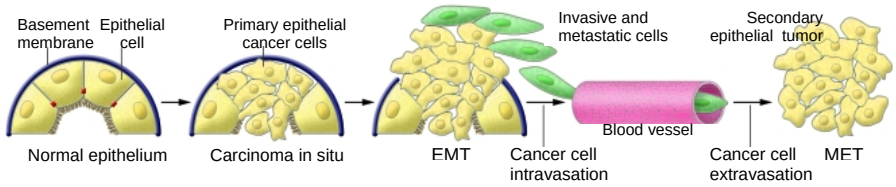

Figure 12: General description of the EMT process. Progression from normal epithelium to invasive carcinoma goes through several stages. Epithelial cells loose their polarity and detach from the basement membrane for cells to become invasive and metastatic. The next step involves EMT and an angiogenic switch. Progression from this stage to metastatic cancer also involves EMTs, enabling cancer cells to enter the circulation and exit the blood stream at a remote site, where they may form micro- and macro-metastases, which may involve METs and thus a reversion to an epithelial phenotype. EMT: epithelial-to-mesenchymal transition, MET: mesenchymal-to-epithelial transition (Kalluri and Weinberg, 2009).

Tumor cells have to be able to form transient attachment for metastasizing. They have to attach to the ECM or to other cells. Integrins are proteins highly involved in the attachment of tumor cells to the ECM. They provide the essential link between the actin cytoskeleton and the ECM during cell migration (Kopfstein and Christofori, 2006). They are involved in a large variety of signalling pathways (Woodhouse et al., 1997; Gupta and Massague, 2006), supporting various key cellular functions such as proliferation, survival, polarity, motility and differentiation (Kopfstein and Christofori, 2006; Christofori, 2006).

1.5.2 The premetastatic niches

Circulating cancer cells are released into the blood flow. But only 0,1% of these cells will generate micrometastases. This is called the metastasis inefficiency. Indeed, metastatic cells leaving the primary tumor have to survive in different hostile environments. Tumor cells must resist to anoikis (programmed cell death associated with loss of cellular contacts), evade from immune recognition and survive to physical shear stress of the circulatory system (Mendoza and Khanna, 2009).

In 1889, Stephan Paget proposed “the seed and soil theory”. He observed that the site for a secondary tumor is made not only by the tumor cells (the seed) but it is also largely influenced by the nature of the target organs (the soil) (Geiger and Peeper, 2009; Fidler, 2003; Paget, 1989). Indeed, the local microenvironment of these organs must be conducive for disseminating tumor cells (Psaila and Lyden, 2009). The secondary tumor will be able to grow only if the microenvironment of the target site is compatible with the circulating tumor cells.

In 1929, Ewing challenged this seed and soil theory, proposing that metastatic development occured by mechanical factors resulting from the anatomical structure of the vascular system (Fidler, 2003; Ribatti et al., 2006). Since a few years, Paget’s theory has come back to light and different groups are now working on how the seed may prepare the soil to allow metastases formation.

The tropism of metastatic cells for specific organs is mediated by chemokines. The local expression of these chemoattractants might guide cognate chemokine receptor-expressing tumor cells to specific destinations, as a result of locally induced chemotaxis and invasion of tumor cells (Joyce and Pollard, 2009).

In 2005, Kaplan et al. published a study supporting the concept of premetastatic niches (Kaplan et al., 2005; Kaplan et al., 2006a), further sustained by Hiratsuka’s publication (Hiratsuka et al., 2006). This work suggested that tumor cells do not solely dictate their own fate but that formation of a hospitable environment is

essential to enable disseminating tumor cells to develop into a secondary tumor (Psaila and Lyden, 2009; Mendoza and Khanna, 2009). In their original study, Kaplan and colleagues showed that after primary tumor implantation in mice but before the metastatic spreading of tumor cells in the lungs, the formation of clusters of BMDC near bronchioles and alveoli was documented (Figure 13). These specific clusters of BMDC were composed of cells expressing VEGFR1, CD133, CD34 and c-kit. Later on, BMDC-expressing VEGFR2 were shown to arrive at the site of the premetastatic niches to allow the passage from micro to macrometastases.

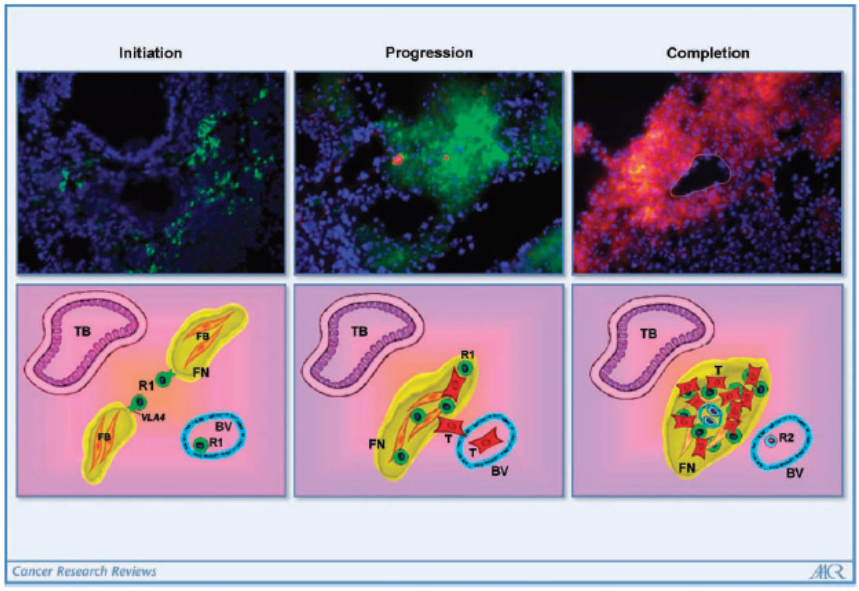

Figure 13: General description of the premetastatic niches. *Initiation:* Hematopoietic progenitor cells (HPC) (in green) form cellular clusters in the lung before tumor cell (in red) arrival. *Progression*, migrating tumor cells adhere and grow specifically at these sites. *Completion*, angiogenic elements, such as VEGFR2$^+$ EPC, are required for completion of the vascularized *Circular outline*, blood vessel within the metastatic tumor. *Bottom row*, a schematic of the metastatic process. There is up-regulation of fibronectin by activated fibroblasts followed by attachment of VLA4$^+$ VEGFR1$^+$ HPC. These cells form clusters that initiate microenvironmental changes necessary for future metastasis. Adhesion and proliferation of tumor cells occur at sites of VEGFR1$^+$ cellular clusters. Influx of endothelial progenitor cells form vasculature to make a mature metastatic lesion. *R1*, VEGFR1$^+$ HPC (*green*); *R2*, VEGFR2$^+$ CEP (*blue*); *T*, tumor (*red*); *yellow*, fibronectin (*FN*); *orange*, fibroblasts (*FB*); *TB*, terminal bronchiole; *BV*, bronchiole vein. (Kaplan et al., 2006b).

The critical roles of VEGFR1 and VEGFR2 in the formation of metastases were confirmed in consecutive studies (Kaplan et al., 2005; Joyce and Pollard, 2009; Kaplan et al., 2006a). Indeed, treatment with monoclonal antibodies against

VEGFR1 was shown to inhibit the initiation of the clusters and to prevent metastasis formation. With anti-VEGFR2 antibodies, the treatment did not inhibit the formation of the clusters but limited metastatic progression.

Kaplan and collaborators also showed that before the recruitment of the BMDC in peripheral tissues, an upregulation of fibronectin expression was observed (Kaplan et al., 2005; Joyce and Pollard, 2009; Kaplan et al., 2006b). This fibronectin expression was also documented after exposure to tumor conditioned media. The injection of tumor conditioned media was documented to modulate the metastasis patterns. Animals were injected with Lewis Lung carcinoma cells (LLc), known to metastasize preferentially to the lungs and the liver or melanoma cells (B16), known to metastasize in a widely disseminated way. Kaplan and colleagues showed that when injecting B16 conditioned media before and after injection of LLc, the mice presented the pattern of metastasis typical for melanoma and not for LLc, showing that chemokines and/or cytokines present in the conditioned media could drive the metastatic fate of tumor cells (Kaplan et al., 2005; Geiger and Peeper, 2009; Oppenheimer, 2006; Kaplan et al., 2006a; Kaplan et al., 2006b).

Deposition of fibronectin was also documented by Erler and colleagues. They found that lysyl oxidase (LOX) co-localized with fibronectin at sites of distant metastases, increasing the further adherence of myeloid cells (Erler et al., 2006). This protein was documented as necessary for hypoxia-dependent metastasis development (Erler and Giaccia, 2006) and in particular, in the recruitment of BMDC into the premetastatic niches (Erler et al., 2009).

In addition, growing evidence indicate that among the BMDC, a particular subset of cells, the MDSC, could be at the origin of the premetastatic niches (Peinado et al., 2011). These cells are derived from myeloid lineage which can give rise to either granulocytes, dendritic cells or macrophages (Ye et al., 2010). MDSC are known to suppress antigen-specific T-cell response. They are recruited, especially via BV8 (Shojaei et al., 2007), and infiltrated in primary tumors and are able to differentiate into tumor-infiltrating macrophages (Sica and Bronte, 2007). They play an important role in tumor angiogenesis but also in metastases development (Ye et al., 2010).

MDSC infiltrate the pre-invasive lesions of cancer whereas effectors T-cells are largely absent (Clark et al., 2007; Yang et al., 2008). They were shown to secrete S100A8 and S100A9 in premetastatic lesions (Hiratsuka et al., 2006). These two proteins were also identified by Rafii and Lyden as chemoattractants for the premetastatic niche formation (Rafii and Lyden, 2006).

2. Cancer in post-genomic era

2.1 Cancer proteomics

High-throughput technologies are now providing new methods to identify biochemical determinants of a disease process (Koomen et al., 2008) through a better understanding of molecular pathways that control growth, differentiation and death of cells (Bitarte et al., 2007). In particular, the future of medicine looks towards mechanistic personalized therapeutic approaches.

Since the human genome has been sequenced, scientists are confronted with the daunting task of explaining the myriad of physiological and pathological functions of a highly complex and adaptable organism by 40 000 genes (Kolch et al., 2005; Koomen et al., 2008). Furthermore, technologies available to date such as microarrays that can identify large numbers of differentially expressed genes fail to take into account the multiple protein products of these genes and their functional significance (Verrills, 2006). Scientists are therefore now logically considering proteomics instead of (or besides) genomics. Genomic changes are relatively static, whereas the proteome is dynamic. It reflects physiological and pathological changes much more acutely and accurately (Kolch et al., 2005; Hanash and Beretta, 2002). In addition, from a therapeutic perspective, the majority of drug targets are proteins and not nucleic acids.

Cancer is commonly described as a genetic disease. Tumorigenesis is a multistep process involving mutations and other genetic events leading to oncogenic gain-of-function and/or deficiency in tumor suppressor gene activity (Alaiya et al., 2000). A gene alone, however, represents only potential information that must be translated into a functional form. A gene is transcribed into mRNA, then translated into protein, which is the final manifestation of the genetic information (Posadas et al., 2005). The tumor phenotype is therefore the result of the many alterations or modifications, occurring at the transcriptional, but also translational and post-translational levels (Posadas et al., 2005; Jain, 2004).

The term proteome was first defined in 1994 and denotes the entirety of proteins expressed by the genome (Habermann et al., 2008; Ullah and Aatif, 2009). The term proteomics has been defined as the study of protein properties on a large-scale that results in a global, integrated view of physiological or disease processes (Poon and Johnson, 2001). In particular, the inherently dynamic nature of the proteome requires to closely monitor changes in the state of a cell, tissue or organism over time (Kolch et al., 2005). Most applications in proteomics are used to determine expression profiles of proteins in cells and tissues in normal or disease states (Bitarte et al., 2007), integrating sequence variations and isoforms, post-translational modifications and protein-protein complexes (Koomen et al., 2008). Because proteins are the acting macromolecules in cells, they are the main candidates for disease targets. Proteomic analysis therefore constitutes a suitable, valuable and powerful tool for studying human diseases. It can be employed as prognostic and diagnostic markers as well as therapeutic targets for the treatment of patients (Seliger and Kellner, 2002; Celis and Moreira, 2010).

In cancer, initial genomic studies focused on changes in global expression levels, using microarrays or serial analysis of gene expression (McHugh et al., 2009). Nowadays proteomics encompasses evaluation of protein expression, activation, modification and degradation, and ambitiously targets protein function (Cho, 2007). The human proteome, due to the variety of post-translational permutations that result in large numbers of isoforms, is actually much more complex than the genome (Bitarte et al., 2007; Cho, 2007; Cho, 2007). Using proteomics-based approach, protein-protein interactions that drive biological processes can be characterized as a fluctuating minute-to-minute information flow within the cell and throughout the organism. The protein pathways in cancer are not confined to the tumor cell but extend to the tumor-host interface and surrounding stromal and vascular compartments (Petricoin and Liotta, 2004).

Survival rates for patients with the most common cancers, especially if detected at an advanced stage remain discouragingly low (Dalton and Friend, 2006). Cancer therapies are still essentially “one size fits all”, meaning that all patients within a

given diagnostic category (typically based on tumor type and stage of disease) receive the same treatment despite the biological heterogeneity known to exist from patient to patient (Dalton and Friend, 2006; Smith et al., 2006). There is therefore a crucial need for early diagnosis or individualized treatment for cancer patients (Koomen et al., 2008).

Bringing such technologies into clinics however present important challenges: stringent requirements for sample collection and preparation, use of limited biological starting material, requirements for potential purification strategies to enrich samples and finally high costs for equipment and staffing in clinics (Koomen et al., 2008; Joshi et al., 2011). Some critical steps for proteome analyses should be taken into account to become achievable: (i) a standard operation procedure for sample preparation, (ii) the reproducibility of the analytical method, (iii) the detection of low-abundant proteins, (iv) the biochemical analysis of proteins of interest, (v) the evaluation of the functional properties of the identified proteins and their clinical relevance (Seliger and Kellner, 2002).

Today, one classical method for resolving proteins from complex mixtures like cells or tissues is two-dimensional electrophoresis. It unravels complex networks of protein interactions (Jungblut et al., 1999). The basic analysis includes subtractive analyses comparing diseases with controls, in order to unravel disease-associated proteins (Figure 14).

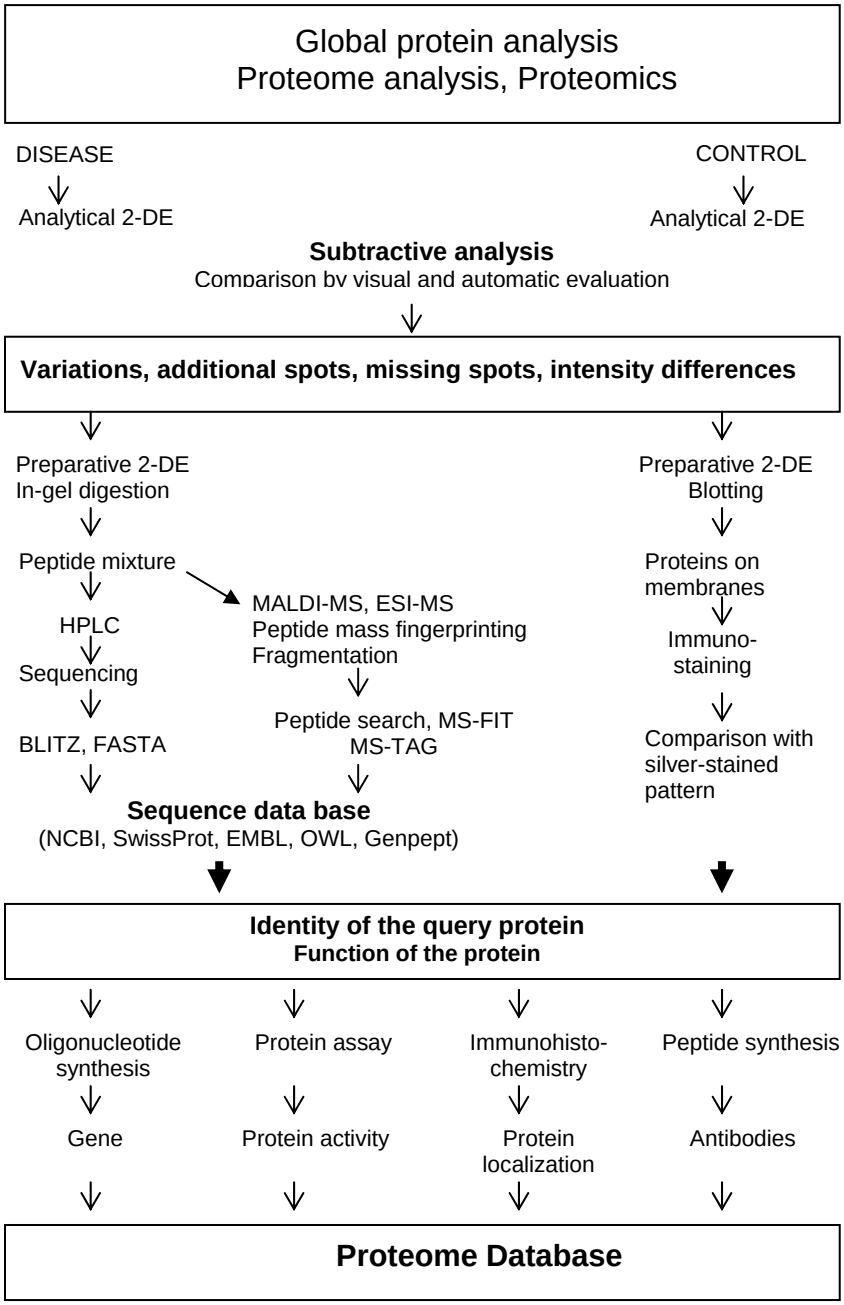

Figure 14: Global scheme of a proteomic-based approach. Analytical gels are firstly performed. After data analysis via subtractive comparisons, preparative gels are prepared either to identify proteins of interest or to immunoblot the membranes. Once the proteins of interest are identified, validation and further studies are required, thereby contributing to the enrichment of the proteome database (Jungblut et al., 1999) .

2.2 Cancer biomarkers

2.2.1 The biomarker concept

It is commonly accepted that a cancer diagnosed at an early stage presents a better prognosis. In the recent years, considerable investment has therefore been made in the detection of cancers. More efficient screening programs and changes in clinical practice have progressively led to the diagnosis of an increasing number of early cancers detected as asymptomatic malignancies or in some instances even as premalignant lesions (Chatterjee and Zetter, 2005). An ideal tumor marker should actually be easily detectable in the patient's blood or urine, but absent in a healthy person (Chatterjee and Zetter, 2005), and should be 100% sensitive and 100% specific. Sensitivity refers to the percentage of individuals with disease who are marker-positive (validity of a positive result), whereas specificity refers to likelihood that a given marker will be altered only in individuals with the disease (validity of a negative result) (Chatterjee and Zetter, 2005).

Tumor biomarkers are produced by the tumor or the host system in response to tumor development, and provide the clinicians with the biological material to detect and classify cancers (Tainsky, 2009). The nature of biomarkers is broad. Because of the genetic nature of cancer, tumor biomarkers include cancer-specific mutations or changes in gene expression or promoter methylation. These nucleic acid-related biomarkers are usually identified after biopsies. However, since cancer cells shed DNA and RNA in the circulation, tumor-specific genetic changes can nowadays also be determined from plasma or other body fluids (Tainsky, 2009; Ullah and Aatif, 2009; Jain, 2008). Tumor-related abundant or variant proteins can be similarly identified from biopsies as well as from the circulation as free, shed proteins or as novel autoantibodies to such proteins (Tainsky, 2009).

Biomarker research focuses on two main areas: (i) the identification of markers that permit early detection of disease, better stratification and are of prognostic value, (ii) the identification of markers for the monitoring of response to therapy (Kolch et al., 2005). Thus, biomarkers are not only useful for diagnostic purpose but also improve

the effectiveness of clinical interventions. Both should ultimately translate to better survival (Tainsky, 2009; Cho, 2007). This need for biomarkers is yet more acute for people with a predicted risk because of the inherited germline mutations in DNA repair or cell cycle control genes. The medical surveillance of people positive for a mutation in a cancer predisposing gene may indeed greatly benefits from the availability of biomarkers reflecting the early progression of the disease (Tainsky, 2009).

Biomarker research is facing different challenges. Indeed, the biological variability of patients' samples makes it difficult to find strong and reliable biomarkers. The huge dynamic range of protein concentrations in tissues and body fluids is another problem. For example, in plasma, the dynamic range exceeds 10 orders of magnitude (Kolch et al., 2005; Cho, 2007; Verrills, 2006). Differences in sample collection, handling or storage, and profiling techniques, may also influence the protein profile obtained from a given sample (Cho, 2007). Finally, to be used in the clinical routine, assays have to be simple, robust, affordable and automated for high-throughput analysis (Kolch et al., 2005; Cho, 2007).

Nowadays, people are convinced that a single biomarker does not exist and could not be used to distinguish between healthy people and cancer patients because of the heterogeneity between cancers and cancer patients. Only the combination of several markers together with adapted statistical analysis may be clinically relevant. Association of several biomarkers has already revealed a good efficiency in term of sensitivity and specificity (Desmetz et al., 2009b; McHugh et al., 2009; Calvo et al., 2005; Tainsky, 2009).

2.2.2 Current clinical protein biomarkers

The first recognized test for a type of common cancer was reported in 1965 by Dr Gold. He found a substance in the blood of patients suffering from colon cancer that was normally found in foetal tissues and named it carcinoembryonic antigen CEA (Gold and Freedman, 1965b). Additional biomarkers developed in the 80s were CA

19-9 for colorectal and pancreatic cancer, CA 15-3 for breast cancer and CA-125 for ovarian cancer (Chatterjee and Zetter, 2005; Jain, 2004; Cho, 2007). These markers are unfortunately not specific for a single cancer.

The best-known biomarker currently used in clinics to detect early disease is the prostate-specific antigen PSA (Chatterjee and Zetter, 2005; Ullah and Aatif, 2009). PSA tests have been widely used in screening for prostate cancer. PSA screening may provide a suspicion of prostate cancer but a clinical diagnosis still needs pathological tissue examination. PSA elevation is also associated with benign prostatic hyperplasia. Therefore, many individuals undergo unnecessary biopsy. Serum PSA is in fact more reliable as a marker of prostate cancer recurrence or as an indicator of treatment efficacy. Its level in the blood will fall after surgical removal of the prostate, radical prostatectomy or treatment of prostate cancer by radiation. Thus, later increase of its level in serum is considered as clinical recurrence of prostate cancer (Chatterjee and Zetter, 2005).

In Table 3 are described the currently used cancer biomarkers in clinics and the purpose of their detection.

Table 3: Cancer biomarkers and their use in clinics. Adapted from (Chatterjee and Zetter, 2005). Description of current biomarkers routinely used in clinics and of recently identified potential new biomarkers.

Biomarkers	Cancers	Use	Refs
Current biomarkers in clinics			
PSA	Prostate cancer	Screening, diagnostic, recurrence prediction	(Ullah and Aatif, 2009)
CEA	Colorectal, lung, breast, liver, pancreatic, thyroid, bladder cancers	Determine recurrence, monitor treatment, efficacy	(Gold and Freedman, 1965a; Yurkovetsky et al., 2010)
CA 125	Ovarian cancer	Diagnostic, monitor treatment, recurrence prediction	(Yurkovetsky et al., 2010)
CA 19.9	Pancreatic and colorectal cancers	Pronostic and monitor treatment	
CA 15.3	Breast cancer	Monitor treatment, recurrence prediction	
Her-2	Breast cancer	Prognosis, response to therapy	(Gao et al., 1997)
Thyroglobulin	Thyroid cancer	Diagnostic	
AFP	Liver and testis cancers	Diagnostic and recurrence prediction	
B2 microglobulin	Multiple myeloma and lymphoma	Prognosis	(Diamandis, 2003)
SCC	Cervical cancer	Diagnostic, monitor treatment	
NSE	Lung cancer	Diagnostic	
Potential biomarkers identified			
BTA	Bladder	Diagnosis, recurrence prediction	
NMP22	Bladder	Diagnosis, recurrence prediction	(Budman et al., 2008; Mungan et al., 2000)
Calreticulin	Bladder	Diagnosis	(Kageyama et al., 2004)
Survivin	Bladder	Diagnosis	(Shariat et al., 2009; Horstmann et al., 2010)
Calcitonin	Thyroid	Diagnosis, monitor treatment and recurrence prediction	(van et al., 2009)
Antizyme inhibitor	Prostate	Prognosis	(Koike et al., 1999)
Collagen XXIII	Prostate, breast and several others	Prognosis	(Banyard et al., 2003)
Osteopontin	Prostate, breast	Prognosis	(Rittling and Chambers, 2004)
Urokinase-type plasminogen activator	Breast	Recurrence	(Borstnar et al., 2002)
ICTP	Ovarian	Prognosis, stage	(Simojoki et al., 2001)
Vimentin	Kidney	Prognosis	(Klatte et al., 2009)
Myc and A1B1	Hepatocellular carcinoma	Prognosis	(Wang et al., 2002)

2.2.3 Autoantibodies as biomarkers

2.2.3.1 Tumor-associated antigens

Our current knowledge of the biology of serum autoantibodies and their target autoantigens is derived from what has been learned from patients with systemic autoimmune diseases such as systemic lupus erythematosus, scleroderma or rheumatoid arthritis (Casiano et al., 2006; Anderson and Labaer, 2005). Results of these investigations can be summarized as follows: (i) autoantibodies are directed against intracellular proteins that participate in important cellular functions, like DNA replication, RNA processing and splicing or mitosis, (ii) autoantibodies have diagnostic and prognostic values as they often precede the first clinical symptoms and are associated with disease severity, (iii) autoantibodies are not considered pathogenic but rather immunological fingerprints of pathological processes associated with the development of systemic autoimmunity (Casiano et al., 2006).

Robert Baldwin published for the first time that the immune system could react to a developing tumor (Desmetz et al., 2009b; Baldwin et al., 1973; Baldwin, 1966). Tumor cells are known to be antigenic but not necessarily immunogenic (Stewart and Abrams, 2008). There are very few tumor-specific antigens. Even MAGE (melanoma antigen) which is supposed to be tumor-specific is found in the testis (Van den Eynde and Van der Bruggen, 1997). Therefore, the expression “Tumor-Associated Antigens” (TAA) is usually preferred since they consist of proteins also present in normal tissues.

The immune system employs common mechanisms to distinguish between self and non self. It deletes or renders tolerant any cells which react to the constant self-repertoire. Sometimes, the immune system responds to self-derived antigens, as seen in cancer. TAA are thought to be altered in a way that renders them immunogenic. These proteins are most of the time self-proteins that can be overexpressed, mutated, misfolded, mislocalized or aberrantly degraded and can therefore induce an immune response in cancer patients (Tan et al., 2009; Desmetz et al., 2009b). These self-proteins can also undergo post-translational modifications, like glycosylation, phosphorylation, oxidation or proteolytic cleavage. This renders them perceived as

foreign by the immune system, inducing an immune response by generating a neo-epitope or by enhancing self-epitope presentation and affinity to the major histocompatibility complex (MHC) or the T-cell receptor (Tan et al., 2009). The induced immune system then produces antibodies against these TAA, so-called autoantibodies which can be used as biomarkers for cancers (see below) (Mintz et al., 2003) (Figure 15).

Many TAA discovered until now are intracellular proteins. Different hypotheses are proposed to explain this phenomenon. Although compensated by tumor cells proliferation, cell death is a frequent event in cancers and modified intracellular proteins can therefore be presented to the immune system in the inflammatory environment induced by necrosis (Lleo et al., 2010). Apoptosis also can be involved in this process (Locher et al., 2010). Indeed, numerous antigens can be presented to cell surface as an early apoptotic event (Tesniere et al., 2008). In addition, when apoptotic engulfment by phagocytes is impaired or when phagocytes take up apoptotic blebs containing intact antigens, it can also induce the production of autoantibodies (Green et al., 2009; Kepp et al., 2009). Also, without any cell death requirement, intracellular proteins that are relocalized to the tumor cell surface may appear unfamiliar, thereby triggering an immune response (Tan et al., 2009). Finally, TAA that bind to heat shock proteins (HSP) may be immunogenic as a result of immunomodulatory properties of the HSP.

One representative example of intracellular protein becoming immunogenic is p53. Although p53 presents a nuclear localization, some publications reported the presence of autoantibodies in various cancers such as lung (Kobold et al., 2010b), breast (Piura and Piura, 2010; Kulic et al., 2010) and ovarian cancers (Anderson et al., 2010; Piura and Piura, 2009). These autoantibodies are present years before the detection of malignant lesions. Unfortunately, because of the presence of anti-p53 antibodies in various inflammatory diseases (Herkel et al., 2002; El-Sayed et al., 2003) and in various malignancies, these autoantibodies could not find any diagnostic or prognostic applications yet. The mutations of p53 may result in the expression of abnormal proteins which have altered functions and increased stability (Tsai-Turton et al., 2009). The abnormal structure of the protein together with the

increased antigenic load and/or its ectopic localization are thought to account for the immunogenic properties of p53 (Tan and Shi, 2003; Cordes et al., 2009).

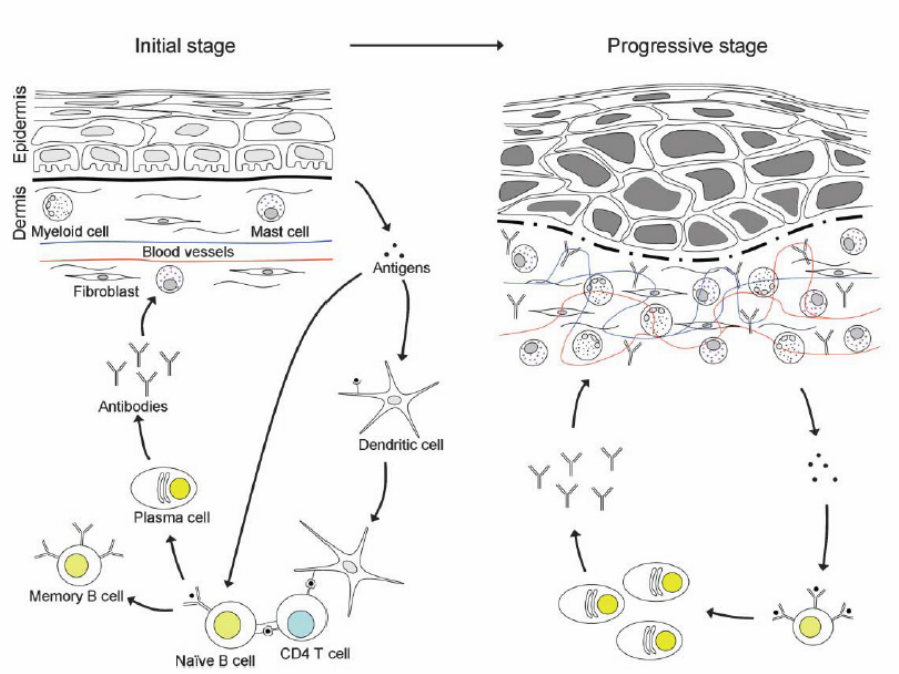

Figure 15: Antibody production by B lymphocyte in early skin carcinogenesis. Naïve B cells are activated by tumor antigens in the presence of CD4 T cells and differentiate into memory B cells and plasma cells. Antibodies produced by plasma cells stimulate resident myeloid cells (macrophages) in the dermis via activating Fc receptors to secrete VEGF, MMPs and other inflammatory signals, recruiting other innate immune cells. All these cells and signaling molecules participate to the tumor expansion. The production of autoantibodies is permanently maintained as tumor antigens are still secreted along with the progression of malignant tumor. Autoantibodies are thus present in the early stages of tumor growth and can represent a source of potential biomarkers (Houghton et al., 2005).

2.2.3.2 Immune systems and cancer

It is well known that the tumor microenvironment contains innate immune cells such as macrophages, neutrophils, mast cells, MDSC, dendritic cells and NK cells but also cells from the adaptive immune system such as B- and T-lymphocytes (Grivennikov et al., 2010) (Table 4).

Table 4: Description of the roles of different immune cell types present in the tumor microenvironment (Grivennikov et al., 2010)

Cell Types	Antitumor	Tumor-Promoting
Macrophages, dendritic cells, myeloid-derived suppressor cells	Antigen presentation; production of cytokines (IL-12 and type I IFN)	Immunosuppression; production of cytokines, chemokines, proteases, growth factors, and angiogenic factors
Mast cells		Production of cytokines
B cells	Production of tumor-specific antibodies?	Production of cytokines and antibodies; activation of mast cells; immunosuppression
$CD8^+$ T cells	Direct lysis of cancer cells; production of cytotoxic cytokines	Production of cytokines?
$CD4^+$ Th2 cells		Education of macrophages; production of cytokines; B cell activation
$CD4^+$ Th1 cells	Help to cytotoxic T lymphocytes (CTLs) in tumor rejection; production of cytokines ($IFN\gamma$)	Production of cytokines
$CD4^+$ Th17 cells	Activation of CTLs	Production of cytokines
$CD4^+$ Treg cells	Suppression of inflammation (cytokines and other suppressive mechanisms)	Immunosuppression; production of cytokines
Natural killer cells	Direct cytotoxicity toward cancer cells; production of cytotoxic cytokines	
Natural killer T cells	Direct cytotoxicity toward cancer cells; production of cytotoxic cytokines	
Neutrophils	Direct cytotoxicity; regulation of CTL responses	Production of cytokines, proteases, and ROS

The immune system can be divided into two categories: the innate immune system and the adaptive immune system. The innate immune system comprises granulocytes, dendritic cells, macrophages, natural killer cells and mast cells. In addition, there is also an important role for the complement system which is a complex network of serum proteins and cell surface receptors. It is often considered as the first line of defense but it is also implicated in the activation and modulation of the adaptive immune responses (de Visser and Coussens, 2005). The adaptive immune system comprises the B- and T-lymphocytes that express antigen-specific receptors (BCR and TCR respectively). Among the T-cells, there are two major subsets: $CD4^+$ (T-helper) and $CD8^+$ (cytotoxic T-cells). The innate and adaptive immune systems do not work separately. When a danger signal is received, the innate immune system is activated and secretes different cytokines, such as IFN, TNFα, IL-12, IL-15 and IL-18. It promotes the differentiation and activation of immature dendritic cells, B- and T-lymphocytes (de Visser and Coussens, 2005). The innate immune cells also regulate the B-lymphocytes response. They will indeed be more efficiently activated if foreign antigens are primed by antigen presenting cells (APC).

The presence of B- and T-lymphocytes inside a tumor suggests that they have been activated by tumor-specific antigens, but this will not necessarily lead to tumor regression. Indeed, tumor-infiltrating lymphocytes are not sufficient for curtailing tumor growth. In a tumor microenvironment, the immune system does not only protect against tumor development, it can also promote tumor growth by selecting tumor cells with reduced immunogenicity (Croci et al., 2007). There are basically three steps in the immunoediting process (Figure 16): (i) the elimination of tumor cells by the innate and adaptive immune systems, (ii) the equilibrium where there is a balance between tumor growth and immune surveillance and finally (iii) the escape, where tumor cells having undergone selection are able to avoid the immune-mediated destruction.

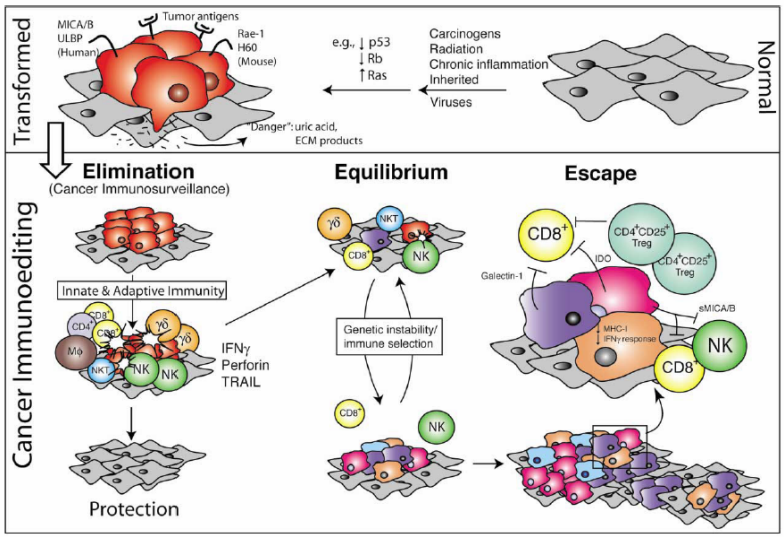

Figure 16: The three phases of the cancer immunoediting process. Normal cells are transformed into tumor cells (red) after different possible events. Tumor cells then release proinflammatory signals that induce their supposed elimination by the innate and adaptive immune systems. Then the tumor will enter in the equilibrium phase where further mutations and selections can occur, allowing some tumor cells to escape from the immunosurveillance. IFN: interferon, TRAIL: TNF-related apoptosis-inducing ligand, NK: natural killers, T reg: regulatory T cells, MICA/B: Major histocompatibility antigen related chain A and B, ULBP: UL16-binding protein, Rae: Retinoic acid early inducible gene-1 (Dunn et al., 2004).

Tumor cells can escape from mass destruction by different strategies. They can produce different tumor-derived factors that facilitate tumor growth, recruit immune

suppressive cell populations (myeloid-derived suppressor cells and T regulatory cells) or suppress directly the innate or adaptive responses (Stewart and Abrams, 2008). Indeed, they can render T-cell activation inefficient because of the absence of inflammatory mediators. Furthermore, they can also decrease the antigen presentation because of mutations that result in the misprocessing or mispresenting of TAA, thereby diminishing the immune response towards the tumor cells (Stewart and Abrams, 2008; El et al., 2008). All these mechanisms lead to an inefficient immune response and a failure in destroying growing tumors.

2.2.3.3 Production of antibodies by B-cells

Antibodies are produced by B-lymphocytes. There are different steps in the production and maturation of these cells that are summarized hereunder.

The B-cell receptor (BCR) expressed at the surface of B-lymphocytes is the key of the regulation of their development, activation, survival or destruction. BCR is composed of an immunoglobulin at the extracellular level and a heterodimer Igα/Igβ which ensures the function of transduction, internalization and intracellular signalling (Figure 17).

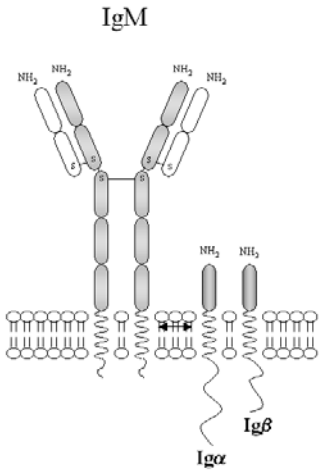

Figure 17: Structure of the receptor of B lymphocytes (BCR). It is composed of an immunoglobulin at the extracellular part and a heterodimer Igα/Igβ (Glaudet F., 2003).

The first step in the development of B-cells is antigen-independent. In the bone marrow, naïve mature B-cell first develop from B-cell progenitors. During this transformation, B-lymphocytes undergo few rearrangements of their heavy and light chains. Immature B-cells express IgM at their surface and at this stage, are submitted to a negative selection. An antibody is composed of two light (L) and two heavy (H) chains, and the genes specifying them are found in the 'H' chain locus and the 'L' chain locus. In the H chain loci there are three regions, V, D and J, which recombine randomly, in a process called VDJ recombination, to produce a unique variable domain in the immunoglobulin of each individual B-cell. Similar rearrangements occur for L chain locus except that there are only two regions, namely V and J (Figure 18).

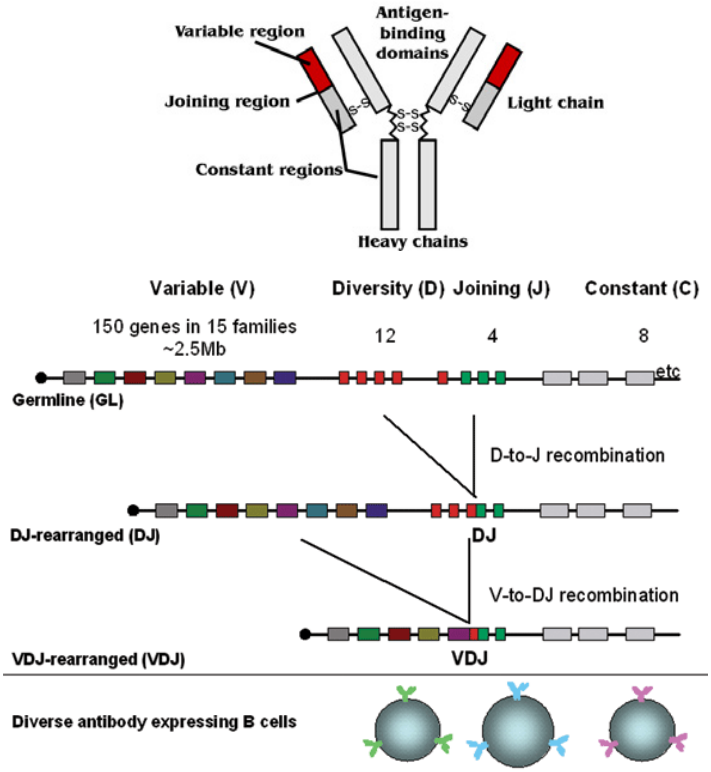

Figure 18: Illustration of the VDJ recombination. In the Pre-B cell phase, when B cells do not produce any immunoglobulin individual gene segments coding for the V, (D) and J regions of the heavy and light chain of the immunoglobulin molecule are randomly assembled to one molecule. The random assembly of 51 V, 27 D and 6 J gene segments provides a minimum of 8.300 different possible combinations for the heavy chain alone, but since the recombination process is not precise and extra nucleotides are inserted the number of possibilities of antibody V region diversity turn out to be greater (Corcoran A., © Babraham Institute 2008).

Thus, if an endogenous ligand is recognized at this step, B-lymphocytes edit the pre-BCR by a rearrangement of the V domains. But if a strong recognition is still maintained, clonal deletion or apoptosis take place or B-cells become anergic. Finally, mature B-cells, expressing BCR at their surface, are formed and move in the blood stream in search for a specific activation. Their receptors are either IgM or IgD (Figure 19).

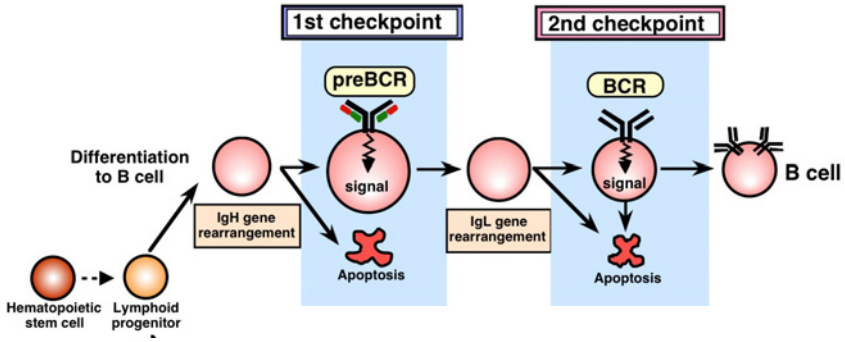

Figure 19: B cell maturation. B lymphocytes are originated from hematopoietic stem cells. After differentiation of lymphoid progenitor into immature B-cells, they undergo IgH gene rearrangement to form the preBCR. B-lymphocytes encounter next negative selection when exposed to endogenous ligands. Depending on the affinity reaction towards the antigen, immature B lymphocytes die from apoptosis or process gene rearrangement of their BCR that further meet a second checkpoint of stimulation. At this step, either they die or they become mature B-cells allowed to reach the blood stream (Melchers et al., 1995).

The second part of the differentiation of the B-lymphocytes happens in secondary lymphoid organs such as the spleen or nodes. A specific recognition of the antigen by the BCR is the first step necessary for the production of a specific and massive response (Amigorena and Savina, 2010). The antigens can be soluble or localized on the surface of a cell. B-lymphocytes, by contrast to T lymphocytes, are able to recognize different types of antigens: lipidic, polysaccharidic or proteic antigens. The further activation of the B-cells can be T lymphocyte-dependent or -independent, according to the nature of the activating antigens (proteic antigens are T-dependent while others are T-independent). Thus, for proteic antigens, the B-cell collaborates with $CD4^+$ Th2 cell (via CD40 and CD40L, and the production of different cytokines such as IL-4, IL-5, IL-6 and IL-10). This kind of specific response will lead to the isotypic commutation and affinity maturation. Some

professional cells in presenting antigens are further needed to activate the $CD4^+$ TH2 cells, that can next interact with B-cells (Robson et al., 2010).

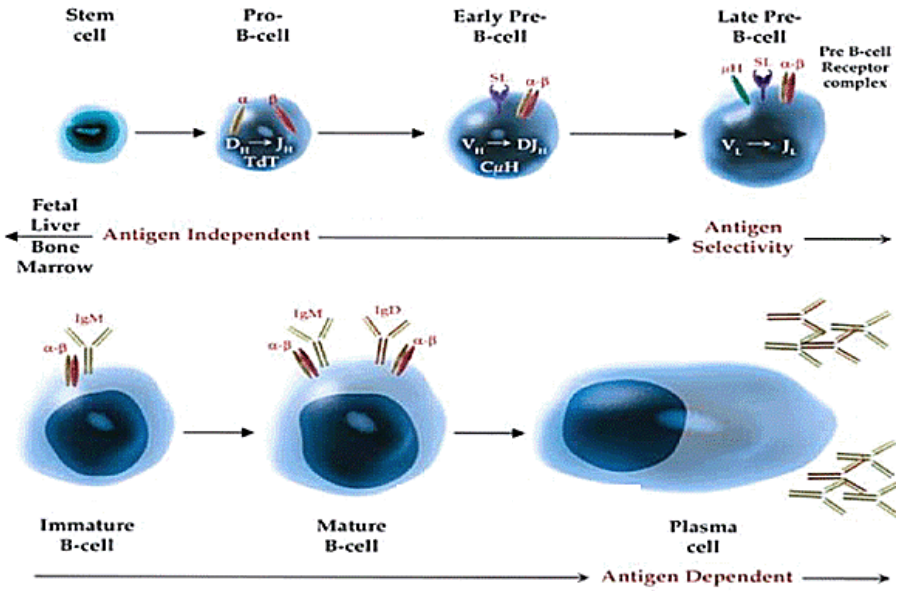

Figure 20: B cell development and maturation. The figure shows the immunoglobulin gene rearrangements and the steps necessary for antibody production and secretion, highlighting the changes that are antigen-independent and consequently autonomous from T-cell interaction. Affinity maturation is the result of cumulative point mutation on the hypervariable region of immunoglobulin genes, resulting from antigenic stimulation and proper co-stimulation of B cells. This process culminates with the emergence of memory B cells and terminally differentiated plasma cells (Kokron et al., 2004).

After this interaction, the B-cell undergoes different modifications that lead to the formation of plasmocytes and memory B-cells (Figure 20). One of the major modifications is the isotypic commutation. This leads to the production of a more specific immunoglobulin: IgG, IgA, IgE, IgD or IgM (Table 3). These antibodies are then responsible for the activation of other pathways of the immune system, like neutralisation, opsonisation or activation of the complement pathways (Figure 21).

Table 5: Description of the potential roles of each immunoglobulin.

Properties	**IgG**	**IgA**	**IgM**	**IgD**	***IgE***
Activation of the classical pathway of the complement	+++	-	++++	-	-
Neutralisation	++	+++	-	+	-
NK activation	+++	-	-	-	-
Opsonisation/phagocytosis	+++	+	-	-	-
Fixation on mast cells	-	-	-	+	+++
Epithelial transport	+	++	+	+	-

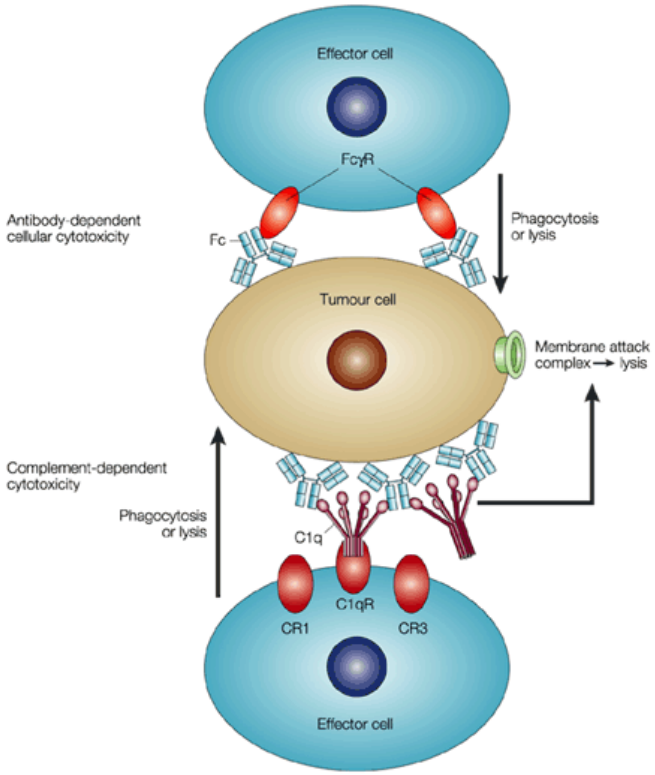

Figure 21: Consequences of antibody production by B-lymphocytes. Tumor-specific antibodies are produced by B-lymphocytes after specific stimulation. The antibodies can then induce cell lysis after fixation to the target cells. They can also activate the complex complement cascade leading to lysis. Finally, they can also be recognized by their receptor FcγR on myeloid cells and subsequently induce antibody-dependent cytotoxicity (Carter, 2001).

2.2.3.4 Autoantibodies in cancer

Natural autoantibodies occur in all individuals, even though this does not mean that we all suffer from autoimmune diseases. These antibodies are directed against self-proteins but they are not specific for a person because they recognize a general repertoire of antigens. They are characterized by a poly-reactivity and present a weak affinity (Oppezzo and Dighiero, 2003; Bei et al., 2009). One can postulate that these autoantibodies serve as a first line barrier against infections, waiting for high-affinity specific antibodies production (Oppezzo and Dighiero, 2003). They present a high-affinity to carbon groups present in the membrane of numerous pathogens and can induce the complement cascade (Lleo et al., 2010). This phenomenon is thought to play a role in the homeostasis of the immune system, being highly conserved among species (Lleo et al., 2010; Oppezzo and Dighiero, 2003). However, the window between self-defense and autoimmunity is extremely narrow and the role of these natural autoantibodies still needs to be clarified.

In cancer patients, autoantibodies are produced against tumor-associated antigens and may thus in theory serve as early molecular signatures for diagnosis of cancer patients (Tan et al., 2009; Kolch et al., 2005; Kijanka and Murphy, 2009). Autoantibodies present indeed an obvious series of advantages. They are easily accessible for screening because they are found in the blood of cancer patients. Autoantibodies are very stable and persist in the serum for a relatively long period. They are not exposed to proteolysis as commonly observed for other polypeptides. Furthermore, they are present in high concentration because they are amplified by the immune system. This is at odd of tumor antigens which, when shed in the blood stream, circulate in low concentrations and are rapidly degraded. Finally, since their biochemical properties are well understood, many reagents are available for the detection of autoantibodies. Sample collection is also simplified as a result of the long half-life of autoantibodies (Tan et al., 2009; Anderson and Labaer, 2005).

Autoantibodies to detect cancer may however suffer from a potential low specificity according to the autoimmune background of the patient and low sensitivity because of the intrinsic heterogeneous nature of cancer (Kobold et al., 2010a).

To note, it is still unclear whether cancer autoantibodies play a tumor-promoting role, whether they take part in immune attack against tumor growing or whether they simply reflect tumor persistence and/or progression (Kobold et al., 2010b).

2.3 Proteomic technologies

2.3.1 Two-dimension electrophoresis

2D-electrophoresis (2-DE) is the classical technique for proteome analysis. For more than 30 years, 2D-electrophoresis has been the mainstay of protein expression profiling (Kolch et al., 2005; McHugh et al., 2009). It is the method of choice because of the power of resolution that it can provide. Indeed, several thousands of proteins can be separated, displayed and stored in one gel. Proteins in the size range from 10 kDa to 200 kDa and with isoelectric points between 3 and 11 can be analyzed. Furthermore, hydrophobic proteins are also included in the analysis because the separation takes place under completely denaturing conditions (Westermeier et al., 2008). It is still the best method for the high-resolution separation of a complex mixture of proteins. Its efficacy in distinguishing post-translationally modified proteins and protein isoforms is unparalleled (Tan et al., 2009; Kolch et al., 2005; Chatterjee and Zetter, 2005; Gorg et al., 2000).

Proteins are first separated according to their isoelectric points using isoelectric focusing in the first dimension and then according to their molecular weight using SDS-PAGE in the second dimension, reason why it is called 2-dimension electrophoresis. The isoelectric point of a protein is the specific pH value at which the sum of negatively and positively charged amino acid residues is equal. At this point, the protein stops its migration within the electric field (Habermann et al., 2008).

2D-electrophoresis can resolve 1500-3000 protein spots per gel. By spreading the pH range across several gels, so called zoom gels, between 5000-10 000 protein spots can be resolved (Kolch et al., 2005). In addition, subcellular fractionation offers the advantage of well-established protocols for many subcellular compartments (Kolch et al., 2005).

2.3.1.1. 2-DE technology

2.3.1.1.1 Principles of electrophoresis

The principle of electrophoresis is the migration of charged particles in an electric field. Because different particles have different sizes and net charges, they migrate with different velocities and form therefore distinct zones. The higher the net charge and the smaller the molecule, the faster is its electrophoretic migration. Proteins and peptides are amphoteric substances, they can become positively or negatively charged, depending on the pH value of their environment. Therefore, they will migrate towards the cathode or the anode respectively.
Most electrophoretic separations in proteomics are performed in gel matrices, which are commonly performed in polyacrylamide gels. Polyacrylamide gels are polymerized from acrylamide monomers and a cross-linking reagent, usually N,N'-methylenebisacrylamide. It should be noted that after the crude gel has formed, there is a consecutive silent polymerization, which takes several hours, and completes the formation of the final matrix. Therefore, the gels should not be used immediately after preparation (Gorg et al., 2000).

2.3.1.1.2. Isoelectric focusing

Isoelectric focusing is performed in a pH gradient. Proteins are amphoteric molecules with acidic and basic buffering groups. They become protonated or deprotonated depending on the pH environment. Accordingly, when an electric field is applied towards the pH gradient, a protein starts to migrate towards the electrode of the opposite sign of its charge and it stops at a pH value corresponding to its isoelectric point (pI) (Figure 22).

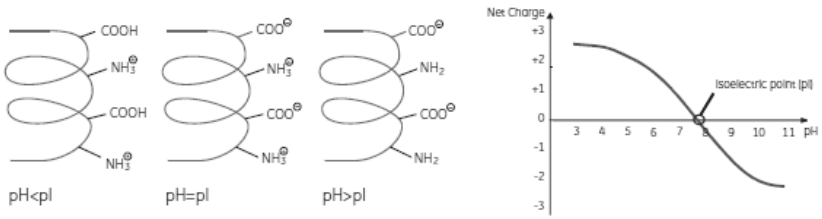

Figure 22: The isoelectric point. When a protein reaches its isoelectric point, it is electrically neutral and presents a net charge of zero, whereas in function of the pH of the solution, the amino acids will be protonated or not (Westermeier et al., 2008).

Historically, the first dimension migration was performed in carrier ampholytes generated pH gradients. The pH gradient was thus established by the electric field. At the beginning, the gel with carrier ampholytes has a uniform mean pH value. When an electric field is applied, the negatively and positively charged carrier ampholytes migrate towards their respective electrode, with velocities depending on their net charges. This was a relatively slow separation method, proteins having only very low net charges when they come close to their isoelectric points (Gorg et al., 2000). These problems were solved with the introduction of immobilized pH gradients (Verrills, 2006; Gorg et al., 2000; Alaiya et al., 2000), generated by buffering acrylamide derivatives copolymerized with the gel matrix. The acrylamide derivatives containing the buffering groups are called Immobilines. A pH gradient is obtained by continuously varying the ratio of Immobilines. Immobilized pH gradient gels are the only electrophoresis slab gels, which do not show any edge effects during the run, when they are cut into strips. Much more reproducible results are obtained, when ready-made IPG strips are used (different pH gradients and lengths provided).

2.3.1.1.3. 2-DE limitations

There are some limitations in resolving certain classes of proteins. Indeed, small, very large, very basic and very hydrophobic proteins are widely excluded. For instance, transmembrane proteins, which are hydrophobic and insoluble are difficult to detect (Desmetz et al., 2009b). Also, it can sometimes be difficult to obtain

reproducible 2D-gels (Tan et al., 2009). The gel-to-gel variations could induce issues in image analysis procedures. The high demand on labour is a serious obstacle for 2D-electrophoresis becoming routine for a clinical laboratory. The low abundant proteins also remain difficult to visualize because of the limited sensitivity of staining methods.

2.3.1.1.4. Typical 2-DE workflow

Hereunder is the description of the different steps that have to be followed in a 2D-gel based proteomic analysis (Figure 23). In a first set of experiments, so-called “analytical gels” are performed to identify proteins of interest (Berth et al., 2007). The material loaded onto 2D-gels is carefully handled and prepared in order to (i) inactivate all cellular processes that may change the proteome composition, (ii) bring a maximum of proteins present in the sample into solution and (iii) get rid of molecules that may disturb the subsequent steps of the 2D protocol.

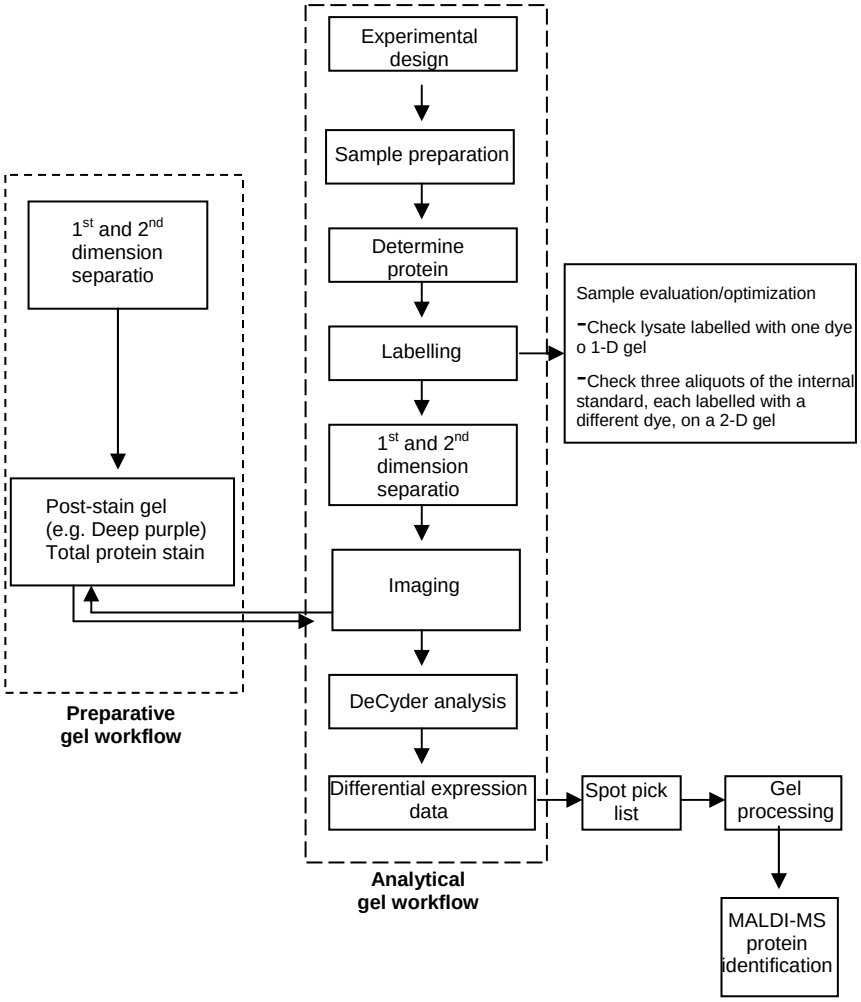

Figure 23: Global scheme of experiments required in a 2D-electrophoresis analysis. First, analytical gels are performed and differential expression analysis is achieved. In a second time, preparative gels are realized to identify proteins of interest. The two-dimensional separations are performed by combining isoelectric focusing in the first and sodium dodecyl sulphate (SDS) electrophoresis in the second dimension. The gel images are captured by using scanners, CCD camera-based, or laser-imaging devices. Proteome maps condense the image information of the whole experiment into one fusion image, also called a proteome map. Spot detection is performed on the proteome map. For spot quantitation and building expression profiles, the consensus spot pattern is applied to all gel images of the experiment (Westermeier et al., 2008).

When spots of interest have been found, “preparative gels” containing higher amounts of proteins are processed in order to pick enough material for further mass spectrometry identification.

2.3.2. 2D-DIGE analysis

Proteomic-based approach can be exploited to study differential protein patterns in cancer biology. One of the major techniques used to investigate the differential expression of proteins in cancer is 2D-electrophoresis and more especially 2D-DIGE (2-Dimension Difference In Gel Electrophoresis) .

Proteomics allows the identification of protein changes caused by a disease process in a relatively high-throughput manner, because it permits the analysis of thousands of modified or unmodified proteins. The DIGE technique resolves the issues that were met in the past in term of reproducibility and accuracy. Using 2D-DIGE, quantitative analysis can be performed and significant target proteins can be identified in numerous fields. It can be used to compare tumor samples *vs* healthy tissues, serum profiles between cancer patients and healthy controls or before and after treatment administration.

One of the critical steps in running proteomic-based analysis in cancer is the enormous heterogeneity of tissues. Indeed, the malignant tissues are contaminated with endothelial cells, fibroblasts, T-cells, dendritic cells and many other non-tumor cells. This should be taken into account in the interpretation of the data obtained. This can however be minimized by the use of laser capture microdissection (LCM). Although this technique is labour-intensive and requires a high-skill level, it represents a valuable tool for proteome analysis. The major limitation is the amount of tissue, which is even more critical when focusing on subproteomes such as the membrane, cytoplasmic or nuclear fractions (Seliger and Kellner, 2002).

2.3.2.1. 2D-DIGE technology

2.3.2.1.1. 2D-DIGE principles

In the last decades, the quantification of proteins has become very accurate with the introduction of highly sensitive fluorescent stains offering a wide dynamic range.

This technology is exploited in the so-called 2D-DIGE technique (Kolch et al., 2005; Habermann et al., 2008; Verrills, 2006).

The protein samples that have to be compared are covalently labelled on lysine groups with a green or red fluorescent fluorophores; the leader in this technology, GE Healthcare, exploits cyanine (Cy) dyes. A mixture of all of the samples in the study is then labelled with a third dye (blue) to serve as internal standard. All three samples are then mixed together and separated by 2D-electrophoresis (Kolch et al., 2005; Bitarte et al., 2007; Lilley and Friedman, 2004). The different protein extracts can then be visualized separately by exciting the different dyes at their specific excitation wavelength (Marouga et al., 2005). The linearity, sensitivity and wide dynamic range of these dyes have made 2D-DIGE into a quantitative technique (Figure 24).

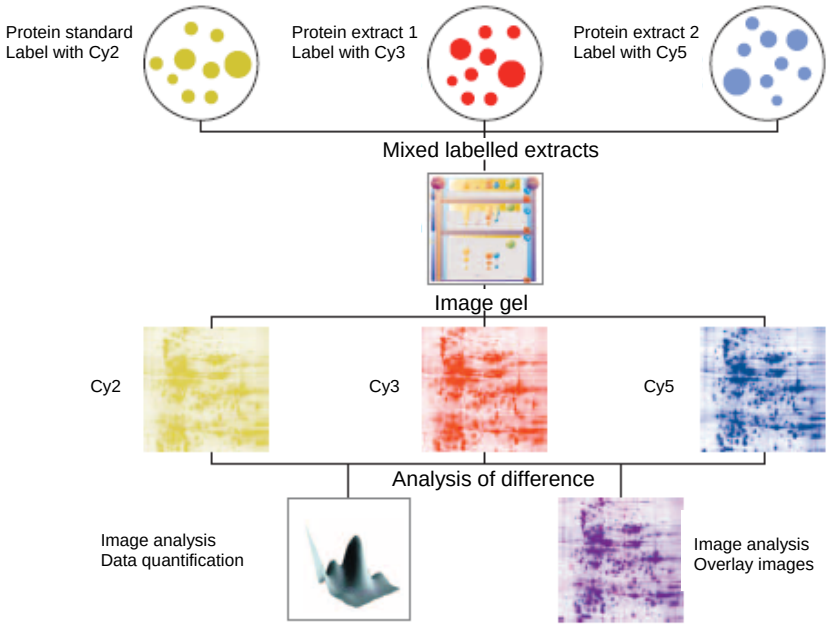

Figure 24: General description of the DIGE labelling and DIGE experiments. The internal standard is labelled with Cy2 and the two samples to compare are labelled with Cy3 and Cy5. The three samples are mixed and the 2D gels are runned. After this, the gels are scanned with the corresponding wavelengths to visualize the three samples individually. With the images obtained, the differential analysis can be performed with the appropriate software (Westermeier et al., 2008).

This technique avoids ambiguities of spot matching as the samples are separated on the same gel and inter-gel comparisons are greatly improved by the common internal standard. The single positive charge of the CyDye replaces the single positive charge of the lysine at neutral and acidic pH keeping the pI of the protein relatively unchanged. A mass of approximately 500 Da is however added by the CyDye to the labelled proteins (Bitarte et al., 2007; Habermann et al., 2008). Since the fluorescent signal is linear over a wide protein concentration range and each spot contains its own internal standard, comparative quantification is very accurate. The individual protein data from the control and diseased/treated (Cy3 or Cy5) samples are normalized against the Cy2 dye-labelled sample. Logarithm abundance ratios are then compared between the control and diseased/treated samples from all the gels using statistical analysis (t-test and ANOVA) (Bitarte et al., 2007). Sensitivity is higher to silver-staining and in addition, fluorescent dyes are fully compatible with mass spectrometry analysis (Kolch et al., 2005).

2.3.2.1.2. Minimal labelling

The proteins of two distinct samples are labelled prior to the electrophoretic separation with different fluorescent dyes. The samples are mixed together and run on the same 2D-gel. In this way, proteins of the two samples migrate under identical conditions, thereby eliminating gel-to-gel variations. The cyanine dyes (CyDye) are chemically modified in a way that they bind to proteins and allow precise co-migration of the same proteins in both dimensions (Lilley and Friedman, 2004) (Figure 25). After electrophoresis the gels are scanned with a fluorescent imager at different wavelengths. There is a linear relation between the labelled protein and the signal measured with the imager, because following excitation of the dye by monochromatic light, the dye emits light in proportion to the amount of labelled compound in the sample. Three spectrally distinct dyes are available: Cy2, Cy3 and Cy5. They can be excited with a blue, red and green laser respectively. In the scanner, the emitted light is amplified with photomultiplier tubes and recorded with computer. The images can be displayed on a computer screen in a false color

representation. The patterns can be overlaid, which is an easy way to visualize differences in protein expression.

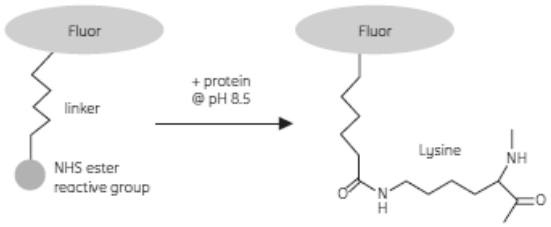

Figure 25: Principles of labelling of proteins with CyDye. The NHS ester reactive group reacts with the primary amine of a protein to generate a covalent link. The proteins are then stably labelled for three to six months in appropriate storage conditions (Westermeier et al., 2008).

There are two methods of labelling with CyDyes: lysine or cysteine tagging. The most applied method is labelling of the lysine because its amino side group is easily accessible and lysine is one of the most frequent amino acids in proteins. The labelling occurs via NHS ester chemistry. Only a small portion of proteins is labelled on the lysine to avoid that proteins become too hydrophobic. It is calculated in a way that 3 to 5% of the proteins will receive a tag. The rest of the proteins remain unlabelled. This is the minimal labelling (Lilley and Friedman, 2004; Miller et al., 2006). Some groups have performed experiments with synthetic peptides containing one or multiple lysine residues in a consecutive sequence. Mass spectrometric analysis of the optimized labelling reactions showed that only one dye molecule is present per protein molecule (Marouga et al., 2005). The relatively high-lysine content of most proteins makes thus amino acids suitable for this labelling strategy, in which small amounts of dye are used.

CyDyes are charge- and size-matched. Therefore, a basic buffering group is added to each of the dyes, so that the isoelectric point does not change. In the second dimension, the proteins migrate to the same point because the molecular weights added are in the range between 434 and 464 for the three dyes. The sensitivity of CyDye DIGE fluor minimal dye Cy2 is 0,075 ng, for Cy3 and Cy5 0,025 ng (in comparison, silver staining has a sensitivity of 1 ng) (Marouga et al., 2005).

2.3.2.1.3 The internal standard

The multiplex feature of DIGE offers the unique possibility to reserve one channel for an internal standard. It is composed of a pool of aliquots taken from each sample of an experiment (Lilley and Friedman, 2004). In order to find significant protein changes with acceptable statistical confidence, at least three biological replicates are required. This requires the pool of at least six samples to create the internal standard. Because the proteins are co-migrating in the gel, no spot matching is needed within the gel. The sample spot volumes can directly be compared to the spot volumes of the standard (Figure 26). Dedicated softwares, such as Decyder (GE Healthcare), do this automatically, employing co-detection algorithm. The result is expressed in spot volume ratios. For the comparison of several gels, the mathematical spot-matching procedure is highly facilitated by the overall identical protein composition within the samples. Finally, full-automated evaluation of a high number of images is made possible by the use of such softwares.

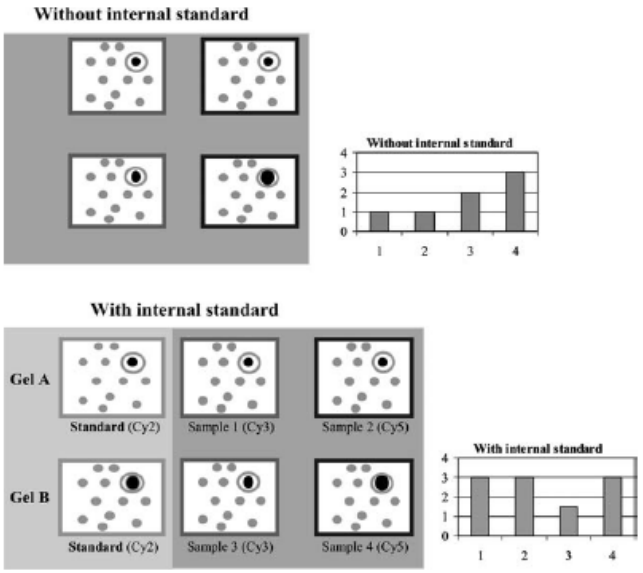

Figure 26: Interest of the internal standard. A. Without internal standard, the third and fourth samples seem to be in higher concentration that the two other samples. B. With the internal standard, the difference between the samples is completely different. The samples are firstly normalized with their own internal standard and are next compared to each others (Marouga et al., 2005).

2.3.2.1.4. DeCyder differential analysis

DeCyder differential analysis software has been developed as part of the DIGE system by GE Healthcare. It is a fully-automated image analysis software for spot detection and accurate measurement of protein differences with statistical confidence (Marouga et al., 2005; Fodor et al., 2005).

Hereunder are described the two main modules available in this software:

- DIA (differential in-gel analysis): The DeCyder DIA module processes the images from a single gel, performing background subtraction, detection and quantitation, in-gel normalization and gel-artefact removal, all automated for high-throughput and reduced user-specific separation. The DIA module quantifies the spot volumes for each image and expresses these values as a ratio, comparing spot volumes on the internal standard image.
- BVA (biological variation analysis) : The DeCyder BVA processes multiple gel images, performing matching of multiple images from different gels for comparison to provide statistical data on different protein abundance levels between multiple groups. This process enables comparison of protein abundance between samples on different gels.

2.3.2.1.5. The identification by mass spectrometry

The most widely used approach of mass spectrometry analysis is proteolytic peptide fingerprinting. The separated protein is first digested with a protease such as trypsin. The masses of a set of peptides are then measured by matrix-assisted laser desorption ionization time of flight mass spectrometry (MALDI-TOF MS) and compared with the theoretical mass spectrum of different proteins in the database (SwissProt or NCBI) (Poon and Johnson, 2001) (Figure 27).
However, it is not possible to identify all proteins by peptide fingerprinting. Indeed, full-length sequences of a large percentage of human proteins are still not represented in the database. Furthermore, some small proteins do not result in a

sufficient number of proteolytic peptides for unambiguous identification. For those peptide sets with unidentified mass spectra, selected peptides can be subjected to quadrupole-TOF MS (Q-TOF MS) for amino acid sequencing. Knowing the mass of a peptide, together with its amino acid sequence, allows to optimize databases searching (Poon and Johnson, 2001).

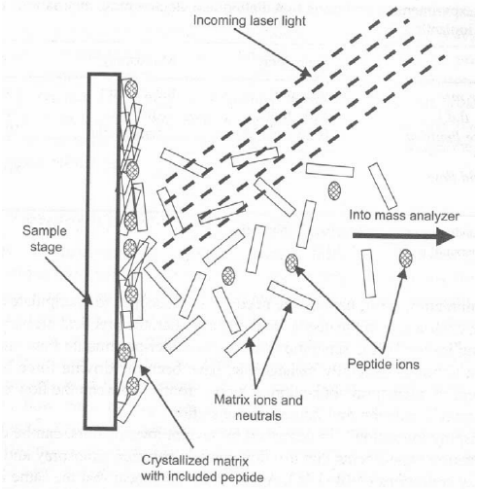

Figure 27: MALDI TOF MS principle. The sample is dispersed in a large excess of matrix material which will strongly absorb the incident light. The matrix contains chromophore for the laser light and since the matrix is in a large molar excess it will absorb essentially all of the laser radiation. The matrix isolates sample molecules in a chemical environment which enhances the probability of ionization without fragmentation. Short pulses of laser light focused on to the sample spot cause the sample and matrix to volatilize. The ions formed are accelerated by a high-voltage supply and then allowed to drift down a flight tube where they separate according to mass (m/z). Arrival at the end of the flight tube is detected and recorded by a high-speed recording device (Kinter and Sherman, 2000).

2.3.3 Serological Proteome Analysis (SERPA)

2.3.3.1 Seric biomarker discovery

The biomarker research can be done using a variety of different technologies, from genomic techniques like microarrays to proteomic techniques using gel-based and gel-free differential analysis together with mass spectrometry analysis. Here, we will focus on the serological proteome analysis and detailed the three main techniques available using serum of patients to discover new biomarkers.

2.3.3.1.1 SEREX (serological analysis of tumor antigens by recombinant cDNA expression cloning)

This technique developed in 1995 involves the identification of TAA by screening patient sera against a cDNA expression library obtained from the autologous tumor tissues (Seliger and Kellner, 2002; Desmetz et al., 2009b; Anderson and Labaer, 2005) (Figure 28). TAA identified by SEREX correspond to linear epitopes expressed by bacteria. Although post-translational modifications are often implicated in autoimmune reactions or cancers, they cannot be detected by SEREX (Tan et al., 2009; Desmetz et al., 2009b) This technique is time-consuming, labour-intensive, not amenable to automation and subject to numerous false positive findings (Desmetz et al., 2009b).

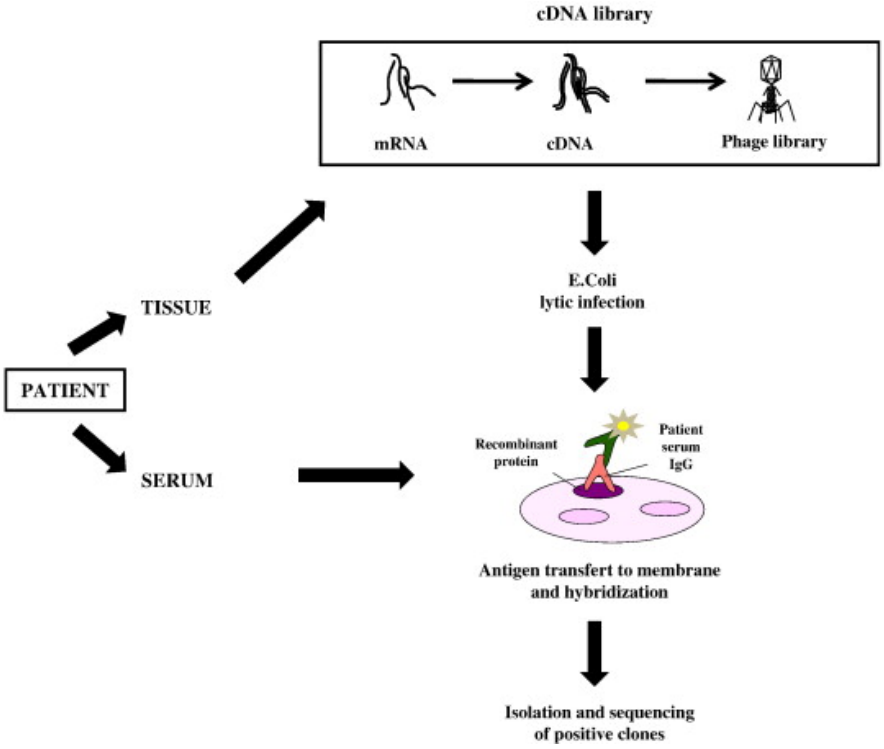

Figure 28: The SEREX strategy. mRNAs are extracted from a tumor tissue. Double-stranded cDNAs are next synthesized and inserted into the phage genome. The amplified recombinant virions will then be used to infect E.Coli bacteria, allowing the production of recombinant proteins. These proteins are then transferred on membranes that will be finally incubated with serum from cancer patient. The positive clones will be isolated and sequenced (Desmetz et al., 2009b).

2.3.3.1.2 Protein microarray

Purified or recombinant proteins, synthetic peptides or fractionated proteins from tumor or cancer cell lysates can be spotted onto microarrays and then incubated with specific sera (Casiano et al., 2006) (Figure 29). This miniature platform allows the use of very low amounts of precious biological fluids. This technique permits high-throughput identification of TAA signatures for the development of cancer diagnostics and vaccines. A major limitation is however the short shelf-life of arrayed proteins and difficulties in purifying or producing native proteins (Tan et al., 2009). Protein microarrays that enable large-scale testing on more than 9000 recombinant antigens have been developed, like ProtoArray (Invitrogen).

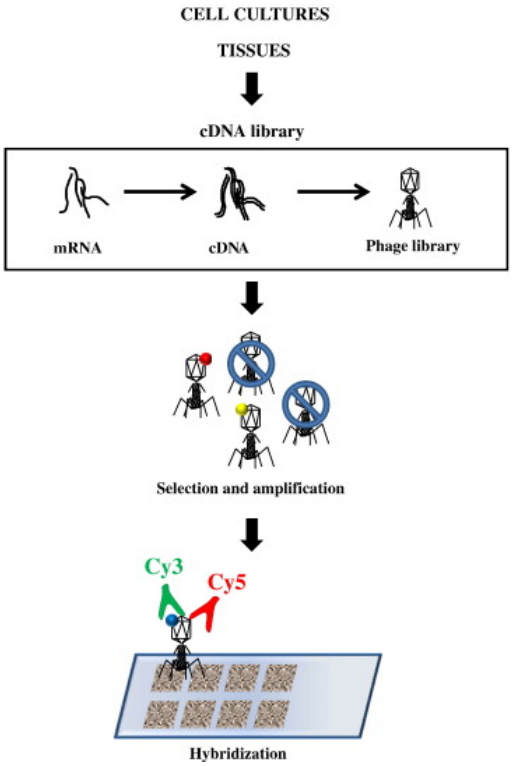

Figure 29: The phage protein-microarray-based strategy. cDNA library is obtained from cell culture or tissue. The cDNA is inserted into the phage genome and a further selection is done by repeating cycles of purification of phages that specifically react with sera from cancer patients. These phages are amplified and spotted on slides, which are hybridized with Cy-5 labelled antibodies from patients with cancer. Labelling intensity is normalized using Cy3-labelled antibody directed against a phage capsid protein. Reactive phages are isolated and cDNA is finally sequenced (Desmetz et al., 2009b).

2.3.3.1.3 SERPA (serological proteome analysis) or PROTEOMEX

This technique combines 2-dimension electrophoresis, Western blotting and mass spectrometry analysis. Total proteins from tissues or cell lines are separated by 2D-electrophoresis, transferred onto membranes by electroblotting and subsequently probed with sera from healthy individuals or patients (Tan et al., 2009). This technique will be described into more details in 2.3.3.2 chapter.

Table 6: Main characteristics of the SEREX and the SERPA/PROTEOMEX techniques (Seliger and Kellner, 2002)**.**

Feature	SEREX	PROTEOMEX/SERPA
Preparation of	mRNA extraction, construction of unidirectional, full-size cDNA libraries in	Protein extraction
Properties of tumor- and pathogen-derived antigens	Recombinant β-gal fusion proteins expressed in lytic plaques by E.Coli, possibly native conformation	Natural, post-translationally modified proteins, urea/SDS denatured
Serological detection of antigens	Extensive pre-adsorption of anti-E.Coli antibodies necessary	Detection of no pre-adsorption required, immune reactivity against pathogenic micro-organisms derived proteome by 2-D immunblot
Specificity controls	-	2-D immunoblots with non tumorous tissue 2-D immunoblots with healthy donor sera
Isolation and identification of antigens	Secondary and tertiary immunoscreening DNA sequencing	Preparative 2-DE MS, sequencing

2.3.3.2 The SERPA technology

2.3.3.2.1. SERPA principles

Klade's team was the first to develop the Serological Proteome Analysis (Desmetz et al., 2009b; Klade et al., 2001) in order to identify antigens associated with humoral response in kidney cancer. The term serological proteome analysis has been proposed for a top-down discovery-driven immunomics method (Caron et al., 2007). It has also been called PROTEOMEX by the group of Seliger et al (Seliger and Kellner, 2002). This technique involves the discovery of TAA using a combination of 2D-electrophoresis, Western blotting and MS analysis. In the field of cancer, proteins from tumor tissues or tumor cell lines are separated by 2D-electrophoresis and then transferred onto membranes by electroblotting and subsequently probed with sera from healthy individuals or patients with cancer (Tan et al., 2009; Jain, 2008; Seliger and Kellner, 2002) (Figure 30). The sera of the patients are supposed

to contain autoantibodies directed against specific TAA. These autoantibodies can be used to detect TAA that have undergone post-translational modifications and are presented as such following 2-DE (Tan et al., 2009; Caron et al., 2007).

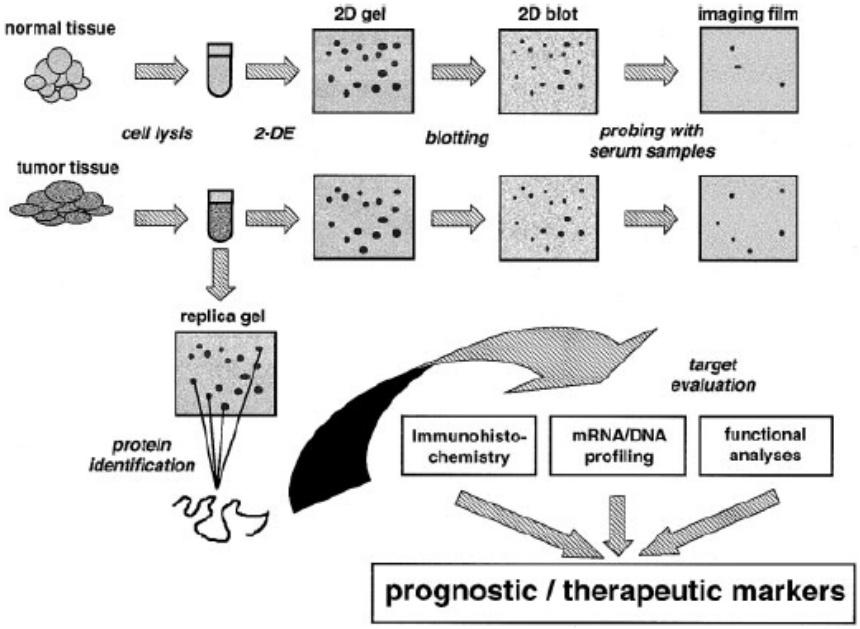

Figure 30: General description of the SERPA strategy. Normal and tumor tissues are lysed and separated by 2D-electrophoresis. Immunoblotting with cancer sera is performed on the membranes. After comparison between the two results obtained, the proteins of interest can be picked up and identified by mass spectrometry. The interest of the biomarker is finally evaluated by further immunohistochemistry, mRNA profiling or functional analyses (Seliger and Kellner, 2002).

The SERPA technique avoids the time-consuming construction of cDNA libraries required for SEREX (Tan et al., 2009). The antigens source results from a simple protein extraction, which present the advantage of maintaining most post-translational modifications (Desmetz et al., 2009b).

The limit of the SERPA technique resides primarily in the limits of 2D-electrophoresis. Indeed, there is a limitation in resolving certain classes of proteins and it can be sometimes difficult to obtain reproducible 2D-gels (Tan et al., 2009). The low abundant proteins remain difficult to visualize because of the limited

sensitivity of staining methods. Transmembrane proteins, which are hydrophobic and insoluble, are also difficult to detect (Desmetz et al., 2009b).

2.3.3.2.2 Identification of cancer biomarkers with the SERPA technique

The SERPA technique can be used in the search for biomarkers in the cancer field but also in other pathologies. Hereunder are summarized few studies using this particular technique in different cancers.

In breast cancer, Hamrita et a.l found 26 proteins that react with the sera of cancer patients. Among them, they reported Hsp60, tumor suppressor prohibitin, β-tubulin, haptoglobin-related protein and peroxiredoxin 2 (Hamrita et al., 2008). Hsp60 was also identified by Desmetz et al. in serum of patients diagnosed in the early stages of breast cancer (Desmetz et al., 2008), along with other 25 proteins, including other chaperones proteins (Hsp70 and Hsp27). They further investigated for a panel of autoantibodies to diagnose breast cancer (Desmetz et al., 2009a), rather than a single biomarker. They identified peroxiredoxin 2, FKBP52 and PPIA as TAA which were able to discriminate between carcinoma *in situ* and healthy controls, whereas Hsp60 and MUC1 were only able to discriminate between early-stage primary breast cancer and controls.

In renal cell carcinoma, different proteins have been identified in patients with high-grade disease. These proteins include annexins I and IV, thymidine phosphorylase, carbonic anhydrase I, Mn-superoxide dismutase and Major Vault Protein (MVP). Further analysis of the tissue expression of some of these proteins shows that MVP is up-regulated in 2/4 of RCC tumors but is also expressed in normal kidney; whereas TP is upregulated in 100% of RCC cases examined with no or minimal expression in normal kidney, indicating a potential use as a therapeutic target (Unwin et al., 2003). Another group working on renal cell carcinoma identified smooth muscle protein 22-alpha and carbonic anhydrase I as tumor-associated antigens. Antibodies to recombinant CAI or SM22-α were detected in sera from

3/11 or 5/11 RCC patients, whereas no serum from healthy patients did react (Klade et al., 2001).

In pancreatic cancer, Hong et al. processed sera from 36 pancreatic cancer patients, 18 patients with chronic pancreatitis, 33 patients with other cancers and 15 healthy subjects. They identified two isoforms of calreticulin. 21 out of 36 cancer patients present autoantibodies directed against this protein in their sera, whereas the frequency of calreticulin isoform 1 immune response was 1/18 for pancreatitis patients and 1/15 in healthy patients and no response against calreticulin isoform 2 was observed (Hong et al., 2004).

In hepatocellular carcinoma, Takashima and colleagues identified four immunoreactive proteins: Hsp70, glyceraldehydes-3-phosphate dehydrogenase, peroxiredoxin and Mn-SOD. In HCC sera, occurrence of autoantibodies against these proteins were 7/15, 5/15, 5/15 and 6/15 respectively whereas 2/20, 7/20, 0/20 and 2/20 were in control sera (Takashima et al., 2006). Li et al. identified 6 HCC-associated antigens and when the combination of the six proteins was analyzed, the sensitivity increased to 90% (Li et al., 2008). An other study revealed calreticulin, cytokeratin 8, nucleoside diphosphate kinase A and F1-ATP synthase b subunit induced autoantibodies in HCC patients, independently of their HBV, HCV status (Le et al., 2002).

In colon cancer, a panel of six TAA eliciting a serological immune response was identified. An optimal ratio between sensitivity and specificity was achieved, grouping reactivity against hnRNP AB, GRP94 and LamC for stage I-II and reactivity against Act4, VCP and AldA for stage III-IV (De et al., 2008).

The same approach was performed for acute leukemia (Cui et al., 2005), for lung squamous carcinoma (Li et al., 2006b), for cutaneous lymphoma (Forgber et al., 2009), for melanoma (Suzuki et al., 2010) and for ovarian cancer (Taylor et al., 2009).

OBJECTIVES

A tumor is composed of tumor cells but also of other cell types including bone marrow-derived cells, endothelial cells and immune cells which composed along with the extracellular matrix the so-called “tumor microenvironment”. The latter is permanently remodelled under the influence of cytokines, proteases, inflammatory signals promoting tumor growth in a first-line and metastasis spreading thereafter. In this work, we studied the influence of a variety of components of the tumor microenvironment, including angiogenesis, hypoxia and secreted cytokines on the humoral and cellular immune responses and how this may influence tumor growth and metastases formation. This work was carried out in a translational research perspective through the development, optimization and use of dedicated proteomics technologies and with the objective to identify new cancer biomarkers and new therapeutic targets.

1. Influence of the anti-cancer humoral response on the nature and titer of circulating autoantibodies used as biomarkers of tumor growth and metastases.

Antibodies directed against tumor-associated antigens circulate in the blood flow of patients in the early and late stages of the disease. Identifying these antibodies may therefore be of interest to diagnose cancer, to improve prognosis and to optimize anti-cancer therapies. These antibodies are directed against different types of antigens, including overexpressed, mutated or mislocalized proteins. Changes in the tumor microenvironment are likely to influence the abundance and the nature of these antigens and thereby to alter the humoral immune response. The development of the tumor vasculature and the consecutive changes in the access of immune cells to the tumor parenchyma is an example of how tumor biology may influence the interpretation of changes in autoantibody titer. At the opposite, in non-vascularized tumor areas, hypoxia should influence the nature of TAA and therefore gives rise to specific serological profiles. The impact of treatments on the tumor microenvironment should also not be underestimated. By inducing myelotoxicity,

chemotherapy may indeed alter the production of autoantibodies while radiotherapy may lead to dramatic perturbation in the repertoire of TAA.
In this part of our work, we first (1.1) used the Lewis Lung carcinoma (LLc) mouse model to evaluate the impact of angiogenesis, chemotherapy and radiotherapy on the titer of paradigmatic autoantibody (directed against GRP78) and (1.2) the mouse mammary tumor MDA-MB-231 model to examine the influence of hypoxia on the serological proteome.

2. Influence of the primary tumor secretome on the metastatic progression

Tumor cells secrete different factors in the extracellular matrix but also in the blood flow. These factors are able to induce the remodelling of the tumor microenvironment facilitating local invasion. Moreover, they are able to act at distance and to recruit bone marrow-derived cells, including endothelial progenitor cells (EPC). EPC are described as key players in tumor angiogenesis through a direct integration into new forming vessels (a process called adult vasculogenesis) or by secreting pro-angiogenic factors stimulating migration and proliferation of endothelial cells originating from pre-existing vessels. In the current work, we focused our attention on a possible role of these cells on metastasis progression (i.e. independently of their role in the tumor vascularization). We used the melanoma B16F10-luciferase mouse model to track the metastasis formation via bioluminescence imaging and studied the influence of EPC on metastasis development.

In the two parts of this study, we used proteomics technologies, SERPA for autoantibodies identification and 2D-DIGE to dissect the proteome of EPC.

RESULTS

Results of this work are summarized in three papers.

1. Defresne F, Bouzin C, Guilbaud C, Dieu M, Delaive E, Michiels C, Raes M, Feron O.
Differential influence of anticancer treatments and angiogenesis on the seric titer of autoantibody used as tumor and metastasis biomarker.
Neoplasia. 2010 Jul;12(7):562-70.

2. Defresne F, Grandjean M, Guilbaud C, Samain J, Feron O.
Hypoxia-driven identification of tumor autoantibodies in a breast cancer mouse model.
In preparation

3. Defresne F, Bouzin C, Grandjean M, Dieu M, Raes M, Hatzopoulos AK, Kupatt C, Feron O.
Preconditioned endothelial progenitor cells reduce the formation of melanoma metastases through SPARC-driven cell-cell interaction and endocytosis.
Cancer Res 2011, accepted.

1. Differential influence of anticancer treatments and angiogenesis on the seric titer of autoantibody used as tumor and metastasis biomarker.

Defresne F, Bouzin C, Guilbaud C, Dieu M, Delaive E, Michiels C, Raes M, Feron O.
Neoplasia. 2010 Jul;12(7):562-70.

Additional informations on GRP78

The endoplasmic reticulum (ER) is a crucial organelle for the synthesis and folding of secretory and membrane proteins. It is also a major intracellular Ca^{++} storage compartment. Stress conditions lead to the unfolded protein response (UPR), consisting of different adaptive pathways triggered by perturbations in the ER. The consequences of the UPR are the arrest of general translation, the upregulation of chaperones and folding enzymes, and degradation of misfolded proteins (Pyrko et al., 2007). If the ER stress is too important, the ultimate step is the cell death through activation of apoptotic pathways (Lee, 2007). Cancer cells present elevated glucose metabolism with increased glycolytic activity supporting high proliferative rate. As a consequence, tumors are often characterized by acidosis and severe hypoxia (Gonzalez-Gronow et al., 2006; Reddy et al., 2003), features associated with the production of misfolded proteins in the ER, triggering the UPR (Lee, 2007).

GRP78 (Glucose-Regulated Protein 78), also called BiP (immunoglobulin heavy-chain binding protein), plays key roles in the proper folding of proteins (Melnick and Argon, 1995). This Ca^{++}-binding protein belongs to the Hsp70 protein family. Its normal localization resides in the ER but GRP78 was shown to migrate to the cell surface under stress conditions (Blass et al., 2001; Gonzalez-Gronow et al., 2006; Shin et al., 2003; Triantafilou et al., 2001). Besides anti-apoptotic properties, GRP78 prevents the aggregation of protein intermediates and targets misfolded protein to proteasomal degradation (Dong et al., 2008; Lee, 2007). For these reasons, GRP78 is described as a major regulator of the homeostasis of the ER (Figure 31).

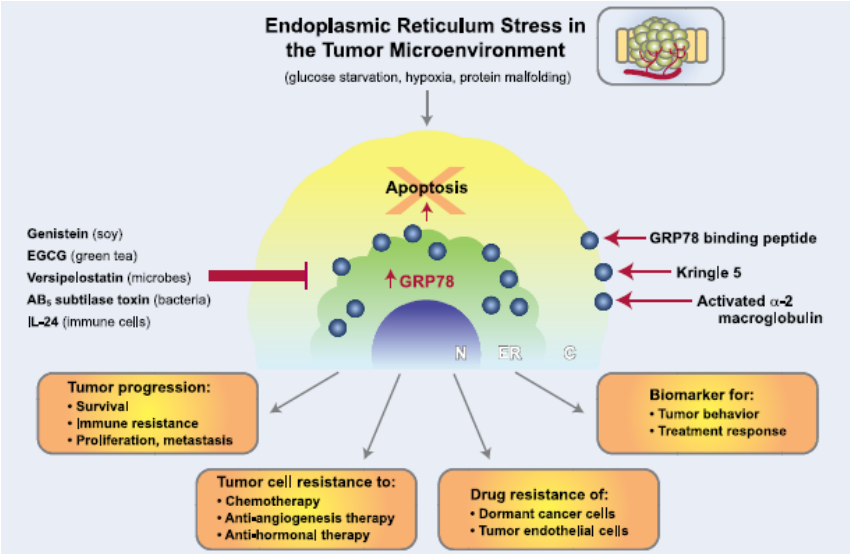

Figure 31: Endoplasmic reticulum stress induction of GRP78 in the tumor microenvironment. GRP78 facilitates tumor progression, immune resistance, metastases and drug resistance (including for dormant cancer cells and tumor endothelial cells). GRP78 has been identified as a cell surface receptor for Kringle 5 of human plasminogen and the activated form of the α2-macroglobulin. GRP78 can also serve as a conduit for cancer-specific delivery of cytotoxic agents via GRP78-binding peptides. GRP78 itself or GRP78 autoantibodies may represent novel biomarkers in stratifying patients for tumor behavior and responsiveness to treatment (Lee, 2007).

Differential influence of anti-cancer treatments and angiogenesis on the seric titer of auto-antibody used as tumor and metastasis biomarker.

Florence Defresne[1], Caroline Bouzin[1], Céline Guilbaud[1], Marc Dieu[2], Edouard Delaive[2], Carine Michiels[2], Martine Raes[2] and Olivier Feron[1]

[1] Université de Louvain, Pole of Pharmacology & Therapeutics (UCL-FATH), Angiogenesis and Cancer Research Laboratory, 52 Avenue E. Mounier, B-1200 Brussels, Belgium
[2] University of Namur-FUNDP, Unit of Research in Cellular Biology (URBC), 61 rue de Bruxelles, B-5000 Namur, Belgium

Address for correspondence: Olivier FERON, Pole of Pharmacology and Therapeutics, UCL-FATH5349, 52 Avenue E. Mounier, B-1200 Brussels, Belgium; Phone: +32-2-764 5264; Fax: +32-2-764 5269; E-mail: olivier.feron@uclouvain.be

Running title: Auto-antibody and anti-cancer treatments

Key words: auto-antibodies, tumor-associated antigens, grp78, radiotherapy, chemotherapy

ABSTRACT

Early detection of tumor-specific autoantibodies (auto-Ab) has the potential to be used for cancer screening and diagnosis. Whether auto-Ab may be useful to track metastatic progression or response to treatment is however largely unknown. To address these issues, the serological proteome was analyzed in an invasive but treatment-responsive mouse tumor model. Among 40 serum-reactive proteins identified by multiplex analysis, we chose to focus on GRP78 (Glucose-Regulated Protein 78), a chaperone protein involved in the endoplasmic reticulum stress response. We first validated GRP78 as a protein overexpressed and mislocalized in tumor cells. We then documented that an increase in GRP78 auto-Ab titer preceded the detection of a palpable tumor mass, correlated with metastatic progression and was influenced by the onset of tumor neovascularization. We also found that chemo- and radiotherapy, both leading to inhibition of tumor growth, oppositely influenced the anti-GRP78 immune response. While radiation increased the concentration of GRP78 auto-Ab by 3-fold, the auto-Ab titer was reduced in response to bolus or metronomic administration of cyclophosphamide. Finally, we established a decrease in auto-Ab-producing B lymphocytes in response to chemotherapy and the overexpression of GRP78 together with a strong Ig response in irradiated tumors. In conclusion, we identified GRP78 auto-Ab as an early marker of tumor and metastatic progressions. However, the multiple influences of anti-cancer treatments on the humoral immune system calls for caution when exploiting such auto-Ab as markers of the tumor response.

Abbreviations: auto-Ab, auto-antibody; TAA, tumor-associated antigen; SERPA, serological proteome analysis.

INTRODUCTION

Auto-antibodies (auto-Ab) are present in the blood of patients who are affected by different malignancies [1,2]. These antibodies are directed against a group of autologous cellular antigens generally known as tumor-associated antigens (TAAs) [3-5]. The expression by tumor cells of proteins which are mutated, mislocalized or produced in abnormal quantities is thought to mainly account for this humoral response. Auto-antibodies circulate for longer time than other polypeptides since they are very stable in the serum and often produced in large amounts. Their biochemical properties are well understood and many available reagents do exist for their detection. Serum profiling of circulating auto-Ab is therefore considered as a very attractive method to diagnose cancer at early stages.

Different proteomic techniques allow detecting auto-Ab and identifying TAAs: SEREX or serological expression cloning and SERPA or serological proteome analysis are among them [6-9]. These methods use patient sera to probe blotted phage expression libraries derived from tumor cells or tumor cell lysates blotted onto a membrane after 2D-gel separation, respectively. Modification of the latter involves spotting of fractionated tumor lysates onto microarrays [10] and for each of these techniques, final identification of the proteins of interest requires mass spectrometry. SERPA has the advantages to allow proteins with their post-translational modifications to be analyzed for their immunogenicity and to reveal, in a single experiment, the global reactivity of a given serum towards a tumor-derived proteome. Multiple studies have already used these techniques to identify auto-antibodies in a variety of cancers including hepatocellular carcinoma [3], colon cancer [11,12], lung cancer [13] and breast cancer [5,14].

Very little is known however about how the auto-Ab-based markers of early cancer stages do evolve when the disease progresses to metastases or when patients undergo anti-cancer treatments. In theory, the ideal auto-Ab candidate would have to be up-regulated when tumor is growing or when metastases are developing and to fall down when the patients respond to the treatment. Collateral effects of treatments on the capacity of tumor or immune cells to contribute to the auto-Ab response should however not be underestimated. Chemotherapy may for instance lead to

lymphodepletion and thereby interfere with the capacity of the humoral immune system to produce auto-Ab. Whether a reduction in auto-Ab reflects the effects of chemotherapy on tumor growth or instead acknowledges a systemic interference with the immune system needs to be addressed to fully exploit information derived from serological proteome analyses.

Here, we applied the SERPA technique to identify the fate of auto-Ab in tumor-bearing mice exposed to different treatments, including chemotherapy, radiotherapy and surgery. Such an animal model allows to reduce inter-individual serological variations under basal conditions as well as in response to treatments and to concentrate in 2-3 weeks, the life of a tumor from the primary tumor emergence to the metastases development. Using SERPA technology, we identified Glucose-Regulated Protein 78 (GRP78) as a reproducible immunogenic TAA in our mouse tumor model. A specific ELISA was developed and confirmed that increase in GRP78 auto-Ab titer was correlated with primary tumor and metastases development. Opposite variations in the GRP78 auto-Ab concentrations after chemo- and radiotherapy however pointed out how treatment-driven modulation of the immune system may interfere with the auto-Ab production and detection.

MATERIALS AND METHODS

Cells and mice.

Lewis Lung carcinoma (LLc) cells were routinely cultured in 175-mm flasks in serum containing Dulbecco's modified Eagle's medium (Invitrogen). Adult C57Bl/6J mice (Elevage Janvier, Le Genest Saint-Isle, France) received intramuscular (i.m.) injections of 10^6 syngeneic LLc cells in the posterior right leg. The tumor diameters were regularly tracked with an electronic caliper. Blood was collected for serological assays through retro-orbital or intra-cardiac routes according to the required amounts. Ten days after tumor cell injection, mice were exposed to radio- or chemotherapy. Local irradiation was administered to mice using a RT-250 device (Philips Medical Systems, Brussels, Belgium) with a dose delivery of 1.2 Gy/min. The tumor was centered in a circular irradiation field, and healthy tissues were protected by a lead mask. Two different protocols were used for chemotherapy: cyclophosphamide (Bayer) was either administered through intra-peritoneal injection of a bolus dose (100mg/kg) or added to the drinking water (renewed every three days) for a so-called metronomic administration [15] to reach a 20mg/kg/day regimen. Each procedure was approved by local authorities according to national animal care regulations.

SERPA technique.

Tumors from three different mice were pooled, lysed in DIGE Labeling (DLA) buffer (7M urea, 2M thiourea, 4% CHAPS and 30mM Tris-pH 8.5), homogenized using Ultra-Turrax T25 (IKA) and clarified by centrifugation at 12,000 *g* for 15 min at 4°C. Protein concentration was determined by the Bradford method and extracts were diluted to reach a final concentration of 5 to 10 µg/µl. pH was adjusted to 8.5 and 25 µg of each sample were labeled with 200 pmol of amine-reactive cyanine Cy5 dye (Amersham GE Healthcare) for 30 min in the dark at 4°C, according to the manufacturer's instructions. Labeling reaction was stopped by incubating the mixture for 10 min with 10 mM lysine (Sigma Aldrich) and non-labeled proteins were added to reach 300 µg. Samples were then diluted in IPG buffer (4% CHAPS, 7 M urea, 2 M thiourea, 30 mM Tris, 30 mM DTT, 1% IPG

buffer 3-11 (v/v) (Amersham GE Healthcare)) and incubated for 20 min in the dark at room temperature.

Proteins were loaded onto rehydrated 18-cm IPGstrips pH 3-11 NL for the isoelecteric focusing on the IPGphor; parameters were as follows: 300 V for 3 h, gradient steps of 1000 V for 8 h and 8000V for 3 h and 8000 V for 45 min at 20°C with a maximum current setting of 50 µA per strip. IPGstrips were subsequently incubated for 15 min with equilibration solutions [6M urea, 30% glycerol, 2% SDS, Tris 1.5M pH 8.8] supplemented with 10mg/ml DTT and 25 mg/ml iodoacetamide, respectively. First-dimension strips were then washed and loaded onto the second-dimension gels (10 % acrylamide). Electrophoresis was performed overnight at 15°C.

Separated proteins were finally transferred onto low-fluorescence PVDF membrane (200 mA for 2 h). All the materials and products were purchased from GE Healthcare, except glycerol from Sigma. Blotted 2D-membranes were incubated for 3h in 5% non-fat dry milk-containing TTBS blocking buffer, and then exposed overnight to either control mouse serum or tumor-bearing mice (dilution 1:100); a pool of sera collected from 15 different mice was used per condition. After several washes in TTBS containing 1% non-fat dry milk, membranes were incubated with horseradish peroxidase-conjugated goat anti-mouse IgG antibody (1:5000, Jackson Immunoresearch) for 2h. Note that this secondary antibody (cat # 115-035) reacts with both heavy and light chains of IgG molecules and may thus also react with other immunoglobulin classes, including IgM. Immunodetection was performed using ECL Plus (GE Healthcare) followed by scanning at the Cy2 wavelength on the Ettan Dige Imager (GE Healthcare) (see Supplementary Figure 1).

Immunoblotting and immunocytochemistry.

Collected tumors were homogenized with an Ultra-Turrax in RIPA lysis buffer containing 1% protease inhibitor cocktail. SDS-PAGE was performed as previously described on 10%-acrylamide gels and after transfer, PVDF membranes were probed overnight at 4°C with anti-GRP78 antibodies (BD Pharmingen and Cell Signaling). HRP-conjugated secondary antibody was used for detection with ECL-Plus.

For immunohistochemical analyses, frozen tumor sections were probed overnight at 4°C with anti-GRP78 antibody (Cell Signaling, dilution 1:50) or with anti-CD31 antibody (Pharmingen, dilution 1:50) after a 30 min blocking procedure in PBS containing 0.1% Tween and 5% BSA. Detection was performed with Alexa Fluor secondary antibodies (1:300 dilution); quantification was performed using ImageJ software. In some experiments, non-permeabilized tumor sections were co-stained with rhodamine-labeled wheat germ agglutinin (Vector Laboratories) to probe plasma membranes.

Laser Doppler Imaging.

Local tumor blood flow was measured with a Laser Doppler imager (Moor Instruments). Mice were anesthetized and fur was removed using a depilatory cream. The animals were placed on a heating pad (37°C) to minimize variations in temperature. The perfusion of the tumor-bearing and control legs can be evaluated on the basis of colored histogram pixels.

In-gel enzymatic digestion and mass spectrometry.

Preparative gels were performed with 300 µg unlabeled proteins according to the protocol described above for the analytical gels. 2D gels were krypton-stained (Pierce) after protein fixation. The proteins of interest were automatically picked from the gels with the Ettan Spot Picker (GE Healthcare). After rinsing, gel pieces were dehydrated in acetonitrile and further dried at 37°C for 20 min. Digestion was performed overnight with trypsin (12.5 ng/µl) in 50 mM ammonium bicarbonate. The extraction step was performed with formic acid 5% for 15 min at 37°C. Peptides were extracted with 5% formic acid at 37°C for 15 min and collected supernatants kept frozen at -20°C until mass spectrometry analysis.

Digested peptides were then processed for identification on the basis of their mass fingerprint obtained using a matrix-assisted laser desorption/ionization MX (Maldi-TOF) (Waters, Mildorf, USA) or using a nanoflow LC-ESI-MS/MS (Waters) on a CapLC Q-TOF2 mass spectrometer (Waters) (see Supplementary data for detailed information). Full-length proteins were identified with Mascot software (version 2.2) (Matrix Sciences) by sequence homology research against mouse protein databases.

GRP78 Enzyme-linked immunosorbent assay (ELISA).

Amounts of circulating auto-antibodies to GRP78 were determined by conventional ELISA. 96-well plates (Reacti-Bind, Thermo Scientific) were coated overnight at room temperature with 5 µg/ml recombinant GRP78 protein (Stressgen). Coating and blocking procedures were carried out using Ultrablock and Neptune buffers from AbD Serotec according to the manufacturer's instructions. Sera (1:100 dilution) were incubated overnight at 4°C and after washing, specific hybridation was measured with a peroxidase-conjugated anti-mouse IgG antibody (1:10 000 dilution) and addition of 3,3',5,5'-tetramethylbenzidine (TMB, Calbiochem). Plates were read at 450 nm in a VictorX4 microplate reader; calibration curve was performed for each single experiment using serial dilutions of GRP78 antibody (BD Pharmingen) (see Supplementary Figure 2).

Immunoprecipitation and immunodetection of natural IgG.

The same volumes of serum and protein G sepharose (slurry 1:1) were mixed together and incubated for 1 hour at 4°C under constant agitation. Pellets were collected from a 10,000 g centrifugation at 4°C and re-suspended in 2x Laemmli buffer. Samples were boiled for 5 minutes and centrifuged; supernatants were analysed by immunoblotting as described above. In some experiments, accumulation of natural IgG was evaluated in tumor sections using an Alexa Fluor 488 anti-mouse IgG.

Flow cytometry analysis.

Blood samples were freshly collected and red blood cells were eliminated by centrifugation on Histopaque-1083 (Sigma). Cells were then labelled with a biotin-conjugated monoclonal antibody from BD Biosciences (anti-B220, clone RA3-6B2) then with PE-conjugated streptavidin. Fluorescence signals were measured using a FACScan apparatus (BD Biosciences) and analyzed by the FlowJo software.

Statistical analysis.

Data are expressed as means ± SEM or as scatter plots. Student's t-test and one-way ANOVA were used where appropriate.

RESULTS

SERPA identification of GRP78 auto-antibodies in tumor-bearing mice

Total proteins extracted from Lewis Lung carcinoma tumors were separated by 2D-PAGE and transferred onto PVDF membranes. Pooled sera from tumor-bearing mice and control mice (n=15 per condition) were probed separately for the presence of auto-antibodies directed against tumor proteins. Multiplexing analysis was performed taking advantage of the Cy5 pre-labelling of tumor proteins and the detection of the anti-IgG peroxidase-conjugated secondary antibody in the Cy2 wavelength (see Suppl. Figure 1). The long-lasting and stable chemiluminescence from the ECL+ reagent used in our experiments gave a stable fluorescence signal. The low inter-individual variability in this mouse tumor model led to the identification of 40 serum-labelled spots on the 2D-blots. The proteins of interest were excised from preparative gels, digested with trypsin and the peptide mixtures were analyzed by MS. This led to the identification of 24 proteins with satisfying scores (see Supplementary Table), among which 12 were tumor-bearing mouse serum-*positive* (Table 1). Only four antigens however were exclusively recognized by the serum of tumor-bearing mice: glucose-regulated protein 78 (GRP78), aldolase A1, vinculin and heterogeneous nuclear ribonucleoprotein L. In the rest of the study, we chose to focus on GRP78 (also called BiP), which was the antigen giving the strongest immunoblot signal (see enlarged spot in Figure 1).

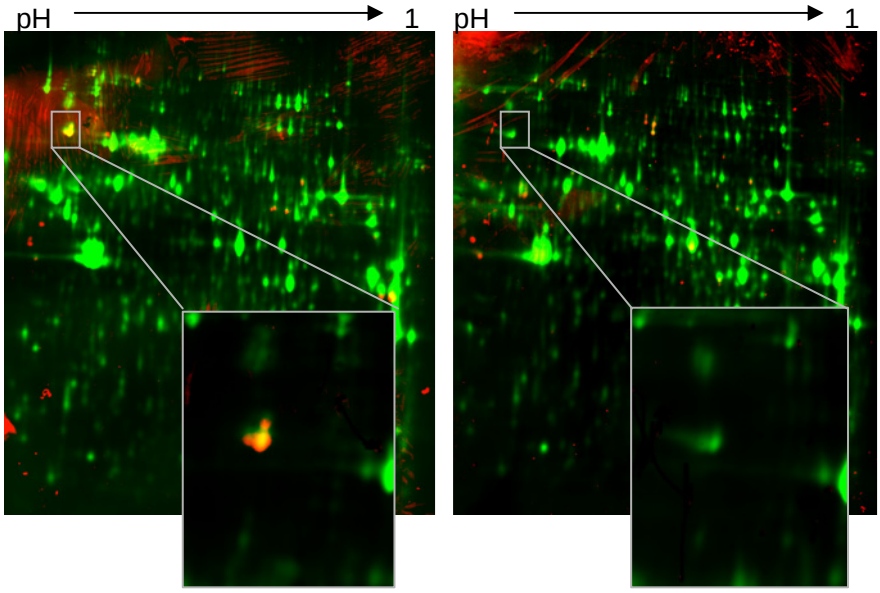

Figure 1. Serological proteome analysis of LLc tumor-bearing mice. Representative immunoblotting with pooled sera from tumor-bearing mice (left panel) or control mice (right panel) (n=15) on Cy5-labelled LLc tumor extracts; yellow/red spots correspond to proteins recognized by auto-Ab present in the sera. This experiment was repeated four times; the enlarged spot corresponds to GRP78, as confirmed following picking, trypsin digestion and consecutive MALDI identification.

Table 1. List of identified tumor proteins detected by 2D-immunobloting with the sera of tumor-bearing mice.

Proteins	pI	MW (kDa)	MASCOT score	Uniprot n°	Queries matched	sequence coverage (%)	p-value (expect)
MALDI identification							
inner membrane protein mitochondrial CRA	6,18	83	148	Q8CAQ8	34	52	1,81E-12
villin 2	5,83	69	245	P26040	41	60	4,50E-20
GRP78	4,79	72	240	P20029	36	56	1,40E-19
heat shock protein 1	4,93	84	125	P07901	29	51	1,80E-08
heterogeneous nuclear ribonucleoprotein L	6,07	70	161	Q499X2	22	47	5,70E-13
heterogeneous nuclear ribonucleoprotein K	5,39	51	119	P61979	18	41	1,80E-07
vimentin	4,77	52	225	P20152	31	59	4,50E-18
Lap 3	7,61	56	153	Q9CPY7	27	56	1,10E-10
lectin, galactose binding, soluble 3	8,50	30	122	P16110	9	80	9,10E-08
QTOF identification							
aldolase 1, A isoform	8,40	40	471	P05064	7		
procollagen lysine, 2-oxoglutarate 5-dioxygenase 3	5,81	85	389	Q9R0E1	4		
vinculin	5,88	117	1160	Q64727	16		

GRP78 auto-antigen validation

The GRP78 identification was confirmed by probing 2D-membranes with commercially available anti-GRP78 antibody (Figure 2A). We then examined by Western blotting the GRP78 expression level in LLc tumor cells and found that it amounted to more than 5-fold the abundance in the host tissue (Figure 2B). Furthermore, while in the host tissue, GRP78 was exclusively found intracellularly in agreement with its ER function, immunohistochemistry revealed that in tumor cells, GRP78 was aberrantly located at the plasma membrane (Figure 2C).

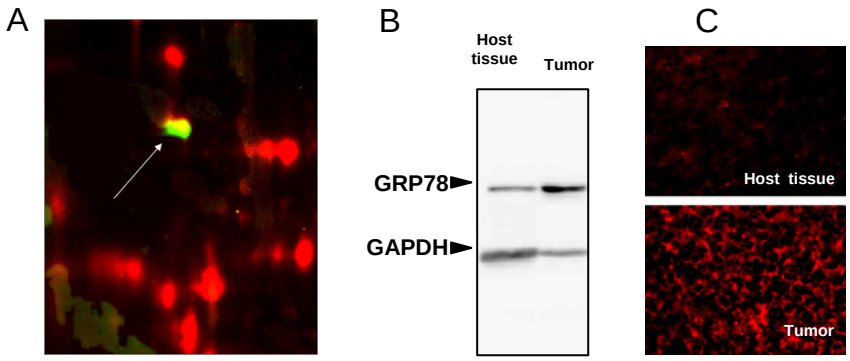

Figure 2. Validation of GRP78 as a tumor auto-antigen. **A**. Immunoblotting with commercial anti-GRP78 of the putative GRP78 spot from LLc tumor extracts separated on 2D-membranes. **B**. Representative Western blot analysis of the expression of GRP78 in host tissue and tumors (n = 4); simultaneous GAPDH immunoblotting was used as a control. **C**. Representative GRP78 immunostaining on host tissue (top) and tumor (bottom) sections; immunostaining experiments were repeated several times with similar results.

GRP78 auto-antibodies as a marker of tumor growth

An enzyme-linked immunosorbent assay (ELISA) was developed using recombinant GRP78 protein in order to confirm the presence of auto-antibodies in the serum of tumor-bearing mice and to track titer changes in response to treatments. Calibration was carried out for each ELISA assay and a linear relationship was consistently observed in the range of antibody concentration detected from the mouse serum (see Supplementary Figure 2). Blood was collected from tumor-bearing mice at days 0, 3, 7, 10, 14 and 17 post-injection (i.m.) with 10^6 tumor cells. ELISA revealed that a net increase in GRP78 auto-antibodies were detectable in the tumor-bearing mouse serum as soon as three days after tumor cell injection. Interestingly, at that early

time, tumor growth, as measured with an electronic calliper, was not yet detectable; tumors were actually palpable from day 7 (Figure 3B). GRP78 auto-Ab signal remained stable from day 3 to day 7 post-injection but peaked at day 10; values detected at days 14 and 17 were barely higher than those observed at day 7. Since day 10 is usually the time required for angiogenesis to become functional, we examined the difference in endothelial staining using anti-CD31 antibody and blood flow around this period. We confirmed a significant increase in large, mature blood vessels at day 14 *vs.* a punctate, angiogenic pattern at day 7 (Figure 3E). A dramatic increase in tumor blood flow was also observed between days 7 and 14, as determined using Laser Doppler imaging (Figure 3F).

In other series of animals aimed to examine the impact of metastases spreading on the anti-GRP78 titer, we stimulated the development of dormant lung metastases by surgically removing the primary tumor (when reaching a 8 mm-diameter), as previously documented in this tumor model [16]. Interestingly, while a net increase in anti-GRP78 antibody was observed 9 days post-surgery (Figure 3C), the detection of metastases required 5 to 10 more days [see day 14 (6 mice out of 9) and day 19 in Figure 3D]. Between days 14 and 19, more than 50% of the mice died because of lung metastases. Interestingly, among the mice alive at day 19, the anti-GRP78 levels were usually in the low percentile range (see Figure 3C).

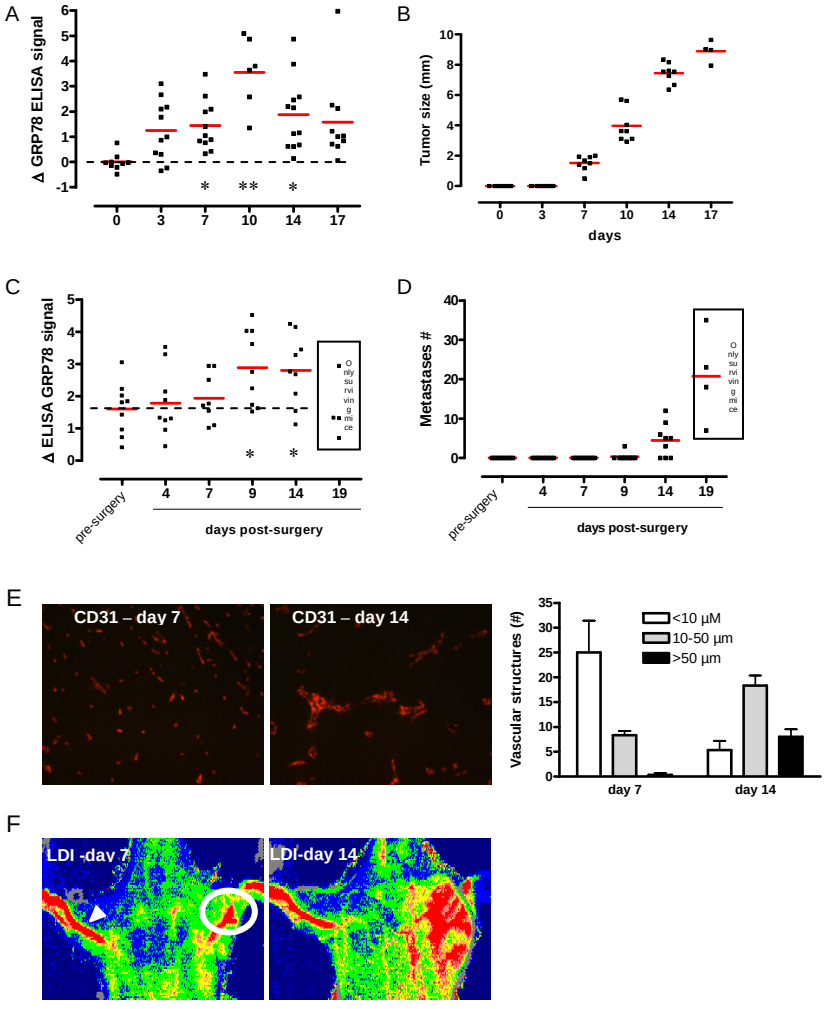

Figure 3. Changes in the titer of anti-GRP78 auto-Ab as a marker of primary tumor growth and metastases. A. GRP78-specific ELISA was performed from sera collected through retro-orbital bleeding of mice before (day 0) and after (days 3, 7, 10, 14 and 17) tumor cell injection. Results are presented as scatter plots; *P<0.05, **P<0.01. **B.** Tumors diameters as measured with a caliper. **C**. GRP78-specific ELISA was performed at the indicated time after primary tumor removal to activate lung metastases. Results are presented as scatter plots; *P<0.05. **D**. Number of lung metastases identified by histological analysis of lungs collected from tumor-bearing mice at the indicated time pre- and post-surgery. Note that at day 19 in panels C and D, only data arising from surviving animals are presented. **E.** Representative CD31 immunostaining of tumor sections at days 7 and 14. Histogram represents the distribution of CD31-positive vascular structures according the indicated sizes. **F.** Representative laser Doppler imaging (LDI) pictures from LLc tumor-bearing mice at day 7 and 14 post-injection of tumor cells. The average perfusions of the tumor-bearing leg (see white circle) and of the control leg (see arrowhead) can be evaluated on the basis of colored histogram pixels.

Impact of radio- and chemotherapy on GRP78 auto-antibody titer.

To study the impact of treatments on the expression of GRP78 auto-antibodies, we chose radio- and chemotherapy regimens. Accordingly, tumor-bearing mice were exposed to 16 Gy radiations, 100mg/kg cyclophosphamide administered i.p. (bolus, two injections at 5-day interval) or low dose cyclophosphamide in the drinking water (the so-called metronomic chemotherapy). The radiotherapy and bolus cyclophosphamide are known to exert profound anti-tumor effects, as confirmed in Figure 4A and 4C, respectively. Metronomic cyclophosphamide therapy is a therapeutic scheme proposed to have a better benefit/toxicity balance than conventional MTD (maximal tolerated dose) regimen [15]. In this study, we observed an initial response of the tumor to metronomic cyclophosphamide but a loss of efficacy on the longer term (Figure 4E). ELISA revealed that radiotherapy led to an increase in circulating anti-GRP78, peaking at 5-fold the level observed 5 days before the radiation exposure (Figure 4B). Of note, local irradiation of control animals (ie, without tumor) failed to lead to any changes in anti-GRP78 concentrations (not shown). Chemotherapy gave rise to an opposite pattern with a significant reduction of anti-GRP78 auto-Ab concentration (Figures 4D and 4F). Note the continuous decrease in anti-GRP78 auto-Ab with metronomic chemotherapy despite the lesser inhibitory effect of this drug regimen on tumor growth (see Figure 4F).

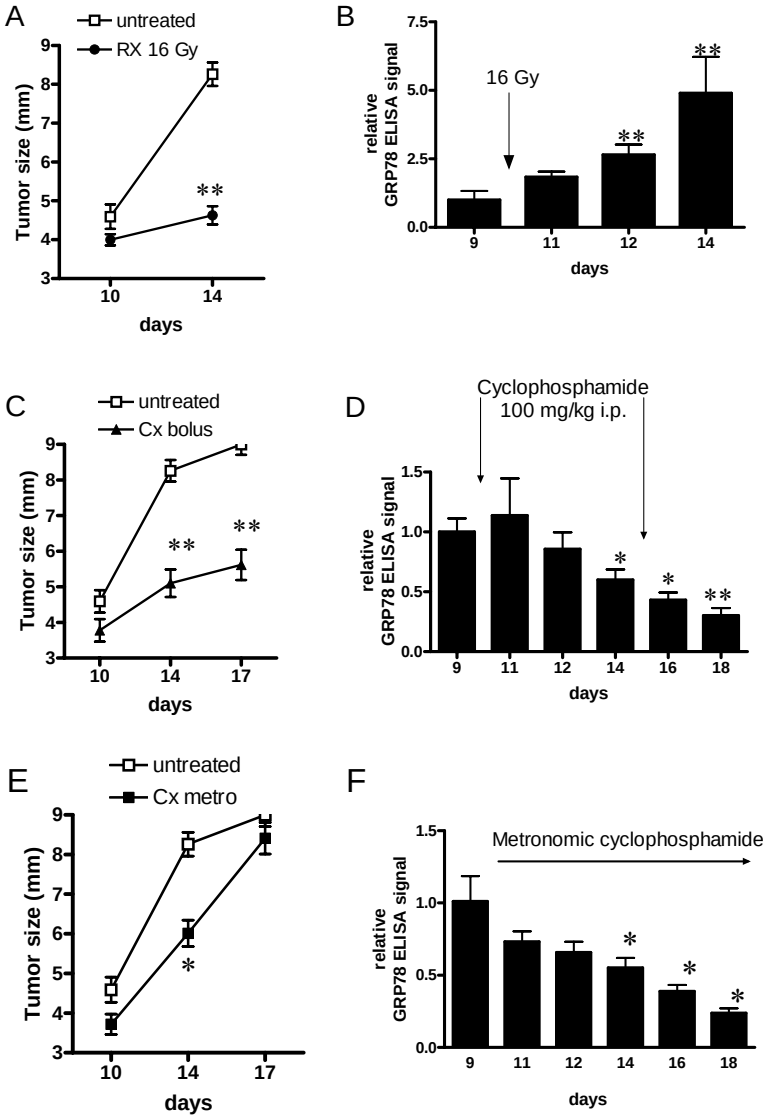

Figure 4. Differential influence of radio- and chemotherapy on GRP78 auto-antibodies titer. Changes in tumor growth and seric GRP78 auto-Ab signal (detected by ELISA) observed after radiotherapy, or cyclophosphamide under bolus (100 mg/kg i.p.) or metronomic (through the drinking water) administrations. Panels **A**, **C** and **E** show the effects of either treatment on tumor growth; **p<0.01 *vs* day 10. Bar graphs represent the effects of either treatment on GRP78 auto-Ab signal from tumor-bearing (Panels **B**, **D**, **F**). *p<0.05, **p<0.01 *vs* day 9 (before treatment administration).

Immune response towards the different treatments

To understand the reasons of the decrease in anti-GRP78 auto-Ab post-chemotherapy, we evaluated whether systemic cytotoxic effects of cyclophosphamide could influence the humoral response by antibody-producing lymphocytes. We therefore used flow cytometry to evaluate potential changes in the extent of B cells in treated *vs* untreated tumor-bearing mice (Figure 5A). We observed that while radiotherapy did not alter the amounts of B-220-positive B cells, cyclophosphamide administration led to a 20-50% reduction in B cells (Figure 5B). The reduction in B cell numbers post-chemotherapy did correlate with a reduction in the extent of circulating IgG as determined by immunoprecipitation from cyclophosphamide-exposed mouse sera (Figure 5C). Since radiotherapy led to a similar reduction in circulating IgG despite a maintained amount of B cells, we further examined whether antibodies could be trapped into the irradiated tumor. Figure 5D shows that overall detection of IgG from tumor sections was indeed significantly increased in response to radiotherapy (*vs* untreated tumors, n=5). Immunohistochemical analysis of the same tumor sections further revealed that GRP78 expression was also dramatically increased in irradiated tumors (Figure 5D).

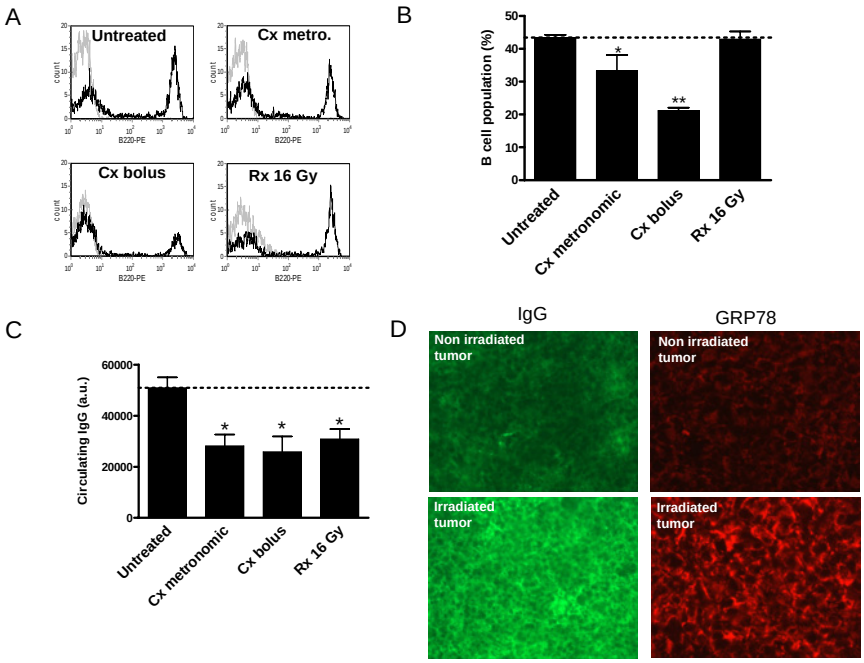

Figure 5. Humoral immune responses of tumor-bearing mice to radio- or chemotherapy. B cell number determination from the blood of control or treated tumor-bearing mice (see Figure 4 legend for treatment details): representative flow cytometry analyses of B220-expressing blood cells **(A)** and quantification **(B)** are presented; *p<0.05, **p<0.01 (n = 3). **C.** Changes in the total amounts of circulating IgG were also determined after immunoprecipitation from the blood of tumor-bearing mice; *p<0.05 (n = 3). **D.** Representative pictures of immunohistochemical analyses of tumor sections documenting the trapping of IgG (left) or the extent of GRP78 protein expression (right) in non-irradiated (top) or irradiated (bottom) tumors. These experiments were repeated on 5 different tumors per condition with similar results; staining and optic conditions were strictly identical between untreated and irradiated tumors.

DISCUSSION

The major findings of this study are that (i) increase in circulating anti-GRP78 auto-Ab is associated with the detection of primary tumor and metastases at earlier times than with palpation and microscopic analysis of the invaded tissues, respectively; (ii) chemo- and radiotherapy have opposite impact on the extent of circulating anti-GRP78 auto-Ab, prompting caution in interpreting changes in auto-Ab titers in response to anticancer treatments; (iii) Cy-dyes multiplex analysis may optimize the SERPA workflow.

An increasing number of studies report the identification of auto-Ab in cancer patients as potential new biomarkers for cancer detection and prognosis [1-14]. Although several good candidates are making their route toward validation in larger studies, a variable proportion of patients with a given cancer type are usually positive for the considered auto-Ab. The large majority of these studies aiming to identify auto-Ab as new cancer biomarkers are carried out by comparing sera of cancer patients with the sera of healthy volunteers or patients with cancer-predisposing diseases (eg, polyps, cirrhosis, viral infection). The status of patients at the time of the serum collection is therefore variable and the influence of treatments (targeting cancer or pre-cancerous lesions) is rarely integrated in the interpretation of the results. Another related issue is the potential and reliability of auto-Ab-based markers to follow the response to treatments. From a theoretical point of view, eradication of a tumor should lead to a decrease in tumor-associated antigens and thus in the corresponding circulating auto-Ab.

Here, we used a mouse tumor model to work with a more condensed process of tumor growth and consecutive metastatic spreading than what is observed in the course of the disease in humans. Such an animal model also allows to reduce the inter-individual variability observed with patients. A multiplex analysis was further applied to optimize the detection of auto-Ab, through the co-registration of the Cy5 staining of tumor cell proteins separated on 2D-gels and the Cy2-channel detection of the ECL-driven chemiluminescence from the peroxidase-conjugated secondary antibody. This multiplex strategy which advantageously replaced the conventional approach matching the immunoblot with Coomassie blue- or silver-stained gels, led

us to identify a rather limited number of spots. From the short list of proteins selectively recognized by the sera of tumor-bearing mice, we have selected GRP78 (ie, the highest immune signal after serum immunoblotting) to address the issues of changes in auto-Ab titer with metastatic spreading and treatments.

GRP78, a member of the heat shock protein 70 (Hsp70) family, plays key roles in the endoplasmic reticulum (ER) stress response [17]. In tumor cells, ER stress is a common phenomenon observed in response to nutrient deprivation, acidosis or hypoxia [18]. In these hostile conditions, GRP78 facilitates proper protein folding and targets misfolded protein for proteasome degradation [18,19]. Shedding of GRP78 protein was reported to sign the presence of cancer [18] and a recent study identified critical roles of GRP78 in tumor cell survival and angiogenesis [19]. Interestingy, anti-GRP78 auto-antibodies were recently identified as biomarkers of the clinical progression of prostate [20,21] and ovarian cancers [22]. In these human studies, serum reactivity against GRP78 correlated positively with natural cancer progression, allowing to discriminate between organ-confined, locally advanced and metastatic prostate cancers [20] and between early stages and stages III/IV of ovarian cancer [21]. The choice of anti-grp78 as a generic auto-antibody detected in our mouse tumor model appears therefore supported by clinical data validating this marker of cancer progression. In our study, the immunogenicity of GRP78 is likely to find its origin in the overexpression and the mislocalization of GRP78 at the plasma membrane of tumor cells (see Figure 2). Importantly, we showed that anti-GRP78 auto-Ab was detected in the serum of mice well before the detection of the tumor by palpation or caliper measurements (see Figures 3A and 3B).

Taking advantage of the induction of dormant lung metastases after the removal of the primary tumor [16], we showed that an increase in anti-GRP78 auto-Ab concentrations was detectable at a time when microscopic evaluation of the lungs failed to identify metastases (see Figures 3C and 3D). These results give credential to the use of anti-GRP78 antibody as early biomarkers of both primary tumor emergence and activation of dormant metastases following surgery. We found however that the titer of circulating anti-GRP78 auto-Ab did not increase linearly with the tumor burden (see Figures 3A and 3B). In particular, the onset of a

functional vascularization in the tumor (see Figures 3E and 3F) was associated with an acute increase in auto-Ab detection (see day 10 in Figure 3A).

The data establishing GRP78 as a key immunogenic protein in our tumor model led us to evaluate whether anti-GRP78 auto-Ab could also be exploited as a marker of the response to radio- and chemotherapy. Although we used a 16 Gy irradiation and bolus cyclophosphamide that inhibited tumor growth to the same extent (see Figures 4A and 4C), we found that chemotherapy administration was associated with a reduction in the serum titer of anti-GRP78 antibodies whereas radiotherapy increased it (see Figures 4B and 4D). We found that the decrease in anti-GRP78 auto-Ab (and circulating Ig in general) following cyclophosphamide administration could be related to the observed net reduction in lymphocytes, in particular the antibody-producing B cell population (Figures 5A and 5B). Moreover, the metronomic scheme of cyclophosphamide administration used in this study, although less efficient to inhibit tumor growth, did not spare the anti-GRP78 titer which also decreased with time (Figure 4F). Altogether, these observations stress that myelotoxic treatments, as observed with most chemotherapeutic strategies [23-25], could be misguiding by inadequately linking reductions in tumor biomarker concentrations and in tumor mass.

By contrast, as anticipated, local irradiation of the tumor did not influence the number of B cells in treated animals. The observed radiation-driven increase in anti-GRP78 auto-Ab may instead be related to an overall increased stress response favoring the expression of functional GRP78 (as shown in Figure 5D); additional mechanisms could involve radiation-triggered degradation of GRP78 protein, thereby increasing the pool of peptides presented by the MHC class I pathway. The observed local increase in IgG abundance in the tumor (Figure 5D) and overall decrease in circulating IgG post-radiation (Figure 5C) support this hypothesis of an overall stimulated immune response. Also, the response was tumor-selective since we did not observe any increase in anti-GRP78 auto-Ab by irradiating the host tissue (in non-tumor-bearing mice) (not shown). Together with the observation that in response to radiotherapy, the circulating anti-GRP78 auto-Ab titer increased despite the overall decrease in circulating antibodies (see Figures 4B and 5C), our data

confirm that GRP78 is one of the key protein against which an immune response is mounted in tumors.

In conclusion, we identified the anti-GRP78 auto-Ab as an early seric marker of tumor and metastatic progression and showed how its titer may be differently influenced by radio- and chemotherapy. Although not excluding the use of auto-Ab as markers of response to conventional anti-cancer treatments, this study with an archetypical auto-Ab emphasizes the need to integrate factors such as B cells depletion or promotion of the antigen-presenting process to interpret the data. Our study therefore brings new insights in the process of identifying new biomarkers from the serological proteome by (i) drawing the attention to the therapeutic status of cancer patients recruited in studies aiming to identify new auto-Abs as cancer biomarkers and (ii) reporting the integration of CyDyes multiplex technology as a way to improve SERPA-based detection of tumor auto-antibodies.

ACKNOWLEDGEMENTS.

This work was supported by grants from the Fonds de la Recherche Scientifique Médicale, the Fonds national de la Recherche Scientifique (FNRS), the Télévie, the Belgian Federation Against Cancer, the J. Maisin Foundation, the Région Bruxelles-Capitale and an Action de Recherche Concertée (ARC 09/14-020) from the Communauté Française de Belgique. FD is FNRS Research Assistant and OF is FNRS Research Director.

Reference List

[1] Caron M, Choquet-Kastylevsky G, and Joubert-Caron R (2007). Cancer immunomics using autoantibody signatures for biomarker discovery. Mol. Cell Proteomics. **6,** 1115-1122.

[2] Desmetz C, Cortijo C, Mange A, and Solassol J (2009). Humoral response to cancer as a tool for biomarker discovery. J. Proteomics. **72,** 982-988.

[3] Zhang JY, Megliorino R, Peng XX, Tan EM, Chen Y, and Chan EK (2007). Antibody detection using tumor-associated antigen mini-array in immunodiagnosing human hepatocellular carcinoma. J. Hepatol. **46,** 107-114.

[4] Tan EM, and Zhang J (2008). Autoantibodies to tumor-associated antigens: reporters from the immune system. Immunol. Rev. **222,** 328-340.

[5] Lu H, Goodell V, and Disis ML (2008). Humoral immunity directed against tumor-associated antigens as potential biomarkers for the early diagnosis of cancer. J. Proteome. Res **7,** 1388-1394.

[6] Ludwig N, Keller A, Heisel S, Leidinger P, Klein V, Rheinheimer S, Andres CU, Stephan B, Steudel WI, Graf NM et al (2009). Improving seroreactivity-based detection of glioma. Neoplasia. **11,** 1383-1389.

[7] Banks RE, Craven RA, Harnden P, Madaan S, Joyce A, and Selby PJ (2007). Key clinical issues in renal cancer: a challenge for proteomics. World J. Urol. **25,** 537-556.

[8] Hardouin J, Lasserre JP, Sylvius L, Joubert-Caron R, and Caron M (2007). Cancer immunomics: from serological proteome analysis to multiple affinity protein profiling. Ann. N. Y. Acad. Sci. **1107,** 223-230.

[9] Tan HT, Low J, Lim SG, and Chung MC (2009). Serum autoantibodies as biomarkers for early cancer detection. FEBS J. **276,** 6880-6904.

[10] Kijanka G, and Murphy D (2009). Protein arrays as tools for serum autoantibody marker discovery in cancer. J. Proteomics. **72,** 936-944.

[11] De ML, Sanvito F, Olivieri S, Vigano F, Doglioni C, Frasson M, Braga M, Bachi A, Dellabona P, Protti MP et al (2008). Serological immunoreactivity against colon cancer proteome varies upon disease progression. J. Proteome. Res. **7,** 504-514.

[12] Ran Y, Hu H, Zhou Z, Yu L, Sun L, Pan J, Liu J, and Yang Z (2008). Profiling tumor-associated autoantibodies for the detection of colon cancer. Clin. Cancer Res **14,** 2696-2700.

[13] Qiu J, Choi G, Li L, Wang H, Pitteri SJ, Pereira-Faca SR, Krasnoselsky AL, Randolph TW, Omenn GS, Edelstein C et al (2008). Occurrence of autoantibodies to annexin I, 14-3-3 theta and LAMR1 in prediagnostic lung cancer sera. J. Clin. Oncol. **26,** 5060-5066.

[14] Desmetz C, Bascoul-Mollevi C, Rochaix P, Lamy PJ, Kramar A, Rouanet P, Maudelonde T, Mange A, and Solassol J (2009). Identification of a new panel of serum autoantibodies associated with the presence of in situ carcinoma of the breast in younger women. Clin. Cancer Res **15,** 4733-4741.

[15] Man S, Bocci G, Francia G, Green SK, Jothy S, Hanahan D, Bohlen P, Hicklin DJ, Bergers G, and Kerbel RS (2002). Antitumor effects in mice of low-dose (metronomic) cyclophosphamide administered continuously through the drinking water. Cancer Res. **62,** 2731-2735.

[16] O'Reilly MS, Holmgren L, Shing Y, Chen C, Rosenthal RA, Moses M, Lane WS, Cao Y, Sage EH, and Folkman J (1994). Angiostatin: a novel angiogenesis inhibitor that mediates the suppression of metastases by a Lewis lung carcinoma. Cell **79,** 315-328.

[17] Melnick J, and Argon Y (1995). Molecular chaperones and the biosynthesis of antigen receptors. Immunol. Today **16,** 243-250.

[18] Lee AS (2007). GRP78 induction in cancer: therapeutic and prognostic implications. Cancer Res. **67,** 3496-3499.

[19] Dong D, Ni M, Li J, Xiong S, Ye W, Virrey JJ, Mao C, Ye R, Wang M, Pen L et al (2008). Critical role of the stress chaperone GRP78/BiP in tumor proliferation, survival, and tumor angiogenesis in transgene-induced mammary tumor development. Cancer Res. **68,** 498-505.

[20] Mintz PJ, Kim J, Do KA, Wang X, Zinner RG, Cristofanilli M, Arap MA, Hong WK, Troncoso P, Logothetis CJ et al (2003). Fingerprinting the circulating repertoire of antibodies from cancer patients. Nat. Biotechnol. **21,** 57-63.

[21] Gonzalez-Gronow M, Cuchacovich M, Llanos C, Urzua C, Gawdi G, and Pizzo SV (2006). Prostate cancer cell proliferation in vitro is modulated by antibodies against glucose-regulated protein 78 isolated from patient serum. Cancer Res. **66,** 11424-11431.

[22] Taylor DD, Gercel-Taylor C, and Parker LP (2009). Patient-derived tumor-reactive antibodies as diagnostic markers for ovarian cancer. Gynecol. Oncol. **115,** 112-120.

[23] Machiels JP, Reilly RT, Emens LA, Ercolini AM, Lei RY, Weintraub D, Okoye FI, and Jaffee EM (2001). Cyclophosphamide, doxorubicin, and paclitaxel enhance the antitumor immune response of granulocyte/macrophage-colony stimulating factor-secreting whole-cell vaccines in HER-2/neu tolerized mice. Cancer Res. **61,** 3689-3697.

[24] Zitvogel L, Apetoh L, Ghiringhelli F, and Kroemer G (2008). Immunological aspects of cancer chemotherapy. Nat. Rev. Immunol. **8,** 59-73.

[25] Zitvogel L, Apetoh L, Ghiringhelli F, Andre F, Tesniere A, and Kroemer G (2008). The anticancer immune response: indispensable for therapeutic success? J. Clin. Invest **118,** 1991-2001.

SUPPLEMENTARY DATA

1. MATERIALS AND METHODS.

MALDI identification

Peptides digest were desalted on C18 Geloader pipette Tips (Proxeon Biosystems) and directly eluted on the target with a mix (1:1 v/v) of α-cyano-4-hydroxyciannamic acid (in 7:3 v/v acetonitrile/5% formic acid) and 2,5-dihydroxybenzoic acid (in 7:3 v/v acetonitrile/0.1% trifluoracetic acid). Peptide mass fingerprints were obtained using a MALDI-MX mass spectrometer (Walters, Mildorf, USA). ProteinLynx Global Server 2.2.5 (Waters) was used as peaklist generating software. Two external calibrations were used: lockmass with ADH digest and lockmass with 1618.84 Da. The trypsin autodigestion peak at 2211.1046 Da was used for the internal calibration. In house Mascot 2.2 server was used as database search engine, PMF search was performed on *Mus Musculus* subset of the National Center for Biotechnology Information non-redundant database (NCBInr; 138000 entries in 2008 sequences). Parameters for peptide matching were a peptide tolerance of 100 ppm, a maximum of one missed cleavage, carbamidomethylation was allowed as a fixed modification and oxidation of methionine was allowed as a variable modification. For all protein identifications, a minimal individual score of 64 (identity score) and expect value below 1 were used for the identification criteria.

QTOF identification

Peptides were analyzed by using a nanoflow LC-ESI-MS/MS (Waters) instrument on a CapLC Q-TOF2 mass spectrometer (Waters). The digests were separated by reverse phase liquid chromatography using a 75-µm x 150-mm reverse phase NanoEase column (Waters) in a CapLC (Waters) liquid chromatography system. Mobile phase A was 95% 0.1% formic acid in water and 5% acetonitrile. Mobile phase B was 0.1% formic acid in acetonitrile. The digest (1 µl) was injected, and the organic content of the mobile phase was increased linearly from 5% B to 40% in 40 min and from 40% B to 100% B in 5 min. The column effluent was connected to a

PicoTip emitter (New Objective) inside the Q-TOF source. Peptides were analyzed in data-dependent acquisition mode on a Q-TOF2 (Waters) instrument. In a survey scan, MS spectra were acquired for 1 s in the m/z range between 450 and 1500. For MS/MS raw data, peak lists were created using Distiller (Matrix Science) and in house Mascot 2.2 (Matrix Science) server was used as database search engine. Enzyme specificity was set to trypsin, and the maximum number of missed cleavages per peptide was set at 1. Carbamidomethylation was allowed as a fixed modification, and oxidation of methionine was allowed as a variable modification. Mass tolerance for the monoisotopic precursor peptide window and MS/MS tolerance window were set to ±0.3 Da. We also specified ESI-Q-TOF as instrument. The peak lists were searched against the *Mus Musculus* subset of the National Center for Biotechnology Information non-redundant (NCBInr) database (138000 entries in 2008). Control searches of all the files against the whole NCBInr database (5,454,477 entries in 2008) was used to confirm the identification. For all protein identifications in MSMS, a minimal individual peptide score of 36 (below this score no identity or homology was found for the analyzed peptides) and expect value below 1 were used for the initial identification criteria. Moreover the correlation between theoretical pI and molecular mass of the protein with the position of the corresponding spot in the 2D gel was also taken into account.

2. RESULTS.

We identified 40 serum-labelled spots on the 2D-blots. The proteins of interest were excised from preparative gels, digested with trypsin and the peptide mixtures were analyzed by MS. This led to the identification of 24 different proteins with satisfying scores (see criteria above) [see Supplementary Table below], among which 12 were recognized by pooled sera of tumor-bearing mice. The extensive data sets corresponding to the identification of the tumor serum-*positive* antigens is provided in the associated Excel file (Supplementary data sets).

Supplementary Table.

Table W1. List of identified tumor proteins detected by two-dimensional immunoblot analysis with the sera of control and/or tumor-bearing mice.

	Proteins recognized by control mouse serum	Proteins recognized by tumor-bearing mouse serum
inner membrane protein mitochondrial, isoform CRA_a et b	+	+
Villin 2	+	+
glucose regulated protein GRP78		+
Sorting-nexin 9	+	
heat shock protein 1	+	+
heterogeneous nuclear ribonucleoprotein L		+
heterogeneous nuclear ribonucleoprotein K	+	
Lamin A/C	+	
Septin 11	+	
vimentin	+	+
Lap 3	+	+
similar to actin	+	
pyrophosphatase	+	
lectin, galactose binding, soluble 3	+	+
alanyl-tRNA synthetase	+	
ubiquitin specific protease 5 (isopeptidase T)	+	
aldolase 1, A isoform		+
gamma-actin	+	
annexin A11	+	
heat shock protein HSP 90 -beta Hsp 84	+	
procollagen-lysine, 2-oxoglutarate 5-dioxygenase 3	+	+
protein 40 kD	+	+
gelsolin-like capping protein	+	
vinculin		+

3. SUPPLEMENTARY FIGURES.

Suppl. Figure 1. Schematic overview of the multiplex-based detection of auto-Ab.
Cy5-labelling of tumor extracts is co-registered with ECL (enhanced chemiluminescence)-based detection of the peroxidase-conjugated secondary antibody using the Cy2 channel detection.

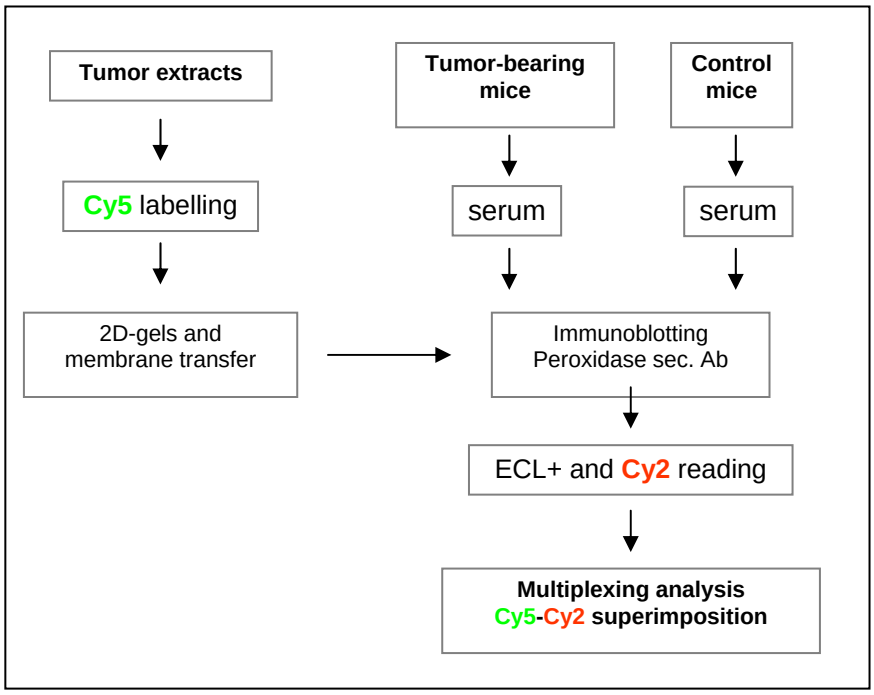

Suppl. Figure 2. Representative anti-GRP78 ELISA calibration.
96-well plates coated with 5 µg/ml recombinant GRP78 protein (Stressgen) were used. Specific hybridation using serial dilutions of GRP78 antibody (BD Pharmingen) was measured with a peroxidase-conjugated anti-mouse IgG antibody (1:10 000 dilution) and addition of 3,3',5,5'-tetramethylbenzidine (TMB, Calbiochem). Plates were read at 450 nm in a VictorX4 microplate reader.

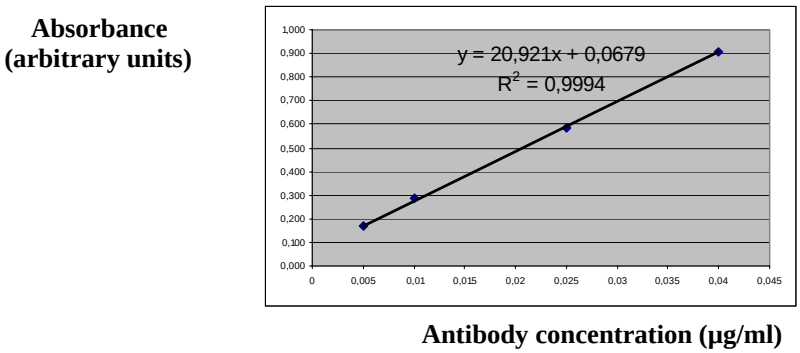

Table W2. List of tumor antigens and related digested peptides identified on basis of their mass fingerprint

inner membrane protein, mitochondrial, isoform CRA_a and CRA_b

Score: **169** Expect: **1.8e-012**

Number of unique mass values matched: **34**

Sequence Coverage: **52%**

Start-End	Observed	Mr(expt)	Mr(calc)	ppm	Miss	Sequence
85 - 101	1805.9049	1804.8976	1804.9797	-45	0	K.LFGMVLGSAPYTVPLPK.K Oxidation
102 - 110	953.5324	952.5251	952.5706	-48	0	K.KPVQSGPLK.I
131 - 158	2777.3716	2776.3643	2776.3879	-9	1	K.TKGDTPASAAGDTLSVPAPAVQHEDTIK.T
169 - 183	1617.7565	1616.7492	1616.7166	20	0	K.STSETTEEAFSSSVR.E
184 - 193	1153.6104	1152.6031	1152.5887	13	0	R.ERPPEEVAAR.L
219 - 238	2031.1125	2030.1052	2030.1008	2	0	R.TSSVTLQTITAQNAAVQAVK.A
293 - 301	1064.5860	1063.5787	1063.5583	19	1	K.MKTIIEDAK.K Oxidation (M)
295 - 302	917.4857	916.4784	916.5229	-49	1	K.TIIEDAKK.R
304 - 318	1493.7893	1492.7820	1492.7634	12	0	R.EIAGATPHITAAEGR.L
319 - 331	1509.7992	1508.7919	1508.8021	-7	0	R.LHNMIVDLDNVVK.K
319 - 331	1525.8120	1524.8047	1524.7970	5	0	R.LHNMIVDLDNVVK.K Oxidation (M)
319 - 332	1653.8451	1652.8378	1652.8920	-33	1	R.LHNMIVDLDNVVKK.V Oxidation (M)
342 - 354	1527.8447	1526.8374	1526.8205	11	0	K.VVSQYHELVVQAR.D
359 - 373	1699.8602	1698.8529	1698.8828	-18	1	R.KELDSITPDITPGWK.G
360 - 373	1571.7997	1570.7924	1570.7879	3	0	K.ELDSITPDITPGWK.G
360 - 378	2046.0180	2045.0107	2045.0139	-2	1	K.ELDSITPDITPGWKGMTGK.L
379 - 393	1662.8756	1661.8683	1661.8485	12	0	K.LSTDDLNSLIAHAHR.R
394 - 400	914.5229	913.5156	913.5093	7	1	R.RIDQLNR.E
411 - 419	1080.6227	1079.6154	1079.5975	17	0	K.QHIELALEK.H
469 - 478	1119.5969	1118.5896	1118.5581	28	0	R.QAAAHTDHLR.D
490 - 499	1229.6070	1228.5997	1228.5612	31	0	K.YEFEQGLSEK.L
500 - 508	1150.6001	1149.5928	1149.5666	23	0	K.LSEQELEFR.R
500 - 509	1306.6755	1305.6682	1305.6677	0	1	K.LSEQELEFRR.R
511 - 528	2089.9753	2088.9680	2088.9422	12	0	R.SQEQMDSFTLDINTAYAR.L
511 - 528	2105.9668	2104.9595	2104.9371	11	0	R.SQEQMDSFTLDINTAYAR.L Oxidation
531 - 547	1823.9110	1822.9037	1822.8809	13	0	R.GIEQAVQSHAVAEEEAR.K
531 - 548	1951.9814	1950.9741	1950.9759	-1	1	R.GIEQAVQSHAVAEEEARK.A
548 - 560	1522.8652	1521.8579	1521.8667	-6	1	R.KAHQLWLSVEALK.Y
549 - 564	1903.9325	1902.9252	1903.0025	-41	1	K.AHQLWLSVEALKYSMK.T
565 - 583	1930.0057	1928.9984	1928.9877	6	0	K.TSSAEMPTIPLGSAVEAIR.V
565 - 583	1946.0005	1944.9932	1944.9826	5	0	K.TSSAEMPTIPLGSAVEAIR.V Oxidation
584 - 606	2534.2175	2533.2102	2533.2119	-1	0	R.VNCSDNEFTQALTAAIPPESLTR.G
607 - 615	1053.5651	1052.5578	1052.5138	42	0	R.GVYSEETLR.A
627 - 635	1090.5702	1089.5629	1089.5601	3	1	R.RVAMIDETR.N
656 - 672	2003.0452	2002.0379	2002.0411	-2	0	K.QLKPPAELYPEDINTFK.L
673 - 691	2153.0630	2152.0557	2152.0510	2	0	K.LLSYASYCIEHGDLELAAK.F
702 - 709	1015.5961	1014.5888	1014.5611	27	1	R.RVAQDWLK.E

villin 2

Score: **245** Expect: **4.5e-020**

Number of unique mass values matched: **45**
Sequence Coverage: **60%**

Start - End	Observed	Mr(expt)	Mr(calc)	ppm	Miss	Sequence
9 - 27	2082.0090	2081.0017	2080.9987	1	0	R.VTTMDAELEFAIQPNTTGK.Q Oxidation
28 - 35	976.5739	975.5666	975.5389	28	0	K.QLFDQVVK.T
41 - 53	1660.8175	1659.8102	1659.7933	10	0	R.EVWYFGLQYVDNK.G
65 - 72	916.5323	915.5250	915.5138	12	1	K.VSAQEVRK.E
72 - 79	989.5712	988.5639	988.5342	30	1	R.KENPVQFK.F
73 - 81	1164.5922	1163.5849	1163.6087	-20	1	K.ENPVQFKFR.A
82 - 100	2237.0789	2236.0716	2236.1263	-24	1	R.AKFYPEDVAEELIQDITQK.L
84 - 100	2038.0107	2037.0034	2036.9942	5	0	K.FYPEDVAEELIQDITQK.L
108 - 133	2809.3713	2808.3640	2808.3891	-9	0	K.DGILSDEIYCPPETAVLLGSYAVQAK.F
140 - 151	1439.7047	1438.6974	1438.6510	32	1	K.EMHKSGYLSSER.L Oxidation
144 - 156	1505.7611	1504.7538	1504.7998	-31	1	K.SGYLSSERLIPQR.V
152 - 162	1364.7168	1363.7095	1363.7394	-22	1	R.LIPQRVMDQHK.L
163 - 171	1204.6127	1203.6054	1203.5632	35	1	K.LSRDQWEDR.I
172 - 180	1175.6383	1174.6310	1174.5996	27	0	R.IQVWHAEHR.G
185 - 193	1085.5432	1084.5359	1084.5110	23	0	K.DSAMLEYLK.I Oxidation (M)
194 - 209	1946.9786	1945.9713	1945.9495	11	0	K.IAQDLEMYGINYFEIK.N
194 - 209	1962.9620	1961.9547	1961.9444	5	0	K.IAQDLEMYGINYFEIK.N Oxidation
238 - 246	1104.6127	1103.6054	1103.5764	26	0	K.IGFPWSEIR.N
247 - 254	965.5443	964.5370	964.4978	41	1	R.NISFNDKK.F
255 - 262	959.5816	958.5743	958.5851	-11	0	K.FVIKPIDK.K
255 - 263	1087.7021	1086.6948	1086.6801	14	1	K.FVIKPIDKK.A
263 - 273	1310.7156	1309.7083	1309.6819	20	1	K.KAPDFVFYAPR.L
264 - 273	1182.6233	1181.6160	1181.5869	25	0	K.APDFVFYAPR.L
280 - 293	1793.8982	1792.8909	1792.8422	27	0	R.ILQLCMGNHELYMR.R Oxidation (M)
280 - 293	1809.8549	1808.8476	1808.8372	6	0	R.ILQLCMGNHELYMR.R 2 Oxidation
295 - 306	1488.8021	1487.7948	1487.7766	12	1	R.RKPDTIEVQQMK.A Oxidation
296 - 306	1332.6926	1331.6853	1331.6755	7	0	R.KPDTIEVQQMK.A Oxidation
296 - 310	1742.8824	1741.8751	1741.9145	-23	1	R.KPDTIEVQQMKAQAR.E
317 - 327	1401.7443	1400.7370	1400.7259	8	1	K.QLERQQLETEK.K
321 - 328	1003.5543	1002.5470	1002.5345	12	1	R.QQLETEKK.R
343 - 350	1063.5746	1062.5673	1062.5379	28	1	R.EKEELMLR.L Oxidation (M)
372 - 379	987.5424	986.5351	986.5032	32	0	K.ALQLEEER.R
372 - 380	1143.6357	1142.6284	1142.6043	21	1	K.ALQLEEERR.R
382 - 393	1416.6907	1415.6834	1415.6640	14	1	R.AQEEAERLEADR.M
413 - 427	1651.8317	1650.8244	1650.8100	9	0	K.SQEQLAAELAEYTAK.I
428 - 435	914.5594	913.5521	913.5232	32	0	K.IALLEEAR.R
428 - 436	1070.6385	1069.6312	1069.6243	6	1	K.IALLEEARR.R
438 - 448	1484.7191	1483.7118	1483.6691	29	1	R.KEDEVEEWQHR.A
439 - 448	1356.6317	1355.6244	1355.5742	37	0	K.EDEVEEWQHR.A
449 - 458	1116.6097	1115.6024	1115.5822	18	1	R.AKEAQDDLVK.T
530 - 542	1472.8320	1471.8247	1471.7994	17	0	R.QLLTLSNELSQAR.D
548 - 559	1493.7607	1492.7534	1492.6841	46	0	R.THNDIIHNENMR.Q
548 - 559	1509.7062	1508.6989	1508.6790	13	0	R.THNDIIHNENMR.Q Oxidation
578 - 586	1138.5610	1137.5537	1137.5124	36	1	K.QRIDEFEAM.-
578 - 586	1154.5375	1153.5302	1153.5074	20	1	K.QRIDEFEAM.- Oxidation (

heat shock protein 5, GRP78, BiP

Score: **240** Expect: **1.4e-019**

Number of unique mass values matched: **36**
Sequence Coverage: **56%**

Start-End	Observed	Mr(expt)	Mr(calc)	ppm	Miss	Sequence
51 - 61	1228.6202	1227.6129	1227.6207	-6	0	R.VEIIANDQGNR.I
62 - 75	1566.7715	1565.7642	1565.7726	-5	0	R.ITPSYVAFTPEGER.L
83 - 97	1677.8042	1676.7969	1676.8006	-2	0	K.NQLTSNPENTVFDAK.R
83 - 98	1833.9252	1832.9179	1832.9017	9	1	K.NQLTSNPENTVFDAKR.L
103 - 114	1430.6766	1429.6693	1429.6838	-10	0	R.TWNDPSVQQDIK.F
124 - 139	1732.9292	1731.9219	1731.9519	-17	1	K.KTKPYIQVDIGGGQTK.T
125 - 139	1604.8522	1603.8449	1603.8570	-8	0	K.TKPYIQVDIGGGQTK.T
140 - 153	1536.7827	1535.7754	1535.7905	-10	0	K.TFAPEEISAMVLTK.M
140 - 153 (M)	1552.7710	1551.7637	1551.7854	-14	0	K.TFAPEEISAMVLTK.M Oxidation
165 - 182	2016.0774	2015.0701	2015.0589	6	1	K.KVTHAVVTVPAYFNDAQR.Q
166 - 182	1887.9794	1886.9721	1886.9639	4	0	K.VTHAVVTVPAYFNDAQR.Q
183 - 198	1645.8024	1644.7951	1644.8617	-40	1	R.QATKDAGTIAGLNVMR.I
187 - 198	1217.6151	1216.6078	1216.6234	-13	0	K.DAGTIAGLNVMR.I
187 - 198 (M)	1233.6101	1232.6028	1232.6183	-13	0	K.DAGTIAGLNVMR.I Oxidation
199 - 214	1659.8882	1658.8809	1658.8879	-4	0	R.IINEPTAAAIAYGLDK.R
199 - 215	1815.9974	1814.9901	1814.9890	1	1	R.IINEPTAAAIAYGLDKR.E
263 - 269	903.4670	902.4597	902.4684	-10	0	R.VMEHFIK.L
263 - 269	919.4646	918.4573	918.4633	-7	0	R.VMEHFIK.L Oxidation (M)
299 - 307	997.5024	996.4951	996.5101	-15	0	R.ALSSQHQAR.I
308 - 325	2149.0159	2148.0086	2147.9899	9	0	R.IEIESFFEGEDFSETLTR.A
326 - 337	1512.7393	1511.7320	1511.7442	-8	1	R.AKFEELNMDLFR.S
326 - 337 (M)	1528.7340	1527.7267	1527.7391	-8	1	R.AKFEELNMDLFR.S Oxidation
328 - 337	1313.6123	1312.6050	1312.6122	-5	0	K.FEELNMDLFR.S
328 - 337	1329.6118	1328.6045	1328.6071	-2	0	K.FEELNMDLFR.S Oxidation (M)
354 - 368	1588.8383	1587.8310	1587.8468	-10	1	K.KSDIDEIVLVGGSTR.I
355 - 368	1460.7462	1459.7389	1459.7518	-9	0	K.SDIDEIVLVGGSTR.I
378 - 387	1210.5690	1209.5617	1209.5778	-13	1	K.EFFNGKEPSR.G
448 - 465	1965.0668	1964.0595	1964.0215	19	1	K.KSQIFSTASDNQPTVTIK.V
449 - 465	1836.9268	1835.9195	1835.9265	-4	0	K.SQIFSTASDNQPTVTIK.V
466 - 475	1191.6201	1190.6128	1190.6295	-14	0	K.VYEGERPLTK.D
476 - 493	1934.0173	1933.0100	1933.0058	2	0	K.DNHLLGTFDLTGIPPAPR.G
494 - 511	1999.0449	1998.0376	1998.0786	-21	0	R.GVPQIEVTFEIDVNGIIR.V
534 - 541	986.5020	985.4947	985.5080	-13	0	R.LTPEEIER.M
542 - 554	1525.6866	1524.6793	1524.6766	2	1	R.MVNDAEKFAEEDK.K
564 - 574	1316.6240	1315.6167	1315.6295	-10	0	R.NELESYAYSLK.N
564 - 580	1972.0381	1971.0308	1970.9585	37	1	R.NELESYAYSLKNQIGDK.E
593 - 602	1193.6044	1192.5971	1192.5645	27	1	K.ETMEKAVEEK.I
603 - 618	1974.9236	1973.9163	1973.9007	8	0	K.IEWLESHQDADIEDFK.A
603 - 620	2174.0360	2173.0287	2173.0327	-2	1	K.IEWLESHQDADIEDFKAK.K
623 - 634	1397.7736	1396.7663	1396.7813	-11	0	K.ELEEIVQPIISK.L
635 - 655	2177.9883	2176.9810	2176.9648	7	1	K.LYGSGGPPPTGEEDTSEKDEL.-

heat shock protein 1

Score: **129** Expect: **1.8e-008**

Number of unique mass values matched: **29**
Sequence Coverage: **51%**

Start - End	Observed	Mr(expt)	Mr(calc)	ppm	Miss	Sequence
42 - 58	1949.9768	1948.9695	1949.0105	-21	1	K.EIFLRELISNSSDALDK.I
47 - 60	1560.8112	1559.8039	1559.8155	-7	1	R.ELISNSSDALDKIR.Y
59 - 69	1308.6798	1307.6725	1307.6721	0	1	K.IRYESLTDPSK.L
75 - 84	1163.6835	1162.6762	1162.6710	5	0	K.ELHINLIPSK.Q
75 - 87	1562.8463	1561.8390	1561.8576	-12	1	K.ELHINLIPSKQDR.T
88 - 100	1349.6902	1348.6829	1348.7272	-33	0	R.TLTIVDTGIGMTK.A
88 - 100	1365.7347	1364.7274	1364.7221	4	0	R.TLTIVDTGIGMTK.A Oxidation
101 - 112	1242.7079	1241.7006	1241.6979	2	0	K.ADLINNLGTIAK.S
154 - 173	2255.9658	2254.9585	2254.9516	3	0	K.HNDDEQYAWESSAGGSFTVR.T
174 - 185	1249.6283	1248.6210	1248.5769	35	1	R.TDTGEPMGRGTK.V
186 - 201	2015.0460	2014.0387	2014.0371	1	1	K.VILHLKEDQTEYLEER.R
192 - 201	1311.6171	1310.6098	1310.5626	36	0	K.EDQTEYLEER.R
210 - 224	1778.9131	1777.9058	1777.9403	-19	0	K.HSQFIGYPITLFVEK.E
285 - 293	1151.5782	1150.5709	1150.5506	18	0	K.YIDQEELNK.T
294 - 300	901.5515	900.5442	900.5181	29	0	K.TKPIWTR.N
301 - 315	1833.7950	1832.7877	1832.7741	7	0	R.NPDDITNEEYGEFYK.S
316 - 328	1541.7775	1540.7702	1540.7522	12	0	K.SLTNDWEEHLAVK.H
329 - 339	1348.6805	1347.6732	1347.6572	12	0	K.HFSVEGQLEFR.A
347 - 356	1264.6609	1263.6536	1263.6360	14	1	R.RAPFDLFENR.K
348 - 356	1108.5677	1107.5604	1107.5349	23	0	R.APFDLFENR.K
348 - 357	1236.6509	1235.6436	1235.6299	11	1	R.APFDLFENRK.K
369 - 387	2415.1660	2414.1587	2414.1650	-3	0	R.VFIMDNCEELIPEYLNFIR.G
388 - 401	1513.8016	1512.7943	1512.7784	11	0	R.GVVDSEDLPLNISR.E
388 - 408	2374.1216	2373.1143	2373.1846	-30	1	R.GVVDSEDLPLNISREMLQQSK.I Oxidation (M)
448 - 457	1168.6049	1167.5976	1167.5632	29	0	K.LGIHEDSQNR.K
448 - 458	1296.6459	1295.6386	1295.6582	-15	1	K.LGIHEDSQNRK.K
466 - 479	1550.7599	1549.7526	1549.6970	36	0	R.YYTSASGDEMVSLK.D
487 - 500	1707.8091	1706.8018	1706.8628	-36	1	K.ENQKHIYFITGETK.D
491 - 500	1208.6445	1207.6372	1207.6237	11	0	K.HIYFITGETK.D
501 - 511	1235.6523	1234.6450	1234.5942	41	0	K.DQVANSAFVER.L

heterogeneous nuclear ribonucleoprotein L

Score: **174** Expect: **5.7e-013**

Number of unique mass values matched: **22**
Sequence Coverage: **47%**

Start - End	Observed	Mr(expt)	Mr(calc)	ppm	Miss	Sequence
29 - 46	1475.7546	1474.7473	1474.7133	23	1	R.AGAMVKMAAAGGGGGGGR.Y
29 - 46	1491.7107	1490.7034	1490.7082	-3	1	R.AGAMVKMAAAGGGGGGGR.Y Oxidation (M)
47 - 56	1029.4589	1028.4516	1028.4312	20	0	R.YYGGGNEGGR.A
63 - 94	2840.1410	2839.1337	2839.1415	-3	0	K.TENAGDQHGGGGGGGSGAAGGGGGENYDDPHK.T
95 - 104	1076.6338	1075.6265	1075.6138	12	0	K.TPASPVVHIR.G
176 - 186	1204.5929	1203.5856	1203.5480	31	0	K.ISRPGDSDDSR.S
226 - 243	1993.9883	1992.9810	1992.9687	6	1	R.KNGVQAMVEFDSVQSAQR.A
226 - 243	2009.9849	2008.9776	2008.9636	7	1	R.KNGVQAMVEFDSVQSAQR.A Oxidation (M)
227 - 243	1865.9003	1864.8930	1864.8738	10	0	K.NGVQAMVEFDSVQSAQR.A
227 - 243	1881.8894	1880.8821	1880.8687	7	0	K.NGVQAMVEFDSVQSAQR.A Oxidation (M)
246 - 261	1729.8187	1728.8114	1728.7811	18	0	K.ASLNGADIYSGCCTLK.I
262 - 269	977.5530	976.5457	976.5341	12	0	K.IEYAKPTR.L
275 - 300	2890.2610	2889.2537	2889.2550	-0	1	K.NDQDTWDYTNPNLSGQGDPGSNPNKR.Q
342 - 350	907.4661	906.4588	906.4494	10	0	R.MGPPVGGHR.R
342 - 350	923.4672	922.4599	922.4443	17	0	R.MGPPVGGHR.R Oxidation
342 - 351	1063.5692	1062.5619	1062.5505	11	1	R.MGPPVGGHRR.G
342 - 351	1079.5763	1078.5690	1078.5454	22	1	R.MGPPVGGHRR.G Oxidation
396 - 408	1588.7927	1587.7854	1587.7756	6	0	R.VFNVFCLYGNVEK.V
396 - 410	1815.9719	1814.9646	1814.9389	14	1	R.VFNVFCLYGNVEKVK.F
414 - 431	1867.8966	1866.8893	1866.8604	15	0	K.SKPGAAMVEMADGYAVDR.A
414 - 431	1883.8937	1882.8864	1882.8553	17	0	K.SKPGAAMVEMADGYAVDR.A Oxidation (M)
414 - 431	1899.8689	1898.8616	1898.8502	6	0	K.SKPGAAMVEMADGYAVDR.A 2 Oxidation (M)
432 - 445	1634.8174	1633.8101	1633.8035	4	0	R.AITHLNNNFMFGQK.M
432 - 445	1650.8053	1649.7980	1649.7984	-0	0	R.AITHLNNNFMFGQK.M Oxidation (M)
453 - 472	2187.9920	2186.9847	2186.9612	11	0	K.QPAIMPGQSYGLEDGSCSYK.D
453 - 472	2203.9854	2202.9781	2202.9562	10	0	K.QPAIMPGQSYGLEDGSCSYK.D Oxidation (M)
453 - 478	2909.2666	2908.2593	2908.2644	-2	1	K.QPAIMPGQSYGLEDGSCSYKDFSESR.N
539 - 549	1208.5940	1207.5867	1207.5721	12	0	R.SSSGLLEWDSK.S
550 - 565	1866.8724	1865.8651	1865.8982	-18	0	K.SDALETLGFLNHYQMK.N
550 - 565	1882.8845	1881.8772	1881.8931	-8	0	K.SDALETLGFLNHYQMK.N Oxidation (M)
566 - 576	1263.6481	1262.6408	1262.6295	9	0	K.NPNGPYPYTLK.L
577 - 586	1121.5149	1120.5076	1120.4971	9	0	K.LCFSTAQHAS.-

heterogeneous nuclear ribonucleoprotein K

Score: **119** Expect: **1.8e-007**

Number of unique mass values matched: **18**
Sequence Coverage: **41%**

Start - End	Observed	Mr(expt)	Mr(calc)	ppm	Miss	Sequence
22 - 34	1579.7118	1578.7045	1578.6984	4	0	K.RPAEDMEEEQAFK.R
22 - 34	1595.7205	1594.7132	1594.6933	12	0	K.RPAEDMEEEQAFK.R Oxidation (M)
22 - 35	1735.8105	1734.8032	1734.7995	2	1	K.RPAEDMEEEQAFKR.S
22 - 35	1751.8088	1750.8015	1750.7944	4	1	K.RPAEDMEEEQAFKR.S Oxidation (M)
36 - 46	1349.6874	1348.6801	1348.6405	29	1	R.SRNTDEMVELR.I
38 - 46	1106.5227	1105.5154	1105.5074	7	0	R.NTDEMVELR.I
70 - 86	1780.8070	1779.7997	1779.7911	5	0	R.TDYNASVSVPDSSGPER.I
87 - 102	1714.9431	1713.9358	1713.9764	-24	0	R.ILSISADIETIGEILK.K
87 - 103	1843.0535	1842.0462	1842.0713	-14	1	R.ILSISADIETIGEILKK.I
140 - 148	1098.4559	1097.4486	1097.4448	4	0	K.GSDFDCELR.L
149 - 163	1518.9264	1517.9191	1517.9293	-7	0	R.LLIHQSLAGGIIGVK.G
180 - 191	1549.6561	1548.6488	1548.6450	2	0	K.LFQECCPHSTDR.V
192 - 201	1053.6368	1052.6295	1052.6342	-4	0	R.VVLIGGKPDR.V
208 - 219	1340.7977	1339.7904	1339.7962	-4	0	K.IILDLISESPIK.G
306 - 316	1194.6909	1193.6836	1193.6921	-7	0	R.NLPLPPPPPPR.G
317 - 325	997.4449	996.4376	996.4335	4	0	R.GGDLMAYDR.R
317 - 326	1153.5441	1152.5368	1152.5346	2	1	R.GGDLMAYDRR.G
317 - 326	1169.5442	1168.5369	1168.5295	6	1	R.GGDLMAYDRR.G Oxidation (M)
378 - 396	1917.0377	1916.0304	1916.0255	3	0	R.GSYGDLGGPIITTQVTIPK.D
423 - 433	1259.6279	1258.6206	1258.5677	42	0	K.IDEPLEGSEDR.I
434 - 456	2589.3845	2588.3772	2588.3810	-1	0	R.IITITGTQDQIQNAQYLLQNSVK.Q

vimentin

Score: **225** Expect: **4.5e-018**

Number of unique mass values matched: **31**
Sequence Coverage: **59%**

Start - End	Observed	Mr(expt)	Mr(calc)	ppm	Miss	Sequence
59 - 77	2126.0708	2125.0635	2125.0579	3	0	R.LLQDSVDFSLADAINTEFK.N
81 - 93	1587.8036	1586.7963	1586.7900	4	1	R.TNEKVELQELNDR.F
85 - 93	1115.5687	1114.5614	1114.5618	-0	0	K.VELQELNDR.F
110 - 119	1169.7110	1168.7037	1168.7067	-3	0	K.ILLAELEQLK.G
110 - 123	1539.9098	1538.9025	1538.9032	-0	1	K.ILLAELEQLKGQGK.S
124 - 135	1497.7247	1496.7174	1496.6929	16	1	K.SRLGDLYEEEMR.E
126 - 135	1254.5704	1253.5631	1253.5598	3	0	R.LGDLYEEEMR.E
126 - 135	1270.5632	1269.5559	1269.5547	1	0	R.LGDLYEEEMR.E Oxidation
151 - 164	1688.8242	1687.8169	1687.8199	-2	1	R.VEVERDNLAEDIMR.L
151 - 164 Oxidation (M)	1704.8322	1703.8249	1703.8148	6	1	R.VEVERDNLAEDIMR.L
156 - 164	1076.5090	1075.5017	1075.4968	5	0	R.DNLAEDIMR.L
167 - 176	1303.6754	1302.6681	1302.6601	6	1	R.EKLQEEMLQR.E
167 - 176	1319.6547	1318.6474	1318.6551	-6	1	R.EKLQEEMLQR.E Oxidation
169 - 176	1046.5367	1045.5294	1045.5226	7	0	K.LQEEMLQR.E
169 - 187	2324.1113	2323.1040	2323.1114	-3	1	K.LQEEMLQREEAESTLQSFR.Q
177 - 187	1296.6482	1295.6409	1295.5993	32	0	R.EEAESTLQSFR.Q
204 - 215	1405.7172	1404.7099	1404.7500	-29	0	K.VESLQEEIAFLK.K
204 - 216	1533.8573	1532.8500	1532.8450	3	1	K.VESLQEEIAFLKK.L
263 - 272	1309.6221	1308.6148	1308.5986	12	0	K.NLQEAEEWYK.S
273 - 284	1308.6484	1307.6411	1307.6469	-4	1	K.SKFADLSEAANR.N
275 - 284	1093.5385	1092.5312	1092.5200	10	0	K.FADLSEAANR.N
294 - 301	1081.5227	1080.5154	1080.4948	19	1	K.QESNEYRR.Q
302 - 314	1490.7515	1489.7442	1489.7446	-0	0	R.QVQSLTCEVDALK.G
302 - 322	2377.1685	2376.1612	2376.1591	1	1	R.QVQSLTCEVDALKGTNESLER.Q
326 - 344	2200.9910	2199.9837	2199.9742	4	0	R.EMEENFALEAANYQDTIGR.L
326 - 344 Oxidation (M)	2216.9970	2215.9897	2215.9691	9	0	R.EMEENFALEAANYQDTIGR.L
345 - 358	1734.8265	1733.8192	1733.8076	7	1	R.LQDEIQNMKEEMAR.H
345 - 358 Oxidation (M)	1750.8184	1749.8111	1749.8025	5	1	R.LQDEIQNMKEEMAR.H
345 - 358 Oxidation (M)	1766.8461	1765.8388	1765.7974	23	1	R.LQDEIQNMKEEMAR.H 2
362 - 370	1121.5856	1120.5783	1120.5764	2	0	R.EYQDLLNVK.M
371 - 381	1295.6661	1294.6588	1294.6591	-0	0	K.MALDIEIATYR.K
371 - 381 Oxidation (M)	1311.6470	1310.6397	1310.6540	-11	0	K.MALDIEIATYR.K
371 - 382	1423.7529	1422.7456	1422.7540	-6	1	K.MALDIEIATYRK.L
382 - 390	1060.5632	1059.5559	1059.5560	-0	1	R.KLLEGEESR.I
391 - 404	1557.9036	1556.8963	1556.8926	2	0	R.ISLPLPTFSSLNLR.E
405 - 419	1682.8700	1681.8627	1681.8523	6	0	R.ETNLESLPLVDTHSK.R
405 - 420	1838.9209	1837.9136	1837.9534	-22	1	R.ETNLESLPLVDTHSKR.T
431 - 446	1836.8154	1835.8081	1835.7922	9	0	R.DGQVINETSQHHDDLE.-

Lap3

Score: **151** Expect: **1.1e-010**

Number of unique mass values matched: **27**
Sequence Coverage: **56%**

Start - End	Observed	Mr(expt)	Mr(calc)	ppm	Miss	Sequence
1 - 11	1215.6342	1214.6269	1214.6845	-47	0	-.MYLLPLPAAAR.V
1 - 11	1231.6321	1230.6248	1230.6794	-44	0	-.MYLLPLPAAAR.V
Oxidation (M)						
35 - 43	933.5963	932.5890	932.5695	21	0	K.GLVLGIYAK.D
67 - 79	1467.8285	1466.8212	1466.8279	-5	1	K.LREMLNISGPPLK.A
67 - 79	1483.8193	1482.8120	1482.8228	-7	1	K.LREMLNISGPPLK.A
Oxidation (M)						
69 - 79	1198.6508	1197.6435	1197.6427	1	0	R.EMLNISGPPLK.A
69 - 79	1214.6564	1213.6491	1213.6376	9	0	R.EMLNISGPPLK.A
Oxidation (M)						
85 - 103	2063.0933	2062.0860	2062.0888	-1	0	R.TFYGLHQDFPSVVVVGLGK.R
105 - 118	1571.7098	1570.7025	1570.6648	24	0	R.SAGVDDQENWHEGK.E
105 - 122	2083.9670	2082.9597	2082.9355	12	1	R.SAGVDDQENWHEGKENIR.A
177 - 188	1341.6648	1340.6575	1340.6361	16	0	K.LHGSGDLEAWEK.G
189 - 200	1232.6888	1231.6815	1231.6673	12	0	K.GVLFASGQNLAR.H
201 - 214	1613.7680	1612.7607	1612.7337	17	0	R.HLMESPANEMTPTR.F
201 - 214	1629.7711	1628.7638	1628.7287	22	0	R.HLMESPANEMTPTR.F
Oxidation (M)						
201 - 214	1645.7744	1644.7671	1644.7236	26	0	R.HLMESPANEMTPTR.F 2
Oxidation (M)						
238 - 253	1840.9200	1839.9127	1839.8713	23	0	K.SWIEEQEMGSFLSVAK.G
238 - 253	1856.9084	1855.9011	1855.8662	19	0	K.SWIEEQEMGSFLSVAK.G
Oxidation (M)						
283 - 294	1194.6176	1193.6103	1193.6292	-16	0	K.GITFDSGGISIK.A
295 - 303	1008.4924	1007.4851	1007.4528	32	0	K.ASANMDLMR.A
304 - 321	1693.8310	1692.8237	1692.8175	4	0	R.ADMGGAATICSAIVSAAK.L
304 - 321	1709.8375	1708.8302	1708.8124	10	0	R.ADMGGAATICSAIVSAAK.L
Oxidation (M)						
322 - 342	2264.1758	2263.1685	2263.2068	-17	0	K.LNLPINIIGLAPLCENMPSGK.A
322 - 342	2280.1638	2279.1565	2279.2017	-20	0	K.LNLPINIIGLAPLCENMPSGK.A
Oxidation (M)						
343 - 351	955.5510	954.5437	954.5247	20	0	K.ANKPGDVVR.A
357 - 368	1318.6875	1317.6802	1317.6161	49	0	K.TIQVDNTDAEGR.L
369 - 384	1846.9454	1845.9381	1845.9447	-4	0	R.LILADALCYAHTFNPK.V
418 - 428	1223.6074	1222.6001	1222.5830	14	0	K.LFEASVETGDR.V
418 - 431	1664.9064	1663.8991	1663.8318	40	1	K.LFEASVETGDRVWR.M
432 - 440	1193.5958	1192.5885	1192.5699	16	0	R.MPLFEHYTR.Q
432 - 440	1209.5900	1208.5827	1208.5648	15	0	R.MPLFEHYTR.Q Oxidation
441 - 455	1686.8605	1685.8532	1685.8407	7	0	R.QVIDCQLADVNNLGK.Y
458 - 469	1195.6106	1194.6033	1194.5815	18	0	R.SAGACTAAAFLR.E
490 - 496	905.5000	904.4927	904.4654	30	0	K.DEIPYLR.K
490 - 497	1033.5830	1032.5757	1032.5604	15	1	K.DEIPYLRK.G
497 - 505	989.5490	988.5417	988.5236	18	1	R.KGMSGRPTR.T
506 - 513	1004.6306	1003.6233	1003.6066	17	0	R.TLIEFLLR.F

lectin, galactose binding, soluble 3

Score: **122** Expect: **9.1e-008**

Number of unique mass values matched: **9**
Sequence Coverage: **80%**

Start - End	Observed	Mr(expt)	Mr(calc)	ppm	Miss	Sequence
4 - 18	1658.9167	1657.9094	1657.9007	5	0	R.MLITIMGTVKPNANR.I
4 - 18	1674.9080	1673.9007	1673.8957	3	0	R.MLITIMGTVKPNANR.I
Oxidation (M)						
4 - 18	1690.8987	1689.8914	1689.8906	1	0	R.MLITIMGTVKPNANR.I 2
Oxidation (M)						
25 - 36	1429.7160	1428.7087	1428.7011	5	1	R.RGNDVAFHFNPR.F
26 - 36	1273.6036	1272.5963	1272.6000	-3	0	R.GNDVAFHFNPR.F
37 - 43	949.4670	948.4597	948.4525	8	1	R.FNENNRR.V
43 - 50	989.5470	988.5397	988.5488	-9	1	R.RVIVCNTK.Q
61 - 73	1469.7491	1468.7418	1468.7351	5	0	R.QSAFPFESGKPFK.I
74 - 84	1298.7118	1297.7045	1297.7030	1	0	K.IQVLVEADHFK.V
85 - 98	1649.8639	1648.8566	1648.8434	8	0	K.VAVNDAHLLQYNHR.M
104 - 124	2171.1120	2170.1047	2170.0940	5	0	R.EISQLGISGDITLTSANHAMI.-
104 - 124	2187.0984	2186.0911	2186.0889	1	0	R.EISQLGISGDITLTSANHAMI.-
Oxidation (M)						

aldolase 1, A isoform

Unique **Queries matched:** 7

Observed	Mr(expt)	Mr(calc)	Delta	Miss	Score	Expect	Rank	Peptide
464.1914	926.3682	926.4168	-0.0485	0	42	0.0092	1	R.CQYVTEK.V
476.2231	950.4316	950.4709	-0.0392	0	29	0.35	1	K.AAQEEYIK.R
522.7621	1043.5097	1043.5611	-0.0514	0	68	4e-005	1	R.QLLLTADDR.V
566.7627	1131.5107	1131.5706	-0.0599	0	93	1.3e-007	1	R.ALANSLACQGK.Y
666.8208	1331.6270	1331.6932	-0.0662	0	88	3.8e-007	1	K.GILAADESTGSIAK.R
745.8178	1489.6211	1489.7008	-0.0797	0	77	2.3e-006	1	R.LQSIGTENTEENR.R
549.5741	1645.7006	1645.8019	-0.1013	1	23	0.59	1	R.LQSIGTENTEENRR.F

procollagen-lysine, 2-oxoglutarate 5-dioxygenase 3

Unique **Queries matched:** 4

Observed	Mr(expt)	Mr(calc)	Delta	Miss	Score	Expect	Rank	Peptide
530.2870	1058.5595	1058.5509	0.0086	0	68	3.9e-005	1	R.TLGLGQEWR.G
535.2190	1068.4234	1068.4295	-0.0061	0	46	0.004	1	K.GVDYEGGGCR.F
619.3055	1236.5964	1236.5986	-0.0022	0	38	0.032	1	R.SEDYVELVQR.K
699.8605	1397.7064	1397.7150	-0.0087	0	108	3.2e-009	1	K.LVGPEEALSAGEAR.D

vinculin

Unique **Queries**
matched: 16

Observed	Mr(expt)	Mr(calc)	Delta	Miss	Score	Expect	Rank	Peptide
500.8037	999.5928	999.5964	-0.0036	0	72	1.6e-005	1	R.IPTISTQLK.I
511.2799	1020.5452	1020.5273	0.0178	1	50	0.0029	1	R.KLEAMTNSK.Q
537.2753	1072.5361	1072.5335	0.0025	0	55	0.00088	1	R.GQGASPVAMQK.A
545.3164	1088.6182	1088.6077	0.0105	0	85	8.6e-007	1	R.SLGEIAALTSK.L
559.8107	1117.6069	1117.5979	0.0090	0	56	0.00055	1	K.STVEGIQASVK.T
566.7986	1131.5826	1131.5706	0.0120	0	60	0.0003	1	R.TNLLQVCER.I
587.3320	1172.6494	1172.6401	0.0093	0	93	1.3e-007	1	R.ALASQLQDSLK.D
588.3175	1174.6205	1174.6016	0.0189	0	53	0.0014	1	K.MSAEINEIIR.V
592.8393	1183.6641	1183.6561	0.0080	0	47	0.0048	1	R.ELTPQVISAAR.I
618.3304	1234.6463	1234.6414	0.0050	0	60	0.00023	1	R.VMLVNSMNTVK.E
635.3468	1268.6791	1268.6725	0.0067	0	69	2.5e-005	1	K.AVAGNISDPGLQK.S
646.8314	1291.6482	1291.6330	0.0152	0	71	1.9e-005	1	K.MTGLVDEAIDTK.S
657.8700	1313.7255	1313.7303	-0.0048	0	97	4e-008	1	K.QVATALQNLQTK.T
702.8710	1403.7275	1403.7144	0.0131	0	56	0.00046	1	K.ETVQTTEDQILK.R
729.4068	1456.7990	1456.7886	0.0104	0	100	1.8e-008	1	K.AQQVSQGLDVLTAK.V
749.3532	1496.6918	1496.6855	0.0063	0	93	9.2e-008	1	R.DPNASPGDAGEQAIR.Q

2. Hypoxia-driven identification of tumor autoantibodies in a breast cancer mouse model.

Defresne F, Grandjean M, Guilbaud C, Samain J, Feron O.

In preparation

Abstract

Early diagnosis of cancer represents a major challenge to improve antitumor treatment efficiency. The serological proteome analysis (SERPA) offers the possibility to identify autoantibodies (autoAb) as a source of early cancer biomarkers. In this work, we modified this technology in order to provide a more relevant repertoire of tumor-associated antigens to detect tumor-selective autoAbs. We exposed cultured mouse MDA-MB-231 mammary tumor cells to either normoxic or hypoxic (1%O_2) conditions before lysis, separation onto 2D-PAGE and membrane blotting. Corresponding extracts were probed with the sera of either healthy or tumor-bearing mice. Only spots positive after tumor serum immunoblotting of hypoxic cell lysates were collected and identified by MS analysis. We focused on proteins described as having a defined role in signaling cascades, excluding therefore nuclear, cytoskeletal and structure proteins. We chose six of the identified proteins, namely protein disulfide-isomerase A3 (PDIA3), calponin 2 (CNN2), Obg-like ATPase 1 (OLA1), peroxiredoxin 6 (PRDX6), aminoacylase 1 (ACY1) and eukaryotic translation initiation factor 3 subunit G (EIF3G). Specific ELISA were developed and confirmed the presence of corresponding autoantibodies in the serum of tumor-bearing mice (*vs* healthy mice); the titer of these autoAbs was also shown to increase with tumor growth. In conclusion, this study provides evidence that integrating the hypoxia criteria in the SERPA technology may increase the specificity and sensitivity of this technique.

Introduction

Most advanced solid tumors present hypoxic and/or anoxic tissue areas, heterogeneously distributed within the tumor mass (Vaupel and Mayer, 2007). When the balance between supply and consumption of oxygen is impaired, hypoxic zones appear among the malignant growing cells. Tumor hypoxia areas may develop in response to (i) structural and functional abnormalities in tumor vessels (referring to acute or cycling hypoxia), (ii) a diffusion-limited oxygen delivery (referring to chronic hypoxia) and (iii) a reduced oxygen transport capacity of the blood (Vaupel and Mayer, 2007; Fukumura and Jain, 2007; Vaupel and Harrison, 2004; Brahimi-Horn et al., 2007). Tumor hypoxia can lead to two different outcomes. On one hand, cells can respond to this particular stress through antiproliferative effects. They restrict proliferation, promote differentiation, apoptosis or necrosis (Vaupel and Mayer, 2007; Vaupel, 2008). On the other hand, some tumor cells may overcome oxygen and nutrient deprivation through metabolic adaptation or stimulation of angiogenesis (Vaupel and Mayer, 2007; Vaupel, 2008).

Tumor cell responses to hypoxic stress are largely driven by the master transcription factor HIF family. As a consequence, the proteome of tumor cells is largely modified under hypoxia (*vs* normoxic conditions). The specific repertoire of tumor-associated antigens (TAA) is thus also likely to be greatly influenced by the hypoxic conditions. This issue is largely underestimated in the studies aiming to identify circulating autoantibodies as cancer biomarkers by using cultured cells extracts as a source of antigens (Kobold et al., 2010; Zhang et al., 2007; Bei et al., 2009; Robson et al., 2010). The SERPA method indeed aims to identify autoAbs by using cancer patient sera to probe tumor or tumor cell lysates blotted on membranes after 2D-PAGE separation (Caron et al., 2007; Yang et al., 2007). In this study, we showed that the reactivity of the sera of mouse bearing mammary MDA-MB-231 tumors greatly differs according to the normoxic or hypoxic conditions used to culture tumor cells before processing 2D analyses. We identified 19 hypoxic-specific TAA associated with the production of autoantibodies in tumor-bearing mice. Specific

ELISA confirmed the validity of some of these proteins to track cancer progression, and thus the interest to use hypoxia as an additional filter to unravel autoantibodies.

Materiel and methods

Cells and mice

Breast cancer cell lines MDA-MB231 cells and HEK293 cells were routinely cultured in serum containing respectively RPMI and Dulbecco's modified Eagle's medium (Invitrogen). MDA-MB231 cells were submitted to hypoxia (1% oxygen) in a hypoxic chamber Invivo2 500 (LED Techno, Belgium) for 48h. Cells were scrapped under hypoxic conditions with appropriate lysis buffer. Adult Nude NMRI nu/nu mice (Elevage Janvier, Le Genest Saint-Isle, France) received subcutaneous injections of 3.10^6 syngeneic MDA-MB231 cells in the flank. The tumor diameters were regularly tracked with an electronic caliper. Sera were collected for serological assays through retro-orbital or intra-cardiac routes according to the required amounts. Each procedure was approved by local authorities according to national animal care regulations.

SERPA technique

Cell extracts were lysed in a buffer containing 7M urea, 2M thiourea, 4% CHAPS and 30mM Tris-pH 8.5. Protein concentration was determined by Bradford assay. 300 µg of proteins were loaded onto IPGstrips pH 3-11 NL for the isofocusing on the IPGphor (300 V for 900 Vhr, 1000 V for 8h followed by 8000V for 3h45); a fraction of these proteins were labelled with Cy5 dye, according to the manufacturer's protocol (GE Healthcare). The IPGstrips were next equilibrated in a solution of 6M urea, 30% glycerol, 2% SDS, Tris 1.5M pH 8.8, containing 10mg/ml DTT and then 25 mg/ml iodoacetamide. The first-dimension strips were loaded onto the second-dimension gels (10 % acrylamide) and the migration run overnight at 15°C. The proteins were finally transferred onto low-fluorescence PVDF membrane (200 mA for 2 h). All the materials and products were purchased from GE Healthcare, except glycerol from Sigma. Blotted 2D-membranes were incubated for 3h in 5% non-fat dry milk-containg TTBS (Tween-Tris buffer saline) blocking

buffer, and then exposed overnight to either control mouse serum or tumor-bearing mice (dilution 1:100). After several washes in TTBS containing 1% non-fat dry milk, membranes were incubated with horseradish peroxidase-conjugated anti-mouse IgG antibody (1:5000, Jackson Immunoresearch) for 2h. Immunodetection was performed using ECL Plus (GE Healthcare) followed by scanning at the Cy2 wavenlength on the Ettan Dige Imager (GE Healthcare).

In-gel enzymatic digestion and mass spectrometry

The 2D gels were krypton-stained (Pierce) after protein fixation. The proteins of interest were automatically picked from the gels with the Ettan Spot Picker (GE Healthcare). After rinsing, gel pieces were dehydrated in acetonitrile at 37°C. Digestion was performed overnight at 37°C with trypsin (12.5 ng/ml) in 100 mM ammonium bicarbonate. The extraction step was performed with formic acid 5% for 15 min at 37°C. The supernatants were then used for the identification of the proteins of interest with a MALDI-TOF apparatus (MALDI MX, Waters). Proteins of interest were identified thanks to the MASCOT program (matrixscience) connected to a mouse protein databank (NCBI).

Production of recombinant proteins

Myc-DDK-tagged-ORF-plasmids were purchased from Origene for each protein of interest. Plasmids were then transfected into HEK293 cells with Lipofectamin 2000 (Invitrogen) following the manufacturer's instructions. After 48h, transfected cells were lysed and total protein extracts were loaded on purification columns made of anti-Flag resin (Sigma). After several washes with TBS, elution was performed using 150ng/µl (final concentration) of 3x-Flag solution (Sigma). Fractions were collected and protein concentration was determined by Bradford assay.

Enzyme-linked immunosorbent assay (ELISA)

Amounts of circulating autoantibodies directed against proteins of interest were determined by conventional ELISA. 96-well plates (Reacti-Bind, Thermo Scientific) were coated overnight at room temperature with 5 µg/ml recombinant protein. Coating and blocking procedures were carried out using dedicated buffers from AbD Serotec as previously described (Defresne et al., 2010). Sera (1:50 dilution) were

incubated overnight at 4°C and after washing, specific hybridation was determined with a peroxidase-conjugated anti-mouse IgG antibody (1:10 000 dilution) and addition of 3,3',5,5'-tetramethylbenzidine (TMB, Calbiochem). Plates were read at 450 nm in a VictorX4 microplate reader.

Statistical analysis

Data are expressed as means ± SEM or as whisker plots (median ± quartiles). Student's t-test and one-way ANOVA were used where appropriate.

Results

Hypoxia-driven identification of autoantibodies in MDA-MB231 mouse model

MDA-MB231 cells were exposed to hypoxia (1% oxygen) for 48h or maintained under normoxia (21% oxygen). We previously validated by 2D-DIGE analysis that after such a period of hypoxia, profound changes in the proteome of tumor cells were induced (data not shown). Tumor lysates were then processed through 2D-PAGE and transferred onto PVDF membranes. Pooled sera from tumor-bearing and control mice were then used to probe membranes. Multiplexing analysis was performed taking advantage of the Cy5 pre-labelling of tumor proteins and the detection of the anti-IgG peroxidase-conjugated secondary antibody in the Cy2 wavelength (Figure 1A). A subtractive analysis of the immunoblots was performed to identify spots only present in the experimental hypoxic lysates probed with tumor sera (Figure 1B). We identified 27 reactive spots in this particular condition (Figure 1C). The proteins of interest were excised from preparative gels, digested with trypsin and the peptide mixtures were analyzed by MALDI-TOF MS. This led to the identification of 19 proteins (Table 1). Based on the nature and the role of some of these proteins (see discussion), we chose to focus on six of them in the rest of this study, namely protein disulfide-isomerase A3 (PDIA3), calponin 2 (CNN2), Obg-like ATPase 1 (OLA1), peroxiredoxin 6 (PRDX6), aminoacylase 1 (ACY1) and eukaryotic translation initiation factor 3 subunit G (EIF3G).

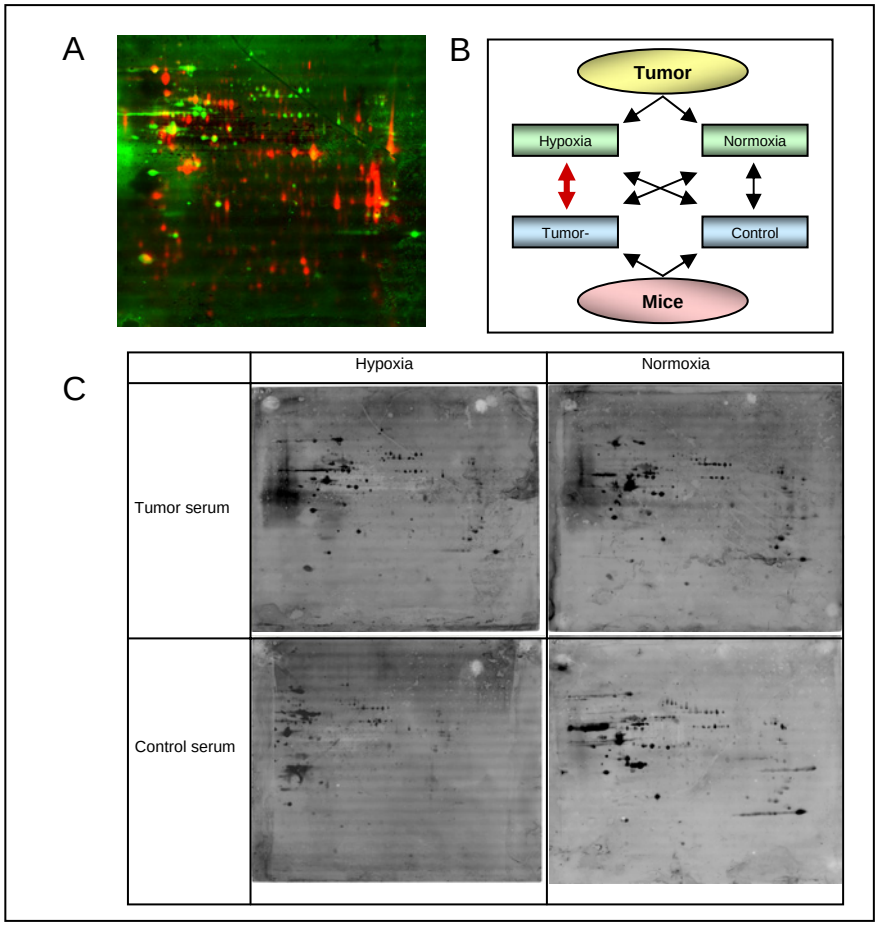

Figure 1: SERPA from MDA-MB-231 tumor-bearing mice. A. Representative multiplex immunoblots with pooled sera from tumor bearing mice (green) on hypoxic lysates (red). B. General scheme of the subtractive analysis processed to identify spots only present in the experimental hypoxic lysates probed with tumor sera. C. Comparative analysis of immunblots obtained after probing sera from tumor-bearing mice (upper panels) or control mice (lower panels) in hypoxic (left) and normoxic cell lysates (right). Analysis was repeated 2 times.

Table 1: List of identified tumor proteins detected by two-dimensional immunoblot analysis with the sera of tumor-bearing mice on hypoxic lysates.

Name	pI	MW (kDa)	Mascot score	p (expect)	queries matched	sequence coverage (%)	UNIPROT
Heat shock cognate 71 kDa protein	5,37	71082	88	3,20E-05	13	26	P11142
Sialic acid synthase	6,29	40738	147	4,10E-11	17	48	Q9NR45
Protein disulfide-isomerase A3	**5,98**	**57146**	**113**	**1,00E-07**	**18**	**33**	**P30101**
Heterogeneous nuclear ribonucleoprotein Q	8,68	69788	121	1,60E-08	23	36	O60506
Lupus La protein	6,68	46979	99	2,80E-06	10	23	P05455
Calponin-2	**6,95**	**34074**	**91**	**1,70E-05**	**14**	**43**	**Q99439**
Calcium-binding mitochondrial carrier protein SCaMC-1	6,00	53548	112	1,30E-07	16	31	Q6NUK1
Septin-11	6,36	49652	119	2,60E-08	13	29	Q9NVA2
Obg-like ATPase 1	**7,64**	**44943**	**253**	**1,00E-21**	**20**	**65**	**Q9NTK5**
Serine hydroxymethyltransferase, mitochondrial	8,76	56414	214	8,10E-18	20	44	P34897
RuvB-like 2	5,49	51296	214	8,10E-18	30	63	Q9Y230
Heterogeneous nuclear ribonucleoproteins C1/C2	4,95	33707	74	0,00078	11	32	P07910
Vimentin	5,06	53676	130	2,00E-09	20	39	P08670
Heterogeneous nuclear ribonucleoproteins A2/B1	8,97	37464	171	1,60E-13	19	57	P22626
Peroxiredoxin-6	**6,00**	**25133**	**179**	**2,60E-14**	**17**	**75**	**P30041**
Aminoacylase-1	**5,77**	**46084**	**62**	**0,013**	**8**	**19**	**Q03154**
Proteasome activator complex subunit 1	5,78	28876	150	4,10E-17	23	63	Q06323
Eukaryotic translation initiation factor 3 subunit G	**5,87**	**35874**	**111**	**1,60E-07**	**10**	**37**	**O75821**
Heterogeneous nuclear ribonucleoprotein D	7,62	38581	56	0,047	5	13	Q14103

Autoantibodies against ACY1, CNN2 and PDIA3 as markers of tumor growth

Enzyme-linked immunosorbent assays (ELISA) were then developed using recombinant proteins in order to confirm the presence of autoantibodies in the serum of tumor-bearing mice. Blood was collected from tumor-bearing mice at days 0, 7, 14, 21, 28 and 35 after s.c. injection of 3.10^6 tumor cells. Recombinant proteins were obtained after transfection of HEK cells with tagged-ORF plasmids and purified with anti-Flag affinity columns.

ELISA revealed that the titer of ACY1, CNN2, PRDX6 and PDIA3 autoantibodies were significantly higher in the tumor-bearing mouse serum whereas EIF3G and OLA1 only showed a trend towards an immunoreactivity with tumor-bearing mouse sera (Figure 2). A tumor-dependent increase in the titer of the ACY1, CNN2, PDIA3 and PRDX6 autoantibodies was further observed in parallel with tumor growth (Figure 3A and 3B).

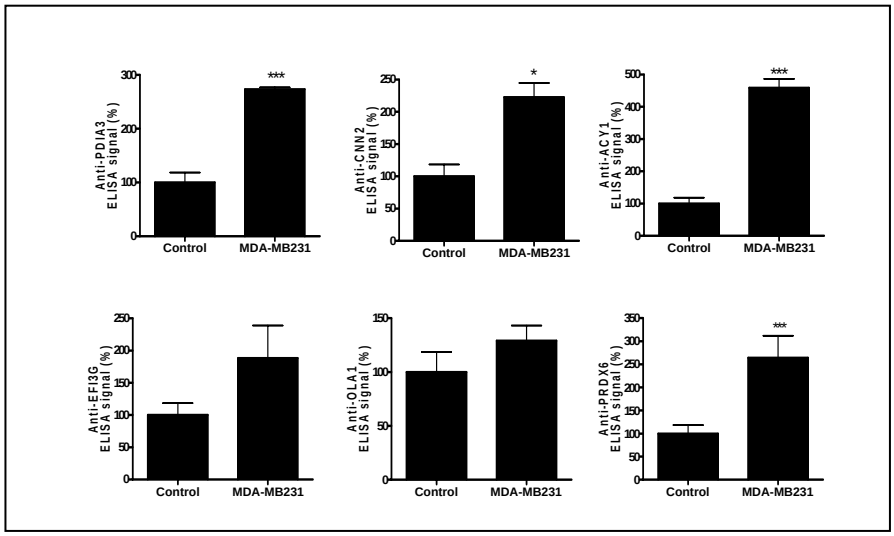

Figure 2: Changes in the titer of autoantibodies in tumor-bearing mice directed against the six proteins of interest identified by SERPA analysis. Specific PDIA3/CNN2/ACY1/EIF3G/OLA1 and PRDX6 ELISA were performed from sera collected by intracardiac punction at day 35 after tumor injection. Results are presented as bar graphs (n=3). * $p<0.05$, ** $p<0.01$, *** $p<0.001$.

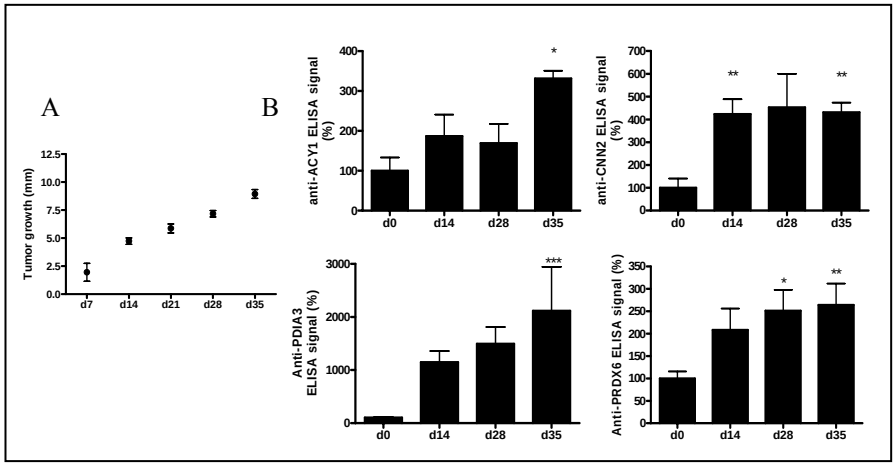

Figure 3: Anti-ACY1/CNN2/PDIA3 and PRDX6 autoantibodies as markers of tumor growth. A. Tumors diameters are measured regularly with a caliper after subcutaneous tumor injection. B. Specific ACY1/CNN2/PDIA3 and PRDX6 ELISA were performed from sera collected through retro-orbital bleeding of mice at day 0, 14, 28 and 35 after tumor injection. Results are presented as bar graphs (n=3). * $p<0.05$, ** $p<0.01$, *** $p<0.001$

Discussion

The major finding of this study is that the SERPA technology may greatly benefit from the use of tumor cells exposed to hypoxia in order to provide the most relevant antigen repertoire to detect circulating autoantibodies. Our data actually illustrate that some TAA are strictly expressed under hypoxic conditions but also that other reactive antigens collected from normoxic tumor cells disappear from the proteome of hypoxic cells. An approach based on the use of the proteome of hypoxic tumor cells may thus lead to a gain of specificity and sensitivity in the search for autoantibodies as cancer biomarkers.

In addition, our study led us to identify potentially promising hypoxia-dependent TAA. In particular, we showed that autoantibodies directed against CNN2, ACY1, PDIA3 and PRDX6 are detectable in the early stages of tumor growth. Although not previously described as hypoxia-induced proteins, these antigens were all reported to play key roles in tumor development, as briefly summarized here below. We focus our attention on proteins already described as playing defined roles in signaling cascades, excluding thus nuclear proteins, structural and cytoskeletal proteins.

Aminoacylase 1 (ACY1) is a cytosolic, homodimeric, zinc-binding enzyme that catalyzes the hydrolysis of acylated L-amino acids. ACY1 is proposed to have a tumor suppressor role in renal cell carcinoma (Zhong et al., 2009) and small cell lung cancer (Cook et al., 1998). It was further shown to be downregulated in neuroblastoma (Long et al., 2010) and in breast cancer MCF-7 (Lee et al., 2006).

Calponin 2 (CNN2) is a calcium-binding protein. Calponin tonically inhibits the ATPase activity of myosin in smooth muscle. Phosphorylation of calponin by a protein kinase, which is dependent upon calcium binding to calmodulin, releases the calponin's inhibition of the smooth muscle ATPase. Calponin 1 was shown to be upregulated after hypoxia (Zacour et al., 2002). Two studies demonstrated a positive labelling of tumors for calponin 1 (Kusafuka et al., 2010; Roy et al., 2010). Less is known about calponin 2. The sequence conservation between calponin 1 and

calponin 2 points however to a similar function. Calponin 2 was shown to play a role in cytoskeletal organization, but also in vascular development (Tang et al., 2006).

Protein disulfide isomerase family A, member 3 (PDIA3) is an isomerase enzyme (also known as GRP58 or ERp57). The PDIA3 protein has protein disulfide isomerase activity. PDIA3 is also part of the major histocompatibility complex (MHC) class I peptide-loading complex, which is essential for the formation of the final antigen conformation and export from the endoplasmic reticulum to the cell surface. Thus, it plays an important role in immune response of cells but its function in the petide-loading complex remains unclear (Komurasaki et al., 2010). This protein was shown to be upregulated in pancreatic cancer (Mikuriya et al., 2007), small cell lung cancer (Buhrens et al., 2009) and in glioma (Deighton et al., 2010). PDIA3 is necessary for the translocation of calreticulin at the membrane and for the subsequent immunogenic cell death; PDIA itself is translocated to the surface membrane (Obeid, 2008; Panaretakis et al., 2008). Interestingly, Komurasaki et al. showed that autoantibodies against ERp57 (PDIA3) were present in the sera of hepatitis patients (Komurasaki et al., 2010).

Obg-like ATPase 1 (OLA1) is a novel Obg-like ATPase. It functions as a negative regulator of the cellular antioxidant response through non-transcriptional/post-translational processes, which is distinct from most known antioxidant systems that depend on transcriptional pathways. Zhang et al published that inhibition of cancer migration and invasion could be achieved by suppression of OLA1 in breast cancer (Zhang et al., 2009).

Peroxiredoxin 6 (PRDX6) is a member of the thiol-specific antioxidant protein family. This protein is a bifunctional enzyme with two distinct active sites. It is involved in redox regulation of the cell; it can reduce H_2O_2 and short chain organic, fatty acid, and phospholipid hydroperoxides. It may play a role in the regulation of phospholipid turnover as well as in protection against oxidative injury. It promotes invasion and metastasis of lung cancer cells (Ho et al., 2010) and is increased in squamous cell carcinoma of the tongue (Huang et al., 2010). Furthermore, anti-

PRDX6 autoantibodies have already been identified in oesophageal squamous cell carcinoma (Fujita et al., 2006).

Eukaryotic translation initiation factor 3, subunit G (EIF3G) is a component of the eukaryotic translation initiation factor 3 (eIF-3) complex, which is required for several steps in the initiation of protein synthesis. EIF3 was shown to be upregulated in squamous cervival cancer (Lomnytska et al., 2010) and oral squamous cell carcinoma (Hayashi et al., 2009).

Further studies are ongoing to evaluate the reactivity of the identified mouse TAA against autoantibodies present in the sera of breast cancer patients. Other experiments are also planned to understand the cause of induction of the humoral response towards these TAA. In preliminary results obtained by Western blot with commercial antibodies (data not shown), we showed that CNN2, EIF3G, OLA1 and PRDX6 were not affected by hypoxia. PDIA3 was slighty increased whereas ACY1 appeared to be decreased, as previously described by Lee and colleagues in another model of breast cancer, MCF7 cells (Lee et al., 2006). This differential expression reinforces the principle that overexpression of TAA is not the only cause of induction of autoimmunity. Indeed, other modifications such as mislocalization or post-translational modifications (phosphorylation, glycosylation) can render the proteins immunogenic.

Reference List

Bei,R., Masuelli,L., Palumbo,C., Modesti,M., and Modesti,A. (2009). A common repertoire of autoantibodies is shared by cancer and autoimmune disease patients: Inflammation in their induction and impact on tumor growth. Cancer Lett. *281*, 8-23.

Brahimi-Horn,M.C., Chiche,J., and Pouyssegur,J. (2007). Hypoxia and cancer. J. Mol. Med. *85*, 1301-1307.

Buhrens,R.I., Amelung,J.T., Reymond,M.A., and Beshay,M. (2009). Protein expression in human non-small cell lung cancer: a systematic database. Pathobiology *76*, 277-285.

Caron,M., Choquet-Kastylevsky,G., and Joubert-Caron,R. (2007). Cancer immunomics using autoantibody signatures for biomarker discovery. Mol. Cell Proteomics. *6*, 1115-1122.

Cook,R.M., Franklin,W.A., Moore,M.D., Johnson,B.E., and Miller,Y.E. (1998). Mutational inactivation of aminoacylase-I in a small cell lung cancer cell line. Genes Chromosomes. Cancer *21*, 320-325.

Defresne,F., Bouzin,C., Guilbaud,C., Dieu,M., Delaive,E., Michiels,C., Raes,M., and Feron,O. (2010). Differential influence of anticancer treatments and angiogenesis on the seric titer of autoantibody used as tumor and metastasis biomarker. Neoplasia. *12*, 562-570.

Deighton,R.F., McGregor,R., Kemp,J., McCulloch,J., and Whittle,I.R. (2010). Glioma pathophysiology: insights emerging from proteomics. Brain Pathol. *20*, 691-703.

Fujita,Y., Nakanishi,T., Hiramatsu,M., Mabuchi,H., Miyamoto,Y., Miyamoto,A., Shimizu,A., and Tanigawa,N. (2006). Proteomics-based approach identifying autoantibody against peroxiredoxin VI as a novel serum marker in esophageal squamous cell carcinoma. Clin. Cancer Res. *12*, 6415-6420.

Fukumura,D. and Jain,R.K. (2007). Tumor microenvironment abnormalities: causes, consequences, and strategies to normalize. J. Cell Biochem. *101*, 937-949.

Hayashi,E., Kuramitsu,Y., Fujimoto,M., Zhang,X., Tanaka,T., Uchida,K., Fukuda,T., Furumoto,H., Ueyama,Y., and Nakamura,K. (2009). Proteomic profiling of differential display analysis for human oral squamous cell carcinoma: 14-3-3 sigma Protein is upregulated in human oral squamous cell carcinoma and dependent on the differentiation level. Proteomics. Clin. Appl. *3*, 1338-1347.

Ho,J.N., Lee,S.B., Lee,S.S., Yoon,S.H., Kang,G.Y., Hwang,S.G., and Um,H.D. (2010). Phospholipase A2 activity of peroxiredoxin 6 promotes invasion and metastasis of lung cancer cells. Mol. Cancer Ther. *9*, 825-832.

Huang,C.F., Sun,Z.J., Zhao,Y.F., Chen,X.M., Jia,J., and Zhang,W.F. (2010). Increased expression of peroxiredoxin 6 and cyclophilin A in squamous cell carcinoma of the tongue. Oral Dis.

Kobold,S., Lutkens,T., Cao,Y., Bokemeyer,C., and Atanackovic,D. (2010). Autoantibodies against tumor-related antigens: incidence and biologic significance. Hum. Immunol. *71*, 643-651.

Komurasaki,R., Imaoka,S., Tada,N., Okada,K., Nishiguchi,S., and Funae,Y. (2010). LKM-1 sera from autoimmune hepatitis patients that recognize ERp57, carboxylesterase 1 and CYP2D6. Drug Metab Pharmacokinet. *25*, 84-92.

Kusafuka,K., Itoh,H., Sugiyama,C., and Nakajima,T. (2010). Low-grade salivary duct carcinoma of the parotid gland: report of a case with immunohistochemical analysis. Med. Mol. Morphol. *43*, 178-184.

Lee,S.U., Kim,B.T., Min,Y.K., and Kim,S.H. (2006). Protein profiling and transcript expression levels of heat shock proteins in 17beta-estradiol-treated human MCF-7 breast cancer cells. Cell Biol. Int. *30*, 983-991.

Lomnytska,M.I., Becker,S., Hellman,K., Hellstrom,A.C., Souchelnytskyi,S., Mints,M., Hellman,U., Andersson,S., and Auer,G. (2010). Diagnostic protein marker patterns in squamous cervical cancer. Proteomics. Clin. Appl. *4*, 17-31.

Long,P.M., Stradecki,H.M., Minturn,J.E., Wesley,U.V., and Jaworski,D.M. (2010). Differential aminoacylase expression in neuroblastoma. Int. J. Cancer.

Mikuriya,K., Kuramitsu,Y., Ryozawa,S., Fujimoto,M., Mori,S., Oka,M., Hamano,K., Okita,K., Sakaida,I., and Nakamura,K. (2007). Expression of glycolytic enzymes is increased in pancreatic cancerous tissues as evidenced by proteomic profiling by two-dimensional electrophoresis and liquid chromatography-mass spectrometry/mass spectrometry. Int. J. Oncol. *30*, 849-855.

Obeid,M. (2008). ERP57 membrane translocation dictates the immunogenicity of tumor cell death by controlling the membrane translocation of calreticulin. J. Immunol. *181*, 2533-2543.

Panaretakis,T., Joza,N., Modjtahedi,N., Tesniere,A., Vitale,I., Durchschlag,M., Fimia,G.M., Kepp,O., Piacentini,M., Froehlich,K.U., van,E.P., Zitvogel,L., Madeo,F., and Kroemer,G. (2008). The co-translocation of ERp57 and calreticulin determines the immunogenicity of cell death. Cell Death. Differ. *15*, 1499-1509.

Robson,N.C., Hoves,S., Maraskovsky,E., and Schnurr,M. (2010). Presentation of tumour antigens by dendritic cells and challenges faced. Curr. Opin. Immunol. *22*, 137-144.

Roy,P., Bullock,M.J., Perez-Ordonez,B., Dardick,I., and Weinreb,I. (2010). Epithelial-myoepithelial carcinoma with high grade transformation. Am. J. Surg. Pathol. *34*, 1258-1265.

Tang,J., Hu,G., Hanai,J., Yadlapalli,G., Lin,Y., Zhang,B., Galloway,J., Bahary,N., Sinha,S., Thisse,B., Thisse,C., Jin,J.P., Zon,L.I., and Sukhatme,V.P. (2006). A critical role for calponin 2 in vascular development. J. Biol. Chem. *281*, 6664-6672.

Vaupel,P. (2008). Hypoxia and aggressive tumor phenotype: implications for therapy and prognosis. Oncologist. *13 Suppl 3*, 21-26.

Vaupel,P. and Harrison,L. (2004). Tumor hypoxia: causative factors, compensatory mechanisms, and cellular response. Oncologist. *9 Suppl 5*, 4-9.

Vaupel,P. and Mayer,A. (2007). Hypoxia in cancer: significance and impact on clinical outcome. Cancer Metastasis Rev. *26*, 225-239.

Yang,F., Xiao,Z.Q., Zhang,X.Z., Li,C., Zhang,P.F., Li,M.Y., Chen,Y., Zhu,G.Q., Sun,Y., Liu,Y.F., and Chen,Z.C. (2007). Identification of tumor antigens in human lung squamous carcinoma by serological proteome analysis. J. Proteome. Res. *6*, 751-758.

Zacour,M.E., Teoh,H., Halayko,A.J., and Ward,M.E. (2002). Mechanisms of aortic smooth muscle hyporeactivity after prolonged hypoxia in rats. J. Appl. Physiol *92*, 2625-2632.

Zhang,J.W., Rubio,V., Zheng,S., and Shi,Z.Z. (2009). Knockdown of OLA1, a regulator of oxidative stress response, inhibits motility and invasion of breast cancer cells. J. Zhejiang. Univ Sci. B *10*, 796-804.

Zhang,J.Y., Megliorino,R., Peng,X.X., Tan,E.M., Chen,Y., and Chan,E.K. (2007). Antibody detection using tumor-associated antigen mini-array in immunodiagnosing human hepatocellular carcinoma. J. Hepatol. *46*, 107-114.

Zhong,Y., Onuki,J., Yamasaki,T., Ogawa,O., Akatsuka,S., and Toyokuni,S. (2009). Genome-wide analysis identifies a tumor suppressor role for aminoacylase 1 in iron-induced rat renal cell carcinoma. Carcinogenesis *30*, 158-164.

3. Preconditioned endothelial progenitor cells reduce the formation of melanoma metastases formation through SPARC-driven cell-cell interaction and endocytosis.

Defresne F, Bouzin C, Grandejan M, Dieu M, Raes M, Hatzopoulos AK, Kupatt C, Feron O.

Cancer Res 2011, accepted.

Additional informations on SPARC

SPARC (Secreted Protein, acidic and rich in cysteine), also called BM-40 or osteonectin is a calcium binding matricellular glycoprotein secreted by many different types of cells (Yan and Sage, 1999). It has been shown to influence integrin clustering and to interact with different ECM components like collagens, laminin, fibronectin or vitronectin (Podhajcer et al., 2008; Lane and Sage, 1994; Arnold and Brekken, 2009). SPARC modulates cell-matrix interactions and cell function without participating in the structural scaffold of the ECM (Tai and Tang, 2008; Clark and Sage, 2008). SPARC is, in particular, reported to be expressed during morphogenesis, development, tissue injury, tissue remodelling and cancer (Clark and Sage, 2008; Nozaki et al., 2006). This protein presents counteradhesive and antiproliferative effects that lead to cell rounding and changes in cell shape that result in the disruption of cell-matrix interactions (Yan and Sage, 1999). Different effects were attributed to SPARC: (i) disruption of cell adhesion, (ii) promotion of changes in cell shape, (iii) inhibition of the cell cycle, (iv) regulation of cell differentiation, (v) inactivation of cellular response to growth factors, (vi) regulation of MMP production (Yan and Sage, 1999; Clark and Sage, 2008). The counteradhesive effect of SPARC can be mediated through a tyrosine phosphorylation dependent pathway, while its antiproliferative function is partially dependent on signal transduction via a G-protein coupled receptor (Yan and Sage, 1999).

The contradictory roles of SPARC in cancer

SPARC is differentially expressed in tumors and its surrounding stroma in various cancers in comparison to the normal tissue (Tai and Tang, 2008; Yan and Sage, 1999). The capacity of SPARC to promote or inhibit tumor progression is apparently dependent on the initiating cell-type, the tumor stage and the tumor microenvironment (Arnold and Brekken, 2009). These informations are summarized in Tables 7 and 8.

Table 7: SPARC expression correlated with poor prognosis in different tumors. Adapted from (Arnold and Brekken, 2009; Clark and Sage, 2008; Podhajcer et al., 2008)

Cancer	Expression	Refs
Bladder cancer	Increased stromal SPARC, Positive correlation	(Nimphius et al., 2007)
Leukemia	Increased SPARC expression	(Martinez et al., 2003; De et al., 2002)
Osteosarcoma	Positive correlation	(Dalla-Torre et al., 2006)
Glioblastoma, astrocytoma and meningioma	Positive correlation, SPARC expression increased in invasive benign and malignant tumors	(Huang et al., 2000; Pen et al., 2007; Rich et al., 2005)
Breast cancer	High stromal SPARC, positive correlation	(Amatschek et al., 2004; Barth et al., 2005; Bellahcene and Castronovo, 1995; Bergamaschi et al., 2008; Helleman et al., 2008; Jones et al., 2004; Parker et al., 2004; Porter et al., 2003; Sarrio et al., 2008; Watkins et al., 2005; Woelfle et al., 2003)
Colorectal cancer	SPARC expression increased in tumor, tumor stroma and at metastatic sites	(Lussier et al., 2001; Madoz-Gurpide et al., 2006; St et al., 2000; Wiese et al., 2007)
Oesophageal squamous cell carcinoma	Positive correlation	(Brabender et al., 2005; Che et al., 2006; Luo et al., 2004; Mitas et al., 2005; Porte et al., 1998; Wong et al., 2009; Xue et al., 2006; Yamashita et al., 2003)
Head and neck cancer	Positive correlation	(Chin et al., 2005; Choi et al., 2008)

Kidney cancer	SPARC expression increased in tumors	(Amatschek et al., 2004; Gieseg et al., 2002; Sakai et al., 2001)
Hepatocellular carcinoma	Positive correlation	(Goldenberg et al., 2002; Lau et al., 2006; Le et al., 1999)
Lung carcinoma	High stromal SPARC, positive correlation	(Amatschek et al., 2004; Koukourakis et al., 2003)
Ovarian cancer	High stromal SPARC, positive correlation	(Paley et al., 2000)
Pancreatic cancer	High stromal SPARC, positive correlation	(Guweidhi et al., 2005; Infante et al., 2007; Mantoni et al., 2008; Prenzel et al., 2006; Ryu et al., 2001)
Prostate cancer	Increased SPARC expression at the metastatic site, positive correlation	(Best et al., 2005; Lapointe et al., 2004; Thomas et al., 2000)
Melanoma	Positive correlation, serum SPARC levels useful as a diagnostic indicator	(Alonso et al., 2007; Ikuta et al., 2005)
Gastric cancer	High stromal SPARC, positive correlation	(Inoue et al., 2002; Maeng et al., 2002; Takeno et al., 2008; Wang et al., 2004)
Thyroid cancer	High stromal SPARC expression in poorly differentiated tumors	(Takano et al., 2002)
Cervical and endometrial carcinoma	High stromal SPARC	(Chen et al., 2003; Rodriguez-Jimenez et al., 2007)

Table 8: SPARC expression correlated with good prognosis in different tumors. Adapted from (Arnold and Brekken, 2009; Clark and Sage, 2008; Podhajcer et al., 2008)

Cancer	Expression	Refs
Acute myeloid leukemia	SPARC expression decreased	(Bullinger et al., 2004; Ross et al., 2004)
Neuroblastoma	Inverse correlation	(Chlenski et al., 2002)
Breast carcinoma	Inverse correlation, increased stromal SPARC	(Bergamaschi et al., 2008; Beck et al., 2008)
Colorectal cancer	Inverse correlation	(Cheetham et al., 2008; Tai et al., 2005; Yang et al., 2007)
Lung cancer	Inverse correlation	(Suzuki et al., 2005)
Ovarian cancer	Inverse correlation	(Socha et al., 2009; Yiu et al., 2001)
Pancreatic cancer	SPARC methylation, inverse correlation	(Brune et al., 2008; Hong et al., 2008; Sato et al., 2003)
Cervical and endometrial carcinoma	Inverse correlation	(Rodriguez-Jimenez et al., 2007; Sova et al., 2006; Kahn et al., 2008)

Preconditioned endothelial progenitor cells reduce the formation of melanoma metastases through SPARC-driven cell-cell interaction and endocytosis

Florence Defresne[1], Caroline Bouzin[1], Marie Grandjean[1], Marc Dieu[2], Martine Raes,[2]
Antonis K. Hatzopoulos[3], Christian Kupatt[4] and Olivier Feron[1]

[1] Université de Louvain, Pole of Pharmacology & Therapeutics (UCL-FATH), Angiogenesis & Cancer Research Laboratory, 52 Avenue E. Mounier, B-1200 Brussels, Belgium
[2] University of Namur-FUNDP, Unit of Research in Cellular Biology (URBC), 61 rue de Bruxelles, B-5000 Namur, Belgium
[3]Department of Medicine, Division of Cardiovascular Medicine, and Department of Cell and Developmental Biology, Vanderbilt University, Nashville, TN 37232, USA
[4]Medical Department I, Cardiology, Ludwig-Maximilians University, Klinikum Großhadern,
15 Marchioninistr., 81377 Munich, Germany

Running title: SPARC-driven macrophagic potential of EPC

Key words: endothelial progenitor cells, metastasis, SPARC

This work was supported by grants from the Fonds de la Recherche Scientifique FRS-FNRS, the Fonds de la Recherche Scientifique Médicale, the Télévie, the Belgian Federation against cancer, the J. Maisin Foundation and an Action de Recherche Concertée (ARC 09/14-020) from the Communauté Française de Belgique. FD is a FRS-FNRS Research Assistant and OF a FRS-FNRS Research Director.

Address for correspondence: Olivier FERON, Pole of Pharmacology and Therapeutics, UCL-FATH5349, 52 avenue E. Mounier, B-1200 Brussels, Belgium; phone : +32-2-764 5264; fax : +32-2-764 5269; E-mail : olivier.feron@uclouvain.be

Abstract

Tumor progression is associated with the release of signaling substances from the primary tumor into the bloodstream. Tumor-derived cytokines are known to promote the mobilization and the recruitment of cells from the bone marrow, including endothelial progenitor cells (EPC). Here, we examined whether such paracrine influence could also influence the capacity of EPC to interfere with circulating metastatic cells. We therefore consecutively injected EPC pre-stimulated by tumor conditioned medium (CM-EPC) and luciferase-expressing B16 melanoma cells to mice. A net decrease in metastases spreading (vs non-stimulated EPC) led us to carry out a 2D-DIGE proteomic study to identify possible mediators of EPC-driven protection. Among 33 proteins exhibiting significant changes in expression, SPARC presented the highest induction after EPC exposure to CM. We then showed that contrary to control EPC, SPARC-silenced EPC were not able to reduce the extent of metastases when injected with B16 melanoma cells. Using adhesion tests and the hanging drop assay, we further documented that cell-cell interactions between CM-EPC and melanoma cells were promoted in a SPARC-dependent manner. This interaction led to the engulfment of melanoma cells by CM-EPC, a process prevented by SPARC silencing and mimicked by recombinant SPARC. Finally, we showed that contrary to melanoma cells, the pro-metastatic human breast cancer cell line MDA-MB231-D3H2 reduced SPARC expression in human EPC and stimulated metastases spreading. Our findings unravel the influence of tumor cells on EPC phenotypes through a SPARC-driven accentuation of macrophagic capacity associated with limitations to metastatic spread.

Introduction

Several populations of bone marrow derived cells (BMDC) have been reported to contribute to tumor growth and metastatic progression such as myeloid progenitors, macrophages and endothelial progenitor cells (EPC) (Gao and Mittal, 2009; Mbeunkui and Johann, Jr., 2009; Witz and Levy-Nissenbaum, 2006). The frontier between these different BMDC is not clearly established. A controversy even exists about the identity and functions of EPC, some investigators claiming a major involvement of these cells in tumor neovascularization while others only reporting anecdotic recruitment in the tumor microenvironment (Wickersheim et al., 2009; Ahn and Brown, 2009; Gao et al., 2009; Gao and Mittal, 2009). Besides obvious differences such as mouse strains or tumor sizes, the lack of consensus about the panel of cell surface markers to define EPC also contributes to these apparent discrepancies. There is actually a continuum between bone marrow stem cells and differentiated endothelial cells which renders difficult the task of delimiting one single type of EPC. This probably accounts for subtle differences in the roles of EPC recruited in tumors. EPC may indeed stimulate the formation of new blood vessels by the release of growth factors (eg, VEGF) which in turn stimulate local angiogenesis or they may be directly incorporated in neo-forming vessels as part of the cell assembly (Wels et al., 2008; Gao and Mittal, 2009; Shaked and Voest, 2009). Bone marrow-derived progenitor cells are also reported to favor the formation of pre-metastatic niches which precondition the environment to facilitate the implantation of tumor cells and the consecutive recruitment of other progenitor cells to promote the neovascularization of metastases (Wels et al., 2008; Gao et al., 2009; Joyce and Pollard, 2009). More recently, EPC were documented to act as antigen-presenting cells similar to monocytes (Raemer et al., 2009; Asakage et al., 2006), confirming previous reports identifying EPC as cells with an intermediate phenotype expressing both endothelial and macrophage properties (Nakul-Aquaronne et al., 2003).

Many studies exploring the role of EPC in the tumor angiogenic process are based on the systemic injection of EPC in tumor- or metastases-bearing mice. This model bypasses the mobilization step and provides key insights on the downstream steps

including adhesion to tumor endothelial cells, extravasation and migration into the tumor stroma. One aspect underestimated in this model is the influence of cytokines released by the primary tumor in the blood stream and influencing bone marrow progenitor cells. We and others however showed that tumor-derived SDF-1 and VEGF interact with their cognate receptors at the surface of bone marrow EPC (Asahara et al., 1999; Yamaguchi et al., 2003; Sbaa et al., 2006; Sonveaux et al., 2004). These studies allowed us to better understand the migration from the endosteal niche to the BM vessel vicinity and the further EPC intravasation step. One may therefore postulate that the phenotype of EPC still located in the bone marrow or on their way to the blood stream is more globally preconditioned by the exposure to the myriads of circulating substances produced by tumor cells and other cell types present in the tumor microenvironment. In this study, we aimed to examine the effect of preconditioned EPC by the tumor cell secretome on tumor progression and in particular on metastases formation. We were actually rapidly intrigued by the capacity of such preconditioned EPC to physically interact with tumor cells and we set up experiments to address the possible protective effects of EPC in reducing the survival of circulating tumor cells. We used embryonic mouse EPC offering the advantage of easy maintenance in culture and transfectability (Wei et al., 2004) together with B16 melanoma cells to dissect the anti-metastatic capacity of prechallenged EPC. 2D-DIGE proteomic analysis led us to identify osteonectin/SPARC (Secreted Protein, Acidic and Rich in Cysteine) as the glue leading to preconditioned EPC physical interaction with melanoma cells and the consecutive engulfment of the latter. The inverse relationship between SPARC expression in EPC and the metastatic potential of tumor cells was further verified using a pro-metastatic breast cancer cell line. Conditioned medium from this cell line actually reduced SPARC expression in EPC which led to a reduced cell-cell interaction and an increase in metastases spreading. This macrophagic behavior of EPC adds a new layer of complexity in the role of so-called endothelial progenitor cells in tumor progression.

Materials and methods

Cell culture and mouse models

Luciferase-expressing mouse B16 melanoma cells (B16-luc) and human MDA-MB231-D3H2 breast cancer cells (MDA-luc) (Xenogen, Caliper), embryonic mouse endothelial progenitor cells (EPC) (Hatzopoulos et al., 1998; Kupatt et al., 2005), human umbilical cord-derived EPC (hEPC) (Lonza) and 3T3 mouse fibroblasts were routinely cultured in the presence of fetal calf serum. In preconditioning experiments, EPC and hEPC were exposed for 24 hours to B16-luc and MDA-luc culture supernatants collected after a 2-day period, respectively. In some experiments, recombinant mouse and human SPARC (R&D) (30µg/ml) was added to EPC and hEPC, respectively. For animal studies, 8-weeks old C57Bl/6 male or nude NMRI nu/nu female mice (Elevage Janvier, Le Genest Saint-Isle, France) were used in experiments with mouse B16-luc and human MDA-luc cells, respectively. In the metastases experiments, EPC and hEPC (10^5 cells) were administered 24h before B16-luc and MDA-luc cells (10^6 cells), respectively, through intravenous or intra-cardiac injections. Metastases were tracked by i.p. injection of a single dose of luciferin (150 mg/kg) to anesthetized and depilated mice. Bioluminescence was detected 15 min after luciferin injection with a IVIS50 imaging system (Xenogen, Caliper). In primary tumor experiments, a mixture of EPC (10^5cells) and B16F10luc melanoma cells (10^6 cells) was injected subcutaneously. These procedures were approved by the local authorities according to national animal care regulations.

Real-time PCR and shRNA silencing

Total RNA was extracted with the TriPure reagent (Roche, Belgium). Reverse transcription was performed using SuperScript II RNase H^- reverse transcriptase (Invitrogen) and random hexamer primers. Sybr Green Supermix (BioRad) was used for qPCR. Primers were designed by Invitrogen primer tool: for mouse SPARC, forward primer was 5'- GGCCTGGATCTTCTTTCTCC -*3'* and reverse primer was 5'- CACGGTTTCCTCCTCCACTA -*3'* and for human SPARC, forward primer was 5'- GATGAGACAGAGGTGGTGGA -*3'* and reverse primer was 5'-

CTCCTCTTCGGTTTCCTCTG -*3'*. β-actin transcripts were used for normalization. For silencing experiments, EPC were transfected with a pLKO.1 vector coding for a shRNA targeting mouse SPARC sequence (Mission shRNA plasmid DNA, Sigma, Bornem, Belgium); a control vector was used in parallel experiments. Plasmids were amplified and purified using NucleoBond columns according to the manufacturer's protocol and transfections were performed with Lipofectamin 2000 (Invitrogen). Prolonged incubation with puromycin (Calbiochem) was used to establish selection of clones and qPCR was used to select the EPC clone with the highest silencing effect. The shRNA sequence of the selected clone (named EPC SPARC KO in our study) was the following: CCGGGAAGGTATGCAGCAATGACAACTCGAGTTGTCATTGCTGCATACC TTCTTTTTG

Immunoblotting, flow cytometry and immunocytochemistry

Immunoblotting was performed with species-specific antibodies against SPARC (R&D), Tie-2 (R&D) and VE-cadherin (Bender Medsystems); gel loading was normalized with GAPDH (Cell signaling), or actin (Sigma) antibody. TUNEL assay (TMR-Red In situ cell death detection kit, Roche) was performed according to the manufacturer's instructions. Immunocytochemistry analysis was performed on paraformaldehyde-fixed cells. Representative pictures were taken with a CCD camera coupled to a Zeiss Axioskop 40 microscope (40 x objective). For flow cytometry characterization of EPC, cell suspensions were labelled with conjugated antibodies (described in Supplemental Materials) using a FACScan apparatus (BD Biosciences).

Cell-cell interaction, adhesion and hanging drop assays

EPC and B16-luc melanoma cells or hEPC and MDA-luc breast cancer cells were placed in MEMα medium and submitted to gentle agitation for 24h in non-adherent plastic dishes. To evaluate the interaction between the two cell types, progenitor cells were pre-labelled with calcein (green) and tumor cells with CMDil (red) according to the manufacturer's protocols. The extent of cell-cell interaction was

evaluated based on the detection of double colored aggregates using a Zeiss Axiovert microscope. Adhesion assays were also carried out in 96-well plates coated with fibronectin (Sigma, 20 µg/ml). Calcein-labelled EPC (40.000 cells per well) were allowed to adhere for 1h at 37°C in conditioned or control medium. After four washes with PBS containing 10% FBS to eliminate all non adherent cells, calcein signal was measured in Victor X4 plate reader (Perkin Elmer). Quantification was performed using the calcein signal ratio (postwash vs prewash). For the so-called hanging drop assay, $1.5.10^4$ tumor cells and $1.5.10^3$ progenitor cells were mixed in 30 µl full medium and placed onto the inner surface of the lid of a 24-well plate and then allowed to aggregate for 24h at 37°C; the corresponding bottom wells were filled with PBS to prevent evaporation. To assay for tightness of cell-cell interactions, cells were subjected to shear force by passing them 10 times through standard 200µl pipet tips. The extents of aggregated and remaining isolated cells were determined within 20 min using a Zeiss Axiovert microscope.

Phagocytosis assays

Fluorescent latex beads (Sigma, L3030, 2 µm) were seeded on confluent EPC pre-exposed or not to B16-luc melanoma cell conditioned medium (with a ratio of three beads per cell) in 12-well plates for 3h at 37°C; similar experiments were carried out with hEPC pre-exposed to MDA-luc cell conditioned medium. Cells were then washed four times to remove non-phagocyted beads and fixed in 4% paraformaldehyde. After DAPI counterstaining, number of beads ingested were determined using a Zeiss Axiovert microscope (10x objective); quantification was performed using ImageJ software. In another set of experiments, B16F10 cells were labelled with calcein-AM and cultured overnight to minimize spontaneous leakage of dye. B16 cells were then added to EPC or SPARC KO EPC (stimulated or not with conditioned media). Cells were harvested 6h later and analyzed by flow cytometry after EPC counter-staining with phycoerythrin-conjugated c-kit antibody. The extents of double calcein- and c-kit positive cells were quantified using FlowJo software. Finally, in a last set of experiments, calcein-labelled B16 melanoma cells were seeded in V-bottom 96-well plate in contact with EPC cells (with ratios ranging from 1:50 to 1:0.5) and allowed to interact for 24h at 37°C. Plates were then

centrifuged and 100 µl of cell supernatant were transferred into flat-bottom 96-well plates to detecrt possible release of calcein in a Victor X4 microplate reader (Perkin Elmer).

Statistics

Results are expressed as mean ± SEM. Student's *t* test, 1-way ANOVA (Tukey's post-hoc test), were used where indicated. *P < 0.05 or **P<0.01 was considered statistically significant in the different experiments.

2D-DIGE-related protocols are provided as Supplementary data.

Results

Preconditioned EPC inhibits metastasis formation

To mimic the modulation of EPC phenotype by cytokines released in the blood circulation from primary tumors and to study the potential impact on metastases formation, we set up experiments where we pre-exposed EPC for 24h to the culture supernatant of B16 melanoma cells. We then injected intravenously pre-stimulated or control EPC followed by luciferase-expressing B16 melanoma cells (1:10 ratio, respectively) to track metastases formation through the detection of bioluminescence. We found that conditioned medium-exposed EPC (EPC-CM) dramatically reduced the extent of metastases as measured at day 10 post-injection. Control EPC did not influence the metastases formation when compared with B16 melanoma cells injected alone (Figure 1A and 1B, upper panels). Using mouse 3T3 fibroblasts instead of EPC, we failed to detect an effect of conditioned medium pre-treatment on the extent of metastases spreading from B16 melanoma cells (Figures 1A and 1B, lower panels).

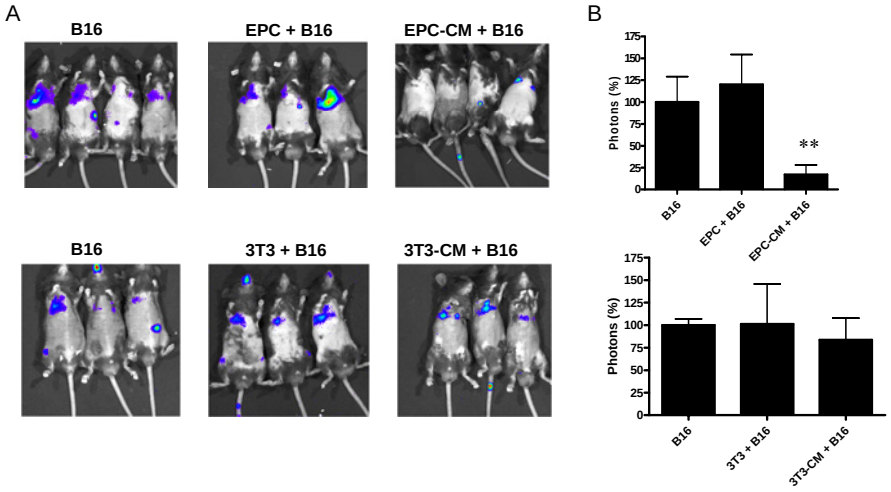

Figure 1. Influence of EPC i.v. administration on the capacity of B16 melanoma cell to form metastases. A. Representative pictures of bioluminescence detection in mice i.v. injected with 10^6 luciferase-expressing B16 melanoma cells 24 hours after i.v. sham or EPC or 3T3 cell injections (10:1 ratio); EPC or 3T3 cells pre-exposed to the tumor conditioned medium (EPC-CM, 3T3-CM) were also used in these experiments. **B.** Bar graphs represent the corresponding extent of photons detected 10 days post-injection (expressed as % of photons detected in sham conditions); **P<0.01, n=15-20 mice for each B16 and B16/EPC group and n=5-10 for each 3T3 and 3T3/EPC group.

SPARC silencing in EPC-CM stimulates metastatic progression

We then used 2D-DIGE technology to compare the proteome of EPC exposed or not to the tumor-conditioned medium (Figure 2A). Using mass spectrometry to identify spots of interest, we identified 33 different proteins with significant (> 2-fold) changes in expression (Table 1). The abundance of 9 of them was increased in response to the exposure to B16 melanoma cell conditioned medium. With a ~9-fold increase in expression, SPARC protein showed the largest induction. To validate the 2D-DIGE data, we then performed immunoblotting and immuno-cytochemistry experiments. We found a three-fold increase in SPARC signal from lysates of EPC-CM (Figure 2B) and a similar increase in membrane SPARC expression on intact EPC-CM (Figure 2C).

Table 1: 2D-DIGE-identified proteins in tumor conditioned media-stimulated EPC.
Mean changes in expression (*vs* control EPC) are indicated in the "average" column; positive values indicate upregulation whereas negative values indicate downregulation in response to CM exposure (P<0.005).

Upregulated Proteins	average	pI	molecular weight (kDa)	MASCOT score	Uniprot ref
hyaluronan mediated motility receptor (RHAMM)	2,46	5,4	92	110	Q5NC88
calreticulin precursor	2,29	4,33	48	78	S06763
vimentin	2,11	4,96	51	158	VIME_MOUSE
heterogeneous nuclear ribonucleoprotein K	2,26	5,39	51	87	S41495
prolyl 4-hydroxylase alpha subunit	2,05	5,6	61	96	P4HA1_MOUSE
glucose regulated protein	2,22	5,88	57	171	PDIA3_MOUSE
secreted acidic cysteine rich glycoprotein SPARC	9,01	4,77	35	102	Q5NBV5
Lrpap1 protein	5,17	6,68	35	88	Q6PB52
triosephosphate isomerase	2,12	5,6	23	66	Q64513

Downregulated proteins	average	pI	molecular weight (kDa)	MASCOT score	Uniprot ref
phosphosribosylglycinamide formyltransferase	-2,34	6,3	108	134	Q64737
elongation factor 2 EF-2	-2,08	6,4	96	144	EF2_MOUSE
lysyl hydroxylase 2 LH2	-2,12	6,3	85	67	PLOD2_MOUSE
lysyl hydroxylase 1 LH1	-2,26	6,08	84	83	Q9R0E2
cysteinyl-tRNA synthetase	-2,45	6,3	95	113	Q9ER72
aspartyl-tRNA synthetase cytoplasmic	-2,11	6,07	57	170	Q922B2
asparagine synthetase	-2,05	6,12	65	97	ASNS_MOUSE
ero1-like	-2,51	6,12	55	139	ERO1A_MOUSE
Fscn-1 protein	-2,05	6,57	52	74	FSCN1_MOUSE
Ndufs2 protein	-2,18	6,43	54	114	Q99L23
serine/threonine-protein phosphatase 2A (PP2A)	-2,09	5,8	52	72	Q6P1F6
adenylosuccinate lyase	-2,17	6,9	55	160	Q8VCD4
eno1 protein	-3,35	7,67	50	104	Q5XKE1
Liver copper binding protein CUBP	-2,29	6,08	48	175	P50247
tubulin beta-7 chain	-2	4,78	50	222	P07437
actin	-2,74	5,6	41	85	P63260
activator of 90kDa heat shock protein ATPase homolog 1	-2,12	5,4	38	88	Q8BK64
proteinase inhibitor Spi3	-2,13	5,3	43	95	Q60854
spermidine synthase	-2,16	5,4	34	185	Q64674
Sid478p	-3	6,7	31	77	Q9R0P3
Cdc2a protein	-2,04	8,7	34	114	Q99JW7
phosphoglycerate mutase 1	-2,06	6,75	29	169	Q9DBJ1
GTP-binding protein Ran/TC4	-2,17	7,01	24	83	P62827
proteasome subunit alpha type 6	-2,51	6,3	28	100	Q9QUM9

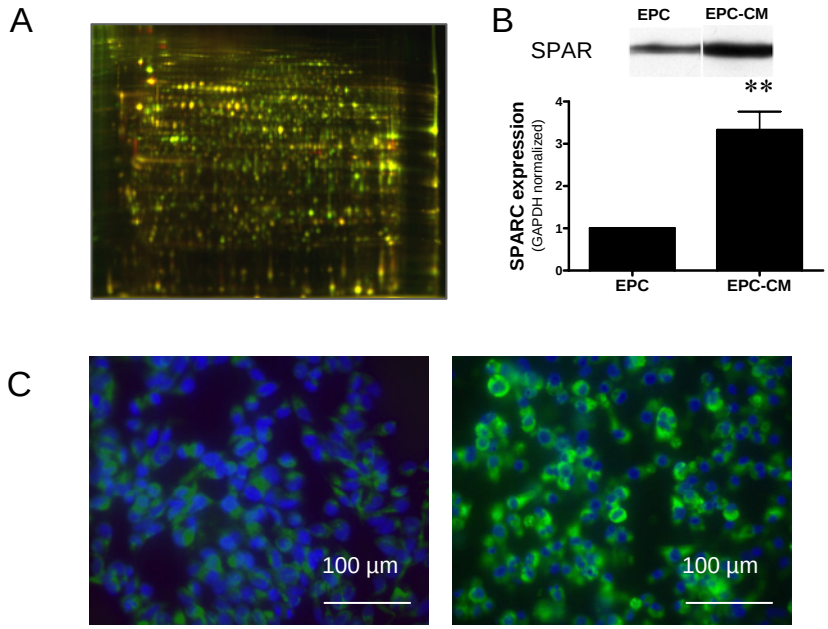

Figure 2. Expression of SPARC is increased in EPC exposed to B16 melanoma conditioned medium. A. Typical 2D-DIGE analysis of EPC proteome exposed or not to the B16 melanoma culture supernatant; control EPC were labelled with Cy3, EPC-CM with Cy5 and a mixture of both used as internal standard was labeled with Cy2. **B.** SPARC immunoblotting performed on EPC and EPC-CM lysates; GAPDH immunoblotting was used as a loading control. Bar graph represents the normalized expression of SPARC in EPC and EPC-CM; **P<0.01, n=3. **C.** SPARC immunocytochemical detection in EPC and EPC-CM; cell nuclei are counterstained with DAPI.

To study a potential role of SPARC in the reduced metastatic progression, we used a dedicated shRNA construct (RNAi consortium, Sigma). Stable transfection and further antibiotic selection led us to isolate several EPC clones. We selected one of them (named here below SPARC-KO-EPC) showing 97% inhibition of SPARC transcript expression in control EPC by qPCR (Figure 3A); immunoblotting analyses confirmed these results (Figure 3B). Importantly, the stimulatory effect of the tumor-conditioned medium on SPARC expression was also significantly blunted in the SPARC KO EPC clone (Figure 3C).

We then compared the influence of SPARC-KO EPC-CM and control EPC-CM injection on the metastatic potential of melanoma cells injected 24h later, as previously described (see Figure 1). Interestingly, SPARC silencing in EPC restored the extent of metastases formation observed when B16 melanoma cells were injected alone (see Figures 3D and 3E). To further evaluate the impact of EPC

prechallenged with tumor CM on the metastasis formation, we also used a model wherein cells were injected directly in the heart in order to bypass the potential cell trapping in the lungs after intravenous injection (Figure 3F). We found again that the pre-injection of SPARC KO EPC-CM favored an increase in the extent of metastases formation, as measured by detecting luciferase-driven bioluminescence 10 days later (Figure 3G).

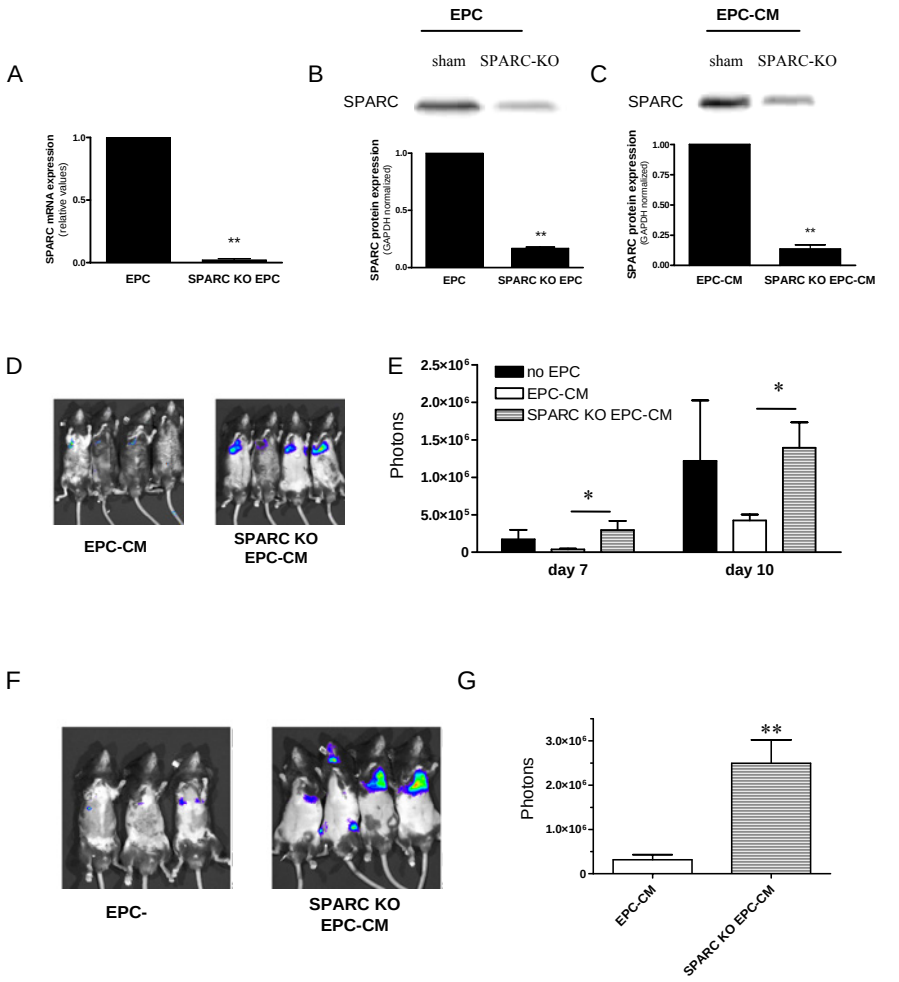

Figure 3. SPARC shRNA reduces induction of SPARC in EPC exposed to tumor cell conditioned medium and stimulates metastases formation. A. Bar graph represents SPARC mRNA expression in EPC and a selected EPC clone stably transfected with a SPARC shRNA; **P<0.01, n=3. **B.** SPARC immunoblotting performed on EPC and SPARC KO EPC; GAPDH immunoblotting was used as a loading control. Bar graph represents the normalized expression of SPARC in EPC and SPARC-KO EPC; **P<0.01, n=3. **C.** Same as in B, but carried out on EPC exposed to tumor conditioned medium (CM). Representative pictures of bioluminescence detection in mice after intravenous (**D**) or intracardiac (**F**) injection of 10^6 luciferase-expressing B16 melanoma cells 24 hours after EPC-CM or SPARC KO EPC-CM administration through the same route (10:1 ratio). Bar graphs represent the corresponding numbers of photons detected 7 and 10 days after intravenous injection (**E**) or 10 days after intracardiac injection (**G**); the extent of bioluminescence obtained in the absence of EPC co-injection is shown as control in E. *P<0.05, **P<0.01 vs EPC-CM condition, n=12-15 mice for each group.

SPARC silencing prevents physical interactions between EPC-CM and melanoma cells

Since SPARC is a protein involved in cell adhesion, we then examined whether a SPARC-driven interaction between EPC and melanoma cells could be involved in the observed reduction in metastases formation. We first co-cultured *in vitro* EPC-CM and B16 cells for 24h in a dish precluding cell attachment on plastic. While control EPC-CM and melanoma cells formed aggregates, physical interaction between SPARC KO EPC-CM and tumor cells was reduced (Figure 4A). To further examine the capacity of EPC-CM to interact with B16 melanoma cells in a SPARC-dependent manner, we used the hanging drop assay (Mariner et al., 2004; Thoreson et al., 2000; Crooke et al., 2009). A similar deficit in aggregate formation was observed when SPARC KO EPC-CM were used in the assay (*vs* control CM-EPC). (Figure 4B). To extract quantitative data from this assay, we counted the remaining isolated cells in the drop, leading to a mirror profile of aggregation (Figure 4C). The use of SPARC KO-EPC-CM actually showed a number of isolated cells (ie, a deficit in aggregation) similar to that observed when tumor cells were used alone in the hanging drop assay (Figure 4C). Interestingly, the addition of mouse recombinant SPARC to EPC mimicked the effect of CM exposure with a significant reduction in isolated cell numbers (ie, an increased aggregation); this pro-aggregant effect of recombinant SPARC was also observed when co-incubating B16 melanoma cells and SPARC KO EPC (Figure 4C).

To get further insights on the SPARC-driven interaction mechanisms between EPC and tumor cells, we examined whether fibronectin abundantly secreted at the extracellular pole of melanoma cells (Kashani-Sabet et al., 2009) and known to bind SPARC protein (Sangaletti et al., 2008) could represent an intermediary ligand for EPC. EPC were therefore labeled with calcein and allowed to adhere on fibronectin-coated wells for 1 hour. After several washes to remove all non-adherent cells, calcein signal was measured and quantified. The extent of EPC-CM adhesion on fibronectin amounted to 10-fold the level reached with control EPC (Figure 4D). Importantly, SPARC silencing led to a dramatic decrease in the capacity of EPC-CM to adhere on fibronectin (Figure 4D).

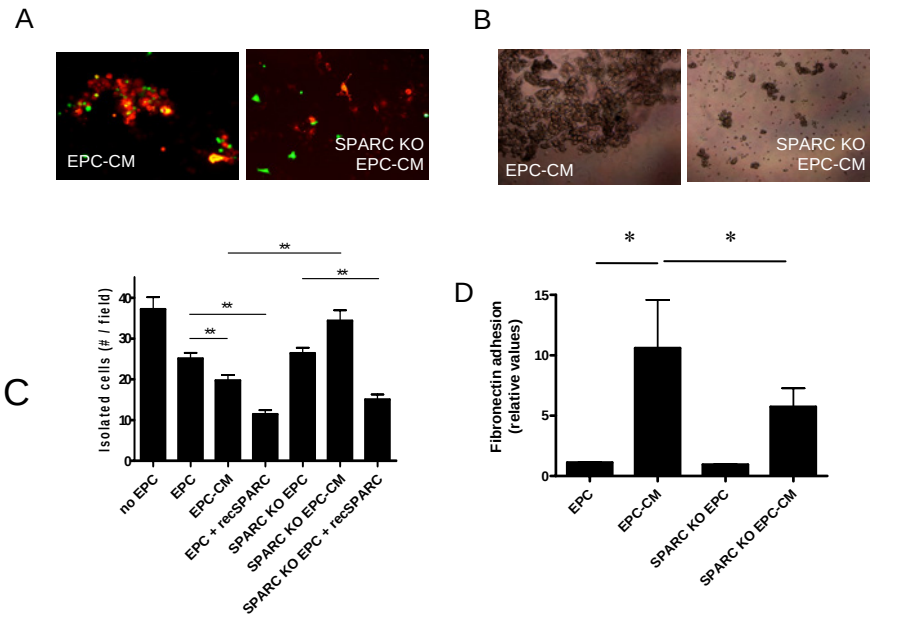

Figure 4. SPARC silencing in EPC reduces interactions with B16 melanoma cells. Representative pictures of EPC and melanoma cells aggregation detected (**A**) by the extent of double staining of B16 melanoma cells and EPC pre-labelled with calcein (green) and CM-Dil (red), respectively, and (**B**) using the hanging drop assay as detailed in the Methods section. (**C**) Bar graph represents the extent of non-aggregated B16 melanoma cells per microscopic field determined in the absence or the presence of EPC (exposed or not to conditioned medium (CM); with or without SPARC silencing (SPARC KO) or addition of recombinant mouse SPARC (recSPARC); ** $p<0.01$, n=3. **(D)** Bar graph represents the extent of EPC adhesion on fibronectin as determined by calcein signal detected after several washes; * $p<0.05$, **$p<0.01$, n = 3.

SPARC expression supports the phagocytic potential of EPC-CM

The capacity of EPC-CM to interact with melanoma cells led us to consider a possible macrophagic behavior of progenitor cells which would reduce the number of tumor cells available to form metastases. We first performed immunoblotting and flow cytometry to characterize the phenotype of EPC and EPC-CM. EPC used in our study were originally isolated from mouse embryos (18) and extensively characterized for their vascular progenitor potential (19, 25). Both EPC and EPC-CM showed a strong expression of Tie-2, VE-cadherin and c-kit but a lack of CD31 labelling confirming that these cells were not yet fully engaged in the endothelial lineage (Figure 5A). We also found that EPC-CM were negative for myeloid markers including CD11b and Gr1 and the pan-hematopoietic surface antigen CD45, but slightly positive for the macrophagic markers F4/80 and CD68 (Figures 5A). Of note, the isolation of circulating c-kit-positive cells from B16 melanoma-bearing mice allowed us to document a 6.2-fold increase in SPARC mRNA expression in this cell population ($n = 4$, $P<0.01$ *vs* circulating c-kit-positive cells from healthy mice), thereby confirming the *in vivo* relevance of our *in vitro* model of pre-conditionned EPC.

The potential macrophagic feature of EPC was confirmed in a phagocytosis assay using fluorescent microbeads. We found that when pre-exposed to the tumor cell conditioned medium, EPC-CM phagocytosed microbeads to a much larger extent than control EPC (see Figures 5B and 5C). Interestingly, SPARC silencing largely prevented this capacity to capture microbeads and conversely, the addition of recombinant mouse SPARC to non-stimulated EPC recapitulated the CM effects (Figures 5B and 5C). To more directly evaluate the ability of EPC to phagocytose tumor cells, we seeded B16 melanoma cells labeled with calcein on confluent EPC and SPARC KO EPC, stimulated or not with tumor cell conditioned media. Flow cytometry analysis performed after extensive rinsing to eliminate cells not captured by EPC showed that EPC-CM could phagocytose tumor cells in a SPARC-dependent manner, as documented by the double staining of cells positive for calcein and c-kit (Figure 5D). To investigate a possible lytic effect of EPC on melanoma cells, we examined whether tumor cells released calcein following exposure to EPC. We did not observe any difference in the extent of calcein

recovered from the co-culture between B16 melanoma cells and EPC-CM vs SPARC KO EPC-CM, confirming that the observed reduction in viable melanoma cells arose from engulfment and not cytolysis (Figure 5E); incubation with Triton 1% was used as a control condition associated with major calcein leak from lysed B16 melanoma cells (Figure 5E). Finally, we also examined the extent of apoptotic cell death occurring in the lungs of mice i.v. injected with B16 melanoma cells 24 hours after EPC administration (ratio B16-EPC 10:1). Interestingly, we only found TUNEL-positive staining in the lungs of mice pre-administered with EPC-CM but failed to detect cell death signal when EPC or SPARC-KO EPC-CM were used, thereby supporting a role of SPARC-expressing EPC in the reduction in metastases formation (Figure 5F).

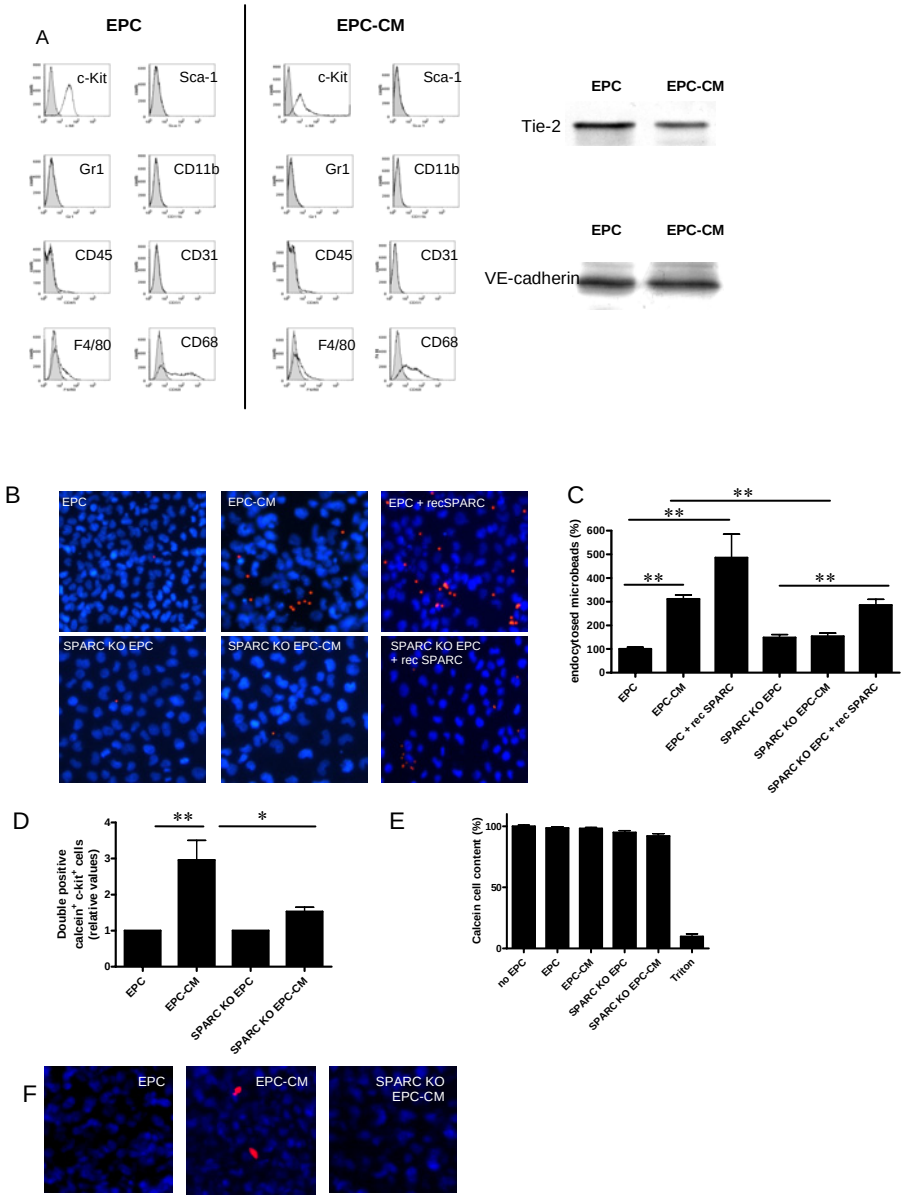

Figure 5. SPARC-driven macrophagic phenotype and activity of EPC-CM. **A.** Representative flow cytometry analyses of EPC and EPC-CM for expression of cKit, Sca-1, CD11b, Gr1, CD45, CD31, CD68 and F4/80. **B.** Representative pictures of the phagocytosis of fluorescent microbeads by EPC and SPARC KO EPC (exposed or not to conditioned media); the effect of recombinant mouse SPARC is also represented. **C.** Quantification of endocytosed microbeads in corresponding conditions; **p<0.01, n = 3. **D**. Bar graph represent the extent of endocytosed calcein-preloaded B16 melanoma cells in different EPC populations, as determined by double staining for calcein and c-kit; *p<0.05; **p<0.01, n = 3. **E**. Bar graph represents the calcein cell content (ie, the lack of cytolysis) after a 24h-co-incubation between tumor cells and EPC (ratio 10:1); Triton was used as a positive control of a calcein leaking condition (n = 3). **F.** Representative pictures of TUNEL-positive staining (red) and DAPI nuclei counterstaining (blue) in lung sections from mice i.v. injected with B16 melanoma cells 24 hours after EPC, EPC-CM and SPARC-KO EPC-CM i.v. administration (ratio B16-EPC 10:1).

Conditioned medium from highly invasive MDA-MB231-D3H2 cells reduces SPARC functional expression in hEPC and increases metastases spreading

We then wondered whether a lack of SPARC induction in EPC could participate in the exacerbation of the metastatic potential of more aggressive tumor cells. We used a luciferase-expressing MDA-MB231 D3H2 breast cancer cell line obtained after several rounds of *in vivo* selection for their high metastatic potential (Jenkins et al., 2005) and a human model of endothelial progenitor cells (hEPC) derived from human umbilical cord. We showed that hEPC exposed to the CM of MDA-MB231-D3H2 cells led to a reduction in SPARC mRNA and protein expression (Figures 6A and 6B); in these conditions, the interaction between the two cells types (ie, as measured in the hanging drop assay by counting the number isolated cells) and the macrophagic potential of hEPC-CM (as measured with microfluorescent beads) were also significantly reduced (Figures 6C and 6D). Finally, we showed that injection of hEPC-CM together with MDA-luc cells significantly increased the extent of metastases spreading (Figure 6E).

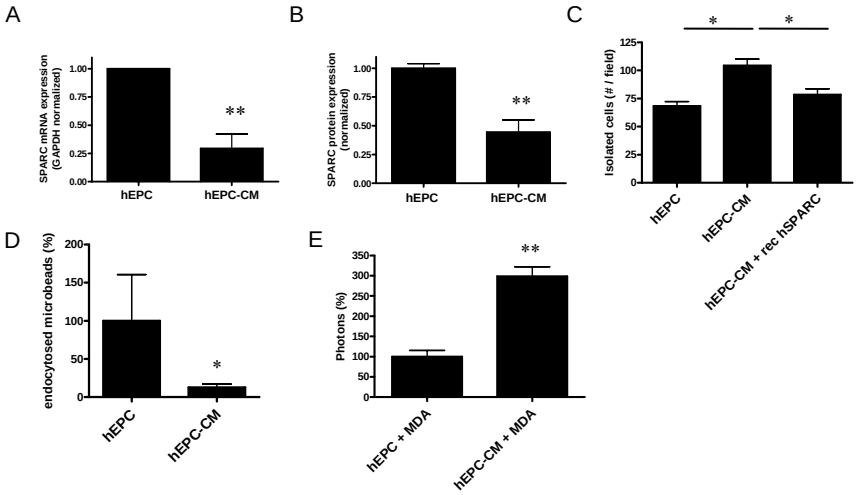

Figure 6. Conditioned medium of highly metastatic MDA-MB231-D3H2 breast cancer cells reduces SPARC expression in human EPC and increases metastases spreading. Bar graphs represent (**A**) SPARC mRNA expression and (**B**) SPARC protein expression in hEPC exposed or not to MDA-MB231-D3H2 conditioned medium (CM). (**C**) Bar graph represents the extent of non-aggregated MDA-MB231-D3H2 cells per microscopic field determined in the presence of EPC or EPC-CM, with or without recombinant human SPARC (rec hSPARC), using the hanging drop assay as detailed in the Methods section; ** $p<0.01$, n=3. (**D**) Bar graph represents the extent of endocytosed fluorescent microbeads by hEPC and hEPC-CM; *$p<0.05$, n = 3. (**E**) Bar graph represents the extent of photons detected post-injection of 10^6 luciferase-expressing MDA-MB231-D3H2 cells 24 hours after i.v. hEPC or hEPC-CM injections (10:1 ratio); **$P<0.01$, n=10-15 for each group.

Discussion

The major findings of this study are that (i) endothelial progenitor cells may exert a protective role against metastases development and that (ii) SPARC plays a key role in the capacity of EPC to physically interact with and phagocyte tumor cells. Interestingly, expression of SPARC and associated anti-metastatic effect are driven by EPC preconditioning by the tumor secretome. By exposing naïve EPC to the culture supernatant of melanoma cells, we indeed aimed to mimic the paracrine influence of primary tumor on bone marrow progenitor cells, and in particular EPC. That EPC are under the influence of growth factors or cytokines released by tumor cells is a concept well established for the mobilization step of these cells from the bone marrow: we and other documented that VEGF and SDF-1 play active roles to favor the local migration and intravasation of EPC (Sbaa et al., 2006; Sonveaux et al., 2004; Asahara et al., 1999; Yamaguchi et al., 2003). Here, we show that this mobilization may also be envisioned as a defense mechanism where the macrophagic characteristics of EPC can confer these cells with the capacity to eliminate circulating tumor cells (eg, B16 melanoma cells). Conversely, the high pro-metastatic potential of tumor cells (eg, MDA-MB231-D3H2 breast cancer cells) could in part arise from their capacity to switch-off the SPARC-mediated macrophagic activity of host-derived circulating cells such as mobilized EPC.

There are several reports documenting the phenotypic proximity beween monocytes and EPC suggesting either a common ancestor or at least important parenthood between these cell types (De and Naldini, 2006; Ribatti, 2007; Rehman et al., 2003). In our hands, we found that EPC, when pre-challenged with the conditioned medium of melanoma cells could stimulate physical interactions between the two cell types and lead to phagocytosis. Our data do not exclude a pro-angiogenic role of EPC when primary tumors are implanted but emphasize that EPC released from the bone marrow are not yet completely engaged in the endothelial lineage and share some properties characteristic of immune cells. Recently, Raemer and colleagues reported that EPC may act as antigen-presenting cells (Raemer et al., 2009). Now, we show that these cells, when exposed to a cocktail of secreted substances from tumor cells, are also endowed with engulfment or phagocytosis properties.

2D-DIGE experiments led us to identify SPARC as a protein the expression of which was dramatically increased in EPC following exposure to conditioned tumor cell media. SPARC is a calcium-binding matricellular glycoprotein which acts as an extracellular scaffolding protein which binds to the ECM, integrins and growth factor receptors (Yan and Sage, 1999; Tai and Tang, 2008). We observed that conditioned medium-mediated overexpression of SPARC induced a strong aggregation between melanoma cells and EPC, an effect mimicked by the use of recombinant SPARC. Of note, all our attempts to measure native SPARC in the culture medium of conditioned EPC failed, indicating that "active" SPARC is likely to be extracellular but entrapped within the extracellular matrix of EPC. The high affinity of SPARC for fibronectin (as shown in Figure 4D) supports the role of "glue" for SPARC which could account for the favored interaction between EPC-CM and fibronectin-producing melanoma cells. This pro-adhesive role of SPARC differs from other reports attributing anti-adhesive properties to SPARC (Said et al., 2007). Schultz et al. (Schultz et al., 2002) however documented that according to the amounts of SPARC, both pro- and anti-adhesive properties could be observed. Interestingly, using SPARC-null mice, Brekken and colleagues reported that lack of SPARC expression by the host (*vs* tumor cells) enhanced tumor growth (Brekken et al., 2003). These authors actually reported that the tumor burden was increased in SPARC KO mice after tumor cells were injected subcutaneously but also intravenously: a significant increase in detectable tumor colonies was observed on the surface of the lungs. Similarly, in our study, we found that highly metastatic MDA-MB231-D3H2 breast cancer cells reduced SPARC expression in hEPC in a paracrine manner, leading to a decrease in the SPARC-mediated macrophagic potential of progenitor cells and an associated increased metastatic burden. Brekken and colleagues further documented in a model of pancreatic carcinoma that increased tumor burden in the absence of host SPARC was a consequence of reduced collagen deposition and a disrupted vascular basement membrane but was also attributable to an immune-tolerant microenvironment (Arnold et al., 2010). They actually found that macrophage recruitment and polarization to the M2 phenotype was augmented in the absence of SPARC. Together with our data identifying a role for SPARC in the phagocytic capacity of EPC, this indicates that

the expression of SPARC by host-derived macrophage-like progenitor cells directly influences the metastatic progression of the disease. More generally, these data emphasize the critical role of SPARC expressed by non-tumor cells, in cancer progression, which appears at odds with the well-characterized tumorigenic role of SPARC expressed by tumor cells, in particular in melanoma (Ledda et al., 1997b; Ledda et al., 1997a).

In conclusion, our study unravels the influence of tumor cells on the phenotype of EPC characterized by a SPARC-driven modulation of their macrophagic capacity. This observation adds new layers of complexity to the roles of EPC and SPARC. We now show that (i) besides their largely advertised capacity to stimulate angiogenesis, the so-called EPC can also prevent metastases spreading and (ii) despite a pro-invasive role of SPARC when expressed in tumor cells, SPARC expression in EPC may drive the interaction with and elimination of circulating tumor cells. More generally, the plasticity of EPC and the multiple role of SPARC in tumor and host tissues need therefore to be carefully evaluated before considering therapeutic modalities based on anti-vasculogenic strategies or SPARC inhibition.

References

Reference List

Ahn,G.O. and Brown,J.M. (2009). Role of endothelial progenitors and other bone marrow-derived cells in the development of the tumor vasculature. Angiogenesis. *12*, 159-164.

Arnold,S.A., Rivera,L.B., Miller,A.F., Carbon,J.G., Dineen,S.P., Xie,Y., Castrillon,D.H., Sage,E.H., Puolakkainen,P., Bradshaw,A.D., and Brekken,R.A. (2010). Lack of host SPARC enhances vascular function and tumor spread in an orthotopic murine model of pancreatic carcinoma. Dis. Model. Mech. *3*, 57-72.

Asahara,T., Takahashi,T., Masuda,H., Kalka,C., Chen,D., Iwaguro,H., Inai,Y., Silver,M., and Isner,J.M. (1999). VEGF contributes to postnatal neovascularization by mobilizing bone marrow-derived endothelial progenitor cells. EMBO J. *18*, 3964-3972.

Asakage,M., Tsuno,N.H., Kitayama,J., Kawai,K., Okaji,Y., Yazawa,K., Kaisaki,S., Osada,T., Watanabe,T., Takahashi,K., and Nagawa,H. (2006). Early-outgrowth of endothelial progenitor cells can function as antigen-presenting cells. Cancer Immunol. Immunother. *55*, 708-716.

Brekken,R.A., Puolakkainen,P., Graves,D.C., Workman,G., Lubkin,S.R., and Sage,E.H. (2003). Enhanced growth of tumors in SPARC null mice is associated with changes in the ECM. J. Clin. Invest *111*, 487-495.

Crooke,C.E., Pozzi,A., and Carpenter,G.F. (2009). PLC-gamma1 regulates fibronectin assembly and cell aggregation. Exp. Cell Res. *315*, 2207-2214.

De,P.M. and Naldini,L. (2006). Role of haematopoietic cells and endothelial progenitors in tumour angiogenesis. Biochim. Biophys. Acta *1766*, 159-166.

Gao,D. and Mittal,V. (2009). The role of bone-marrow-derived cells in tumor growth, metastasis initiation and progression. Trends Mol. Med. *15*, 333-343.

Gao,D., Nolan,D., McDonnell,K., Vahdat,L., Benezra,R., Altorki,N., and Mittal,V. (2009). Bone marrow-derived endothelial progenitor cells contribute to the angiogenic switch in tumor growth and metastatic progression. Biochim. Biophys. Acta *1796*, 33-40.

Hatzopoulos,A.K., Folkman,J., Vasile,E., Eiselen,G.K., and Rosenberg,R.D. (1998). Isolation and characterization of endothelial progenitor cells from mouse embryos. Development *125*, 1457-1468.

Jenkins,D.E., Hornig,Y.S., Oei,Y., Dusich,J., and Purchio,T. (2005). Bioluminescent human breast cancer cell lines that permit rapid and sensitive in vivo detection of mammary tumors and multiple metastases in immune deficient mice. Breast Cancer Res *7*, R444-R454.

Joyce,J.A. and Pollard,J.W. (2009). Microenvironmental regulation of metastasis. Nat. Rev. Cancer *9*, 239-252.

Kashani-Sabet,M., Rangel,J., Torabian,S., Nosrati,M., Simko,J., Jablons,D.M., Moore,D.H., Haqq,C., Miller,J.R., III, and Sagebiel,R.W. (2009). A multi-marker assay to distinguish malignant melanomas from benign nevi. Proc. Natl. Acad. Sci. U. S. A *106*, 6268-6272.

Kupatt,C., Horstkotte,J., Vlastos,G.A., Pfosser,A., Lebherz,C., Semisch,M., Thalgott,M., Buttner,K., Browarzyk,C., Mages,J., Hoffmann,R., Deten,A., Lamparter,M., Muller,F., Beck,H., Buning,H., Boekstegers,P., and Hatzopoulos,A.K. (2005). Embryonic endothelial progenitor cells expressing a broad range of proangiogenic and remodeling factors enhance vascularization and tissue recovery in acute and chronic ischemia. FASEB J. *19*, 1576-1578.

Ledda,F., Bravo,A.I., Adris,S., Bover,L., Mordoh,J., and Podhajcer,O.L. (1997a). The expression of the secreted protein acidic and rich in cysteine (SPARC) is associated with the neoplastic progression of human melanoma. J. Invest Dermatol. *108*, 210-214.

Ledda,M.F., Adris,S., Bravo,A.I., Kairiyama,C., Bover,L., Chernajovsky,Y., Mordoh,J., and Podhajcer,O.L. (1997b). Suppression of SPARC expression by antisense RNA abrogates the tumorigenicity of human melanoma cells. Nat. Med. *3*, 171-176.

Mariner,D.J., Davis,M.A., and Reynolds,A.B. (2004). EGFR signaling to p120-catenin through phosphorylation at Y228. J. Cell Sci. *117*, 1339-1350.

Mbeunkui,F. and Johann,D.J., Jr. (2009). Cancer and the tumor microenvironment: a review of an essential relationship. Cancer Chemother. Pharmacol. *63*, 571-582.

Nakul-Aquaronne,D., Bayle,J., and Frelin,C. (2003). Coexpression of endothelial markers and CD14 by cytokine mobilized CD34+ cells under angiogenic stimulation. Cardiovasc. Res. *57*, 816-823.

Raemer,P.C., Haemmerling,S., Giese,T., Canaday,D.H., Katus,H.A., Dengler,T.J., and Shankar,S.G. (2009). Endothelial progenitor cells possess monocyte-like antigen-presenting and T-cell-co-stimulatory capacity. Transplantation *87*, 340-349.

Rehman,J., Li,J., Orschell,C.M., and March,K.L. (2003). Peripheral blood "endothelial progenitor cells" are derived from monocyte/macrophages and secrete angiogenic growth factors. Circulation *107*, 1164-1169.

Ribatti,D. (2007). The discovery of endothelial progenitor cells. An historical review. Leuk. Res. *31*, 439-444.

Said,N., Najwer,I., and Motamed,K. (2007). Secreted protein acidic and rich in cysteine (SPARC) inhibits integrin-mediated adhesion and growth factor-dependent survival signaling in ovarian cancer. Am. J. Pathol. *170*, 1054-1063.

Sangaletti,S., Di,C.E., Gariboldi,S., Miotti,S., Cappetti,B., Parenza,M., Rumio,C., Brekken,R.A., Chiodoni,C., and Colombo,M.P. (2008). Macrophage-derived SPARC bridges tumor cell-extracellular matrix interactions toward metastasis. Cancer Res. *68*, 9050-9059.

Sbaa,E., Dewever,J., Martinive,P., Bouzin,C., Frerart,F., Balligand,J.L., Dessy,C., and Feron,O. (2006). Caveolin plays a central role in endothelial progenitor cell mobilization and homing in SDF-1-driven postischemic vasculogenesis. Circ. Res *98*, 1219-1227.

Schultz,C., Lemke,N., Ge,S., Golembieski,W.A., and Rempel,S.A. (2002). Secreted protein acidic and rich in cysteine promotes glioma invasion and delays tumor growth in vivo. Cancer Res. *62*, 6270-6277.

Shaked,Y. and Voest,E.E. (2009). Bone marrow derived cells in tumor angiogenesis and growth: are they the good, the bad or the evil? Biochim. Biophys. Acta *1796*, 1-4.

Sonveaux,P., Martinive,P., Dewever,J., Batova,Z., Daneau,G., Pelat,M., Ghisdal,P., Gregoire,V., Dessy,C., Balligand,J.L., and Feron,O. (2004). Caveolin-1 expression is critical for vascular endothelial growth factor-induced ischemic hindlimb collateralization and nitric oxide-mediated angiogenesis. Circ. Res *95*, 154-161.

Tai,I.T. and Tang,M.J. (2008). SPARC in cancer biology: its role in cancer progression and potential for therapy. Drug Resist. Updat. *11*, 231-246.

Thoreson,M.A., Anastasiadis,P.Z., Daniel,J.M., Ireton,R.C., Wheelock,M.J., Johnson,K.R., Hummingbird,D.K., and Reynolds,A.B. (2000). Selective uncoupling of p120(ctn) from E-cadherin disrupts strong adhesion. J. Cell Biol. *148*, 189-202.

Wei,J., Blum,S., Unger,M., Jarmy,G., Lamparter,M., Geishauser,A., Vlastos,G.A., Chan,G., Fischer,K.D., Rattat,D., Debatin,K.M., Hatzopoulos,A.K., and Beltinger,C. (2004). Embryonic endothelial progenitor cells armed with a suicide gene target hypoxic lung metastases after intravenous delivery. Cancer Cell *5*, 477-488.

Wels,J., Kaplan,R.N., Rafii,S., and Lyden,D. (2008). Migratory neighbors and distant invaders: tumor-associated niche cells. Genes Dev. *22*, 559-574.

Wickersheim,A., Kerber,M., de Miguel,L.S., Plate,K.H., and Machein,M.R. (2009). Endothelial progenitor cells do not contribute to tumor endothelium in primary and metastatic tumors. Int. J. Cancer *125*, 1771-1777.

Witz,I.P. and Levy-Nissenbaum,O. (2006). The tumor microenvironment in the post-PAGET era. Cancer Lett. *242*, 1-10.

Yamaguchi,J., Kusano,K.F., Masuo,O., Kawamoto,A., Silver,M., Murasawa,S., Bosch-Marce,M., Masuda,H., Losordo,D.W., Isner,J.M., and Asahara,T. (2003). Stromal cell-derived factor-1 effects on ex vivo expanded endothelial progenitor cell recruitment for ischemic neovascularization. Circulation *107*, 1322-1328.

Yan,Q. and Sage,E.H. (1999). SPARC, a matricellular glycoprotein with important biological functions. J. Histochem. Cytochem. *47*, 1495-1506.

2D-DIGE analyses.

Sample preparation. EPC (exposed to conditioned medium or control medium for 24h) were rinsed twice with PBS and scrapped with DIGE Labeling (DLA) buffer (CHAPS 4%, urea 7 M, thiourea 2 M, Tris 30 mM pH 8.5). Lysates were then clarified by centrifugation at 13,000 rpm for 15 min at 4°C and protein concentration determined by the Bradford method (BioRad). Extracts were diluted to reach a final concentration of 5 to 10 µg/µl and pH was adjusted to 8.5. 25 µg of each sample (n = 3 per condition) was minimally labelled with CyDyes (Amersham GE Healthcare) for 30 min in the dark (200 pmol of amine-reactive cyanine dyes, Cy3 or Cy5) at 4°C according to the manufacturer's instructions. An internal standard, obtained after pooling an equal amount of the 6 different samples, was labelled with Cy2. Labelling reaction was stopped by incubating the mixture 10 min with10 mM lysine (Sigma Aldrich). Samples were then diluted twice (CHAPS 4%, Urea 7 M, thiourea 2 M, Tris 30 mM, DTT 30 mM, IPG buffer 3-11 (v/v) 1% (Amersham GE Healthcare) and reduced 20 min in the dark at room temperature before clarification by centrifugation at 13,000 rpm during 10 min. Each gel was then loaded with 25 µg of mixed labelled samples and 25 µg of the internal standard.

Electrophoresis. The first dimension was performed with Immobiline DryStrips (IPG strip, continuous pH 3-11 gradient, 24 cm; Amersham GE Healthcare). IPG strips were rehydrated in an Immobiline DryStrip reswelling tray (Amersham GE Healthcare) for 24 h at room temperature with rehydration buffer (DeStreak solution and IPG buffer 3-11 (v/v) 0.5%) for IPG strip pH 3-11 and covered with DryStrip oil. Samples were loaded in a cupule at the more acidic part of the IPG strips. Isoelectric focusing (IEF) was run on an IPGphor isoelectric focusing system (Amersham GE Healthcare) with the following parameters: 300 V for 3 h, gradient step of 1,000 V for 8 h, gradient step of 8,000 V for 3 h and 8,000 V for 25,600 V.h at 20°C with a maximum current setting of 50 µA/strip. IPG strips were then washed with distilled water and incubated subsequently for 15 min with an equilibration

buffer [Tris-HCl 50mM (pH 8.8), urea 6 M, glycerol (v/v) 30%, SDS (w/v) 2%] supplemented with DTT 10 mg/ml or iodoacetamide 25 mg/ml, respectively. IPG strips were then washed with running buffer [Tris-HCl 50 mM (pH 8.5), glycine 384 mM, SDS 0.2%] twice concentrated and sealed with agarose 0.5% (containing bromophenol blue) on the top of a 10% SDS-PAGE pre-poured between low fluorescent glass plates using an Ettan-DALT caster (Amersham GE Healthcare). Twice concentrated buffer and normal running buffer were added at the top and the bottom of the gels, respectively. Electrophoresis was performed overnight (16 h) at 15°C with 1 W/gel in the EttanDalt six (Amersham GE Healthcare). The 3 gels from a same experiment were run at the same time.

Image acquisition and statistical analysis. In order to observe cyanin-labelled proteins, gels were scanned in fluorescence with Ettan DIGE Imager (GE Healthcare) at a resolution of 100 µm. Cy2 images were obtained from a 488 nm excitation laser coupled to a 520 nm emission filter. Cy3 images were obtained from a 532 nm excitation laser coupled to a 580 nm emission filter. Cy5 images were obtained from a 633 nm excitation laser coupled to a 670 nm emission filter. A total of 9 gels images was generated for each comparative experiment and analyzed using DeCyder Differential Analysis Software v7.0 (Amersham GE Healthcare) for spot detection, matching, quantization and statistical analysis. First, a differential in-gel analysis (DIA) was applied on each gel to eliminate gel-to-gel variance by matching and normalizing every spot gel with the corresponding internal standard. Second, a biological variation analysis (BVA) software, using student's t test ($p < 0.005$), was run to detect statistical differential protein expression between the control and treated groups.

Sample recovering. Two preparative 2D gels were performed with 300 µg of unlabelled proteins. The protocol remained unchanged as for analytical gels except that the sample was loaded in two times for the first dimension in order to decrease protein precipitation; and for the second dimension, one of the low fluorescent glass plates was pre-treated with bind-silane (Amersham GE Healthcare). At the end, the

plate without bind-silane was removed and the gel was incubated in a fixating solution (ethanol 30%, acetic acid 10%) for 5 h. Gels were then washed 3 times for 30 min with a solution of 20% ethanol before overnight protein staining with 7 µl of 20 mM Ruthenium II solution [Ruthenium II tris (bathophenantroline disulfonate)]. Gels were then washed three times with distilled water (Milli-Q system, Millipore) for 15 min. Gels were scanned with Ettan DIGE Imager (GE Healthcare) using a 532 nm excitation laser coupled to a 610 nm emission filter. After matching the preparative gel picture to the master analytical gel image, spots of interest were localized on the preparative gel and picked with an automated Ettan Spot Picker (GE Healthcare) following the manufacturer's instructions. Spots were transferred in a 96-well plate and kept frozen at -20°C until protein digestion.

Protein extraction and digestion. Gel fragments were washed twice with distilled water (Milli-Q system, Millipore) and once with acetonitril (ACN) 100% at 1000 rpm and 21°C for 10 min. Pellets were then dried at 37°C during 20 min. Proteins were first digested on ice with trypsin 12.5 ng/µl (Promega, Madison, USA) in 50 mM NH_4CO_3 for 45 min, and then overnight at 37°C. Peptides were extracted with 10 µl acid formic 5% at 37°C for 15 minutes and the collected supernatants were kept frozen at – 20°C until mass spectrometry analysis.

Protein identification. Proteins were identified on the basis of their "peptide mass fingerprint" with a matrix-assisted laser desorption/ionization MX (Maldi) (Waters). Peptide mass maps were acquired in the reflectron mode with delayed extraction. Mass spectra were internally calibrated with trypsin autolysis peaks. Full-length proteins were identified with Mascot software (version 2.2) (Matrix Sciences) by sequence homology research against adequate protein databases.

Real-time PCR and shRNA silencing. Primers sequences were designed by Invitrogen primer tool: for mouse SPARC, forward primer was 5'-GGCCTGGATCTTCTTTCTCC -*3'* and reverse primer was 5'-CACGGTTTCCTCCTCCACTA -*3'* and for human SPARC, forward primer was 5'-

GATGAGACAGAGGTGGTGGA -*3'* and reverse primer was 5'-CTCCTCTTCGGTTTCCTCTG -*3'*. Mouse β-actin and human tubulin-β transcripts were used for normalization. For silencing experiments, EPC were transfected with a pLKO.1 vector coding for a shRNA targeting mouse SPARC sequence (Mission shRNA plasmid DNA, Sigma, Bornem, Belgium); a control vector was used in parallel experiments. Plasmids were amplified and purified using NucleoBond columns according to the manufacturer's protocol and transfections were performed with Lipofectamin 2000 (Invitrogen). Prolonged incubation with puromycin (Calbiochem) was used to establish selection of clones and qPCR was used to select the EPC clone with the highest silencing effect. The shRNA sequence of the selected clone (named EPC SPARC KO in our study) was the following: CCGGGAAGGTATGCAGCAATGACAACTCGAGTTGTCATTGCTGCATACC TTCTTTTTG

Flow cytometry. For flow cytometry characterization of EPC, cell suspensions were labelled with PE-conjugated c-kit antibody (BD Biosciences), FITC-conjugated Sca-1 antibody (BD Biosciences), PE-conjugated CD11b antibody (BD Biosciences) and APC-conjugated CD45 antibody (Immunosource). F4/80 (Invitrogen) and CD68 (Serotec) antibodies were also used together with Alexa 488-conjugated secondary antibodies (BD Biosciences) as well as biotin-conjugated Gr1 (BD Biosciences) and CD31 antibodies (BD Biosciences) together with PE-conjugated streptavidin (BD Biosciences). Control experiments included incubation in the absence of primary antibody or with an irrelevant conjugated primary antibody. Fluorescence intensity was measured using a FACScan apparatus (BD Biosciences) and was analyzed by the FlowJo software.

CONCLUSION-PERSPECTIVES

A tumor is composed of a complex network of tumor cells and host cells, including fibroblasts and macrophages. The tumor also secretes various factors which remodel the tumor microenvironment through the stimulation of angiogenesis or the recruitment of immune cells and eventually favor proliferation, local invasion and metastases.

In this work, we examined how intrinsic characteristics of the tumor microenvironment as well as treatment-induced alterations thereof influence (1) the humoral immune response and (2) the dialog with bone marrow-derived cells.

1. Influence of the anti-cancer humoral response on circulating autoantibodies used as biomarkers of tumor growth and metastases.

In this part of our work, we used different mouse tumor models to evaluate the impact of angiogenesis, therapies and hypoxia on the nature and the titer of autoantibodies. We also took advantage of this study to optimize the SERPA technology, by integrating the CyDyes multiplex detection.

We first investigated the impact of angiogenesis and anti-cancer treatments on the biology of autoantibodies in the Lewis lung carcinoma model. We identified anti-GRP78 autoantibodies as an early marker of tumor growth and also of the metastatic progression following surgical removal of the primary tumor. We then tracked the changes in the anti-GRP78 autoantibodies titer following anti-cancer treatments. Most cancer patients are exposed to chemo- and radiotherapy and these treatments are likely to impact the presence and production of autoantibodies. In this study, we found that chemotherapy was associated with a reduction in the serum titer of anti-GRP78 antibodies whereas radiotherapy increased it. We provided evidence that the decrease in anti-GRP78 autoantibodies (and circulating IgG in general) following cyclophosphamide administration could be related to the observed net reduction in lymphocytes, in particular the antibody-producing B cell population. The myelotoxicity of chemotherapy (Machiels et al., 2001; Zitvogel et al., 2008b;

Zitvogel et al., 2008a) may thus be misguiding by indirectly leading to a reduction in autoantibody-based biomarker concentrations. As anticipated, local irradiation of the tumor did not influence the number of B-cells in treated animals. The observed radiation-driven increase in anti-GRP78 autoantibodies was instead related to an overall increased stress response favoring the expression of functional GRP78. Additional mechanisms could involve radiation-triggered degradation of GRP78 protein, thereby increasing the pool of peptides presented by the MHC class I pathway (Zitvogel et al., 2008a). The observed local increase in IgG abundance in the tumor and overall decrease in circulating IgG post-radiation support the hypothesis of an overall-stimulated immune response.

Chemotherapy and radiotherapy are believed to kill cancer cells by apoptosis (Ma et al., 2011). Conventionally, apoptosis is considered as a non immunogenic-cell death modality contrary to necrosis (Zitvogel et al., 2008b). Indeed, apoptosis is a rapid form of cell death, characterized by the rounding of cell, retraction of pseudopodes, chromatin condensation, nuclear fragmentation, plasma membrane blebbing and importantly clearing of the resulting apoptotic bodies (Ullrich et al., 2008; Gregory and Pound, 2010). By contrast, necrosis is characterized by the swelling of cytoplasm and organelles, leading to the disruption of the plasma membrane, thereby creating local pro-immunogenic inflammation (Ullrich et al., 2008). This view however recently changed and immunogenicity now appears to be also induced by apoptosis according to the anticancer strategies. Kroemer and collaborators actually documented that radiotherapy, doxorubicin and oxaliplatin (among many anticancer drugs screened) were able to induce immunogenic cell death, relying on two major checkpoints, calreticulin exposure (“eat me” signal) and HMGB1 release (“danger” signal) (Apetoh et al., 2007; Obeid et al., 2007). These events in turn prompt dendritic cells for antigen uptake and TLR4-dependent antigen processing (Apetoh et al., 2007). Thus, based on these reports, in our study, ionizing radiations induced an immunogenic cell death, while chemotherapy (cyclophosphamid) preferentially induced a non-immunogenic cell death, further supporting the differential impact of grp78 autoantibodies titer.

This part of our study therefore emphasizes the limitations in exploiting autoantibodies as cancer biomarkers in cancer patients exposed to conventional therapeutic modalities.

In the second part of our work on the serological proteome, we focused on the influence of hypoxia on the expression of tumor-associated antigens and in consequence on the nature of circulating autoantibodies. Hypoxia is one of the most common features of cancer. Cancer cells proliferate very rapidly and intervessel distances may increase to such extent that local deficiency in pO_2 is observed. Hypoxia is known to increase mutations occurrence and more generally to induce changes in gene expression. Hypoxia therefore induces proteomic changes that determine the phenotype of tumor cells.

In the SERPA technique, protein extracts of tumor cells cultured *in vitro* are used as substrates for the detection of autoantibodies present in the serum. In order to better mimick the *in vivo* conditions, we have exposed MDA-MB-231 mammary tumor cells to hypoxia before processing the SERPA screening. After subtractive analysis of the immunoblots, we were able to demonstrate the presence of hypoxia-selective tumor-associated antigens. After identification of the proteins of interest, we focused our attention on six proteins: protein-disulfide isomerase A3, calponin-2, Obg-like ATPase 1, peroxiredoxin-6, aminoacylase-1, eukaryotic translation initiation factor 3 subunit G. We further confirmed in ELISA assays the presence of higher titers of corresponding autoantibodies in tumor-bearing mice.

Although validation with patient sera is needed, this study underscores the interest to work with a hypoxia-induced repertoire of tumor antigens to identify relevant autoantibodies as biomarkers of cancer.

2. Influence of the primary tumor secretome on the metastatic progression

In the last part of our work, we examined how the secretome of tumor cells can influence the metastatic progression of B16 melanoma in mice. Tumor cells are known to mobilize bone marrow-derived cells and to recruit them at the primary tumor site or in so-called premetastatic niches. Here, we examined whether one type of bone marrow-derived cells, namely EPC, already described to support tumor angiogenesis, were also involved in metastases formation.

We exposed EPC to the conditioned medium of luciferase-expressing B16 melanoma cells and further injected them intravenously along with tumor cells. Surprisingly, we observed that preconditioned EPC protect mice against the development of metastases. A 2D-proteomic-based approach allowed us to compare the profile of control EPC and EPC exposed to the secretome of tumor cells. Among the identified proteins, we focused on SPARC, the most upregulated protein. We demonstrated that the incidence of metastases increased when SPARC was knocked down in EPC. We showed that EPC and melanoma cells physically interact in a SPARC-dependent manner and that consecutively, EPC could phagocytose melanoma cells. We confirmed that stimulated EPC presented phagocytic properties using intracellularly labelled tumor cells and fluorescent microbeads. We also found that highly metastatic MDA-MB231-D3H2 breast cancer cells reduced SPARC expression in human EPC in a paracrine manner, leading to a decrease in the SPARC-mediated macrophagic potential of progenitor cells and an associated increased metastatic burden.

Altogether, our data indicate that the expression of SPARC by host-derived macrophage-like progenitor cells directly influences the metastatic progression of the disease. More generally, these data emphasize the critical role of SPARC expressed by non-tumor cells, in cancer progression, which appears at odds with the well-characterized tumorigenic role of SPARC expressed by tumor cells, in particular in melanoma (Ledda et al., 1997b; Ledda et al., 1997a).

Targeting SPARC to cure cancer as proposed by some authors needs to be carefully evaluated. Some studies suggested therapies in order to decrease SPARC expression in tumor cells and surrounding stroma because of SPARC association to tumor aggressiveness (Lopez et al., 2006; Shi et al., 2007; Yin et al., 2010; Seno et al., 2009; Horie et al., 2010). However, we and others documented that overexpression of SPARC could instead provide some benefits by reducing tumor development and metastatic progression (Atorrasagasti et al., 2010). This points out (1) how the multiple roles of SPARC (in proliferation, angiogenesis, cell-cell interaction, cell-matrix interaction) can differentially influence the outcome of tumor growth and (2) how the expression of SPARC can be modulated in function of the tumor type.

3. Final conclusion and perspectives

The aim of this work was to use proteomics to focus on the influence of what we could call “the extra-tumor compartment” on the progression of cancer (see Figure 32).

Accordingly, we first examined the influence of various components of the tumor microenvironment on the humoral immune response. In this context, the extra-tumor actors are the immune cells and in particular B-lymphocytes, the circulating autoantibodies but also the antigens which even if originally part of proteins expressed by tumor cells are processed by specialized cells to mount the immune response. We showed that the couple ‘hypoxia-angiogenesis’ could modulate the immune response, the former by promoting the expression of a specific antigen repertoire, the second by facilitating the access of (probably both) circulating cells and antibodies to the tumor. We also documented that through different mechanisms, chemo- and radiotherapy could perturb the local or bone marrow homeostasis and thereby alter our interpretation of changes in circulating autoantibody titers (Figure 32).

On a translational research perspective, this part of our work provides new insights to improve the serological proteome analysis but also the interpretation of the data. Our studies also led to the identification of unsuspected mammary tumor-associated antigens and the possible use of corresponding autoantibodies to detect early stages of the disease. The ELISA tests that we have developed will allow us to examine the potential of these biomarkers by comparing the sera from breast cancer patients and healthy volunteers.

Our work certainly pleads for the use of 2D-technology to identify autoantibodies but limitations need however to be considered. Indeed, 2D-gels are inefficient to resolve hydrophobic proteins and are very sensitive to the dynamic range and quantitative distribution issues. Development of gel-free-based methods is thus legitimately advertised to circumvent these issues. These methods are based on the high-throughput “shotgun” analysis of peptides from a digested complex protein

sample using an on-line high performance liquid chromatography method, prior to identification using mass spectrometry, such as electrospray ionization-MS.

However, 2D-technology still presents numerous advantages. Indeed, this technique has been tested worldwide and, *in fine*, the most critical variable remains the sample preparation and analysis of the data rather than the 2D-gel process. In addition, most of detection methods are now mass-spectrometry compatible, focusing the identification on the protein of interest and not polluted by contaminating proteins. Based on the ability to analyze simultaneously all the proteins present in the sample at high resolution, 2D-proteomics remains a method of choice to analyse complex samples.

The current view of exploiting 2D-electrophoresis looks now towards an optimization of the samples which have to be separated following the principle “the lower the complexity, the better the performance”. In particular, to improve the separation of membrane proteins, blue-native electrophoresis can be performed (Reisinger and Eichacker, 2006). This technique consists in native electrophoresis for high-resolution separation of enzymatically active protein complexes from tissue homogenates and cell fractions. The separation principle relies on binding of Coomassie blue G250 which provides negative charges to the surface of the protein. An additional advantage of 2D-electrophoresis which warrants the holding of this technology in the next decades is its use for immunodetection purposes. The value of this process relies on parameters such as specificity, reproducibility of 2D-gels and the resolving power where antibodies can identify minor proteins, no more masked by major and unrelated proteins. The immunoblotting can be exploited to identify, as we did in our work, antigens recognized by the immune system (in case of autoimmune diseases, infections and cancers) but also to study post-translational modifications like phosphorylation, citrullination or protein carbonylation. Thus, 2D-technique retains a prominent place in the proteomic field and allows numerous applications to take place in various domains.

Very little is known about the role of autoantibodies on tumor growth or metastasis development. IgG appeared to aggregate in tumors (Nakahara et al., 2006; Tan and Coussens, 2007) and triggered inflammation, recruiting cells from the innate immune system (Andreu et al., 2010; de Visser et al., 2005). Understanding better

why and how autoantibodies are produced and their role in tumorigenesis could be of great interest for new biomarkers identification and potential new therapeutic targets. It is now commonly accepted that tumors are infiltrated by immune cells, including B-lymphocytes (Pages et al., 2010; DeNardo et al., 2008). The binding of autoantibodies to their secreted or released antigen is known to lead to the formation of immune complexes. The concept of circulating immune complexes has been more deeply studied in autoimmune diseases (Sokolove et al., 2011). However, different groups identified circulating immune complexes in ovarian (Cramer et al., 2010), oral (Parveen et al., 2010), breast (Dass et al., 1992) and genitourinary cancers (Aziz et al., 1997). Immune complexes have also been found to be trapped inside tumors. The role of these immune complexes could be mediated through the receptor of the Fc of the immunoglobulins (FcγR for IgG) (Nimmerjahn and Ravetch, 2007b; Nimmerjahn and Ravetch, 2007a). FcγR are expressed on many immune cells. This further highlights the role of myeloid cells in tumor and metastases progression. The involvement of the immune complexes in the humoral immune response and in the recruitment of bone marrow-derived cells to the tumor site and/or to metastatic sites represents therefore an exciting subject of further investigations.

In the second part of our work, the extra-tumor compartment relates to the secretome of tumor cells and to bone marrow-derived cells (BMDC) (Figure 32). In particular, we showed that among the various factors that are produced at the primary site of the tumor, some may influence distant metastatic spreading. SPARC is a marker of such influence of the tumor cell secretome on BMDC, namely endothelial progenitor cells.

Although we showed that whether tumor cells lead to an increase or a decrease in SPARC expression in EPC, it may either prevent or promote metastases formation (through macrophage-like activity), the mechanism through which tumor cells modulates SPARC expression in EPC warrants further studies. Indeed, the factors inducing changes on SPARC expression still need to be identified. Cytokine arrays on tumor conditioned media could help to identify key players. In addition, studies on the promoter of SPARC could also bring critical informations to identify key transcription factors. Finally, Affymetrix studies or 2D-DIGE analysis on tumor

conditioned media of melanoma and breast cancer cells could be of great interest to identify groups of genes or proteins typical for the tumor type. The further screening on other cell lines for these identified clusters of genes/proteins could then also be performed.

More generally, the plasticity of EPC and the multiple role of SPARC in tumor and host tissues need also to be carefully re-evaluated before considering therapeutic modalities based on anti-vasculogenic strategies or SPARC inhibition.

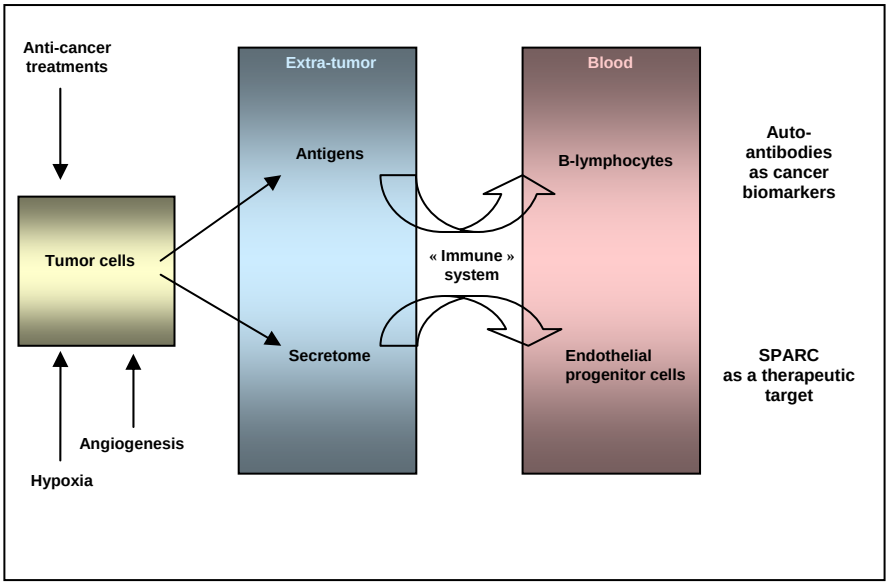

Figure 32: Tumor influences the extra-tumor compartment via its secretome and its antigens. On one hand, tumor cells, by expressing tumor-associated antigens, initiate a humoral immune response leading to the formation of autoantibodies directed against these tumor antigens; autoantibodies can serve as early biomarkers of tumor growth and metastases development. Anticancer treatments, hypoxia and angiogenesis bring their contribution by altering the nature and the blood titer of these autoantibodies. On the other hand, the secretome of tumor cells mobilizes endothelial progenitor cells and induces changes in the expression of various proteins including SPARC. Depending on the tumor types, SPARC will be differentially expressed, its upregulation fostering interaction with tumor cells and reducing metastatic spreading. Thus the "extra-tumor" compartment appears to play key roles in the global stimulation of the immune system via the production of antibodies by B-lymphocytes and the recruitment of progenitor cells endowed with macrophagic functions.

REFERENCES

Reference List

Ahn,G.O. and Brown,J.M. (2009). Role of endothelial progenitors and other bone marrow-derived cells in the development of the tumor vasculature. Angiogenesis. *12*, 159-164.

Alaiya,A.A., Franzen,B., Auer,G., and Linder,S. (2000). Cancer proteomics: from identification of novel markers to creation of artifical learning models for tumor classification. Electrophoresis *21*, 1210-1217.

Alonso,S.R., Tracey,L., Ortiz,P., Perez-Gomez,B., Palacios,J., Pollan,M., Linares,J., Serrano,S., Saez-Castillo,A.I., Sanchez,L., Pajares,R., Sanchez-Aguilera,A., Artiga,M.J., Piris,M.A., and Rodriguez-Peralto,J.L. (2007). A high-throughput study in melanoma identifies epithelial-mesenchymal transition as a major determinant of metastasis. Cancer Res. *67*, 3450-3460.

Amatschek,S., Koenig,U., Auer,H., Steinlein,P., Pacher,M., Gruenfelder,A., Dekan,G., Vogl,S., Kubista,E., Heider,K.H., Stratowa,C., Schreiber,M., and Sommergruber,W. (2004). Tissue-wide expression profiling using cDNA subtraction and microarrays to identify tumor-specific genes. Cancer Res. *64*, 844-856.

Amigorena,S. and Savina,A. (2010). Intracellular mechanisms of antigen cross presentation in dendritic cells. Curr. Opin. Immunol. *22*, 109-117.

Anderson,K.S. and Labaer,J. (2005). The sentinel within: exploiting the immune system for cancer biomarkers. J. Proteome. Res. *4*, 1123-1133.

Anderson,K.S., Wong,J., Vitonis,A., Crum,C.P., Sluss,P.M., Labaer,J., and Cramer,D. (2010). p53 autoantibodies as potential detection and prognostic biomarkers in serous ovarian cancer. Cancer Epidemiol. Biomarkers Prev. *19*, 859-868.

Andreu,P., Johansson,M., Affara,N.I., Pucci,F., Tan,T., Junankar,S., Korets,L., Lam,J., Tawfik,D., DeNardo,D.G., Naldini,L., de Visser,K.E., De,P.M., and Coussens,L.M. (2010). FcRgamma activation regulates inflammation-associated squamous carcinogenesis. Cancer Cell *17*, 121-134.

Apetoh,L., Ghiringhelli,F., Tesniere,A., Obeid,M., Ortiz,C., Criollo,A., Mignot,G., Maiuri,M.C., Ullrich,E., Saulnier,P., Yang,H., Amigorena,S., Ryffel,B., Barrat,F.J., Saftig,P., Levi,F., Lidereau,R., Nogues,C., Mira,J.P., Chompret,A., Joulin,V., Clavel-Chapelon,F., Bourhis,J., Andre,F., Delaloge,S., Tursz,T., Kroemer,G., and Zitvogel,L. (2007). Toll-like receptor 4-dependent contribution of the immune system to anticancer chemotherapy and radiotherapy. Nat. Med. *13*, 1050-1059.

Arnold,S.A. and Brekken,R.A. (2009). SPARC: a matricellular regulator of tumorigenesis. J. Cell Commun. Signal.

Asahara,T. and Kawamoto,A. (2004). Endothelial progenitor cells for postnatal vasculogenesis. Am. J. Physiol Cell Physiol *287*, C572-C579.

Asahara,T., Murohara,T., Sullivan,A., Silver,M., van der,Z.R., Li,T., Witzenbichler,B., Schatteman,G., and Isner,J.M. (1997). Isolation of putative progenitor endothelial cells for angiogenesis. Science *275*, 964-967.

Atorrasagasti,C., Malvicini,M., Aquino,J.B., Alaniz,L., Garcia,M., Bolontrade,M., Rizzo,M., Podhajcer,O.L., and Mazzolini,G. (2010). Overexpression of SPARC obliterates the in vivo tumorigenicity of human hepatocellular carcinoma cells. Int. J. Cancer *126*, 2726-2740.

Aziz,M., Das,T.K., and Rattan,A. (1997). Role of circulating immune complexes in prognostic evaluation and management of genitourinary cancer patients. Indian J. Cancer *34*, 111-120.

Baeriswyl,V. and Christofori,G. (2009). The angiogenic switch in carcinogenesis. Semin. Cancer Biol. *19*, 329-337.

Baldwin,R.W. (1966). Tumour-specific immunity against spontaneous rat tumours. Int. J. Cancer *1*, 257-264.

Baldwin,R.W., Embleton,M.J., Jones,J.S., and Langman,M.J. (1973). Cell-mediated and humoral immune reactions to human tumours. Int. J. Cancer *12*, 73-83.

Banyard,J., Bao,L., and Zetter,B.R. (2003). Type XXIII collagen, a new transmembrane collagen identified in metastatic tumor cells. J. Biol. Chem. *278*, 20989-20994.

Barnhart,B.C. and Simon,M.C. (2007). Metastasis and stem cell pathways. Cancer Metastasis Rev. *26*, 261-271.

Barth,P.J., Moll,R., and Ramaswamy,A. (2005). Stromal remodeling and SPARC (secreted protein acid rich in cysteine) expression in invasive ductal carcinomas of the breast. Virchows Arch. *446*, 532-536.

Beck,A.H., Espinosa,I., Gilks,C.B., van de Rijn,M., and West,R.B. (2008). The fibromatosis signature defines a robust stromal response in breast carcinoma. Lab Invest *88*, 591-601.

Bei,R., Masuelli,L., Palumbo,C., Modesti,M., and Modesti,A. (2009). A common repertoire of autoantibodies is shared by cancer and autoimmune disease patients: Inflammation in their induction and impact on tumor growth. Cancer Lett. *281*, 8-23.

Bellahcene,A. and Castronovo,V. (1995). Increased expression of osteonectin and osteopontin, two bone matrix proteins, in human breast cancer. Am. J. Pathol. *146*, 95-100.

Bergamaschi,A., Tagliabue,E., Sorlie,T., Naume,B., Triulzi,T., Orlandi,R., Russnes,H.G., Nesland,J.M., Tammi,R., Auvinen,P., Kosma,V.M., Menard,S., and Borresen-Dale,A.L. (2008). Extracellular matrix signature identifies breast cancer subgroups with different clinical outcome. J. Pathol. *214*, 357-367.

Berth,M., Moser,F.M., Kolbe,M., and Bernhardt,J. (2007). The state of the art in the analysis of two-dimensional gel electrophoresis images. Appl. Microbiol. Biotechnol. *76*, 1223-1243.

Best,C.J., Gillespie,J.W., Yi,Y., Chandramouli,G.V., Perlmutter,M.A., Gathright,Y., Erickson,H.S., Georgevich,L., Tangrea,M.A., Duray,P.H., Gonzalez,S., Velasco,A., Linehan,W.M., Matusik,R.J.,

Price,D.K., Figg,W.D., Emmert-Buck,M.R., and Chuaqui,R.F. (2005). Molecular alterations in primary prostate cancer after androgen ablation therapy. Clin. Cancer Res. *11*, 6823-6834.

Bhowmick,N.A. and Moses,H.L. (2005). Tumor-stroma interactions. Curr. Opin. Genet. Dev. *15*, 97-101.

Bidard,F.C., Pierga,J.Y., Vincent-Salomon,A., and Poupon,M.F. (2008). A "class action" against the microenvironment: do cancer cells cooperate in metastasis? Cancer Metastasis Rev. *27*, 5-10.

Bitarte,N., Bandres,E., Zarate,R., Ramirez,N., and Garcia-Foncillas,J. (2007). Moving forward in colorectal cancer research, what proteomics has to tell. World J. Gastroenterol. *13*, 5813-5821.

Blass,S., Union,A., Raymackers,J., Schumann,F., Ungethum,U., Muller-Steinbach,S., De,K.F., Engel,J.M., and Burmester,G.R. (2001). The stress protein BiP is overexpressed and is a major B and T cell target in rheumatoid arthritis. Arthritis Rheum. *44*, 761-771.

Borstnar,S., Vrhovec,I., Svetic,B., and Cufer,T. (2002). Prognostic value of the urokinase-type plasminogen activator, and its inhibitors and receptor in breast cancer patients. Clin. Breast Cancer *3*, 138-146.

Brabender,J., Marjoram,P., Lord,R.V., Metzger,R., Salonga,D., Vallbohmer,D., Schafer,H., Danenberg,K.D., Danenberg,P.V., Selaru,F.M., Baldus,S.E., Holscher,A.H., Meltzer,S.J., and Schneider,P.M. (2005). The molecular signature of normal squamous esophageal epithelium identifies the presence of a field effect and can discriminate between patients with Barrett's esophagus and patients with Barrett's-associated adenocarcinoma. Cancer Epidemiol. Biomarkers Prev. *14*, 2113-2117.

Brahimi-Horn,M.C., Chiche,J., and Pouyssegur,J. (2007). Hypoxia and cancer. J. Mol. Med. *85*, 1301-1307.

Brune,K., Hong,S.M., Li,A., Yachida,S., Abe,T., Griffith,M., Yang,D., Omura,N., Eshleman,J., Canto,M., Schulick,R., Klein,A.P., Hruban,R.H., Iacobuzio-Donohue,C., and Goggins,M. (2008). Genetic and epigenetic alterations of familial pancreatic cancers. Cancer Epidemiol. Biomarkers Prev. *17*, 3536-3542.

Budman,L.I., Kassouf,W., and Steinberg,J.R. (2008). Biomarkers for detection and surveillance of bladder cancer. Can. Urol. Assoc. J. *2*, 212-221.

Bullinger,L., Dohner,K., Bair,E., Frohling,S., Schlenk,R.F., Tibshirani,R., Dohner,H., and Pollack,J.R. (2004). Use of gene-expression profiling to identify prognostic subclasses in adult acute myeloid leukemia. N. Engl. J. Med. *350*, 1605-1616.

Calvo,K.R., Liotta,L.A., and Petricoin,E.F. (2005). Clinical proteomics: from biomarker discovery and cell signaling profiles to individualized personal therapy. Biosci. Rep. *25*, 107-125.

Capillo,M., Mancuso,P., Gobbi,A., Monestiroli,S., Pruneri,G., Dell'Agnola,C., Martinelli,G., Shultz,L., and Bertolini,F. (2003). Continuous infusion of endostatin inhibits differentiation, mobilization, and clonogenic potential of endothelial cell progenitors. Clin. Cancer Res. *9*, 377-382.

Caron,M., Choquet-Kastylevsky,G., and Joubert-Caron,R. (2007). Cancer immunomics using autoantibody signatures for biomarker discovery. Mol. Cell Proteomics. *6*, 1115-1122.

Carter,P. (2001). Improving the efficacy of antibody-based cancer therapies. Nat. Rev. Cancer *1*, 118-129.

Casiano,C.A., Mediavilla-Varela,M., and Tan,E.M. (2006). Tumor-associated antigen arrays for the serological diagnosis of cancer. Mol. Cell Proteomics. *5*, 1745-1759.

Celis,J.E. and Moreira,J.M. (2010). Challenges and opportunities in oncoproteomics. Mol. Oncol. *4*, 459-460.

Chatterjee,S.K. and Zetter,B.R. (2005). Cancer biomarkers: knowing the present and predicting the future. Future. Oncol. *1*, 37-50.

Chavakis,E., Urbich,C., and Dimmeler,S. (2008). Homing and engraftment of progenitor cells: a prerequisite for cell therapy. J. Mol. Cell Cardiol. *45*, 514-522.

Che,Y., Luo,A., Wang,H., Qi,J., Guo,J., and Liu,Z. (2006). The differential expression of SPARC in esophageal squamous cell carcinoma. Int. J. Mol. Med. *17*, 1027-1033.

Cheetham,S., Tang,M.J., Mesak,F., Kennecke,H., Owen,D., and Tai,I.T. (2008). SPARC promoter hypermethylation in colorectal cancers can be reversed by 5-Aza-2'deoxycytidine to increase SPARC expression and improve therapy response. Br. J. Cancer *98*, 1810-1819.

Chen,Y., Miller,C., Mosher,R., Zhao,X., Deeds,J., Morrissey,M., Bryant,B., Yang,D., Meyer,R., Cronin,F., Gostout,B.S., Smith-McCune,K., and Schlegel,R. (2003). Identification of cervical cancer markers by cDNA and tissue microarrays. Cancer Res. *63*, 1927-1935.

Chin,D., Boyle,G.M., Williams,R.M., Ferguson,K., Pandeya,N., Pedley,J., Campbell,C.M., Theile,D.R., Parsons,P.G., and Coman,W.B. (2005). Novel markers for poor prognosis in head and neck cancer. Int. J. Cancer *113*, 789-797.

Chlenski,A., Liu,S., Crawford,S.E., Volpert,O.V., DeVries,G.H., Evangelista,A., Yang,Q., Salwen,H.R., Farrer,R., Bray,J., and Cohn,S.L. (2002). SPARC is a key Schwannian-derived inhibitor controlling neuroblastoma tumor angiogenesis. Cancer Res. *62*, 7357-7363.

Cho,W.C. (2007). Contribution of oncoproteomics to cancer biomarker discovery. Mol. Cancer *6*, 25.

Choi,P., Jordan,C.D., Mendez,E., Houck,J., Yueh,B., Farwell,D.G., Futran,N., and Chen,C. (2008). Examination of oral cancer biomarkers by tissue microarray analysis. Arch. Otolaryngol. Head Neck Surg. *134*, 539-546.

Christofori,G. (2006). New signals from the invasive front. Nature *441*, 444-450.

Clark,C.E., Hingorani,S.R., Mick,R., Combs,C., Tuveson,D.A., and Vonderheide,R.H. (2007). Dynamics of the immune reaction to pancreatic cancer from inception to invasion. Cancer Res. *67*, 9518-9527.

Clark,C.J. and Sage,E.H. (2008). A prototypic matricellular protein in the tumor microenvironment--where there's SPARC, there's fire. J. Cell Biochem. *104*, 721-732.

Cordes,C., Von,L.J., Gorogh,T., Ambrosch,P., Gottschlich,S., and Hoffmann,M. (2009). Molecular and immunological aspects of p53 and p53-autoantibodies in head and neck squamous cell carcinoma. Oncol. Rep. *22*, 1299-1303.

Cramer,D.W., O'Rourke,D.J., Vitonis,A.F., Matulonis,U.A., Dijohnson,D.A., Sluss,P.M., Crum,C.P., and Liu,B.C. (2010). CA125 immune complexes in ovarian cancer patients with low CA125 concentrations. Clin. Chem. *56*, 1889-1892.

Croci,D.O., Zacarias Fluck,M.F., Rico,M.J., Matar,P., Rabinovich,G.A., and Scharovsky,O.G. (2007). Dynamic cross-talk between tumor and immune cells in orchestrating the immunosuppressive network at the tumor microenvironment. Cancer Immunol. Immunother. *56*, 1687-1700.

Cui,J.W., Li,W.H., Wang,J., Li,A.L., Li,H.Y., Wang,H.X., He,K., Li,W., Kang,L.H., Yu,M., Shen,B.F., Wang,G.J., and Zhang,X.M. (2005). Proteomics-based identification of human acute leukemia antigens that induce humoral immune response. Mol. Cell Proteomics. *4*, 1718-1724.

Dalla-Torre,C.A., Yoshimoto,M., Lee,C.H., Joshua,A.M., de Toledo,S.R., Petrilli,A.S., Andrade,J.A., Chilton-MacNeill,S., Zielenska,M., and Squire,J.A. (2006). Effects of THBS3, SPARC and SPP1 expression on biological behavior and survival in patients with osteosarcoma. BMC. Cancer *6*, 237.

Dalton,W.S. and Friend,S.H. (2006). Cancer biomarkers--an invitation to the table. Science *312*, 1165-1168.

Dass,T.K., Aziz,M., Rattan,A., and Tyagi,S.P. (1992). Clinical utility and monitoring of breast cancer by circulating immune complexes. Indian J. Pathol. Microbiol. *35*, 298-307.

de Visser,K.E. and Coussens,L.M. (2005). The interplay between innate and adaptive immunity regulates cancer development. Cancer Immunol. Immunother. *54*, 1143-1152.

de Visser,K.E., Korets,L.V., and Coussens,L.M. (2005). De novo carcinogenesis promoted by chronic inflammation is B lymphocyte dependent. Cancer Cell *7*, 411-423.

De,M.L., Sanvito,F., Olivieri,S., Vigano,F., Doglioni,C., Frasson,M., Braga,M., Bachi,A., Dellabona,P., Protti,M.P., and Alessio,M. (2008). Serological immunoreactivity against colon cancer proteome varies upon disease progression. J. Proteome. Res. *7*, 504-514.

De,P.M. and Naldini,L. (2006). Role of haematopoietic cells and endothelial progenitors in tumour angiogenesis. Biochim. Biophys. Acta *1766*, 159-166.

De,V.J., Thykjaer,T., Tarte,K., Ensslen,M., Raynaud,P., Requirand,G., Pellet,F., Pantesco,V., Reme,T., Jourdan,M., Rossi,J.F., Orntoft,T., and Klein,B. (2002). Comparison of gene expression profiling between malignant and normal plasma cells with oligonucleotide arrays. Oncogene *21*, 6848-6857.

DeNardo,D.G., Johansson,M., and Coussens,L.M. (2008). Immune cells as mediators of solid tumor metastasis. Cancer Metastasis Rev. *27*, 11-18.

Desmetz,C., Bascoul-Mollevi,C., Rochaix,P., Lamy,P.J., Kramar,A., Rouanet,P., Maudelonde,T., Mange,A., and Solassol,J. (2009a). Identification of a new panel of serum autoantibodies associated with the presence of in situ carcinoma of the breast in younger women. Clin. Cancer Res. *15*, 4733-4741.

Desmetz,C., Bibeau,F., Boissiere,F., Bellet,V., Rouanet,P., Maudelonde,T., Mange,A., and Solassol,J. (2008). Proteomics-based identification of HSP60 as a tumor-associated antigen in early stage breast cancer and ductal carcinoma in situ. J. Proteome. Res. *7*, 3830-3837.

Desmetz,C., Cortijo,C., Mange,A., and Solassol,J. (2009b). Humoral response to cancer as a tool for biomarker discovery. J. Proteomics. *72*, 982-988.

Dewhirst,M.W. (2009). Relationships between cycling hypoxia, HIF-1, angiogenesis and oxidative stress. Radiat. Res. *172*, 653-665.

Diamandis,E.P. (2003). Point: Proteomic patterns in biological fluids: do they represent the future of cancer diagnostics? Clin. Chem. *49*, 1272-1275.

Dittmar,T., Heyder,C., Gloria-Maercker,E., Hatzmann,W., and Zanker,K.S. (2008). Adhesion molecules and chemokines: the navigation system for circulating tumor (stem) cells to metastasize in an organ-specific manner. Clin. Exp. Metastasis *25*, 11-32.

Dome,B., Timar,J., Ladanyi,A., Paku,S., Renyi-Vamos,F., Klepetko,W., Lang,G., Dome,P., Bogos,K., and Tovari,J. (2009). Circulating endothelial cells, bone marrow-derived endothelial progenitor cells and proangiogenic hematopoietic cells in cancer: From biology to therapy. Crit Rev. Oncol. Hematol. *69*, 108-124.

Dong,D., Ni,M., Li,J., Xiong,S., Ye,W., Virrey,J.J., Mao,C., Ye,R., Wang,M., Pen,L., Dubeau,L., Groshen,S., Hofman,F.M., and Lee,A.S. (2008). Critical role of the stress chaperone GRP78/BiP in tumor proliferation, survival, and tumor angiogenesis in transgene-induced mammary tumor development. Cancer Res. *68*, 498-505.

Dunn,G.P., Old,L.J., and Schreiber,R.D. (2004). The immunobiology of cancer immunosurveillance and immunoediting. Immunity. *21*, 137-148.

Eguchi,M., Masuda,H., and Asahara,T. (2007). Endothelial progenitor cells for postnatal vasculogenesis. Clin. Exp. Nephrol. *11*, 18-25.

El,H.F., Abouzahr-Rifai,S., Meslin,F., Mami-Chouaib,F., and Chouaib,S. (2008). [Immune response and cancer]. Bull. Cancer *95*, 57-67.

El-Sayed,Z.A., Farag,D.H., and Eissa,S. (2003). Tumor suppressor protein p53 and anti-p53 autoantibodies in pediatric rheumatological diseases. Pediatr. Allergy Immunol. *14*, 229-233.

Erler,J.T., Bennewith,K.L., Cox,T.R., Lang,G., Bird,D., Koong,A., Le,Q.T., and Giaccia,A.J. (2009). Hypoxia-induced lysyl oxidase is a critical mediator of bone marrow cell recruitment to form the premetastatic niche. Cancer Cell *15*, 35-44.

Erler,J.T., Bennewith,K.L., Nicolau,M., Dornhofer,N., Kong,C., Le,Q.T., Chi,J.T., Jeffrey,S.S., and Giaccia,A.J. (2006). Lysyl oxidase is essential for hypoxia-induced metastasis. Nature *440*, 1222-1226.

Erler,J.T. and Giaccia,A.J. (2006). Lysyl oxidase mediates hypoxic control of metastasis. Cancer Res. *66*, 10238-10241.

Erler,J.T. and Weaver,V.M. (2009). Three-dimensional context regulation of metastasis. Clin. Exp. Metastasis *26*, 35-49.

Fidler,I.J. (2003). The pathogenesis of cancer metastasis: the 'seed and soil' hypothesis revisited. Nat. Rev. Cancer *3*, 453-458.

Fodor,I.K., Nelson,D.O., egria-Hartman,M., Robbins,K., Langlois,R.G., Turteltaub,K.W., Corzett,T.H., and Cutchen-Maloney,S.L. (2005). Statistical challenges in the analysis of two-dimensional difference gel electrophoresis experiments using DeCyder. Bioinformatics. *21*, 3733-3740.

Fokas,E., Engenhart-Cabillic,R., Daniilidis,K., Rose,F., and An,H.X. (2007). Metastasis: the seed and soil theory gains identity. Cancer Metastasis Rev. *26*, 705-715.

Folkman,J. (1971). Tumor angiogenesis: therapeutic implications. N. Engl. J. Med. *285*, 1182-1186.

Forgber,M., Gellrich,S., Sharav,T., Sterry,W., and Walden,P. (2009). Proteome-based analysis of serologically defined tumor-associated antigens in cutaneous lymphoma. PLoS. One. *4*, e8376.

Francavilla,C., Maddaluno,L., and Cavallaro,U. (2009). The functional role of cell adhesion molecules in tumor angiogenesis. Semin. Cancer Biol. *19*, 298-309.

Gao,D. and Mittal,V. (2009). The role of bone-marrow-derived cells in tumor growth, metastasis initiation and progression. Trends Mol. Med. *15*, 333-343.

Gao,D., Nolan,D., McDonnell,K., Vahdat,L., Benezra,R., Altorki,N., and Mittal,V. (2009). Bone marrow-derived endothelial progenitor cells contribute to the angiogenic switch in tumor growth and metastatic progression. Biochim. Biophys. Acta *1796*, 33-40.

Gao,X., Porter,A.T., Grignon,D.J., Pontes,J.E., and Honn,K.V. (1997). Diagnostic and prognostic markers for human prostate cancer. Prostate *31*, 264-281.

Garcia-Barros,M., Paris,F., Cordon-Cardo,C., Lyden,D., Rafii,S., Haimovitz-Friedman,A., Fuks,Z., and Kolesnick,R. (2003). Tumor response to radiotherapy regulated by endothelial cell apoptosis. Science *300*, 1155-1159.

Ge,L., Meng,W., Zhou,H., and Bhowmick,N. (2010). Could stroma contribute to field cancerization? Med. Hypotheses.

Geiger,T.R. and Peeper,D.S. (2009). Metastasis mechanisms. Biochim. Biophys. Acta *1796*, 293-308.

Gieseg,M.A., Cody,T., Man,M.Z., Madore,S.J., Rubin,M.A., and Kaldjian,E.P. (2002). Expression profiling of human renal carcinomas with functional taxonomic analysis. BMC. Bioinformatics. *3*, 26.

Gillies,R.J. and Gatenby,R.A. (2007). Hypoxia and adaptive landscapes in the evolution of carcinogenesis. Cancer Metastasis Rev. *26*, 311-317.

Glaudet F. Contribution à l'étude du rôle du récepteur à l'antigène des cellules B dans l'hypermutation somatique et la commutation isotypique. 2003.
Ref Type: Thesis/Dissertation

Gold,P. and Freedman,S.O. (1965a). DEMONSTRATION OF TUMOR-SPECIFIC ANTIGENS IN HUMAN COLONIC CARCINOMATA BY IMMUNOLOGICAL TOLERANCE AND ABSORPTION TECHNIQUES. J. Exp. Med. *121*, 439-462.

Gold,P. and Freedman,S.O. (1965b). Specific carcinoembryonic antigens of the human digestive system. J. Exp. Med. *122*, 467-481.

Goldenberg,D., Ayesh,S., Schneider,T., Pappo,O., Jurim,O., Eid,A., Fellig,Y., Dadon,T., Ariel,I., de,G.N., Hochberg,A., and Galun,E. (2002). Analysis of differentially expressed genes in hepatocellular carcinoma using cDNA arrays. Mol. Carcinog. *33*, 113-124.

Gonzalez-Gronow,M., Cuchacovich,M., Llanos,C., Urzua,C., Gawdi,G., and Pizzo,S.V. (2006). Prostate cancer cell proliferation in vitro is modulated by antibodies against glucose-regulated protein 78 isolated from patient serum. Cancer Res. *66*, 11424-11431.

Gorg,A., Obermaier,C., Boguth,G., Harder,A., Scheibe,B., Wildgruber,R., and Weiss,W. (2000). The current state of two-dimensional electrophoresis with immobilized pH gradients. Electrophoresis *21*, 1037-1053.

Gothert,J.R., Gustin,S.E., van Eekelen,J.A., Schmidt,U., Hall,M.A., Jane,S.M., Green,A.R., Gottgens,B., Izon,D.J., and Begley,C.G. (2004). Genetically tagging endothelial cells in vivo: bone marrow-derived cells do not contribute to tumor endothelium. Blood *104*, 1769-1777.

Green,D.R., Ferguson,T., Zitvogel,L., and Kroemer,G. (2009). Immunogenic and tolerogenic cell death. Nat. Rev. Immunol. *9*, 353-363.

Gregory,C.D. and Pound,J.D. (2010). Cell death in the neighbourhood: direct microenvironmental effects of apoptosis in normal and neoplastic tissues. J. Pathol.

Grivennikov,S.I., Greten,F.R., and Karin,M. (2010). Immunity, inflammation, and cancer. Cell *140*, 883-899.

Gupta,G.P. and Massague,J. (2006). Cancer metastasis: building a framework. Cell *127*, 679-695.

Guweidhi,A., Kleeff,J., Adwan,H., Giese,N.A., Wente,M.N., Giese,T., Buchler,M.W., Berger,M.R., and Friess,H. (2005). Osteonectin influences growth and invasion of pancreatic cancer cells. Ann. Surg. *242*, 224-234.

Habermann,J.K., Bader,F.G., Franke,C., Zimmermann,K., Gemoll,T., Fritzsche,B., Ried,T., Auer,G., Bruch,H.P., and Roblick,U.J. (2008). From the genome to the proteome--biomarkers in colorectal cancer. Langenbecks Arch. Surg. *393*, 93-104.

Hamrita,B., Chahed,K., Kabbage,M., Guillier,C.L., Trimeche,M., Chaieb,A., and Chouchane,L. (2008). Identification of tumor antigens

that elicit a humoral immune response in breast cancer patients' sera by serological proteome analysis (SERPA). Clin. Chim. Acta *393*, 95-102.

Hanahan,D. and Weinberg,R.A. (2000). The hallmarks of cancer. Cell *100*, 57-70.

Hanash,S.M. and Beretta,L.M. (2002). Operomics: integrated genomic and proteomic profiling of cells and tissues. Brief. Funct. Genomic. Proteomic. *1*, 10-22.

Hanna,E., Quick,J., and Libutti,S.K. (2009). The tumour microenvironment: a novel target for cancer therapy. Oral Dis. *15*, 8-17.

Helleman,J., Jansen,M.P., Ruigrok-Ritstier,K., van,S., I, Look,M.P., Meijer-van Gelder,M.E., Sieuwerts,A.M., Klijn,J.G., Sleijfer,S., Foekens,J.A., and Berns,E.M. (2008). Association of an extracellular matrix gene cluster with breast cancer prognosis and endocrine therapy response. Clin. Cancer Res. *14*, 5555-5564.

Herkel,J., Modrow,J.P., Bamberger,S., Kanzler,S., Rotter,V., Cohen,I.R., and Lohse,A.W. (2002). Prevalence of autoantibodies to the p53 protein in autoimmune hepatitis. Autoimmunity *35*, 493-496.

Hilbe,W., Dirnhofer,S., Oberwasserlechner,F., Schmid,T., Gunsilius,E., Hilbe,G., Woll,E., and Kahler,C.M. (2004). CD133 positive endothelial progenitor cells contribute to the tumour vasculature in non-small cell lung cancer. J. Clin. Pathol. *57*, 965-969.

Hiratsuka,S., Watanabe,A., Aburatani,H., and Maru,Y. (2006). Tumour-mediated upregulation of chemoattractants and recruitment of myeloid cells predetermines lung metastasis. Nat. Cell Biol. *8*, 1369-1375.

Hong,S.H., Misek,D.E., Wang,H., Puravs,E., Giordano,T.J., Greenson,J.K., Brenner,D.E., Simeone,D.M., Logsdon,C.D., and Hanash,S.M. (2004). An autoantibody-mediated immune response to calreticulin isoforms in pancreatic cancer. Cancer Res. *64*, 5504-5510.

Hong,S.M., Kelly,D., Griffith,M., Omura,N., Li,A., Li,C.P., Hruban,R.H., and Goggins,M. (2008). Multiple genes are

hypermethylated in intraductal papillary mucinous neoplasms of the pancreas. Mod. Pathol. *21*, 1499-1507.

Horie,K., Tsuchihara,M., and Nakatsura,T. (2010). Silencing of secreted protein acidic and rich in cysteine inhibits the growth of human melanoma cells with G arrest induction. Cancer Sci. *101*, 913-919.

Horstmann,M., Bontrup,H., Hennenlotter,J., Taeger,D., Weber,A., Pesch,B., Feil,G., Patschan,O., Johnen,G., Stenzl,A., and Bruning,T. (2010). Clinical experience with survivin as a biomarker for urothelial bladder cancer. World J. Urol.

Houghton,A.N., Uchi,H., and Wolchok,J.D. (2005). The role of the immune system in early epithelial carcinogenesis: B-ware the double-edged sword. Cancer Cell *7*, 403-405.

Hristov,M., Erl,W., and Weber,P.C. (2003). Endothelial progenitor cells: mobilization, differentiation, and homing. Arterioscler. Thromb. Vasc. Biol. *23*, 1185-1189.

Huang,H., Colella,S., Kurrer,M., Yonekawa,Y., Kleihues,P., and Ohgaki,H. (2000). Gene expression profiling of low-grade diffuse astrocytomas by cDNA arrays. Cancer Res. *60*, 6868-6874.

Hynes,R.O. (2009). The extracellular matrix: not just pretty fibrils. Science *326*, 1216-1219.

Ikuta,Y., Nakatsura,T., Kageshita,T., Fukushima,S., Ito,S., Wakamatsu,K., Baba,H., and Nishimura,Y. (2005). Highly sensitive detection of melanoma at an early stage based on the increased serum secreted protein acidic and rich in cysteine and glypican-3 levels. Clin. Cancer Res. *11*, 8079-8088.

Infante,J.R., Matsubayashi,H., Sato,N., Tonascia,J., Klein,A.P., Riall,T.A., Yeo,C., Iacobuzio-Donahue,C., and Goggins,M. (2007). Peritumoral fibroblast SPARC expression and patient outcome with resectable pancreatic adenocarcinoma. J. Clin. Oncol. *25*, 319-325.

Inoue,H., Matsuyama,A., Mimori,K., Ueo,H., and Mori,M. (2002). Prognostic score of gastric cancer determined by cDNA microarray. Clin. Cancer Res. *8*, 3475-3479.

Jain,K.K. (2004). Role of oncoproteomics in the personalized management of cancer. Expert. Rev. Proteomics. *1*, 49-55.

Jain,K.K. (2008). Innovations, challenges and future prospects of oncoproteomics. Mol. Oncol. *2*, 153-160.

Jodele,S., Chantrain,C.F., Blavier,L., Lutzko,C., Crooks,G.M., Shimada,H., Coussens,L.M., and DeClerck,Y.A. (2005). The contribution of bone marrow-derived cells to the tumor vasculature in neuroblastoma is matrix metalloproteinase-9 dependent. Cancer Res. *65*, 3200-3208.

Jones,C., Mackay,A., Grigoriadis,A., Cossu,A., Reis-Filho,J.S., Fulford,L., Dexter,T., Davies,S., Bulmer,K., Ford,E., Parry,S., Budroni,M., Palmieri,G., Neville,A.M., O'Hare,M.J., and Lakhani,S.R. (2004). Expression profiling of purified normal human luminal and myoepithelial breast cells: identification of novel prognostic markers for breast cancer. Cancer Res. *64*, 3037-3045.

Joshi,S., Tiwari,A.K., Mondal,B., and Sharma,A. (2011). Oncoproteomics. Clin. Chim. Acta *412*, 217-226.

Joyce,J.A. and Pollard,J.W. (2009). Microenvironmental regulation of metastasis. Nat. Rev. Cancer *9*, 239-252.

Jungblut,P.R., Zimny-Arndt,U., Zeindl-Eberhart,E., Stulik,J., Koupilova,K., Pleissner,K.P., Otto,A., Muller,E.C., Sokolowska-Kohler,W., Grabher,G., and Stoffler,G. (1999). Proteomics in human disease: cancer, heart and infectious diseases. Electrophoresis *20*, 2100-2110.

Kageyama,S., Isono,T., Iwaki,H., Wakabayashi,Y., Okada,Y., Kontani,K., Yoshimura,K., Terai,A., Arai,Y., and Yoshiki,T. (2004). Identification by proteomic analysis of calreticulin as a marker for bladder cancer and evaluation of the diagnostic accuracy of its detection in urine. Clin. Chem. *50*, 857-866.

Kahn,S.L., Ronnett,B.M., Gravitt,P.E., and Gustafson,K.S. (2008). Quantitative methylation-specific PCR for the detection of aberrant DNA methylation in liquid-based Pap tests. Cancer *114*, 57-64.

Kalluri,R. and Weinberg,R.A. (2009). The basics of epithelial-mesenchymal transition. J. Clin. Invest *119*, 1420-1428.

Kaplan,R.N., Psaila,B., and Lyden,D. (2006a). Bone marrow cells in the 'pre-metastatic niche': within bone and beyond. Cancer Metastasis Rev. *25*, 521-529.

Kaplan,R.N., Rafii,S., and Lyden,D. (2006b). Preparing the "soil": the premetastatic niche. Cancer Res. *66*, 11089-11093.

Kaplan,R.N., Riba,R.D., Zacharoulis,S., Bramley,A.H., Vincent,L., Costa,C., MacDonald,D.D., Jin,D.K., Shido,K., Kerns,S.A., Zhu,Z., Hicklin,D., Wu,Y., Port,J.L., Altorki,N., Port,E.R., Ruggero,D., Shmelkov,S.V., Jensen,K.K., Rafii,S., and Lyden,D. (2005). VEGFR1-positive haematopoietic bone marrow progenitors initiate the pre-metastatic niche. Nature *438*, 820-827.

Kassmeyer,S., Plendl,J., Custodis,P., and Bahramsoltani,M. (2009). New insights in vascular development: vasculogenesis and endothelial progenitor cells. Anat. Histol. Embryol. *38*, 1-11.

Kepp,O., Tesniere,A., Schlemmer,F., Michaud,M., Senovilla,L., Zitvogel,L., and Kroemer,G. (2009). Immunogenic cell death modalities and their impact on cancer treatment. Apoptosis. *14*, 364-375.

Kerbel,R.S., Benezra,R., Lyden,D.C., Hattori,K., Heissig,B., Nolan,D.J., Mittal,V., Shaked,Y., Dias,S., Bertolini,F., and Rafii,S. (2008). Endothelial progenitor cells are cellular hubs essential for neoangiogenesis of certain aggressive adenocarcinomas and metastatic transition but not adenomas. Proc. Natl. Acad. Sci. U. S. A *105*, E54.

Kijanka,G. and Murphy,D. (2009). Protein arrays as tools for serum autoantibody marker discovery in cancer. J. Proteomics. *72*, 936-944.

Kinter,M.T. and Sherman,N.E. (2000). Protein sequencing and identification using tandem mass spectrometry.

Klade,C.S., Voss,T., Krystek,E., Ahorn,H., Zatloukal,K., Pummer,K., and Adolf,G.R. (2001). Identification of tumor antigens in renal cell carcinoma by serological proteome analysis. Proteomics. *1*, 890-898.

Klatte,T., Seligson,D.B., LaRochelle,J., Shuch,B., Said,J.W., Riggs,S.B., Zomorodian,N., Kabbinavar,F.F., Pantuck,A.J., and Belldegrun,A.S. (2009). Molecular signatures of localized clear cell renal cell carcinoma to predict disease-free survival after nephrectomy. Cancer Epidemiol. Biomarkers Prev. *18*, 894-900.

Kobold,S., Luetkens,T., Cao,Y., Bokemeyer,C., and Atanackovic,D. (2010a). Prognostic and diagnostic value of spontaneous tumor-related antibodies. Clin. Dev. Immunol. *2010*, 721531.

Kobold,S., Lutkens,T., Cao,Y., Bokemeyer,C., and Atanackovic,D. (2010b). Autoantibodies against tumor-related antigens: incidence and biologic significance. Hum. Immunol. *71*, 643-651.

Koike,C., Chao,D.T., and Zetter,B.R. (1999). Sensitivity to polyamine-induced growth arrest correlates with antizyme induction in prostate carcinoma cells. Cancer Res. *59*, 6109-6112.

Kokron,C.M., Errante,P.R., Barros,M.T., Baracho,G.V., Camargo,M.M., Kalil,J., and Rizzo,L.V. (2004). Clinical and laboratory aspects of common variable immunodeficiency. An. Acad. Bras. Cienc. *76*, 707-726.

Kolch,W., Mischak,H., and Pitt,A.R. (2005). The molecular make-up of a tumour: proteomics in cancer research. Clin. Sci. (Lond) *108*, 369-383.

Koomen,J.M., Haura,E.B., Bepler,G., Sutphen,R., Remily-Wood,E.R., Benson,K., Hussein,M., Hazlehurst,L.A., Yeatman,T.J., Hildreth,L.T., Sellers,T.A., Jacobsen,P.B., Fenstermacher,D.A., and Dalton,W.S. (2008). Proteomic contributions to personalized cancer care. Mol. Cell Proteomics. *7*, 1780-1794.

Kopfstein,L. and Christofori,G. (2006). Metastasis: cell-autonomous mechanisms versus contributions by the tumor microenvironment. Cell Mol. Life Sci. *63*, 449-468.

Koukourakis,M.I., Giatromanolaki,A., Brekken,R.A., Sivridis,E., Gatter,K.C., Harris,A.L., and Sage,E.H. (2003). Enhanced expression of SPARC/osteonectin in the tumor-associated stroma of non-small cell lung cancer is correlated with markers of hypoxia/acidity and with poor prognosis of patients. Cancer Res. *63*, 5376-5380.

Kulic,A., Sirotkovic-Skerlev,M., Jelisavac-Cosic,S., Herceg,D., Kovac,Z., and Vrbanec,D. (2010). Anti-p53 antibodies in serum: relationship to tumor biology and prognosis of breast cancer patients. Med. Oncol. *27*, 887-893.

Kumar,S. and Weaver,V.M. (2009). Mechanics, malignancy, and metastasis: the force journey of a tumor cell. Cancer Metastasis Rev. *28*, 113-127.

Lane,T.F. and Sage,E.H. (1994). The biology of SPARC, a protein that modulates cell-matrix interactions. FASEB J. *8*, 163-173.

Lapointe,J., Li,C., Higgins,J.P., van de Rijn,M., Bair,E., Montgomery,K., Ferrari,M., Egevad,L., Rayford,W., Bergerheim,U., Ekman,P., DeMarzo,A.M., Tibshirani,R., Botstein,D., Brown,P.O., Brooks,J.D., and Pollack,J.R. (2004). Gene expression profiling identifies clinically relevant subtypes of prostate cancer. Proc. Natl. Acad. Sci. U. S. A *101*, 811-816.

Larrivee,B. and Karsan,A. (2007). Involvement of marrow-derived endothelial cells in vascularization. Handb. Exp. Pharmacol. 89-114.

Larrivee,B., Niessen,K., Pollet,I., Corbel,S.Y., Long,M., Rossi,F.M., Olive,P.L., and Karsan,A. (2005). Minimal contribution of marrow-derived endothelial precursors to tumor vasculature. J. Immunol. *175*, 2890-2899.

Lau,C.P., Poon,R.T., Cheung,S.T., Yu,W.C., and Fan,S.T. (2006). SPARC and Hevin expression correlate with tumour angiogenesis in hepatocellular carcinoma. J. Pathol. *210*, 459-468.

Le,B.B., Faouzi,S., Boussarie,L., Guirouilh,J., Blanc,J.F., Carles,J., Bioulac-Sage,P., Balabaud,C., and Rosenbaum,J. (1999). Osteonectin/SPARC is overexpressed in human hepatocellular carcinoma. J. Pathol. *189*, 46-52.

Le,N.F., Brichory,F., Misek,D.E., Brechot,C., Hanash,S.M., and Beretta,L. (2002). A distinct repertoire of autoantibodies in hepatocellular carcinoma identified by proteomic analysis. Mol. Cell Proteomics. *1*, 197-203.

Ledda,F., Bravo,A.I., Adris,S., Bover,L., Mordoh,J., and Podhajcer,O.L. (1997a). The expression of the secreted protein acidic and rich in cysteine (SPARC) is associated with the neoplastic progression of human melanoma. J. Invest Dermatol. *108*, 210-214.

Ledda,M.F., Adris,S., Bravo,A.I., Kairiyama,C., Bover,L., Chernajovsky,Y., Mordoh,J., and Podhajcer,O.L. (1997b). Suppression of SPARC expression by antisense RNA abrogates the tumorigenicity of human melanoma cells. Nat. Med. *3*, 171-176.

Lee,A.S. (2007). GRP78 induction in cancer: therapeutic and prognostic implications. Cancer Res. *67*, 3496-3499.

Li,B., Sharpe,E.E., Maupin,A.B., Teleron,A.A., Pyle,A.L., Carmeliet,P., and Young,P.P. (2006a). VEGF and PlGF promote adult vasculogenesis by enhancing EPC recruitment and vessel formation at the site of tumor neovascularization. FASEB J. *20*, 1495-1497.

Li,C., Xiao,Z., Chen,Z., Zhang,X., Li,J., Wu,X., Li,X., Yi,H., Li,M., Zhu,G., and Liang,S. (2006b). Proteome analysis of human lung squamous carcinoma. Proteomics. *6*, 547-558.

Li,L., Chen,S.H., Yu,C.H., Li,Y.M., and Wang,S.Q. (2008). Identification of hepatocellular-carcinoma-associated antigens and autoantibodies by serological proteome analysis combined with protein microarray. J. Proteome. Res. *7*, 611-620.

Lilley,K.S. and Friedman,D.B. (2004). All about DIGE: quantification technology for differential-display 2D-gel proteomics. Expert. Rev. Proteomics. *1*, 401-409.

Liotta,L.A. and Kohn,E.C. (2001). The microenvironment of the tumour-host interface. Nature *411*, 375-379.

Lleo,A., Invernizzi,P., Gao,B., Podda,M., and Gershwin,M.E. (2010). Definition of human autoimmunity--autoantibodies versus autoimmune disease. Autoimmun. Rev. *9*, A259-A266.

Locher,C., Conforti,R., Aymeric,L., Ma,Y., Yamazaki,T., Rusakiewicz,S., Tesniere,A., Ghiringhelli,F., Apetoh,L., Morel,Y., Girard,J.P., Kroemer,G., and Zitvogel,L. (2010). Desirable cell death during anticancer chemotherapy. Ann. N. Y. Acad. Sci. *1209*, 99-108.

Lopez,M.V., Blanco,P., Viale,D.L., Cafferata,E.G., Carbone,C., Gould,D., Chernajovsky,Y., and Podhajcer,O.L. (2006). Expression of a suicidal gene under control of the human secreted protein acidic and rich in cysteine (SPARC) promoter in tumor or stromal cells led to the inhibition of tumor cell growth. Mol. Cancer Ther. *5*, 2503-2511.

Lorusso,G. and Ruegg,C. (2008). The tumor microenvironment and its contribution to tumor evolution toward metastasis. Histochem. Cell Biol. *130*, 1091-1103.

Luo,A., Kong,J., Hu,G., Liew,C.C., Xiong,M., Wang,X., Ji,J., Wang,T., Zhi,H., Wu,M., and Liu,Z. (2004). Discovery of Ca2+-relevant and differentiation-associated genes downregulated in esophageal squamous cell carcinoma using cDNA microarray. Oncogene *23*, 1291-1299.

Lussier,C., Sodek,J., and Beaulieu,J.F. (2001). Expression of SPARC/osteonectin/BM4O in the human gut: predominance in the stroma of the remodeling distal intestine. J. Cell Biochem. *81*, 463-476.

Luttun,A., Carmeliet,G., and Carmeliet,P. (2002). Vascular progenitors: from biology to treatment. Trends Cardiovasc. Med. *12*, 88-96.

Lyden,D., Hattori,K., Dias,S., Costa,C., Blaikie,P., Butros,L., Chadburn,A., Heissig,B., Marks,W., Witte,L., Wu,Y., Hicklin,D., Zhu,Z., Hackett,N.R., Crystal,R.G., Moore,M.A., Hajjar,K.A., Manova,K., Benezra,R., and Rafii,S. (2001). Impaired recruitment of bone-marrow-derived endothelial and hematopoietic precursor cells blocks tumor angiogenesis and growth. Nat. Med. *7*, 1194-1201.

Ma,Y., Conforti,R., Aymeric,L., Locher,C., Kepp,O., Kroemer,G., and Zitvogel,L. (2011). How to improve the immunogenicity of chemotherapy and radiotherapy. Cancer Metastasis Rev. *30*, 71-82.

Machiels,J.P., Reilly,R.T., Emens,L.A., Ercolini,A.M., Lei,R.Y., Weintraub,D., Okoye,F.I., and Jaffee,E.M. (2001). Cyclophosphamide, doxorubicin, and paclitaxel enhance the antitumor immune response of granulocyte/macrophage-colony stimulating factor-secreting whole-cell vaccines in HER-2/neu tolerized mice. Cancer Res. *61*, 3689-3697.

Madoz-Gurpide,J., Lopez-Serra,P., Martinez-Torrecuadrada,J.L., Sanchez,L., Lombardia,L., and Casal,J.I. (2006). Proteomics-based validation of genomic data: applications in colorectal cancer diagnosis. Mol. Cell Proteomics. *5*, 1471-1483.

Maeng,H.Y., Song,S.B., Choi,D.K., Kim,K.E., Jeong,H.Y., Sakaki,Y., and Furihata,C. (2002). Osteonectin-expressing cells in human stomach cancer and their possible clinical significance. Cancer Lett. *184*, 117-121.

Mantoni,T.S., Schendel,R.R., Rodel,F., Niedobitek,G., Al-Assar,O., Masamune,A., and Brunner,T.B. (2008). Stromal SPARC expression and patient survival after chemoradiation for non-resectable pancreatic adenocarcinoma. Cancer Biol. Ther. *7*.

Marouga,R., David,S., and Hawkins,E. (2005). The development of the DIGE system: 2D fluorescence difference gel analysis technology. Anal. Bioanal. Chem. *382*, 669-678.

Martinez,N., Camacho,F.I., Algara,P., Rodriguez,A., Dopazo,A., Ruiz-Ballesteros,E., Martin,P., Martinez-Climent,J.A., Garcia-Conde,J., Menarguez,J., Solano,F., Mollejo,M., and Piris,M.A. (2003). The molecular signature of mantle cell lymphoma reveals multiple signals favoring cell survival. Cancer Res. *63*, 8226-8232.

Martinive,P., Defresne,F., Bouzin,C., Saliez,J., Lair,F., Gregoire,V., Michiels,C., Dessy,C., and Feron,O. (2006). Preconditioning of the tumor vasculature and tumor cells by intermittent hypoxia: implications for anticancer therapies. Cancer Res. *66*, 11736-11744.

Martinive,P., Defresne,F., Quaghebeur,E., Daneau,G., Crokart,N., Gregoire,V., Gallez,B., Dessy,C., and Feron,O. (2009). Impact of cyclic hypoxia on HIF-1alpha regulation in endothelial cells--new insights for anti-tumor treatments. FEBS J. *276*, 509-518.

Mbeunkui,F. and Johann,D.J., Jr. (2009). Cancer and the tumor microenvironment: a review of an essential relationship. Cancer Chemother. Pharmacol. *63*, 571-582.

McAllister,S.S. and Weinberg,R.A. (2010). Tumor-host interactions: a far-reaching relationship. J. Clin. Oncol. *28*, 4022-4028.

McCawley,L.J. and Matrisian,L.M. (2001). Tumor progression: defining the soil round the tumor seed. Curr. Biol. *11*, R25-R27.

McHugh,S.M., O'Donnell,J., and Gillen,P. (2009). Genomic and oncoproteomic advances in detection and treatment of colorectal cancer. World J. Surg. Oncol. *7*, 36.

Melchers,F., Rolink,A., Grawunder,U., Winkler,T.H., Karasuyama,H., Ghia,P., and Andersson,J. (1995). Positive and negative selection events during B lymphopoiesis. Curr. Opin. Immunol. *7*, 214-227.

Melnick,J. and Argon,Y. (1995). Molecular chaperones and the biosynthesis of antigen receptors. Immunol. Today *16*, 243-250.

Mendoza,M. and Khanna,C. (2009). Revisiting the seed and soil in cancer metastasis. Int. J. Biochem. Cell Biol. *41*, 1452-1462.

Miller,I., Crawford,J., and Gianazza,E. (2006). Protein stains for proteomic applications: which, when, why? Proteomics. *6*, 5385-5408.

Miller-Kasprzak,E. and Jagodzinski,P.P. (2007). Endothelial progenitor cells as a new agent contributing to vascular repair. Arch. Immunol. Ther. Exp. (Warsz.) *55*, 247-259.

Mintz,P.J., Kim,J., Do,K.A., Wang,X., Zinner,R.G., Cristofanilli,M., Arap,M.A., Hong,W.K., Troncoso,P., Logothetis,C.J., Pasqualini,R., and Arap,W. (2003). Fingerprinting the circulating repertoire of antibodies from cancer patients. Nat. Biotechnol. *21*, 57-63.

Mitas,M., Almeida,J.S., Mikhitarian,K., Gillanders,W.E., Lewin,D.N., Spyropoulos,D.D., Hoover,L., Graham,A., Glenn,T., King,P., Cole,D.J., Hawes,R., Reed,C.E., and Hoffman,B.J. (2005). Accurate discrimination of Barrett's esophagus and esophageal adenocarcinoma using a quantitative three-tiered algorithm and multimarker real-time reverse transcription-PCR. Clin. Cancer Res. *11*, 2205-2214.

Mungan,N.A., Vriesema,J.L., Thomas,C.M., Kiemeney,L.A., and Witjes,J.A. (2000). Urinary bladder cancer test: a new urinary tumor marker in the follow-up of superficial bladder cancer. Urology *56*, 787-792.

Nakahara,T., Norberg,S.M., Shalinsky,D.R., Hu-Lowe,D.D., and McDonald,D.M. (2006). Effect of inhibition of vascular endothelial growth factor signaling on distribution of extravasated antibodies in tumors. Cancer Res. *66*, 1434-1445.

Nimmerjahn,F. and Ravetch,J.V. (2007a). Antibodies, Fc receptors and cancer. Curr. Opin. Immunol. *19*, 239-245.

Nimmerjahn,F. and Ravetch,J.V. (2007b). Fc-receptors as regulators of immunity. Adv. Immunol. *96*, 179-204.

Nimphius,W., Moll,R., Olbert,P., Ramaswamy,A., and Barth,P.J. (2007). CD34+ fibrocytes in chronic cystitis and noninvasive and invasive urothelial carcinomas of the urinary bladder. Virchows Arch. *450*, 179-185.

Nolan,D.J., Ciarrocchi,A., Mellick,A.S., Jaggi,J.S., Bambino,K., Gupta,S., Heikamp,E., McDevitt,M.R., Scheinberg,D.A., Benezra,R., and Mittal,V. (2007). Bone marrow-derived endothelial progenitor cells are a major determinant of nascent tumor neovascularization. Genes Dev. *21*, 1546-1558.

Nozaki,M., Sakurai,E., Raisler,B.J., Baffi,J.Z., Witta,J., Ogura,Y., Brekken,R.A., Sage,E.H., Ambati,B.K., and Ambati,J. (2006). Loss of SPARC-mediated VEGFR-1 suppression after injury reveals a novel antiangiogenic activity of VEGF-A. J. Clin. Invest *116*, 422-429.

Obeid,M., Tesniere,A., Ghiringhelli,F., Fimia,G.M., Apetoh,L., Perfettini,J.L., Castedo,M., Mignot,G., Panaretakis,T., Casares,N., Metivier,D., Larochette,N., van,E.P., Ciccosanti,F., Piacentini,M., Zitvogel,L., and Kroemer,G. (2007). Calreticulin exposure dictates the immunogenicity of cancer cell death. Nat. Med. *13*, 54-61.

Oppenheimer,S.B. (2006). Cellular basis of cancer metastasis: A review of fundamentals and new advances. Acta Histochem. *108*, 327-334.

Oppezzo,P. and Dighiero,G. (2003). [Autoantibodies, tolerance and autoimmunity]. Pathol. Biol. (Paris) *51*, 297-304.

Ostrand-Rosenberg,S. (2010). Myeloid-derived suppressor cells: more mechanisms for inhibiting antitumor immunity. Cancer Immunol. Immunother. *59*, 1593-1600.

Pages,F., Galon,J., Dieu-Nosjean,M.C., Tartour,E., Sautes-Fridman,C., and Fridman,W.H. (2010). Immune infiltration in human tumors: a prognostic factor that should not be ignored. Oncogene *29*, 1093-1102.

Paget,S. (1989). The distribution of secondary growths in cancer of the breast. 1889. Cancer Metastasis Rev. *8*, 98-101.

Paley,P.J., Goff,B.A., Gown,A.M., Greer,B.E., and Sage,E.H. (2000). Alterations in SPARC and VEGF immunoreactivity in epithelial ovarian cancer. Gynecol. Oncol. *78*, 336-341.

Parker,B.S., Argani,P., Cook,B.P., Liangfeng,H., Chartrand,S.D., Zhang,M., Saha,S., Bardelli,A., Jiang,Y., St Martin,T.B., Nacht,M., Teicher,B.A., Klinger,K.W., Sukumar,S., and Madden,S.L. (2004). Alterations in vascular gene expression in invasive breast carcinoma. Cancer Res. *64*, 7857-7866.

Parveen,S., Taneja,N., Bathi,R.J., and Deka,A.C. (2010). Evaluation of circulating immune complexes and serum immunoglobulins in oral cancer patients--a follow up study. Indian J. Dent. Res. *21*, 10-15.

Patenaude,A., Parker,J., and Karsan,A. (2010). Involvement of endothelial progenitor cells in tumor vascularization. Microvasc. Res.

Peinado,H., Lavothskin,S., and Lyden,D. (2011). The secreted factors responsible for pre-metastatic niche formation: Old sayings and new thoughts. Semin. Cancer Biol.

Pen,A., Moreno,M.J., Martin,J., and Stanimirovic,D.B. (2007). Molecular markers of extracellular matrix remodeling in glioblastoma vessels: microarray study of laser-captured glioblastoma vessels. Glia *55*, 559-572.

Peranzoni,E., Zilio,S., Marigo,I., Dolcetti,L., Zanovello,P., Mandruzzato,S., and Bronte,V. (2010). Myeloid-derived suppressor cell heterogeneity and subset definition. Curr. Opin. Immunol. *22*, 238-244.

Petricoin,E.F. and Liotta,L.A. (2004). Proteomic approaches in cancer risk and response assessment. Trends Mol. Med. *10*, 59-64.

Piura,B. and Piura,E. (2009). Autoantibodies to tumor-associated antigens in epithelial ovarian carcinoma. J. Oncol. *2009*, 581939.

Piura,E. and Piura,B. (2010). Autoantibodies to tumor-associated antigens in breast carcinoma. J. Oncol. *2010*, 264926.

Podhajcer,O.L., Benedetti,L.G., Girotti,M.R., Prada,F., Salvatierra,E., and Llera,A.S. (2008). The role of the matricellular protein SPARC in the dynamic interaction between the tumor and the host. Cancer Metastasis Rev. *27*, 691-705.

Poon,T.C. and Johnson,P.J. (2001). Proteome analysis and its impact on the discovery of serological tumor markers. Clin. Chim. Acta *313*, 231-239.

Porte,H., Triboulet,J.P., Kotelevets,L., Carrat,F., Prevot,S., Nordlinger,B., DiGioia,Y., Wurtz,A., Comoglio,P., Gespach,C., and Chastre,E. (1998). Overexpression of stromelysin-3, BM-40/SPARC, and MET genes in human esophageal carcinoma: implications for prognosis. Clin. Cancer Res. *4*, 1375-1382.

Porter,D., Lahti-Domenici,J., Keshaviah,A., Bae,Y.K., Argani,P., Marks,J., Richardson,A., Cooper,A., Strausberg,R., Riggins,G.J., Schnitt,S., Gabrielson,E., Gelman,R., and Polyak,K. (2003). Molecular markers in ductal carcinoma in situ of the breast. Mol. Cancer Res. *1*, 362-375.

Posadas,E.M., Simpkins,F., Liotta,L.A., MacDonald,C., and Kohn,E.C. (2005). Proteomic analysis for the early detection and rational treatment of cancer--realistic hope? Ann. Oncol. *16*, 16-22.

Prenzel,K.L., Warnecke-Eberz,U., Xi,H., Brabender,J., Baldus,S.E., Bollschweiler,E., Gutschow,C.A., Holscher,A.H., and Schneider,P.M. (2006). Significant overexpression of SPARC/osteonectin mRNA in pancreatic cancer compared to cancer of the papilla of Vater. Oncol. Rep. *15*, 1397-1401.

Prindull,G. (2005). Hypothesis: cell plasticity, linking embryonal stem cells to adult stem cell reservoirs and metastatic cancer cells? Exp. Hematol. *33*, 738-746.

Psaila,B. and Lyden,D. (2009). The metastatic niche: adapting the foreign soil. Nat. Rev. Cancer *9*, 285-293.

Purhonen,S., Palm,J., Rossi,D., Kaskenpaa,N., Rajantie,I., Yla-Herttuala,S., Alitalo,K., Weissman,I.L., and Salven,P. (2008). Bone marrow-derived circulating endothelial precursors do not contribute to vascular endothelium and are not needed for tumor growth. Proc. Natl. Acad. Sci. U. S. A *105*, 6620-6625.

Pyrko,P., Schonthal,A.H., Hofman,F.M., Chen,T.C., and Lee,A.S. (2007). The unfolded protein response regulator GRP78/BiP as a novel target for increasing chemosensitivity in malignant gliomas. Cancer Res. *67*, 9809-9816.

Rafii,S. and Lyden,D. (2006). S100 chemokines mediate bookmarking of premetastatic niches. Nat. Cell Biol. *8*, 1321-1323.

Rajantie,I., Ilmonen,M., Alminaite,A., Ozerdem,U., Alitalo,K., and Salven,P. (2004). Adult bone marrow-derived cells recruited during angiogenesis comprise precursors for periendothelial vascular mural cells. Blood *104*, 2084-2086.

Rankin,E.B. and Giaccia,A.J. (2008). The role of hypoxia-inducible factors in tumorigenesis. Cell Death. Differ. *15*, 678-685.

Reddy,R.K., Mao,C., Baumeister,P., Austin,R.C., Kaufman,R.J., and Lee,A.S. (2003). Endoplasmic reticulum chaperone protein GRP78 protects cells from apoptosis induced by topoisomerase inhibitors: role of ATP binding site in suppression of caspase-7 activation. J. Biol. Chem. *278*, 20915-20924.

Reisinger,V. and Eichacker,L.A. (2006). Analysis of membrane protein complexes by blue native PAGE. Proteomics. *6 Suppl 2*, 6-15.

Ribatti,D. (2007). The discovery of endothelial progenitor cells. An historical review. Leuk. Res. *31*, 439-444.

Ribatti,D., Mangialardi,G., and Vacca,A. (2006). Stephen Paget and the 'seed and soil' theory of metastatic dissemination. Clin. Exp. Med. *6*, 145-149.

Rich,J.N., Hans,C., Jones,B., Iversen,E.S., McLendon,R.E., Rasheed,B.K., Dobra,A., Dressman,H.K., Bigner,D.D., Nevins,J.R., and West,M. (2005). Gene expression profiling and genetic markers in glioblastoma survival. Cancer Res. *65*, 4051-4058.

Rittling,S.R. and Chambers,A.F. (2004). Role of osteopontin in tumour progression. Br. J. Cancer *90*, 1877-1881.

Robson,N.C., Hoves,S., Maraskovsky,E., and Schnurr,M. (2010). Presentation of tumour antigens by dendritic cells and challenges faced. Curr. Opin. Immunol. *22*, 137-144.

Rodriguez-Jimenez,F.J., Caldes,T., Iniesta,P., Vidart,J.A., Garcia-Asenjo,J.L., and Benito,M. (2007). Overexpression of SPARC protein contrasts with its transcriptional silencing by aberrant hypermethylation of SPARC CpG-rich region in endometrial carcinoma. Oncol. Rep. *17*, 1301-1307.

Rofstad,E.K., Gaustad,J.V., Egeland,T.A., Mathiesen,B., and Galappathi,K. (2010). Tumors exposed to acute cyclic hypoxic stress show enhanced angiogenesis, perfusion and metastatic dissemination. Int. J. Cancer.

Ross,M.E., Mahfouz,R., Onciu,M., Liu,H.C., Zhou,X., Song,G., Shurtleff,S.A., Pounds,S., Cheng,C., Ma,J., Ribeiro,R.C., Rubnitz,J.E., Girtman,K., Williams,W.K., Raimondi,S.C., Liang,D.C., Shih,L.Y., Pui,C.H., and Downing,J.R. (2004). Gene expression profiling of pediatric acute myelogenous leukemia. Blood *104*, 3679-3687.

Ryu,B., Jones,J., Hollingsworth,M.A., Hruban,R.H., and Kern,S.E. (2001). Invasion-specific genes in malignancy: serial analysis of gene expression comparisons of primary and passaged cancers. Cancer Res. *61*, 1833-1838.

Sakai,N., Baba,M., Nagasima,Y., Kato,Y., Hirai,K., Kondo,K., Kobayashi,K., Yoshida,M., Kaneko,S., Kishida,T., Kawakami,S., Hosaka,M., Inayama,Y., and Yao,M. (2001). SPARC expression in

primary human renal cell carcinoma: upregulation of SPARC in sarcomatoid renal carcinoma. Hum. Pathol. *32*, 1064-1070.

Sarrio,D., Rodriguez-Pinilla,S.M., Hardisson,D., Cano,A., Moreno-Bueno,G., and Palacios,J. (2008). Epithelial-mesenchymal transition in breast cancer relates to the basal-like phenotype. Cancer Res. *68*, 989-997.

Sato,N., Fukushima,N., Maehara,N., Matsubayashi,H., Koopmann,J., Su,G.H., Hruban,R.H., and Goggins,M. (2003). SPARC/osteonectin is a frequent target for aberrant methylation in pancreatic adenocarcinoma and a mediator of tumor-stromal interactions. Oncogene *22*, 5021-5030.

Sbaa,E., Dewever,J., Martinive,P., Bouzin,C., Frerart,F., Balligand,J.L., Dessy,C., and Feron,O. (2006). Caveolin plays a central role in endothelial progenitor cell mobilization and homing in SDF-1-driven postischemic vasculogenesis. Circ. Res. *98*, 1219-1227.

Scheel,C., Onder,T., Karnoub,A., and Weinberg,R.A. (2007). Adaptation versus selection: the origins of metastatic behavior. Cancer Res. *67*, 11476-11479.

Seandel,M., Butler,J., Lyden,D., and Rafii,S. (2008). A catalytic role for proangiogenic marrow-derived cells in tumor neovascularization. Cancer Cell *13*, 181-183.

Seliger,B. and Kellner,R. (2002). Design of proteome-based studies in combination with serology for the identification of biomarkers and novel targets. Proteomics. *2*, 1641-1651.

Semenza,G.L. (2002). HIF-1 and tumor progression: pathophysiology and therapeutics. Trends Mol. Med. *8*, S62-S67.

Semenza,G.L. (2008). Hypoxia-inducible factor 1 and cancer pathogenesis. IUBMB. Life *60*, 591-597.

Seno,T., Harada,H., Kohno,S., Teraoka,M., Inoue,A., and Ohnishi,T. (2009). Downregulation of SPARC expression inhibits cell migration and invasion in malignant gliomas. Int. J. Oncol. *34*, 707-715.

Seruga,B., Zhang,H., Bernstein,L.J., and Tannock,I.F. (2008). Cytokines and their relationship to the symptoms and outcome of cancer. Nat. Rev. Cancer *8*, 887-899.

Shaked,Y., Ciarrocchi,A., Franco,M., Lee,C.R., Man,S., Cheung,A.M., Hicklin,D.J., Chaplin,D., Foster,F.S., Benezra,R., and Kerbel,R.S. (2006). Therapy-induced acute recruitment of circulating endothelial progenitor cells to tumors. Science *313*, 1785-1787.

Shaked,Y., Henke,E., Roodhart,J.M., Mancuso,P., Langenberg,M.H., Colleoni,M., Daenen,L.G., Man,S., Xu,P., Emmenegger,U., Tang,T., Zhu,Z., Witte,L., Strieter,R.M., Bertolini,F., Voest,E.E., Benezra,R., and Kerbel,R.S. (2008). Rapid chemotherapy-induced acute endothelial progenitor cell mobilization: implications for antiangiogenic drugs as chemosensitizing agents. Cancer Cell *14*, 263-273.

Shaked,Y. and Voest,E.E. (2009). Bone marrow derived cells in tumor angiogenesis and growth: are they the good, the bad or the evil? Biochim. Biophys. Acta *1796*, 1-4.

Shariat,S.F., Karakiewicz,P.I., Godoy,G., Karam,J.A., Ashfaq,R., Fradet,Y., Isbarn,H., Montorsi,F., Jeldres,C., Bastian,P.J., Nielsen,M.E., Muller,S.C., Sagalowsky,A.I., and Lotan,Y. (2009). Survivin as a prognostic marker for urothelial carcinoma of the bladder: a multicenter external validation study. Clin. Cancer Res. *15*, 7012-7019.

Shi,Q., Bao,S., Song,L., Wu,Q., Bigner,D.D., Hjelmeland,A.B., and Rich,J.N. (2007). Targeting SPARC expression decreases glioma cellular survival and invasion associated with reduced activities of FAK and ILK kinases. Oncogene *26*, 4084-4094.

Shin,B.K., Wang,H., Yim,A.M., Le,N.F., Brichory,F., Jang,J.H., Zhao,R., Puravs,E., Tra,J., Michael,C.W., Misek,D.E., and Hanash,S.M. (2003). Global profiling of the cell surface proteome of cancer cells uncovers an abundance of proteins with chaperone function. J. Biol. Chem. *278*, 7607-7616.

Shinde Patil,V.R., Friedrich,E.B., Wolley,A.E., Gerszten,R.E., Allport,J.R., and Weissleder,R. (2005). Bone marrow-derived lin(-)c-

kit(+)Sca-1+ stem cells do not contribute to vasculogenesis in Lewis lung carcinoma. Neoplasia. *7*, 234-240.

Shojaei,F., Wu,X., Zhong,C., Yu,L., Liang,X.H., Yao,J., Blanchard,D., Bais,C., Peale,F.V., van,B.N., Ho,C., Ross,J., Tan,M., Carano,R.A., Meng,Y.G., and Ferrara,N. (2007). Bv8 regulates myeloid-cell-dependent tumour angiogenesis. Nature *450*, 825-831.

Sica,A. and Bronte,V. (2007). Altered macrophage differentiation and immune dysfunction in tumor development. J. Clin. Invest *117*, 1155-1166.

Simojoki,M., Santala,M., Risteli,J., and Kauppila,A. (2001). Carboxyterminal telopeptide of type I collagen (ICTP) in predicting prognosis in epithelial ovarian cancer. Gynecol. Oncol. *82*, 110-115.

Sivridis,E., Giatromanolaki,A., and Koukourakis,M.I. (2004). "Stromatogenesis" and tumor progression. Int. J. Surg. Pathol. *12*, 1-9.

Smith,L., Lind,M.J., Welham,K.J., and Cawkwell,L. (2006). Cancer proteomics and its application to discovery of therapy response markers in human cancer. Cancer *107*, 232-241.

Socha,M.J., Said,N., Dai,Y., Kwong,J., Ramalingam,P., Trieu,V., Desai,N., Mok,S.C., and Motamed,K. (2009). Aberrant promoter methylation of SPARC in ovarian cancer. Neoplasia. *11*, 126-135.

Sokolove,J., Zhao,X., Chandra,P.E., and Robinson,W.H. (2011). Immune complexes containing citrullinated fibrinogen costimulate macrophages via Toll-like receptor 4 and Fcgamma receptor. Arthritis Rheum. *63*, 53-62.

Sova,P., Feng,Q., Geiss,G., Wood,T., Strauss,R., Rudolf,V., Lieber,A., and Kiviat,N. (2006). Discovery of novel methylation biomarkers in cervical carcinoma by global demethylation and microarray analysis. Cancer Epidemiol. Biomarkers Prev. *15*, 114-123.

St,C.B., Rago,C., Velculescu,V., Traverso,G., Romans,K.E., Montgomery,E., Lal,A., Riggins,G.J., Lengauer,C., Vogelstein,B., and Kinzler,K.W. (2000). Genes expressed in human tumor endothelium. Science *289*, 1197-1202.

Stewart,T.J. and Abrams,S.I. (2008). How tumours escape mass destruction. Oncogene *27*, 5894-5903.

Suriano,R., Chaudhuri,D., Johnson,R.S., Lambers,E., Ashok,B.T., Kishore,R., and Tiwari,R.K. (2008). 17Beta-estradiol mobilizes bone marrow-derived endothelial progenitor cells to tumors. Cancer Res. *68*, 6038-6042.

Suzuki,A., Iizuka,A., Komiyama,M., Takikawa,M., Kume,A., Tai,S., Ohshita,C., Kurusu,A., Nakamura,Y., Yamamoto,A., Yamazaki,N., Yoshikawa,S., Kiyohara,Y., and Akiyama,Y. (2010). Identification of melanoma antigens using a Serological Proteome Approach (SERPA). Cancer Genomics Proteomics. *7*, 17-23.

Suzuki,M., Hao,C., Takahashi,T., Shigematsu,H., Shivapurkar,N., Sathyanarayana,U.G., Iizasa,T., Fujisawa,T., Hiroshima,K., and Gazdar,A.F. (2005). Aberrant methylation of SPARC in human lung cancers. Br. J. Cancer *92*, 942-948.

Tai,I.T., Dai,M., Owen,D.A., and Chen,L.B. (2005). Genome-wide expression analysis of therapy-resistant tumors reveals SPARC as a novel target for cancer therapy. J. Clin. Invest *115*, 1492-1502.

Tai,I.T. and Tang,M.J. (2008). SPARC in cancer biology: its role in cancer progression and potential for therapy. Drug Resist. Updat. *11*, 231-246.

Tainsky,M.A. (2009). Genomic and proteomic biomarkers for cancer: a multitude of opportunities. Biochim. Biophys. Acta *1796*, 176-193.

Takano,T., Hasegawa,Y., Miyauchi,A., Matsuzuka,F., Yoshida,H., Kuma,K., Hayashi,N., Nakamori,S., and Amino,N. (2002). Quantitative analysis of osteonectin mRNA in thyroid carcinomas. Endocr. J. *49*, 511-516.

Takashima,M., Kuramitsu,Y., Yokoyama,Y., Iizuka,N., Harada,T., Fujimoto,M., Sakaida,I., Okita,K., Oka,M., and Nakamura,K. (2006). Proteomic analysis of autoantibodies in patients with hepatocellular carcinoma. Proteomics. *6*, 3894-3900.

Takeno,A., Takemasa,I., Doki,Y., Yamasaki,M., Miyata,H., Takiguchi,S., Fujiwara,Y., Matsubara,K., and Monden,M. (2008).

Integrative approach for differentially overexpressed genes in gastric cancer by combining large-scale gene expression profiling and network analysis. Br. J. Cancer *99*, 1307-1315.

Tan,E.M. and Shi,F.D. (2003). Relative paradigms between autoantibodies in lupus and autoantibodies in cancer. Clin. Exp. Immunol. *134*, 169-177.

Tan,H.T., Low,J., Lim,S.G., and Chung,M.C. (2009). Serum autoantibodies as biomarkers for early cancer detection. FEBS J. *276*, 6880-6904.

Tan,T.T. and Coussens,L.M. (2007). Humoral immunity, inflammation and cancer. Curr. Opin. Immunol. *19*, 209-216.

Taylor,D.D., Gercel-Taylor,C., and Parker,L.P. (2009). Patient-derived tumor-reactive antibodies as diagnostic markers for ovarian cancer. Gynecol. Oncol. *115*, 112-120.

Tesniere,A., Apetoh,L., Ghiringhelli,F., Joza,N., Panaretakis,T., Kepp,O., Schlemmer,F., Zitvogel,L., and Kroemer,G. (2008). Immunogenic cancer cell death: a key-lock paradigm. Curr. Opin. Immunol. *20*, 504-511.

Thomas,R., True,L.D., Bassuk,J.A., Lange,P.H., and Vessella,R.L. (2000). Differential expression of osteonectin/SPARC during human prostate cancer progression. Clin. Cancer Res. *6*, 1140-1149.

Timmermans,F., Plum,J., Yoder,M.C., Ingram,D.A., Vandekerckhove,B., and Case,J. (2009). Endothelial progenitor cells: identity defined? J. Cell Mol. Med. *13*, 87-102.

Triantafilou,M., Fradelizi,D., and Triantafilou,K. (2001). Major histocompatibility class one molecule associates with glucose regulated protein (GRP) 78 on the cell surface. Hum. Immunol. *62*, 764-770.

Trosko,J.E., Chang,C.C., Upham,B.L., and Tai,M.H. (2004). Ignored hallmarks of carcinogenesis: stem cells and cell-cell communication. Ann. N. Y. Acad. Sci. *1028*, 192-201.

Tsai-Turton,M., Santillan,A., Lu,D., Bristow,R.E., Chan,K.C., Shih,I., and Roden,R.B. (2009). p53 autoantibodies, cytokine levels and ovarian carcinogenesis. Gynecol. Oncol. *114*, 12-17.

Ullah,M.F. and Aatif,M. (2009). The footprints of cancer development: Cancer biomarkers. Cancer Treat. Rev. *35*, 193-200.

Ullrich,E., Bonmort,M., Mignot,G., Kroemer,G., and Zitvogel,L. (2008). Tumor stress, cell death and the ensuing immune response. Cell Death. Differ. *15*, 21-28.

Unwin,R.D., Harnden,P., Pappin,D., Rahman,D., Whelan,P., Craven,R.A., Selby,P.J., and Banks,R.E. (2003). Serological and proteomic evaluation of antibody responses in the identification of tumor antigens in renal cell carcinoma. Proteomics. *3*, 45-55.

Urbich,C. and Dimmeler,S. (2004). Endothelial progenitor cells: characterization and role in vascular biology. Circ. Res. *95*, 343-353.

Van den Eynde,B.J. and Van der Bruggen,P. (1997). T cell defined tumor antigens. Curr. Opin. Immunol. *9*, 684-693.

van,V.W., de Groot,J.W., Acton,D.S., Hofstra,R.M., Hoppener,J.W., Links,T.P., and Lips,C.J. (2009). Medullary thyroid carcinoma and biomarkers: past, present and future. J. Intern. Med. *266*, 126-140.

Vaupel,P. and Harrison,L. (2004). Tumor hypoxia: causative factors, compensatory mechanisms, and cellular response. Oncologist. *9 Suppl 5*, 4-9.

Verrills,N.M. (2006). Clinical proteomics: present and future prospects. Clin. Biochem. Rev. *27*, 99-116.

Wang,C.S., Lin,K.H., Chen,S.L., Chan,Y.F., and Hsueh,S. (2004). Overexpression of SPARC gene in human gastric carcinoma and its clinic-pathologic significance. Br. J. Cancer *91*, 1924-1930.

Wang,Y., Wu,M.C., Sham,J.S., Zhang,W., Wu,W.Q., and Guan,X.Y. (2002). Prognostic significance of c-myc and AIB1 amplification in hepatocellular carcinoma. A broad survey using high-throughput tissue microarray. Cancer *95*, 2346-2352.

Watkins,G., Douglas-Jones,A., Bryce,R., Mansel,R.E., and Jiang,W.G. (2005). Increased levels of SPARC (osteonectin) in human breast cancer tissues and its association with clinical outcomes. Prostaglandins Leukot. Essent. Fatty Acids *72*, 267-272.

Wels,J., Kaplan,R.N., Rafii,S., and Lyden,D. (2008). Migratory neighbors and distant invaders: tumor-associated niche cells. Genes Dev. *22*, 559-574.

Westermeier, R., Naven, T., and Hopker, HR. Proteomics in practice. Wiley VCH 1[1-2], 1-479. 2008.
Ref Type: Serial (Book,Monograph)

Wickersheim,A., Kerber,M., de Miguel,L.S., Plate,K.H., and Machein,M.R. (2009). Endothelial progenitor cells do not contribute to tumor endothelium in primary and metastatic tumors. Int. J. Cancer *125*, 1771-1777.

Wiese,A.H., Auer,J., Lassmann,S., Nahrig,J., Rosenberg,R., Hofler,H., Ruger,R., and Werner,M. (2007). Identification of gene signatures for invasive colorectal tumor cells. Cancer Detect. Prev. *31*, 282-295.

Witz,I.P. and Levy-Nissenbaum,O. (2006). The tumor microenvironment in the post-PAGET era. Cancer Lett. *242*, 1-10.

Woelfle,U., Cloos,J., Sauter,G., Riethdorf,L., Janicke,F., van,D.P., Brakenhoff,R., and Pantel,K. (2003). Molecular signature associated with bone marrow micrometastasis in human breast cancer. Cancer Res. *63*, 5679-5684.

Wong,F.H., Huang,C.Y., Su,L.J., Wu,Y.C., Lin,Y.S., Hsia,J.Y., Tsai,H.T., Lee,S.A., Lin,C.H., Tzeng,C.H., Chen,P.M., Chen,Y.J., Liang,S.C., Lai,J.M., and Yen,C.C. (2009). Combination of microarray profiling and protein-protein interaction databases delineates the minimal discriminators as a metastasis network for esophageal squamous cell carcinoma. Int. J. Oncol. *34*, 117-128.

Woodhouse,E.C., Chuaqui,R.F., and Liotta,L.A. (1997). General mechanisms of metastasis. Cancer *80*, 1529-1537.

Xue,L.Y., Hu,N., Song,Y.M., Zou,S.M., Shou,J.Z., Qian,L.X., Ren,L.Q., Lin,D.M., Tong,T., He,Z.G., Zhan,Q.M., Taylor,P.R., and Lu,N. (2006). Tissue microarray analysis reveals a tight correlation between protein expression pattern and progression of esophageal squamous cell carcinoma. BMC. Cancer *6*, 296.

Yamashita,K., Upadhay,S., Mimori,K., Inoue,H., and Mori,M. (2003). Clinical significance of secreted protein acidic and rich in cystein in esophageal carcinoma and its relation to carcinoma progression. Cancer *97*, 2412-2419.

Yan,Q. and Sage,E.H. (1999). SPARC, a matricellular glycoprotein with important biological functions. J. Histochem. Cytochem. *47*, 1495-1506.

Yang,E., Kang,H.J., Koh,K.H., Rhee,H., Kim,N.K., and Kim,H. (2007). Frequent inactivation of SPARC by promoter hypermethylation in colon cancers. Int. J. Cancer *121*, 567-575.

Yang,L., Huang,J., Ren,X., Gorska,A.E., Chytil,A., Aakre,M., Carbone,D.P., Matrisian,L.M., Richmond,A., Lin,P.C., and Moses,H.L. (2008). Abrogation of TGF beta signaling in mammary carcinomas recruits Gr-1+CD11b+ myeloid cells that promote metastasis. Cancer Cell *13*, 23-35.

Ye,X.Z., Yu,S.C., and Bian,X.W. (2010). Contribution of myeloid-derived suppressor cells to tumor-induced immune suppression, angiogenesis, invasion and metastasis. J. Genet. Genomics *37*, 423-430.

Yilmaz,M., Christofori,G., and Lehembre,F. (2007). Distinct mechanisms of tumor invasion and metastasis. Trends Mol. Med. *13*, 535-541.

Yin,J., Chen,G., Liu,Y., Liu,S., Wang,P., Wan,Y., Wang,X., Zhu,J., and Gao,H. (2010). Downregulation of SPARC expression decreases gastric cancer cellular invasion and survival. J. Exp. Clin. Cancer Res. *29*, 59.

Yiu,G.K., Chan,W.Y., Ng,S.W., Chan,P.S., Cheung,K.K., Berkowitz,R.S., and Mok,S.C. (2001). SPARC (secreted protein

acidic and rich in cysteine) induces apoptosis in ovarian cancer cells. Am. J. Pathol. *159*, 609-622.

Yurkovetsky,Z., Skates,S., Lomakin,A., Nolen,B., Pulsipher,T., Modugno,F., Marks,J., Godwin,A., Gorelik,E., Jacobs,I., Menon,U., Lu,K., Badgwell,D., Bast,R.C., Jr., and Lokshin,A.E. (2010). Development of a Multimarker Assay for Early Detection of Ovarian Cancer. J. Clin. Oncol.

Zitvogel,L., Apetoh,L., Ghiringhelli,F., Andre,F., Tesniere,A., and Kroemer,G. (2008a). The anticancer immune response: indispensable for therapeutic success? J. Clin. Invest *118*, 1991-2001.

Zitvogel,L., Apetoh,L., Ghiringhelli,F., and Kroemer,G. (2008b). Immunological aspects of cancer chemotherapy. Nat. Rev. Immunol. *8*, 59-73.

PUBLICATIONS

1. Defresne F, Bouzin C, Guilbaud C, Dieu M, Delaive E, Michiels C, Raes M, Feron O.

Differential influence of anticancer treatments and angiogenesis on the seric titer of autoantibody used as tumor and metastasis biomarker.

Neoplasia. 2010 Jul;12(7):562-70.

2. Defresne F, Bouzin C, Grandjean M, Dieu M, Raes M, Hatzopoulos AK, Kupatt C, Feron O.

Preconditioned endothelial progenitor cells reduce the formation of melanoma metastases through SPARC-driven cell-cell interaction and endocytosis.

Cancer Res 2011, accepted.

3. Martinive P#, Defresne F#, Quaghebeur E, Daneau G, Crokart N, Grégoire V, Gallez B, Dessy C, Feron O.

Impact of cyclic hypoxia on HIF-1alpha regulation in endothelial cells--new insights for anti-tumor treatments.

FEBS J. 2009 Jan;276(2):509-18. Epub 2008 Dec 10.

# Martinive P and Defresne F contributed equally to this work

4. Martinive P, Defresne F, Bouzin C, Saliez J, Lair F, Grégoire V, Michiels C, Dessy C, Feron O.

Preconditioning of the tumor vasculature and tumor cells by intermittent hypoxia: implications for anticancer therapies.

Cancer Res. 2006 Dec 15;66(24):11736-44

5. Daugimont L, Vandermeulen G, Defresne F, Bouzin C, Mir L, Bouquet C, Feron O, Préat V.

Antitumoral and antimetastatic effect of antiangiogenic plasmids in B16 melanoma.

Eur J Pharm Biopharm. 2011 Feb 18.

6. Godechal Q, Defresne F, Danhier P, Leveque P, Ettore Porporato P, Sonveaux P, Baurain JF, Feron O, Gallez B.

Assessment of melanoma extent and melanoma metastases invasion using Electron Paramagnetic Resonance and bioluminescence imaging

Contrast Media Mol Imaging 2011, in press

7. Verrax J, Defresne F, Lair F, Vandermeulen G, Rath G, Dessy C, Préat V, Feron O.

Delivery of soluble VEGF receptor 1 (sFlt1) by gene electrotransfer as a new anti-angiogenic cancer therapy.

Molecular Pharmaceutics 2011, in revision

8. Defresne F, Grandjean M, Guilbaud C, Samain J, Feron O.

Hypoxia-driven identification of tumor autoantibodies in a breast cancer mouse model.

In preparation